University of Cordoba

Analytical Chemistry Department

NEW CONTRIBUTIONS OF ION MOBILITY TECHNIQUES TO ENVIRONMENTAL AND CLINICAL ANALYSIS

NUEVAS CONTRIBUCIONES DE LAS TÉCNICAS DE MOVILIDAD IÓNICA AL ANÁLISIS AMBIENTAL Y CLÍNICO

DOCTORAL THESIS

Laura del Rosario Criado García

Córdoba, 2015

TITULO: *Nuevas contribuciones de las técnicas de movilidad iónica ambiental y clínico*

AUTOR: *Laura del Rosario Criado García*

© Edita: Servicio de Publicaciones de la Universidad de Córdoba. 2016
Campus de Rabanales
Ctra. Nacional IV, Km. 396 A
14071 Córdoba

www.uco.es/publicaciones
publicaciones@uco.es

NUEVAS CONTRIBUCIONES DE LAS TÉCNICAS DE MOVILIDAD IÓNICA AL ANÁLISIS AMBIENTAL Y CLÍNICO

LOS DIRECTORES,

Fdo. **Lourdes Arce Jiménez**
Profesora Titular del Departamento de Química Analítica de la Universidad de Córdoba

Fdo. **Miguel Valcárcel Cases**
Catedrático del Departamento de Química Analítica de la Universidad de Córdoba

Trabajo presentado para aspirar al

Grado de Doctor en Ciencias con Mención Internacional

LA DOCTORANDA,

Fdo. **Laura del Rosario Criado García**

Licenciada en Ciencias Ambientales

Lourdes Arce Jiménez, Profesora Titular del Departamento de Química Analítica de la Universidad de Córdoba y **Miguel Valcárcel Cases**, Catedrático del Departamento de Química Analítica de la Universidad de Córdoba, en calidad de directores de la Tesis Doctoral presentada por **Laura del Rosario Criado García** titulada "Nuevas contribuciones de las técnicas de movilidad iónica al análisis ambiental y clínico",

CERTIFICAN:

1) Que el trabajo experimental de la Tesis Doctoral ha sido desarrollado en los laboratorios del Departamento de Química Analítica de la Universidad de Córdoba (España) y del área de Química Analítica perteneciente al Departamento de Química de la Universidad de Loughborough (Reino Unido).

2) A nuestro juicio, reúne todos los requisitos exigidos a este tipo de trabajo.

3) Laura del Rosario Criado García es la primera autora de todos los trabajos científicos presentados en la Tesis. De acuerdo a la normativa de la Universidad y los acuerdos internos de nuestro grupo de investigación, el primer autor es el responsable por completo de la implementación del trabajo experimental y de la producción de la primera versión del artículo. Además, ella ha participado activamente en las reuniones con sus directores para comprobar y discutir el progreso del trabajo doctoral.

Córdoba, a 17 de Noviembre de 2015

Fdo. **Lourdes Arce Jiménez** Fdo. **Miguel Valcárcel Cases**

Lourdes Arce Jiménez, Lecturer from the Analytical Chemistry Department of the University of Cordoba and **Miguel Valcárcel Cases**, Full Professor from the Analytical Chemistry Department of the University of Cordoba both in quality of supervisors of the Doctoral Thesis of **Laura del Rosario Criado García** entitled "New contributions of ion mobility techniques to environmental and clinical analysis",

CERTIFY THAT:

1) The experimental work of the PhD thesis has been developed in the laboratories of the Department of Analytical Chemistry of the University of Córdoba (Spain) and Analytical Science area, Department of Chemistry of the University of Loughborough (United Kingdom).

2) According to our judgment the Doctoral Thesis meets all the requirements of this type of scientific work.

3) Laura del Rosario Criado García is the first author of all the scientific papers presented in the Thesis. According to the University rules and the internal agreements in our research group, the first author of a paper is the full responsible for the implementation of the experimental work and also to produce the first draft of the paper. In addition, she has also actively participated in the meetings with their supervisors to check and discuss the progress of the doctoral work.

Córdoba, 17th de November 2015

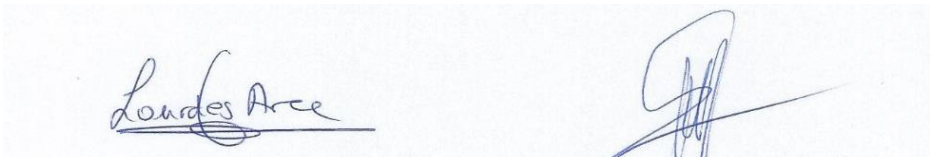

Fdo. **Lourdes Arce Jiménez** Fdo. **Miguel Valcárcel Cases**

TÍTULO DE LA TESIS: Nuevas contribuciones de las técnicas de movilidad iónica al análisis ambiental y clínico

DOCTORANDO/A: Laura del Rosario Criado García

INFORME RAZONADO DE LOS DIRECTORES DE LA TESIS

La licenciada Laura del Rosario Criado García cursó brillantemente la Licenciatura de Ciencias Ambientales y los estudios del máster en Química Fina Avanzada. En el año 2011 accedió a una beca de formación de profesorado universitario para la realización de la Tesis Doctoral, cuya Memoria se presentará para su defensa el próximo mes de enero bajo la modalidad de doctorado internacional y como compendio de publicaciones. La temática de la misma ha sido el desarrollo de nuevos métodos de análisis en el ámbito ambiental y clínico con el uso de las técnicas de movilidad iónica.

El trabajo experimental realizado se ha materializado en ocho artículos científicos, publicados o enviados para su publicación a revistas especializadas del área de química analítica. La doctoranda ha asistido a nueve congresos nacionales e internacionales presentando un total de doce comunicaciones en formato oral, flash o cartel. A lo largo de estos años, ha adquirido formación en el manejo de equipos de movilidad iónica tales como la espectrometría de movilidad iónica con fuente de ionización ultravioleta o de tritio. Durante su estancia de seis meses en la Universidad de Loughborough (Reino Unido) aprendió a usar la espectrometría de movilidad diferencial con fuente de níquel. Además también ha usado instrumentos analíticos clásicos tales como la cromatografía de gases y espectroscopia infrarroja y ha adquirido gran experiencia en el desarrollo de la primera etapa del proceso analítico que incluye el uso de métodos de pretratamiento de muestra y técnicas de extracción para la determinación de analitos de interés en matrices ambientales y biológicas. Con todo el trabajo realizado ha adquirido las competencias técnicas inherentes al trabajo en el laboratorio demostrando una gran iniciativa y capacidad para la resolución de problemas. La Lcda. Criado ha demostrado su capacidad para trabajar en equipos multidisciplinares, tanto con investigadores de la Universidad de Córdoba como de otras universidades extranjeras así como con el personal de distintas empresas (G.A.S. mbH., RAMEM S.A., Magtel S.A. y TSK S.A.). Finalmente tuvo la oportunidad de codirigir con éxito un trabajo fin de master a un alumno extranjero del Master titulado "Forensic Science".

Por todo ello, se autoriza la presentación de la tesis doctoral.

Córdoba, a 17 de Noviembre de 2015

Firma de los directores

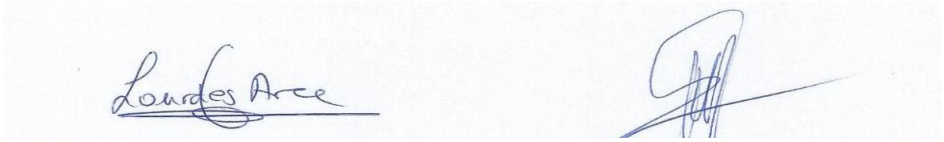

Fdo.: **Lourdes Arce Jiménez** Fdo.: **Miguel Valcárcel Cases**

MENCIÓN DOCTORADO INTERNACIONAL

Mediante la defensa de esta Memoria de Tesis Doctoral se pretende optar a la obtención de la Mención de "Doctorado Internacional" habida cuenta de que la doctoranda reúne los requisitos para tal mención (R.D. 99/2011, de 28 de Enero):

1. Cuenta con los informes favorables de dos doctores pertenecientes a instituciones de Enseñanza Superior de países distintos a España.

2. Uno de los miembros del tribunal que ha de evaluar la Tesis pertenece a un centro de Enseñanza Superior de otro país distinto a España.

3. Parte de la defensa de la Tesis Doctoral se realizará en una lengua distinta de las lenguas oficiales en España.

4. La doctoranda ha realizado una estancia de seis meses en el área de Química Analítica perteneciente al Departamento de Química de la Universidad de Loughborough (Reino Unido), gracias a la concesión de una beca para estancias en el extranjero del ceiA3. El trabajo de investigación desarrollado ha sido aceptado para su publicación en la revista *Journal of Breath Research*.

Córdoba, a 17 de Noviembre de 2015

Fdo. **Lourdes Arce Jiménez** Fdo. **Miguel Valcárcel Cases**

Agradezco al Ministerio de Educación, Cultura y Deporte la concesión de una beca de Formación de Profesorado Universitario (FPU) que ha hecho posible mi dedicación a este trabajo durante los últimos cuatro años.

INDEX/ INDICE

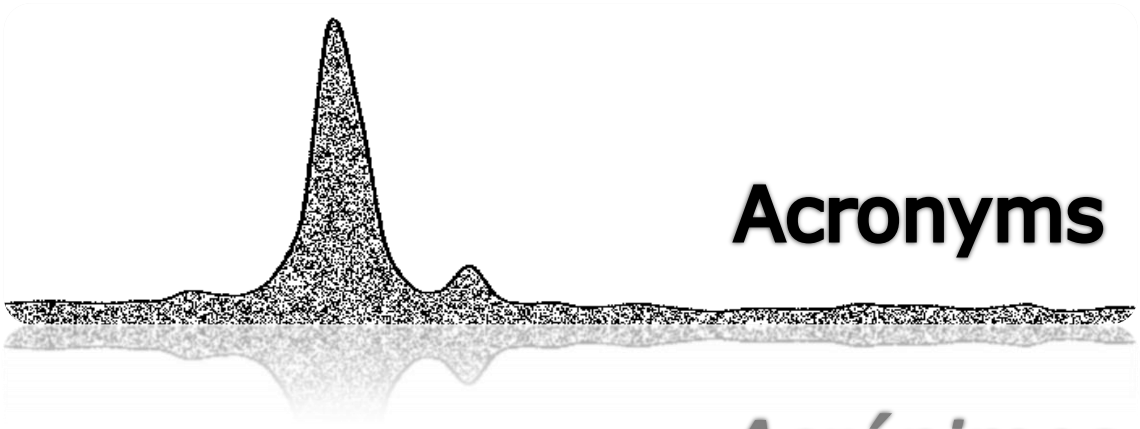

Acronyms

Acrónimos

- AIMS — Aspiration ion mobility spectrometry
  Espectrometría de movilidad iónica de aspiración
- ^{241}Am — Americium source
  Fuente de americio
- APCI — Atmospheric pressure chemical ionization
  Ionizacion química a presión atmosférica
- BTX — Benzene, toluene, *m*-xylene, *o*-xylene and *p*-xylene
  Benceno, tolueno, *m*-xileno, *o*-xileno and *p*-xileno
- BTEX — Benzene, toluene, ethylbenzene, *m*-xylene, *o*-xylene and *p*-xylene
  Benceno, tolueno, etilbenceno, *m*-xileno, *o*-xileno and *p*-xileno
- CWA — Chemical warfare agents
  Agentes químicos de guerra
- CD — Corona discharge
  Descarga corona
- CDI — Clostridium difficile infection
  Infección de clostridium difficile
- CF — Cross flow
  Flujo cruzado
- COPD — Chronic obstructive pulmonary disease
  Enfermedad pulmonar obstrucción crónica
- CPC — Condensation particle counter
  Contador de particulas condensadas
- CRC — Colorectal cancer
  Cáncer de colon
- CV — Compensation voltage
  Voltaje de compensación
- DBBP — Dibutyl phosphonate
  Dibutil fosfonato
- DC — Difussion cell
  Celda de difusión
- DEEP — Diethyl phosphonate
  Dietil fosfonato
- DEIP — Diethylisopropyl phosphonate
  Dietilisopropil fosfonato
- DEMP — Diethylmethyl phosphonate
  Dietilmetil fosfonato
- DIMP — Diisopropylmethyl phosphonate
  Diisopropilmetil fosfonato

- DMA — Differential mobility analyzer
  Analizador de movilidad diferencial
- DMMP — Dimethylphosphonate
  Dimetilfosfonato
- DMS — Differential mobility spectrometry
  Espectrometría de movilidad diferencial
- DOE — Design of experiment
  Diseño de experimento
- DV — Dispersion voltage
  Voltaje de dispersión
- EDF — Exponential dilution flask
  Frasco de dilución exponencial
- EPA — Environmental protection agency
  Agencia de protección ambiental (EEUU)
- ESI — Electrospray ionization source
  Fuente de ionización de electrospray
- FAIMS — Field asymmetric ion mobility spectrometry
  Espectrometría de movilidad iónica de campo
- c-FAIMS — Cylindrical field asymmetric ion mobility spectrometry
  Espectrometría de movilidad iónica de campo cilíndrico
- p-FAIMS — Planar field asymmetric ion mobility spectrometry
  Espectrometría de movilidad iónica de campo plano
- FID — Flame ionization detector
  Detector de ionización de llama
- FT-MIR — Fourier transform-mid infrared
  Espectroscopia de transformada de fourier-infrarrojo cercano
- GC — Gas chromatography
  Cromatografía de gases
- GHB — Gamma hydroxybutyric acid
  Acido gamma hidroxibutírico
- ^{3}H — Tritium
  Tritio
- HF — Hollow fiber
  Fibra hueca
- HS — Headspace
  Espacio de cabeza
- HSCC — High speed capillary column
  Columna capilar de alta velocidad
- HTF — Heat transfer fluid

Fluido transmisor de calor

- ✧ IL — Ionic liquid
  Liquido iónico
- ✧ IMS — Ion mobility spectrometry
  Espectrometría de movilidad iónica
- ✧ IMMS — Ion mobility spectrometry-mass spectrometry
  Espectrometría de movilidad iónica-espectrometría de masas
- ✧ LC — Liquid chromatography
  Cromatografía de líquidos
- ✧ LOD — Limit of detection
  Límite de detección
- ✧ LOQ — Limit of quantification
  Límite de cuantificación
- ✧ LPME — Liquid phase microextraction
  Microextracción en fase líquida
- ✧ MCC — Multicapillary column
  Columna multicapilar
- ✧ MEU — Membrane extraction unit
  Unidad de extracción de membrana
- ✧ MI — Membrane inlet
  Sistema de membrana
- ✧ MIBK — Methyl isobutyl ketone
  Metil isobutil cetona
- ✧ MIPS — Molecularly imprinted polymer
  Polímero de impresión molecular
- ✧ MS — Mass spectrometry
  Espectrometría de masas
- ✧ MTBE — Methyl tert-butyl ether
  Metil tert-butil-éter
- ✧ MWCNTs — Multiwalled carbon nanotubes
  Nanotubos de carbono de pared múltiple
- ✧ ^{63}Ni — Nickel
  Níquel
- ✧ NIOSH — National institute of occupational safety and health
  Instituto nacional de seguridad y salud ocupacional (EEUU)
- ✧ OLIMS — Open loop ion mobility spectrometry
  Espectrometría de movilidad iónica de circuito abierto
- ✧ OMS — Overtone mobility spectrometry
  Espectrometría de movilidad harmónico

✧ Py	Pyrolysis Pirólisis
✧ R^2	Regression coefficient Coeficiente de regresión
✧ RH	Relative humidity Humedad relativa
✧ RIP	Reactant ion peak Pico del ion reactante
✧ RSD	Relative standard deviation Desviación estándar relativa
✧ RTGC	Room temperatura-gas chromatography Cromatografía de gases-temperatura ambiente
✧ SBSE	Stir-bar sorptive extractor Extracción en barra agitada
✧ SDME	Single drop microextraction Microextracción en gota
✧ SELDI	Surface enhanced laser desorption ionization Ionización de desorpción laser superficie mejorada
✧ SIS	Sample introduction system Sistema de introducción de muestra
✧ SPE	Solid phase extraction Extracción en fase sólida
✧ μSPE	Microsolid phase extraction Extracción en fase microsólida
✧ SPME	Solid phase microextraction Microextracción en fase sólida
✧ STEL	Short-term exposure limit Límite de exposición de corta duración
✧ TBN	Tri-n-buthyl phosphate Tri-n-butil fosfato
✧ TD	Thermal desorption Desorción térmica
✧ TENAX TA	Porous polymer adsorbent Polímero poroso adsorbente
✧ TEP	Triethyl phosphonate Trietil fosfonato
✧ TIMS	Trapped ion mobility spectrometry Espectrometría de movilidad iónica de circuito cerrado
✧ TMA	Trimethylamine Trimetilamina
✧ TMB	1,2,4-trimethylbenzene

1,2,4-trimetilbenceno

- TMP — Trimethyl phosphate
  Trimetil fosfato
- TPP — Triprophyl phosphate
  Tripropil fosfato
- TWIMS — Travelling wave ion mobility spectrometry
  Espectrometría de movilidad iónica de onda
- TOF — Time of flight detector
  Detector de tiempo de vuelo
- UV — Ultraviolet source
  Fuente ultravioleta
- VOCs — Volatile Organic Compounds
  Compuestos Orgánicos Volátiles

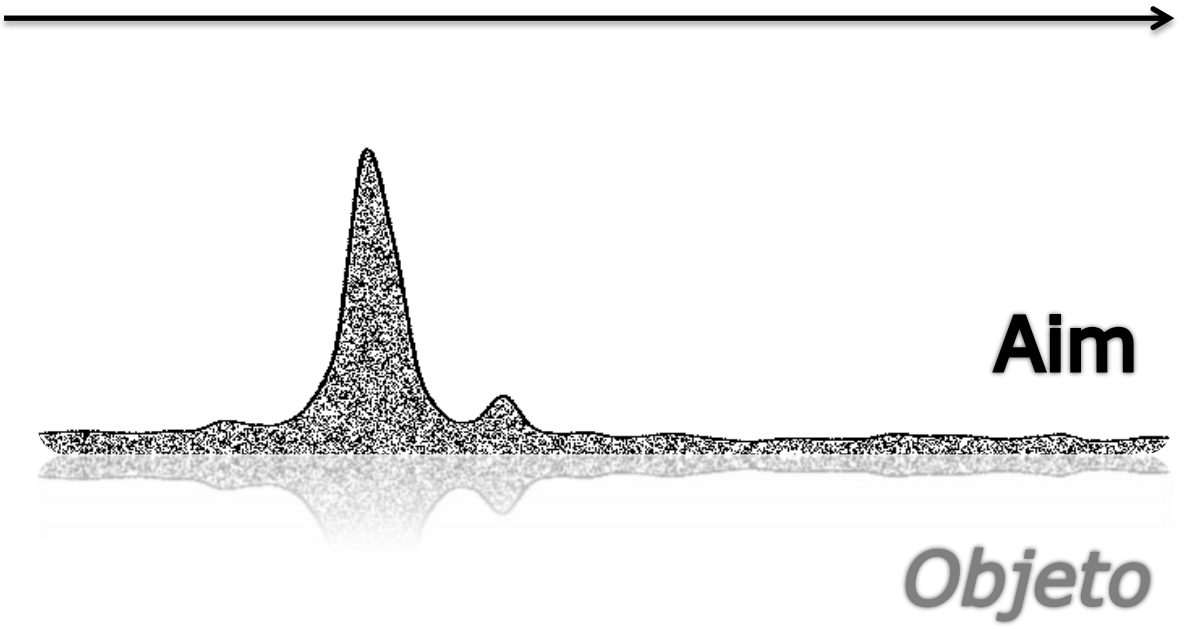
Aim
Objeto

Nowadays, routine analysis laboratories need to process a large number of samples periodically. Hence, the increasing development of new breakthrough technologies to provide quickly and reliably necessary information requested by the client, constituting one of the objectives of the current Analytical Chemistry. Framed within the cutting edge (vanguard) techniques are the ion mobility techniques. Currently, it is expanding due to the advantages they offer as simplicity, reliability, fast response and low cost. Ion mobility techniques are a useful tool in many areas such as detection of warfare agents and explosives. It is noteworthy the use of the instrument as a screening method in the environmental field and in the diagnosis of diseases in the clinical setting by detecting biomarkers and toxics.

The direct application of ion mobility techniques to the determination of target compounds in complex matrices such as environmental and human samples is challenging because the analytical methods and tools necessary to carry out it, are under development. Moreover, having the commitment to sort out problems related to low selectivity and in specific cases low sensitivity of ion mobility spectrometry, coupling techniques of gas chromatography and extraction modules for the separation and preconcentration of the analytes of interest can enhance analytical properties of this technology.

Considering the above, the main objective of the Doctoral Thesis presented in this Memory is the development of analytical methodologies using ion mobility spectrometry to solve problems in environmental and clinical field. With this overall objective, specific objectives of the research to develop are:

- ✧ Develop and compare different efficient methods to generate gaseous standards in order to calibrate an ion mobility spectrometer with ultraviolet source.

- ✧ Develop a system based on a membrane set-up coupled to an ultraviolet source ion mobility spectrometer in order to avoid the moisture interference on the ion mobility signal.
- ✧ Improve the selectivity of an analytical method used to determine analytes present in gaseous samples with the ultraviolet source ion mobility spectrometer by including a pre-separation step.
- ✧ Demonstrate the applicability of ion mobility spectrometry to obtain qualitative and quantitative information related to degradation and volatile compounds generated in the thermosolar fluid.
- ✧ Assess the potential of using solid and micro-solid phase extraction and other sorbent materials to improve the analytical performance of analytical methods based on the use of ion mobility instruments applied to the determination of toxic compounds in environmental and biological samples, respectively.

Of the wide variety of ion mobility instruments and variants described, this Doctoral Thesis has focused on the most widespread and representative ones such as ion mobility spectrometer with linear drift tube with tritium or ultraviolet ionization source, and differential mobility spectrometer with nickel ionization source.

En la actualidad, los laboratorios de análisis de rutina requieren procesar un gran número de muestras periódicamente. De ahí, el creciente desarrollo de nuevas técnicas de vanguardia que proporcionen la información necesaria demandada por el cliente de forma rápida y fiable, constituyendo uno de los objetivos de la Química Analítica actual. Enmarcada dentro de las técnicas de vanguardia se encuentran las técnicas de espectrometría de movilidad iónica. Actualmente en expansión debido a las ventajas que aportan como la simplicidad, fiabilidad, rapidez de respuesta y bajo coste. Las técnicas de movilidad iónica pueden ser útiles en numerosas áreas tal como detección de agentes de guerra y explosivos. Destacando el uso de la tecnología IMS como método de *screening* en el ámbito ambiental y en el diagnóstico de enfermedades en el ámbito clínico mediante la detección de biomarcadores y tóxicos.

La aplicación directa de las técnicas de movilidad iónica para la determinación de compuestos de interés en matrices complejas tales como muestras ambientales y/o clínicas constituye un reto que resulta complicado de abordar debido a que los métodos analíticos y las herramientas necesarias se encuentran en fase de desarrollo. Existiendo además el compromiso por mejorar los problemas asociados a la baja selectividad y en algunas ocasiones de sensibilidad de la movilidad iónica, los cuales pueden solucionarse mediante el acoplamiento a técnicas de separación tipo cromatografía de gases y módulos de extracción para la separación y preconcentración de los analitos de interés para mejorar las propiedades analíticas de esta tecnología.

Teniendo en cuenta lo anteriormente expuesto, el objetivo principal de la Tesis Doctoral que se presenta en esta Memoria es el desarrollo de metodologías analíticas mediante el uso de la espectrometría de movilidad iónica para resolver problemas en el ámbito ambiental y clínico. Con este objetivo global, los objetivos específicos de la investigación a desarrollar son los siguientes:

- ✧ Desarrollar y comparar diferentes métodos eficientes para la generación de estándares gaseosos y calibrar el equipo de movilidad iónica con fuente de ionización de ultravioleta.
- ✧ Desarrollar un sistema de membrana acoplado al espectrómetro de movilidad iónica con fuente de ionización ultravioleta para evitar la influencia de la humedad en la señal de movilidad iónica.
- ✧ Mejorar la selectividad del método analítico usado para determinar analitos presentes en muestras gaseosas con el espectrómetro de movilidad iónica con fuente de ionización ultravioleta incluyendo una etapa previa de pre-separación.
- ✧ Demostrar la aplicabilidad de la espectrometría de movilidad iónica para obtener información cualitativa y cuantitativa sobre compuestos de degradación volátiles generados en el aceite termosolar.
- ✧ Evaluar el potencial del uso de técnicas de extracción en fase sólida y micro sólida y otros materiales sorbentes para mejorar la selectividad y sensibilidad de los métodos analíticos basados en el uso de equipos de movilidad iónica aplicados a la determinación de compuestos tóxicos en muestras ambientales y biológicas, respectivamente.

Del amplio rango de instrumentos de movilidad iónica y variantes descritas hasta la fecha, esta Tesis Doctoral se ha centrado en las de uso más extendido y representativas tales como el espectrómetro de movilidad iónica con tubo de deriva lineal con fuente de ionización de tritio o ultravioleta y el espectrómetro de movilidad diferencial con fuente de ionización de níquel.

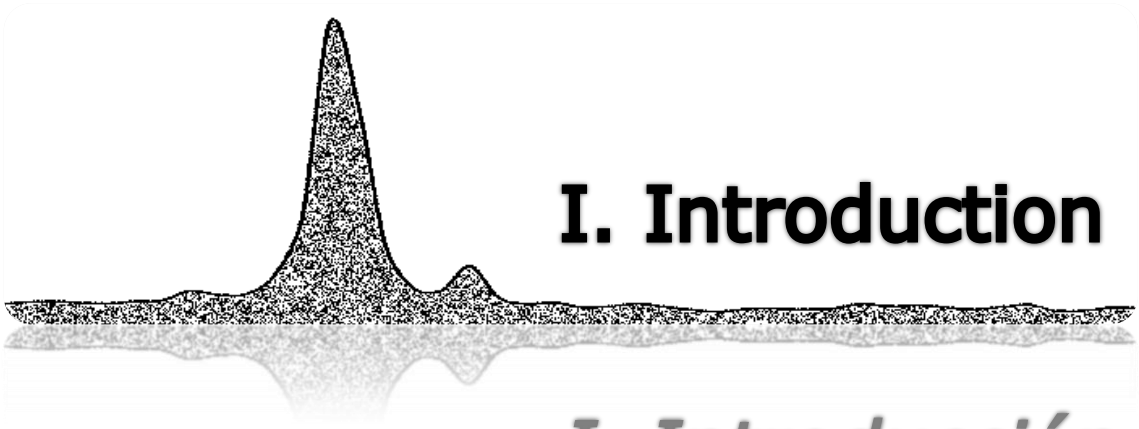

I. Introduction

I. Introducción

I.1. General overview

Ion mobility spectrometry (IMS) is a technique developed at the end of 1960s for the detection of organic compounds in air. In **Figure 1** are shown the increasing number of publications related with this technology along years. The interest in this technique has increased from late 1900s to these days due to their inherent advantages such as high sensitivity, instrumental simplicity, low cost, analytical flexibility, and real-time monitoring capability which are especially good in applications such as environmental monitoring and clinical analysis.

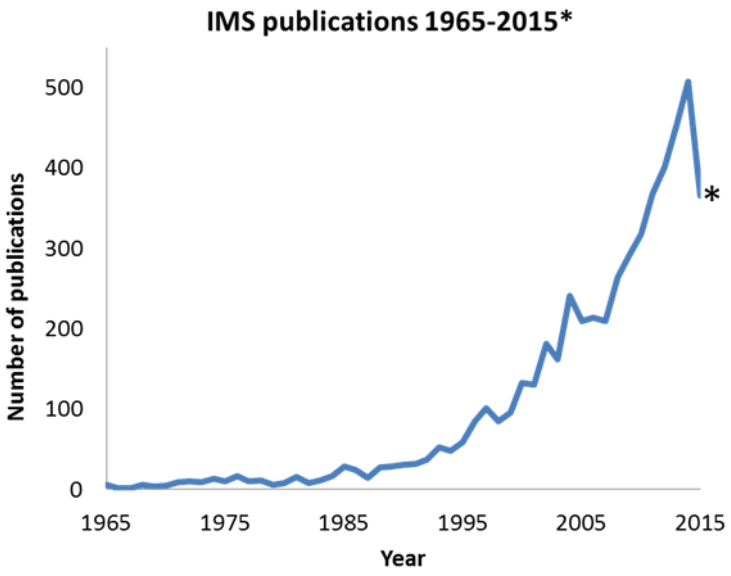

Fig. 1. Contribution of ion mobility spectrometry (IMS) in the years 1965-2015*. *Data extracted from Scopus database, last accessed September 2015.

In **Table 1** are summarized the advantages and disadvantages of IMS and it is also compared with common analytical techniques widely used in clinical and environmental fields. As can be seen, IMS is a technique that offers several advantages in comparison with other classical analytical techniques. However, it presents limitations such as low selectivity and the

occurrence of ion-molecule reactions and competitive ionization which can result in strong or even complete signal suppression for some analytes.

Table 1. Advantages of some analytical methods that currently are more used in clinical and environmental analysis.

Analytical method	Advantages	Disadvantages
IMS	▪ Low cost ▪ Portable ▪ Ease of use ▪ Rapid time analysis ▪ Work at ambient pressure ▪ Highly sensitive ▪ Robust	▪ Charge and exchange reactions and competitive ionization ▪ Low selectivity
Electronic nose	▪ Low size ▪ Low cost ▪ Low energy consumption ▪ Combination with other sensors is also possible	▪ Low reproducibility ▪ Short life-time ▪ Low selectivity
FT-MIR	▪ Rapid analysis ▪ No derivatization needed	▪ Extremely convoluted spectra ▪ More than one peak per component
GC-MS	▪ Sensitive ▪ Selective ▪ Robust ▪ Large commercial and public library	▪ High cost and maintenance ▪ Often requires derivatization
GC-FID	▪ Sensitive ▪ Low maintenance requirement	▪ Cannot detect inorganic substances
LC-MS	▪ Sensitive ▪ Selective ▪ Many modes of separation available	▪ High cost and maintenance ▪ Limited commercial libraries

IMS: ion mobility spectrometry, FT-MIR: fourier transform-mid infrared spectroscopy, GC-MS: gas chromatography-mass spectrometry, GC-FID: gas chromatography-flame ionization detector, LC-MS: liquid chromatography-mass spectrometry. This table has been adapted from [1].

I.2. Principle of operation

The principle of IMS is very simple. When a gaseous ion at atmospheric pressure is placed in a constant electric field, it accelerates down the field until it collides with a neutral molecule, accelerates again until it has another collision, and so forth. This chaotic sequence of accelerations and collisions at the molecular level translates into a constant ion velocity over macroscopic distances. The ratio of the ion velocity to the magnitude of the electric field is called the ion mobility, and separation of ions on the basis of mobility differences is called ion mobility spectrometry [2]. The ratio of the ion velocity is determined by the number of collisions it experiences within the drift tube with the neutral gas-drift molecules in an electric field. And this is directly proportional to the electric field, E (V cm^{-1}), as can be seen in equation (1):

$$v = KE \tag{1}$$

where K is the ion mobility coefficient. The K, which can be seen as drift velocity normalized to field, is characteristic of the ion, and it is the basis of identification of ions in IMS devices. The time the ions need to cover the drift distance from the shutter grid to the detector under the influence of an electric field is called drift time, which is characterized for the analyte ion. The number of the detected ions is a measure of the concentration of analytes. A plot of current versus drift time yields an ion mobility spectrum from which the mobility can be calculated as shown in equation (2):

$$K = \frac{l^2}{V\,t} \tag{2}$$

where K is the ion mobility constant, l is the length of the drift region in cm; V is the applied voltage across the drift tube in V and t is the drift time of the ion in s. From the drift time and the instrumental parameters the reduced ion mobility K_0 can be calculated, considering the influence of ambient pressure and temperature as it is showed in equation (3).

$$K_0 = \left(\frac{l}{tE}\right)\left(\frac{P\,T_0}{P_0 T}\right) \quad (3)$$

Where *l* is the length of the drift region, in cm; *E* is the electric field strength, in V cm^{-1}, *t* is the drift time, in s; *P* is the atmospheric pressure (P_0= 101325 Pa) and *T* is the temperature of the drift gas (T_0= 273 K) [2, 3]. In theory, K_0 values are constant for a given compound in a given buffer gas. They are a qualitative indicator of the ion's identity [4]. In practice K_0 values do not always match with those values reported in the literature by other authors. These variations are generally attributed to instrumental parameters such as inhomogeneities in temperature and electrical field, which are not often well characterized [5].

The mobility of an ion also depends on the collision cross section (Ω) and the number density (*N*, the number of molecules per unit volume), and according to the theory of Chapman-Enskog, Mason-Champ equation (4) can be obtained:

$$K = \frac{3}{16}\left(\frac{2\pi}{\mu\, k_B T}\right)^{1/2}\frac{ze}{N\Omega} \quad (4)$$

where μ is the reduced mass of the pair of the diffusing ions and carrier gas molecules with respective masses of *m* and *M* [$\mu = mM\,(m + M)$]; k_B is the Boltzmann constant (1.38065 x 10^{-23} J K^{-1}), *T* is the gas temperature (K), *z* is the number of elemental charges (dimensionless), and e is the elementary charge (1.602 x 10^{-19} C).

I.3. Parts in an ion mobility instrument

Each ion mobility instrument has three main parts namely ionization source, drift tube (where separation and selection occurs and detector). Besides, we consider in this section the sample introduction system (SIS) because it is an essential supplement to the IMS since if analytes are inefficiently extracted from samples or transferred, measurements can hardly be representative of the analytical problem at hand [6].

I.3.1. Sample introduction system

There is a wide variety of devices which are currently in use to introduce volatiles from gas, liquid or solid samples into the IMS instruments. Because IMS is a method that separates gas phase ions through collisions with a buffer gas, all analytes must be transported from the sample matrix and converted to a gas phase ion before ion mobility separation and detection can be performed [3]. Permeation tubes [7], purge vessels and dilution gas flask [8], headspace samplers [9], pyrolyzers [10], membrane inlets systems [11], thermal desorption (TD) units [12], solid-phase microextraction (SPME) units [13], stir-bar sorptive extractors (SBSE) [14], chromatographic columns [15] are the most common SISs coupled to IMS devices.

I.3.2. Ionization source

Of all the components of an IMS instrument, the ion source defines the response, utilization and possible applications of an IMS analyzer since the measurement of mobility may be regarded as a universal technique. Ionization in analytical IMS commonly occurs in air at ambient pressure. There are a wide variety of ionization sources such as radioactive source, being ^{63}Ni and ^{3}H the most used, UV-lamp, corona discharge (CD), electrospray (ESI) and laser sources.

I.3.2.1. Radioactive sources

Radioactive sources are favoured for use in IMS analyzers providing stable and reliable operation, with ionization chemistry that is well suited for most current applications of IMS. Furthermore, radioactive foils do not require an external power supply and have no moving parts or maintenance requirements [3]. Radioactive isotopes other than ^{63}Ni have been used with IMS drift tubes, including a beta-emitting tritium source. The use of beta radiation sources is discouraged today mainly because radioactive sources require special permits and licensing procedures. However, tritium poses less radiation hazard than ^{63}Ni sources and has been used as an ionization source in some study related to environmental monitoring. IMS instruments

with ^{3}H are described in *Block IV (chapter 4 and 5)*, *Block V (chapter 8)* and ^{63}Ni in *Block V (chapter 7)* of this Doctoral Thesis.

Collision between β particles (17 KeV) and molecules such as N_2, H_2O and O_2 yields positive and negative ions (5) which can be employed to ionize substances introduced into the reaction region of the drift tube:

$$N_2 + \beta \rightarrow N_2^+ + \beta' + e^- \quad (5)$$

Reactant ions are formed from the supporting atmosphere inside the IMS drift tube by high energy primary electrons emitted by β source. These energetic electrons collide with molecules of the supporting atmosphere, forming ions and producing secondary electrons. A sequence of ion-molecule reactions with nitrogen, oxygen and water vapor in purified air (6) result in the formation of a reservoir of ions of $H^+(H_2O)_n$ in positive polarity and $O_2^-(H_20)_n$ in negative polarity. In this case a sequence of reactions for the formation of reactant ions using a tritium source in positive mode is shown in equation (6):

$$^{3}H^+ \text{ (primary electrons)} + N_2 \rightarrow N_2^+ + e^- \text{primary} + e^- \text{secondary} \quad (6)$$

$$N_2^+ + 2N_2 \rightarrow N_4^+ + N_2$$

$$N_4^+ + H_2O \rightarrow 2N_2 + H_2O^+$$

$$H_2O^+ + H_2O \rightarrow H_3O^+ + OH$$

$$H_3O^+ + H_2O + N_2 \rightarrow H^+(H_2O)_2 + N_2$$

$$H^+(H_2O)_2 + H_2O + N_2 \rightarrow H^+(H_2O)_3 + N_2$$

The total charge of the reactant ions is governed by the size of the ionization source and establishes the upper limit of the number of molecules that can be ionized. The dominant process of product ion generation is through proton transfer, which occurs if the sample molecules (M) have a greater proton affinity than that of the reactant ions [16]. Sample molecules

(M) are ionized by collisions with reactant ions, forming products ions that are stabilized through the displacement of water molecules bound to the cluster ion, as shown in equation (7):

$$M + H^+(H_2O)_n \rightarrow MH^+(H_2O)_n \rightarrow MH^+(H_2O)_{n-x} + xH_2O \quad (7)$$

$$\text{Sample} + \text{Reactant ion} \rightarrow \text{Cluster ion} \rightarrow \text{Product ion} + \text{Water}$$

Theoretically, it can also occur in some cases that when the concentration of the sample increased, a second product ion is formed with a decline in intensity of the reactant-ion peaks and the peak of the protonated monomer called proton bond dimer as shown in equation (8):

$$MH^+(H_2O)_n + M \rightarrow M_2H^+(H_2O)_{n-x} + xH_2O \quad (8)$$

$$\text{Protonated monomer} + \text{Sample} \rightarrow \text{Proton} - \text{bound dimer} + \text{Water}$$

The formation of reactant ions in negative polarity occurs by means of resonant electron capture, and therefore, it occurs between low-energy electrons and neutrals such as oxygen. Ion-molecule reactions can take place between reactant ions and sample molecule (M), leading to the formation of product ion as was also described for positive polarity, shown in equation (9):

$$M + O_2^-(H_20)_n \rightarrow MO_2^-(H_20)_{n-x} + xH_20 \quad (9)$$

$$\text{Sample} + \text{Negative reactant ion} \rightarrow \text{Product ion} + \text{Water}$$

3.2.2. Photodischarge lamps

Photodischarge lamps emit photons from the electrical excitation of gases filled in the lamp [17]. The formation of positive ions with photons has been described as direct ionization through the reaction given in equation (10):

$$h\nu + M \rightarrow M^+ + e^- \quad (10)$$

where hν is the photon energy and M is the neutral molecule. The energy needed for this, the ionization potential, with organic compounds is generally between 7 and 10 eV, and M^+ ions are routinely observed with aromatic hydrocarbons [18]. The main advantage of photodischarge sources is that some selectivity in response may be ensured by the choice of an appropriate ionization energy or wavelength. The disadvantages are the requirement for an external power supply and the need to replace them periodically due to the finite lifetimes of such lamps. IMS with UV lamp was used in the experimental works shown in *Block III, chapter 1, 2 and 3*.

I.3.3. Drift tube

Before the entrance to the drift tube there is an ion gate that blocks ions flowing into the drift region, admitting them in a brief pulse (normally fixed between 10 μs and 1 ms) which is initiated by a user or which automatically sampling the reaction region at different frequencies (scales of Hz), this parameter is called as grid pulse width [19]. The heart of the instrument is the drift tube, which provides a region of constant electric field (V cm^{-1}) where the ions are created and allowed to migrate. Ions under the influence of this electric field move toward the detector. The high voltage supply needs to deliver voltages of 100-10000 V to establish a strong electric field in the drift tube, a conventional design for drift tubes (with 5-12 cm average length) is based upon stacks of ring-shaped electrodes held at fixed intervals with insulating spacers. A uniform electric field is created within the tube by applying potentials to each electrode in constant voltage drops.

I.3.4. Detector

At the end of the drift region, ions collide with a detector. Most commercial IMS use ions counter devices such as a faraday plate detector, ions are detected as they strike a metal plate and induce a current. Faraday plate detection is simple, inexpensive, and can be used for both positive and negative ions. Finally, the signals are amplified and sent to an automated recorded where the data is stored. The ion mobility spectrum is usually a

plot of ion intensity current a function of elapsed drift time that ions takes to reach the detector after the ion gate has been opened [20]. IMS spectra not only give qualitative information (the peak position is related with the compound shape and size because the drift time is related with the mobility of ions), but they also give quantitative information (the peak intensity or area is related to the compound concentration).

I.4. Types of ion mobility spectrometers

In addition of the traditional IMS, different types of IMS devices are currently available [21]. Travelling wave-IMS (TWIMS) consists of a stacked-ring ion guide to which a travelling voltage wave is applied; high field asymmetric waveform ion mobility spectrometer (FAIMS) in which a strong time-dependent electric field as periodic asymmetric waveform is implemented; differential mobility spectrometry (DMS) which is the planar version of FAIMS that consist of two flat parallel electrodes separated by an analytical gap through which ions are transported by a gas flow perpendicular to the electric field; trapped IMS (TIMS) based on the use of a non-uniform electric field to hold ions stationary against a moving gas, so that the force is compensated by the electric field and ion packages are separated based on their size-to-charge ratio; aspiration IMS (AIMS) or also called open loop IMS (OLIMS) and differential mobility analyzer (DMA) where ions with different electrical mobilities are separated in the space as with FAIMS; transversal modulation IMS (TMIMS) which separates ions according to their mobility using only electric fields; overtone mobility spectrometry (OMS) based on the transport of ions through multiple identical drift regions, each with an elimination and transmission region. A summary of the main used IMS instrument used is given in this section. The main characteristics of each of them are represented in **Table 2**.

I.4.1. Linear ion mobility spectrometer

The linear IMS or also called drift time ion mobility spectrometer (DTIMS) is the classical equipment in which ions move through a

homogeneous and continuous electric field in the drift tube in the presence of neutral gas molecules [22]. A schema of working principle of the instrument is plotted in **Figure 2**.

Table 2. Summary of main characteristics of IMS instruments.

Parameter	**Linear IMS**	**FAIMS**	**DMS**	**DMA**
Electric field *E*	Uniform low *E* (<1000 V cm^{-1})	Alternating asymmetric high/ low *E* (>10000 V cm^{-1})		Uniform high *E*
Configuration	Stacked ring electrodes along a linear drift tube	Cylindrical	Planar	Cylindrical and planar
Transport gas	Yes	Yes	Yes	Yes (high fluid field is required)
Common ionization source	UV, ^{3}H, ^{63}Ni, CD	ESI	ESI, ^{3}H, ^{63}Ni, CD	UV, CD, ESI
Ion shutter	Yes	No	No	No
Polarity	Single	Both	Both	Single
Hyphenated techniques	MCC-IMS, GC-IMS, IMS-MS, GC-IMS-MS, LC-IMS-MS	GC-FAIMS, FAIMS-MS, ESI-FAIMS, Py-FAIMS	DMS-MS, GC-DMS, TD-GC-DMS	DMA-MS, DMA-IMS-CPC
Advantages	-High resolving power -Directly measurement of collision cross sections	-Higher resolution -Better suited for coupling with MS -Positive and negative ions can be separated simultaneously - Reduced size compared with DTIMS (millimetre range)		-Capable of measured nanometre sized particles -Continuous classification of ions

UV: ultraviolet lamp, ^{3}H: tritium source, ^{63}Ni: nickel source, CD: corona discharge, ESI: electrospray ionization, MCC: multicapillary column, GC: gas chromatography, IMS: ion mobility spectrometer, MS: mass spectrometer, LC: liquid chromatography, FAIMS: field asymmetric ion mobility spectrometer, Py: pyrolysis, DMS: differential mobility spectrometer, TD: thermal desorber, CPC: condensation particle counter.

The carrier gas and the gaseous sample are introduced into the ionization region, forming the sample gas; while a flow of a pure gas (most usually nitrogen or even synthetic gas) called drift gas is introduced in the opposite direction of the entrance of volatile molecules. In linear IMS instruments, the mobility *K* can be reduced showing that while in low electric fields (<1000 V cm^{-1}) it does not depend on *E*, it depends on the number density (*N*). For ions in a fixed *E*, having a constant velocity *v*, the

displacement *L* is proportional to time $L = K E t$, so the drift time that an ion needs to pass through the drift region is proportional to the inverse of the mobility [3]. In this Doctoral Thesis three linear IMS were used; two of them with tritium source with 5 and 10 cm of drift tube length, respectively; and another IMS with an UV lamp and a 12 cm drift tube.

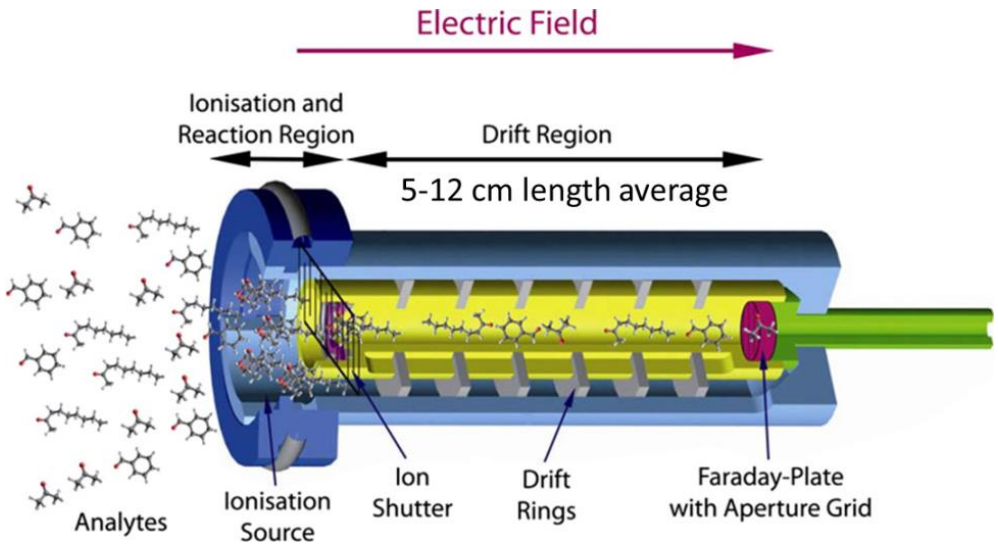

Fig. 2. Schema of a conventional linear IMS. Adapted from ref. 21 with permission from IOP publishing.

I.4.2. High field asymmetric waveform ion mobility spectrometer

FAIMS works as an ion-mobility filter and can be set to continuously transmit one type of ion with a variant electric field (> 10000 V cm^{-1}). Two main electrode configurations have been developed with FAIMS, planar (p-FAIMS) and cylindrical (c-FAIMS). The planar version is also known as Differential Mobility Spectrometry (DMS) and consists of two flat parallel electrodes separated by an analytical gap through which ions are transported by a gas flow perpendicular to the electric field [23]. In **Figure 3** is shown a schema of the DMS working principle. This IMS instrument was used in the experimental work which is explained in *Block V chapter 7*.

FAIMS and also DMS are spatial electrical mobility spectrometer rather than a time-based separation device such as DTIMS.

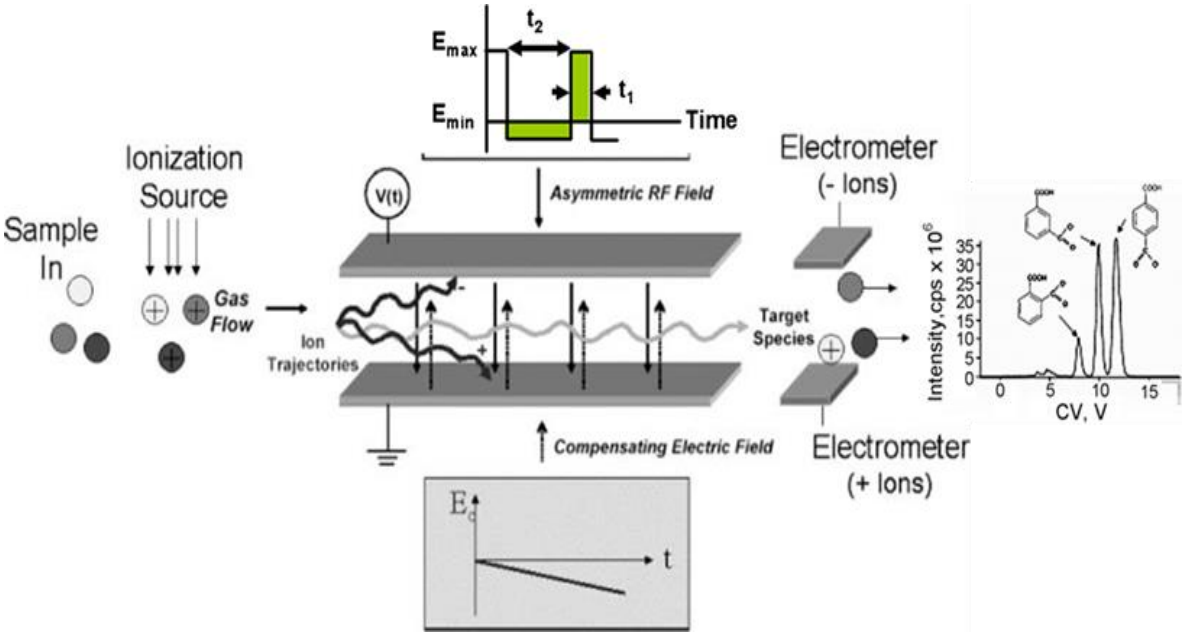

Fig. 3. Differential mobility spectrometer configuration overview. Adapted from ref. 22 with permission from American Chemical Society.

In FAIMS and DMS chromatograms, intensity instead of time is plotted against the sweeping compensation voltage (CV) or compensation field or having dispersion plot in which both compensation (low DC voltage) and dispersion voltage (high frequency asymmetric voltage) are swept. The mobility coefficient is not measured and instead the differences in mobility at extremes of field are determined. The main advantage of FAIMS and DMS is that with this technology positive and negative ions can be detected simultaneously. As well with the elimination of ion shutter and low-duty cycle from gating ions as with the time of flight method, allowing simplification of the drift tube manufacture.

I.4.3. Differential mobility analyzer

A Differential Mobility Analyser (DMA) is a particular configuration of an IMS instrument. In DMA ions with different electrical mobilities migrate between the two electrodes held at different potentials while being transported by a stream of gas (initially clean) following parallel to the electrodes. A diagram of the DMA is plotted in **Figure 4**.

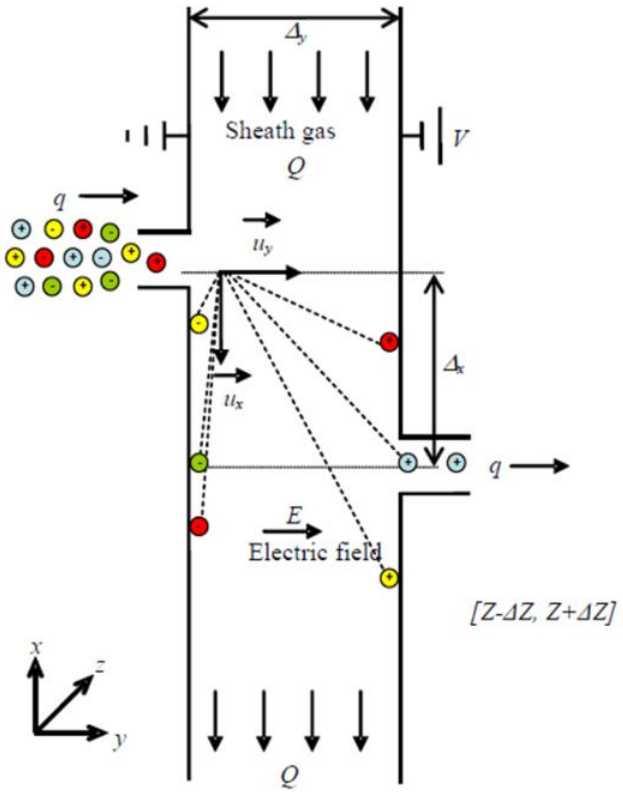

Fig. 4. Schema of a differential mobility analyzer instrument. Reproduced from ref. 24 with permission from Royal Society of Chemistry.

The classification of DMA is done using high carrier flow rates which lead to the use of space instead of time (drift time) [24]. This fact can offer the advantage of achieving higher resolving powers and sensitivities. Two possible configurations of DMA are found. The more used DMAs have cylindrical configuration that consist of two cylindrical and concentric metal

electrodes, widely used for aerosols measurements. In a planar ion-DMA, a carrier gas which transports the ionized species enters to the DMA through a slit and joins particle-free carrier gas or also called sheath gas which flows between the two parallel electrodes. An electric field is superimposed in the perpendicular direction so that ions are driven by the combination of the electrical force and high gas flow. Only the ions of a given electrical mobility leave the DMA through a slit which is made in the outer electrode and collected by an ion plate connected to an electrometer [25].

For mobility analysis, the analyte ions are introduced at ambient gas pressure into a voltage gradient or electric field (*E*). Thus, ions attain a velocity (*v*) that is proportional to the electric field strength equation (11)

$$v = ZE \tag{11}$$

where *Z* is the "mobility coefficient" of the ion. The electrical mobility allows the characterization of the molecular size. For the case of particles much larger than atomic dimensions although much smaller than the gas mean free path, *Z* is an inverse measure of the cross-section area of the particle, whenever these molecules are considered as spherical particles. An equation based on an approximation of the Millikan law to identify different molecules as a function of their size using DMA was proposed by Tammet [26] equation (12):

$$Z = 0.441 \frac{ze(Kt/m)^{1/2}}{P(d_\rho + d_0)^2} \tag{12}$$

where *P* is the pressure, *T* the absolute temperature and m is the molecular mass of the background gas (purified air), *k* is the Boltzmann's constant, *z* is the ion charge, and *dρ* and d_0 are the molecule diameter and the gas molecule diameter of the surrounding particles (d_0= 0.3 nm) [27]. Based on this approach and on the reactivity of the species, which is related to the ionization source, analyte molecules can be identified form the mobility spectrum.

I.4.4. IMS coupled with others instruments

Unfortunately, IMS has in some cases low resolution power, lack of positive identification as well such detection does not afford additional qualitative information associated with the separation of ions. To overcome this problem, modifications of the instrument and combination with other equipment are possible as it is illustrated in the **Figure 5**.

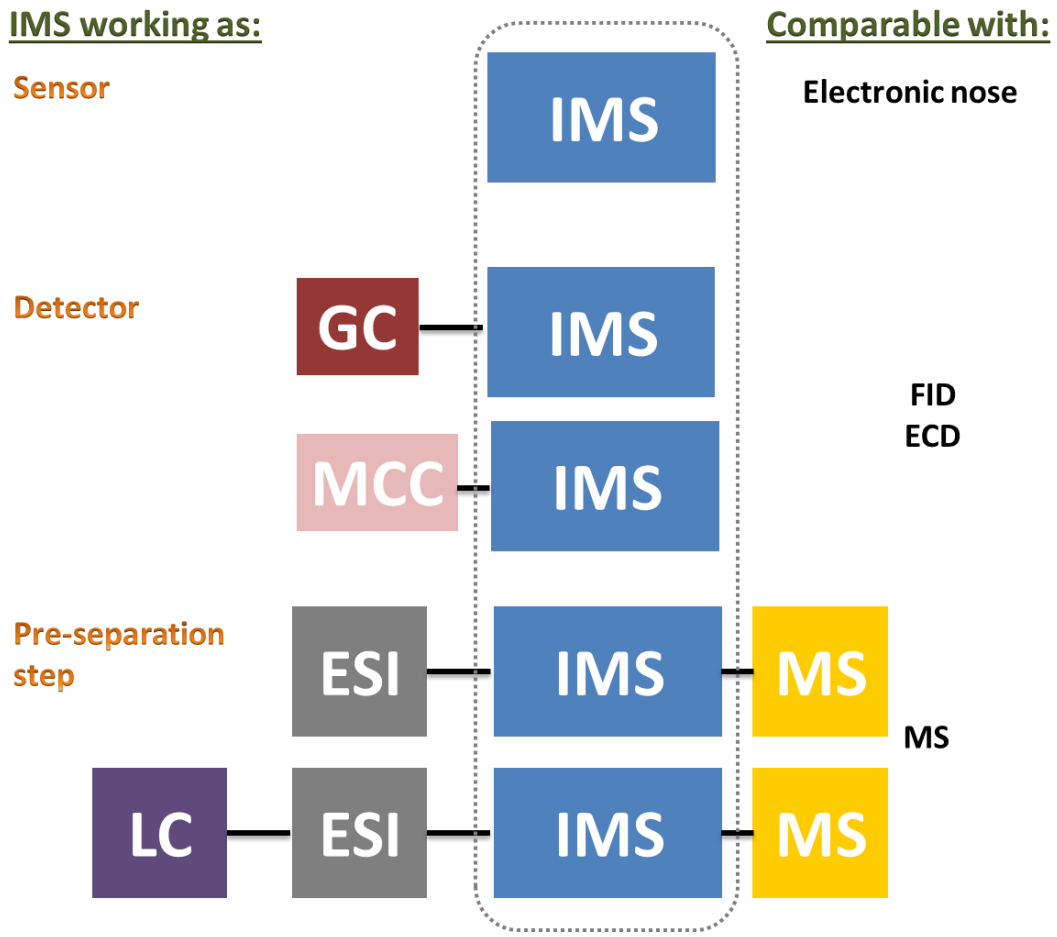

Fig 5. Examples of possible working operation modes of the IMS technology.

GC: gas chromatography, MCC: multicapillary column, LC: liquid chromatography, ESI: electrospray source, MS: mass spectrometry, FID: flame ionization detector, ECD: electron capture detector.

The classical view of IMS is working as a sensor for screening purposes. Moreover, IMS can work as a detector when coupled to a GC or

MCC column used for pre-separation in complex samples. Also, IMS can be used coupled to a mass spectrometer in order to enhance separation achieved with MS. Possible combinations with IMS instruments are described in sections 5, 6, 7, and 8.

I.5. Improvement of sensitivity

There are some applications in the clinical and environmental field which required detecting low concentration values in order to meet the legislative requirement or detect a disease at its early stage. Sensitivity can be improved in IMS mainly by changing the ionization source, by using a preconcentration step before the IMS analysis, or by coupling a semipermeable membrane to reduce the interference of non-target substances.

I.5.1. Ionization source

Directly sensitivity can be improved by selecting a proper ionization source according to the type of sample and the chemical characteristics of the analyte. CD and ^{63}Ni ionization sources permit more sensitive detection for halogenated compounds. The principal advantage of CD over ^{63}Ni as ionization source is the increased total ion current it provides (approx. an order the magnitude greater), which leads to improve sensitivity, signal-to-nose ratio and dynamic range [28]. Photo ionization is indicated for aromatics compounds [3]. Other sources such as ESI or laser based ionization sources are more appropriated for the determination of analytes in liquid or solid samples.

I.5.2. Preconcentration methods

The use of extraction techniques before IMS detection not only removes interfering substances but also reduces the final volume of sample, leading to an improvement of the sensitivity achieved. Solid phase extraction (SPE) [29] and molecularly imprinted polymer-solid phase extraction (MIPS-SPE) [30-34] were used in the clinical field to retain target analytes in complex clinical samples, improving detection limits as result.

SPME is a simple, fast, solvent-free extraction technique integrating sampling, extraction, concentration and sample introduction in a single step. LOD of herbicides and others contaminants when using SPME were in the range of few ppb [35-37]. Headspace SPME provides several advantages over direct immersion; including protection of the fiber and reducing interferents low detection limits were obtained with HS-SPME in clinical analysis [37-40]. Combination of ionic liquid-headspace-single drop microextraction (IL-HS-SDME) with IMS exhibits excellent sensivity with LODs in the range of 0.1-1.5 μg L^{-1} [41]. When using inlet membranes (MI) or membrane extraction unit (MEU), sensitivity was also enhanced due to the preconcentration achieved.

I.6. Improvement of selectivity

I.6.1. Dopants and extraction techniques

The introduction of analytes of complex samples (clinical and environmental) and the determination of several target compounds in a mixture leads to complicated IMS spectra. This difficulty may arise from multiple and competitive ionization interactions as a consequence of the limited reactant ions in chemical-based sources or limited energy available in the ionization source. An initial solution is to change the chemistry of the IMS by introducing dopants (acetone, methanol, dichloromethane, and ammonia). Other solution is to use selective extraction. In that way the use of extraction techniques (membrane inlet (MI), SPME, SPE, SDME) before IMS detection provides selectivity to the measurement minimizing the background interferences and competition between others analytes present in the sample.

I.6.2. Pre-separation with MCC and GC columns

The low selectivity of IMS can also be alleviated by the coupling of MCC or GC to the IMS instruments by the axial introduction of the GC effluent to the IMS drift tube [3, 42]. Thus, the GC brings an advantage to IMS by eliminating cross-sensitivity/ charge competition effects. In addition, because gas chromatography separates in the minute to second time scale,

multiple IMS spectra can be obtained for each gas chromatographic peak [43]. IMS coupled with high resolution capillary gas chromatography is a versatile detector which can function as an FID or ECD [44]. GC-IMS system combines data into a 2D-matrix. The result of this data format is the ability to derive a contour plot revealing both retention time and drift time information. While coupling DMS to GC results in multidimensional separations that rely both on chromatographic retention times and also on differential mobility *K* (inversely proportional to the compensation voltage CV) and the dispersion voltage (DV) providing a highly sensitive and selective analytical tool [23, 45-47].

Gas chromatography coupled with ion mobility spectrometers has been demonstrated to be a powerful method for the determination of compounds in complex samples in clinical analysis [48]. Currently, MCC coupled to IMS techniques are being used to enhance chromatographic separation. MCC columns contained approximately a 1000 parallel capillary tube coated with a stationary phase which permits a considerable efficiency in separation at high flow rates and optimal sample capacity for IMS. Its compact size and the possibility to work at ambient temperature and isothermal separation make it attractive for portable IMS analyzer [49]. Tenax® column coupled to IMS [50], MCC-IMS [51-53] and GC-IMS [41, 54] have been used in environmental trace analysis for determination of pollutants. In the clinical field diagnosis of pathological conditions trough breath analysis by MCC-IMS is rapidly growing [22, 55-64]. In principle, volatile chemicals inhaled by a subject could be observed in respired air or from the skin emissions and could provide a non-invasive assessment of the extent of exposure [3]. Technical advances during the past decade have extended the scope of ion mobility techniques to the biological and biomedical research and a growing presence or capability for IMS in environmental analysis and medical diagnostics has been demonstrated.

I.7. Using IMS as a pre-filter for mass spectrometry system

The coupling of IMS with MS is sometimes referred to as ion mobility–mass spectrometry (IMMS) because the two methods complement and instrumentally match one another so well that they seem to fuse into one analytical measurement [65]. IMS separates ions based on size-to-charge ratios and MS detects ions based on mass-to-charge (m/z) ratios. In IMMS coupling ions are separated based on the size-to-charge ratio in the IMS component and the mass-to-charge ratio in the MS component. A two dimensional separation is obtained based on size and mass [66]. IMMS is a powerful analytical technique that combines the benefits traditionally associated with MS, such as high sensitivity and mass accuracy identifying compounds, with the ability to distinguish ions with identical masses such as regio- and stereo-isomers provided by IMS [67]. Because IMS separates ions on the millisecond time scale which is significantly slower than the average time it takes to acquire a mass spectrum (on the microsecond time scale), this makes the coupling of the two methods easy because for every ion mobility separated peak, several mass spectra can be measured. The difficulty with adding a mass spectrometer to an ion mobility spectrometer is the high cost and the instrument complexity. MS requires a vacuum, which is difficult to maintain on a routine basis in day-to-day field operation [68].

The first ion mobility mass spectrometer coupled with ion mobility spectrometer was built in the 1960s. Since then, different ion mobility instruments have been coupled with many different kinds of mass analyzers. The four types of ion mobility spectrometers more used with mass spectrometers are: linear IMS, TWIMS, FAIMS and DMA. DTIMS, FAIMS and DMA are operated under ambient pressure conditions while TWIMS is operated at reduced pressure. Each of these ion mobility spectrometers can be interfaced to a variety of mass spectrometers such as time-of-flight, quadrupole, ion-trap, ion-cyclotron, or magnetic-sector mass spectrometers [66].

IMS coupled to MS is extensively used in research laboratories to investigate ion–molecule reactions, ion structures, and conformation of biomolecules such as peptides and proteins and separation of isomers [16]. In the clinical field, some works in which ESI-IMS coupled to MS to study conformation of n-linked glycans and metabolites in serum, blood and lymph extracts [69-71] and DMS coupled to MS to determine cancer associated antigen CG1 in serum [72] were found. This combination is advantageous, because IMS offers the possibility for isomer separation, and MS provides valuable information about the mass identification of ions.

I.8. Multiple hyphenated IMS

Tandem IMS has been studied including combinations with FAIMS or DMS devices: IMS-IMS, DMS-IMS, IMS-DMS and DMS-DMS [3, 73-75]. Ions derived from a sample in the reaction region were injected through the first ion shutter into a drift region, and ion swarms were separated by drift time. At the end of this first drift region, another ion shutter synchronized to the first shutter was used to isolate a certain ion swarm and selectively introduce this swarm into a second drift region. Ions in this next drift region were photo fragmented, and these ions were then characterized using a third drift region, preceded with another ion shutter [74].

Since mobility spectrometers are comparatively inexpensive, simple, and with low resolving power compared to MSs, tandem mobility can be achieved for comparatively little additional complexity and cost, particularly in comparison to MSs [3]. With these techniques, the intrinsic correlation of ion size and mass can be altered by changing the ions' shapes. This can improve the detection of low-intensity signals and increase the analytical peak capacity (important for many-component mixtures) [73]. Merenbloom et al. demonstrated a peak capacity for an IMS-IMS separation of peptides (prior to MS) in excess of 1000 [75]. Benefits of a tandem DMS/IMS were observed with a constant resolution over ion mass [74]. New configurations

and applications based in this technology are increasing in the fields of metabolomics, proteomics and medical analysis.

I.9. Applications of ion mobility spectrometry

IMS technology has been successfully applied to a wide variety of analytical purposes [76] including the detection of explosives, chemical warfare agents (CWA), drugs and quality control in industrial process among others. In **Figure 6** is plotted the contribution (number of papers) of IMS in different areas of study.

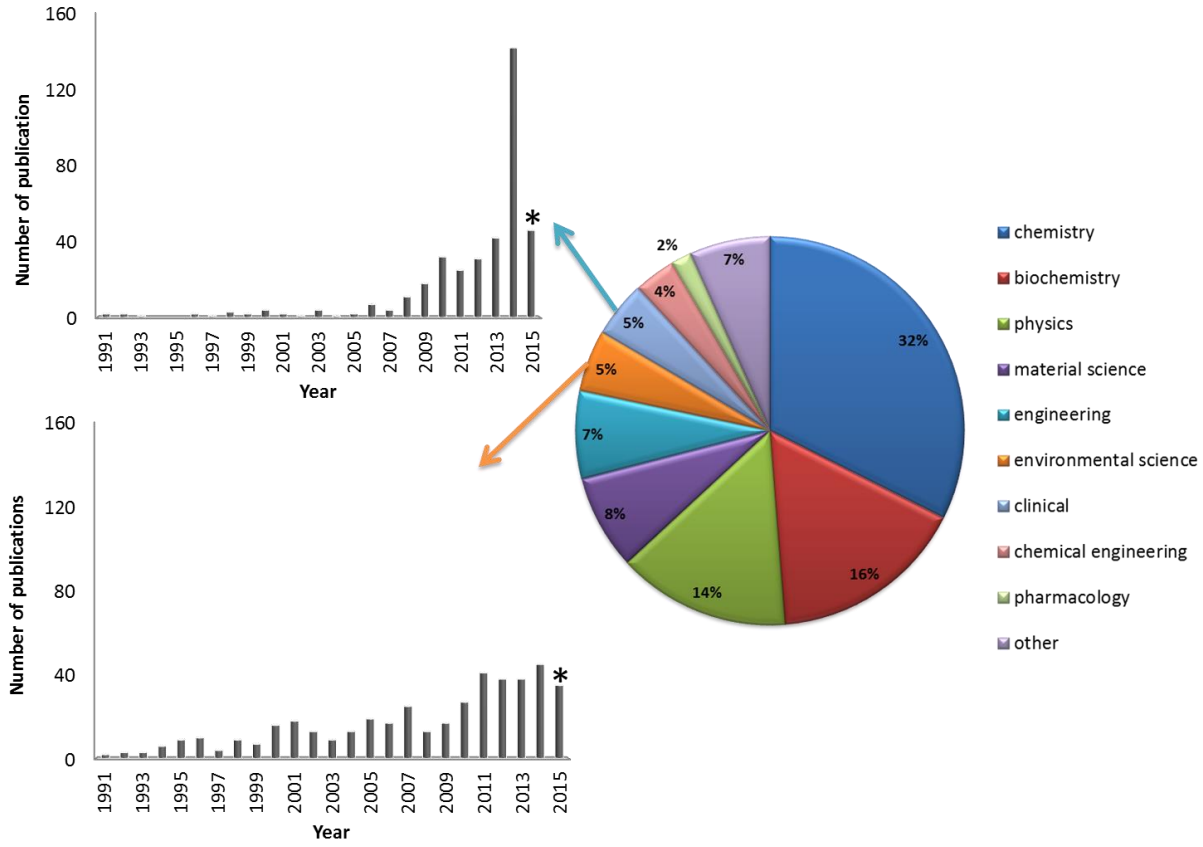

Fig. 6. Contribution of ion mobility spectrometry in the clinical and environmental fields in the years 1991-2015*.
*Data extracted from Scopus database, last accessed 27/09/15.

The percentages were calculated over 5007 publications found in Scopus database. Published papers related to clinical and environmental analysis are represented along years (1991-2015). Only 10% of the total of articles published was found corresponded to less exploited fields such as environmental [77], and clinical and biomedical analysis. However, they are having a recent growing.

I.9.1. Clinical analysis

The fast, accurate and precise responses with the low detections limits provided by IMS makes this technology suitable for clinical analysis. It has been applied for the detection of drugs and toxics compounds and for medical diagnoses based on the determination of biomarkers. Recent applications found for clinical analysis are summarized in **Table 3A** and **3B**; updated and adapted from [76].

Non-invasive analysis is increasing due to the accessibility of the sample, specialty indicated for emergency applications. Drugs presents in several samples as shown in **Table 3A** such as hair [78, 79], sweat [80], skin [81], breath [82-85] and saliva samples [86-89] were analyzed by IMS with nickel source, being the configuration most used. ESI was also used in one work [88] in which thiocyanate was detected at 3 μg L^{-1}. There are a wide variety of sample introduction systems used such as headspace, membrane inlet, thermal desorption and flow injection configuration. As well MCC was coupled to the IMS to determine drugs in breath samples, because in such complex matrix it is necessary to enhance separation [82-84]. Invasive analyses were performed with samples of urine [29, 32, 33, 90-93], plasma [31, 40, 92, 93], serum [30, 34, 38, 39], and blood [32, 37] which were extracted from the patients. In these works SPE or SPME were applied prior to the introduction of the volatile molecules to the IMS to overcome the interferences of biological matrices with IMS analyses and improve detection limits as a result. In this Doctoral Thesis, analytes potentially present in saliva samples were studied, results are shown in *Block V, chapter I, II.*

IMS has also been successfully used in the clinical field to determine biomarkers or diseases by its fingerprints, as it is shown in **Table 3B**.

Table 3A. Determination of drugs in the clinical field by IMS.

Matrix	Compound	SIS	Pre-separation	IMS	LOD	Ref.
Hair	MDMA and MDEA	TD	None	^{63}Ni-IMS	-	[78]
	Methadone	HS	None	^{63}Ni-IMS	0.01 ng g^{-1}	[79]
Sweat	Flunitrazepam, ketamine, and MDMA	TD	None	^{63}Ni-IMS	0.27-2.4 ng	[80]
Skin	Ibuprofen	DC- TD	None	^{63}Ni-IMS	73 ng mL^{-1}	[81]
Exhaled breath	Propofol	None	MCC	^{63}Ni-IMS	-	[82]
		MI	MCC	^{63}Ni-IMS	65 ng mL^{-1}	[83]
		MI	MCC	^{63}Ni-IMS	0.5 µg mL^{-1}	[84]
Breath/ serum	γ-hydroxybutyrate and γ-butyrolactone	TD	None	^{63}Ni-IMS	low ppm range	[85]
Saliva	Cocaine	TD	None	^{63}Ni-IMS	100 µg mL^{-1}	[86]
	MDMA	TD	None	^{63}Ni-IMS	160 µg L^{-1}	[87]
	Thiocyanate	Flow injection	None	ESI-IMS	3 µg L^{-1}	[88]
	Tetrahydrocannabinol	Thermal desorption	None	^{63}Ni-IMS	11 ng	[89]
Urine	Cocaine and metabolites	SPE	None	^{63}Ni-IMS	4-10 µg L^{-1}	[29]
	Ephedrine	SPME	None	^{63}Ni-IMS	50 µg L^{-1}	[90]
	Verapamil	SPME	None	SELDI-IMS	2 µg L^{-1}	[91]
	Testosterone	MIP-SPE	None	CD-IMS	0.9 µg L^{-1}	[33]
Urine/ plasma	Trimipramine and desipramine	HF-LPME	None	ESI-IMS	1 µg L^{-1}	[92]
	Venlafaxine	SPME	None	ESI-IMS	0.2-11µg L^{-1}	[93]
Plasma	Caffeine and theophylline	MIP-SPE	None	ESI-IMS	0.2-0.3 µg L^{-1}	[31]
	Captopril	HS-SPME	None	CD-IMS	6.3 µg L^{-1}	[40]
Serum	Primidone	MIP-SPE	None	ESI-IMS	5.1 µg L^{-1}	[34]
	Metronidazole	MIP-SPE	None	CD-IMS	10 µg L^{-1}	[30]
	Urea	HS-SPME	None	CD-IMS	2 µg mL^{-1}	[39]
	Methamphetamines	HS-SPME	None	CD-IMS	0.04-8 µg L^{-1}	[38]
Blood	Se (IV)	HS-SPME	None	CD-IMS	2 µg L^{-1}	[37]
Urine/ Blood	Salicylic acid	MIP-SPE	None	ESI-IMS	-	[32]

MDMA: 3,4-methylenedioxy-methamphetamine; MDEA: 3,4-methylendioxyethamphetamine; TD: thermal desorption; HS: headspace; MI: membrane inlet; DC- TD: diffusion cell-thermal desorption; ESI: electrospray; SPE: solid phase extraction; SPME: solid phase microextraction; MIP-SPE: molecularly imprinted polymer solid phase extraction; HS-SPME: head space solid phase microextraction; HF-LPME: hollow fiber liquid phase microextraction; MCC: multi-capillary column; ^{63}Ni: nickel source; CD: corona discharge; SELDI: Surface enhanced laser desorption ionization; IMS: ion mobility spectrometer.

Table 3B. Determination of biomarkers and toxics in the clinical field by IMS.

Matrix	Biomarker/ disease	SIS	Pre-separation	IMS	LOD	Ref.
Skin	Octanal, nonanal and decanal	SPME	MCC	^{63}Ni-IMS	0.1-0.3 μg L^{-1}	[94]
Breath	COPD	Exhalation	MCC	^{63}Ni-IMS	-	[57]
	Parkinson, Alzheimer	Exhalation	MCC	^{63}Ni-IMS	-	[55]
	Sarcoidosis	Exhalation	MCC	^{63}Ni-IMS	ppb level	[22, 63]
	Lung diseases	Exhalation	MCC	^{63}Ni-IMS	ppb level	[60, 64]
	Diseases	Exhalation	MCC	^{63}Ni-IMS	ppb level	[56, 62]
	Cancer	Exhalation	MCC	^{63}Ni-IMS	0.1-2.1μg L^{-1}	[61]
		Exhalation	MCC	^{63}Ni-IMS	-	[58, 59]
	Diseases	TD	None	ESI-IMS-MS	ng level	[96]
Stool	CDI	HS	None	FAIMS	-	[99]
Breath/ stool	Bacterial infection	Aspiration pump	None	DMS	-	[97]
Secretions	Vaginal infection	HS	None	^{63}Ni-IMS	-	[98]
Urine	UTI	HS	None	^{241}Am- IMS	-	[100]
	Coeliac disease	HS	None	FAIMS	-	[101]
	CRC	HS	None	FAIMS	-	[102]
	Acetone	HS	None	UV-IMS	4 mg L^{-1}	[103]
Serum	N-linked glycans	Flow injection	None	ESI-IMS-MS/ESI-IMS-MS-MS-MS	-	[70]
	Cancer Associated Antigen, CG1	ESI	None	DMS-MS		[72]
Blood	Metabolites	Flow injection	None	ESI-IMS-MS	-	[69]
Lymph extracts	Metabolites	Flow injection	None	ESI-IMS-MS	-	[71]

COPD: chronic obstructive pulmonary disease; CDI: Clostridium difficile infection ; UTI: urinary tract infection; CRC: colorectal cancer; SPME: solid phase microextraction; TD: thermal desorption; HS: headspace; ESI; electrospray; SPE: solid phase extraction; HS: headspace; HS-SPME: head space-solid phase microextraction; MCC: multi-capillary column; ^{63}Ni: nickel source; ESI: electrospray; ^{241}Am: americium source; UV: ultraviolet source; IMS: ion mobility spectrometer; FAIMS: field asymmetric ion mobility spectrometer; MS: mass spectrometer; DMS: differential mobility spectrometer.

Non-invasive samples such as skin [94], breath [22, 55-60, 62-64, 95-97], and secretions [98] were used to identify biomarkers of diseases. Stool [97, 99], urine [100-103], serum [70, 72], blood [69] and lymph extracts [71] were also used. Disease specific peaks can be identified by comparing topographic plot obtained from patients with a particular disease and others in a control group [62]. Information obtained as a complex

dataset usually require using an appropriate chemometrics tool for evaluation, classification and analyte quantification.

I.9.2. Environmental analysis

IMS is highly suitable for environmental applications due to its advantages such as on-site and real-time analysis. This technique provides a good balance between usable information and ruggedness, reliability and portability. Besides it combines low cost technology with high speed data acquisition. IMS has been successfully used for environmental analysis mainly in the determination of contaminants present in gas phase [50, 52, 54, 104-107], water and discharge effluents [28, 35-37, 41, 53, 108-116] and volatile and semivolatile compounds present in solid samples (soil, sediments and aerosols) [36, 117-121] as summarized in **Table 4**, updated and adapted from [76, 77]. IMS is ideal for the determination of VOCs in air samples by virtue of the ease with which samples can be introduced in the instrument. Much work has focused on the analysis of ambient air for determination of explosives and monitoring of toxic substances such as BTEX [8,107], which have been studied in *Block III, chapter I, II and III*, n-alkanethiols [54] and hydrazines [106]. Aspirations pumps and membrane inlets were the SISs more used when introducing the analytes to the IMS instrument. IMS with UV lamp was used for determining VOCs [52] and terpenes in air samples [51]. However, ^{63}Ni-IMS is the instrument which is widely used also for environmental analysis. Most environmental samples are aqueous. This matrix can be complex enough to require clean-up and preconcentration prior to IMS analysis. MTBE was determined in water samples by using a membrane inlet [108] and HS-SPME [35]. Pesticides residue analyses, present in water samples, have also been accomplished by IMS without any prior separation [111, 112, 114] and with SPME [28, 36] detecting lower concentration levels.

Table 4. Compounds analysed by IMS in environmental samples.

Matrix	Analyte	SIS	Pre-separation	IMS	LOD	Ref.
Air	VOCs	None	None	^{63}Ni-IMS	-	[105]
		Aspiration pump	MCC	UV-IMS	5-1200 μg L^{-1}	[52]
	BTEX	None	None	^{63}Ni-IMS	40-65 μg L^{-1}	[107]
	Perfluorocarbons	MI	None	^{63}Ni-IMS	340-780 ng L^{-1}	[104]
	Dimethylsulfate	None	Tenax®	^{63}Ni-IMS	3 μg L^{-1}	[50]
	Hydrazine, monomethylhydrazine, ammonia	MI	None	^{63}Ni-IMS	6 μg L^{-1}	[106]
	Terpenes	None	MCC	UV-IMS	5-20 mg L^{-1}	[51]
	n-Alkanethiols	None	GC	^{63}Ni-DMS	-	[54]
Water and liquid samples	MTBE	MEU	None	^{63}Ni-IMS	0.1-4 mg L^{-1}	[108]
		HS-SPME	None	CD-IMS	0.7-4.9 μg L^{-1}	[35]
	Tetrachloroethylene and trichloroethylene	MI	None	^{63}Ni-IMS	78-80 μg L^{-1}	[109]
	Trihalomethanes	IL-HS-SDME	RTGC	^{3}H-IMS	100-910 ng L^{-1}	[41]
	Chloroethenes, chlorobenzenes and aromatics	HS-SPME	MCC	UV-IMS	ppb range	[53]
	Chlorophenols	None	LC large bore	ESI-IMS	0.1-2.2 mg L^{-1}	[115]
	Malathion, ethion and dichlorovos	None	None	^{63}Ni-IMS	0.21-0.94 ng	[112]
	Sevin, almitraz, and metalaxyl	None	None	^{63}Ni-IMS	0.45-0.58 ng	[111]
	Ethyl parathion, toluene, 2-4-diisocyanate	Vapor generation	None	^{241}Am-IMS	4.9-30 μg L^{-1}	[114]
	Atrazine, ametryn	HS-SPME	None	CD-IMS	37-23 ng g^{-1}	[36]
	Nitrite and nitrate	None	None	ESI-IMS	10-40 mg L^{-1}	[110]
	Ammoniacal nitrogen	Purge system	None	CD-IMS	9.2 μg L^{-1}	[113]
	Se	HS-SPME	None	CD-IMS	12 μg L^{-1}	[37]
Solids, aerosols, sediments	Diisopropyl-, diethyl, dimethyl-methylphosphonate	SPME	None	^{63}Ni-IMS	6.3-7.6 mg Kg^{-1}	[117]
	CWA	TD	None	^{63}Ni-IMS	<15 pg	[118]
	Atrazine, ametryn	HS-SPME	None	CD-IMS	23-37 ng g^{-1}	[36]
	Chlorocarbons	Exponential dilution	None	^{63}Ni-IMS	6-8 ng L^{-1}	[122]
	VOCs	Exponential dilution	None	^{63}Ni-IMS	-	[120]
	Malathion	UV photolytic vapor generation	None	^{63}Ni-IMS	<0.01 mg m^{-3}	[119]
	Atrazine, ametryn	HS-SPME	None	CD-IMS	37-23 ng g^{-1}	[36]
	α-Pinene	None	None	^{63}Ni-IMS	ppb range	[121]

VOCs: volatile organic compounds, BTEX: benzene, toluene, ethylbenzene, m-xylene, o-xylene, p-xylene, MTBE: methyl tert-butyl ether, CWA: chemical warfare agents, MI: membrane inlet, Se: selenium, MEU: membrane extraction unit, HS-SPME: headspace-solid phase microextraction, IL-HS-SDME: ionic liquid-headspace-single drop microextraction, SPME: solid phase microextraction, TD: thermal desorption, MCC: multicapillary column, GC: gas chromatography, RTGC: room temperature-gas chromatography, ^{63}Ni: nickel source, UV: ultraviolet source, CD: corona discharge, ^{241}Am: americium source, IMS: ion mobility spectrometer, DMS: differential mobility spectrometer.

Halogenated substances have been also determined by using several SISs including polydimethylsiloxane (PDMS) membrane [109], ESI-IMS after liquid chromatography (LC) large-bore pre-separation [115], HS-SPME with MCC-IMS [53], and ionic liquid-headspace (IL-HS) [41]. Inorganic compounds in environmental matrices were determined by IMS [37, 110, 113].

ESI and CD ionization sources were used for determination of nitrite, nitrate and ammonia nitrogen respectively. Derivatization step was done to convert metal ion into volatile forms for determining selenite in water samples. Environmental soil samples have been successfully analysed by IMS with a good sensitivity and selectivity. SPME [36, 117], exponential dilution [120, 122] were applied to determine contaminants in soil surface. TD was used to determine TWA in surface soil [118], direct analysis of α-pinene was performed by IMS [121], and malathion residues in organic and inorganic particles by IMS with UV photolytic vaporization [119].

I.10. Conclusion and future trends

IMS is an analytical technique which provides a rapid detection of volatile compounds at ambient conditions. It offers a wide range of configurations and possibilities to be applied in the clinical and in the environmental field among others. The works found in the scientific literature reveals that it can be used to detect and identify a wide series of biomarkers and pollutants with varied chemistries and structures. However, some limitations related to the technique for detection of target analytes in complex samples and insufficient sensitivity and selectivity can be obtained in some cases. To overcome these problems it is suggested to use an adequate ionization source and preconcentration methods prior to the introduction of the sample. Extraction techniques are also recommended to enhance separation. Pre-separation of the constituents of the sample can be carried out coupling GC and MCC with IMS. Coupling IMS to MS is also advantageous because IMS offers the ability to distinguish isomers with

similar shapes (cross sections) and MS provides valuable information about the mass identification of ions. Also hyphenation of IMS instrument improved resolution. New developments in IMS instrumentation and applications in the clinical and environmental field are expected in the near future and some of them should be based on the results obtained in the experimental work of this Doctoral Thesis.

References

[1] V.Shulaev, Briefings in Bioinformatics. Oxford University Press, 2006, p. 128.

[2] H. H. Hill, W. F. Siems, R. H. Louis, D. G. Mc Minn, Ion mobility spectrometry, Anal. Chem. 62 (1990) 1201-1209.

[3] G. A. Eiceman, Z. Karpas, Ion Mobility Spectrometry. Boca Raton, Fl 33487-2742, 2005.

[4] H. Borsdorf, A comparison of the ion chemistry of mono substitued toluenes and anilines by three methods of atmospheric pressure ionization with ion mobility spectrometry, Talanta 78 (2009) 1464-1475.

[5] G. A. Eiceman, E. G. Nazarov, J. A. Stone, Chemical standards in ion mobility spectrometry, Anal. Chim. Acta 493 (2003) 185-194.

[6] L. Arce, M. Menéndez, R. Garrido-Delgado, M. Valcárcel, Sample-introduction systems coupled to ion-mobility spectrometry equipment for determining compounds present in gaseous, liquid and solid samples, Trac-Trends in Anal. Chem. 27 (2008) 139-150.

[7] H. Borsdorf, H. Schelhorn, J. Flachowsky, R. Döring, J. Stach, Corona discharge ion mobility spectrometry of aliphatic and aromatic hydrocarbons, Anal. Chim. Acta 403 (2000) 235-242.

[8] L. Criado-Garcia, R. Garrido-Delgado, L. Arce, M. Valcárcel, A comparative study between different alternatives to prepare gaseous standards for calibrating UV-Ion Mobility Spectrometers, Talanta 111 (2013) 111-118.

[9] Y. Seto, Determination of volatile substances in biological samples by headspace gas chromatography, J. Chrom. A 674 (1994) 25-62.

[10] S. Prasad, H. Schmidt, P. Lampen, M. Wang, R. Güth, J. V. Rao, G. B. Smith, G. A. Eiceman, Analysis of bacterial strains with pyrolysis-gas chromatography/differential mobility spectrometry, Analyst 131 (2006) 1216-1225.

[11] T.Kotiaho, F.R.Lauritsen, H.Degn, H.Paakkanen, Anal. Chim. Acta 309 (1995) 317.

[12] M. Najarro, M. E. D. Morris, M. E. Staymates, R. Fletcher, G. Gillen, Optimized thermal desorption for improved sensitivity in trace explosives detection by ion mobility spectrometry, Analyst 137 (2012) 2614-2622.

[13] W. Fan, M. Young, J. Canino, J. Smith, J. Oxley, J. Almirall, Fast detection of triacetone triperoxide (TATP) from headspace using planar solid-phase microextraction (PSPME) coupled to an IMS detector, Anal. Bioanal. Chem. 403 (2012) 408.

[14] J. K. Lokhnauth, N. H. Snow, Solid phase microextraction and stir bar sorptive extraction coupled to ion mobility spectrometry, J. Chrom. A 1105 (2006) 33-38.

[15] M. Basanta, R. M. Jarvis, Y. Xu, G. Blackburn, R. Tal-Singer, A. Woodcock, D. Singh, R. Goodacre, C. L. P. Thomas, S. Fowler, Non-invasive metabolomic analysis of breath using differential mobility spectrometry in patients with chronic obstructive pulmonary disease and healthy smokers, Analyst 135 (2010) 315-320.

[16] C. S. Creaser, J. R. Griffiths, C. J. Bramwell, S. Noreen, C. A. Hill, C. L. P. Thomas, Ion mobility spectrometyr: a review. Part 1. Structural analysis by mobility measurement, Analyst 129 (2004) 984-994.

[17] J. N. Driscoll, Evaluation of a new photoionization detector for organic compounds, J. Chrom. A 134 (1977) 49-55.

[18] M. Young, K. M. Douglas, G. A. Eiceman, D. A. ake, M. V. Johnston, Laser desorption- ionization of polycyclic aromatic hydrocarbons from glass surfaces with ion mobility spectrometry analysis, Anal. Chim. Acta 453 (2002) 231-243.

[19] P. V. Johnson, L. W. Beegle, H. I. Kim, G. A. Eiceman, I. Kanik, Ion mobility spectrometry in espace exploration, Int. J. Mass Spectrom. 262 (2007) 1-15.

[20] I. A. Buryakov, E. V. Krylov, E. G. Nazarov, U. Kh. Rasulev, A new method of separation of multi-atomic ions by mobility at atmospheric pressure using a high frequency amplitude-asymmetric strong electric field, Int. J. Mass Spectrom. 128 (1993) 148.

[21] R. Cumeras, E. Figueras, C. E. Davis, J. I. Baumbach, I. Gràcia, Review on ion mobility spectrometry. Part 1: current instrumentation, Analyst 140 (2014) 1376-1390.

[22] A. Bunkowski, B. Bödeker, S. Bader, M. Westhoff, P. Litterst, J. I. Baumbach, MCC/IMS signals in human breath related to sarcoidosis-results of a feasibility study using an automated peak finding procedure, J. Breath. Res. 3 (2009) 1-10.

[23] G. R. Lambertus, C. S. Fix, S. M. Reidy, S. A. Miller, D. Wheeler, E. Nazarov, R. Sacks, Silicon microfabricated column with microfabricated differential mobility spectrometer for GC analysis of volatile organic compounds, Anal. Chem. 77 (2005) 7563-7571.

[24] R. Saleh, A. Shihadeh, A. Khlystov, Determination of evaporation coefficients of semi-volatile organic aerosols using an integrated volume—tandem differential mobility analysis (IV-TDMA) method, J. Aerosol Sci. 40 (2009) 1019-1029.

[25] V. Pomareda, S. López-Vidal, D. Calvo, A. Pardo, S. Marco, A novel differential mobility analyzer as a VOC detector and multivariate techniques for identification and quantification, Analyst 138 (2013) 3512-3521.

[26] H. Tammet, Size and mobility of nanometer particles, clusters and ions, J. Aerosol Sci. 26 (1995) 459-475.

[27] B. K. Ku, J. Fernández de la Mora, Relation between electrical mobility, mass, and size for nanodrops 1-6.5 nm in diameter in air, J. Aerosol Sci.Tech. 43 (2009) 241-249.

[28] M. T. Jafari, H. Saraji, H. Sherafatmand, Polypyrrole/montmorillonite nanocomposite as a new solid phase microextraction fiber combined with gas chromatography-corona discharge ion mobility spectrometry for the simultaneous determination of diazinon and fenthion organophosphorus pesticides, Anal. Chim. Acta 814 (2014) 69-78.

[29] Y. Lu, R. M. O'Donnell, P. B. Harrington, Detection of cocaine and its metabolites in urine using solid phase extraction-ion mobility spectrometry with alternating least squares, Forensic Sci. Int. 189 (2009) 54-59.

[30] M. T. Jafari, B. Rezaei, B. Zaker, Ion Mobility spectrometry as a detector for molecular imprinted polymer separation and metronidazole determination in pharmaceutical and human serum samples, Anal. Chem. 81 (2009) 3585-3591.

[31] M. T. Jafari, B. Rezaei, M. Javaheri, A new method based on electrospray ionisation ion mobility spectrometry (ESI-IMS) for simultaneous determination of caffeine and theophylline, Food Chem. 126 (2011) 1964-1970.

[32] M. T. Jafari, Z. Badihi, E. Jazan, A new approach to determine salicylic acid in human urine and blood plasma based on negative electrospray ion mobility spectrometry after selective separation using a molecular imprinted polymer , Talanta 99 (2012) 520-526.

[33] S. Mirmahdieh, A. Mardihallaj, Z. Hashemian, J. Razavizadeh, H. Ghaziaskar, T. Khayamian, Analysis of testosterone in human urine using molecularly imprinted solid-phase extraction and corona discharge ion mobility spectrometry, J. Sep. Sci. 34 (2011) 107-112.

[34] B. Rezaei, M. T. Jafari, R. Khademi, Selective separation and determination of primidone in the pharmaceutical and human serum samples using molecular imprinted polymer-electrospray ionization ion mobility spectrometry (MIP-ESI-IMS), Talanta 79 (2009) 669-675.

[35] N. Alizadeh, M. Jafari, A. Mohammadi, Headspace-solid-phase microextraction using a dodecylsulfate-doped polypyrrole film coupled to ion mobility spectrometry for analysis methyl tert-butyl ether in water and gasoline, J. Hazard. Mater. 169 (2009) 861-867.

[36] A. Mohammadi, A. Ameli, N. Alizadeh, Headspace solid-phase microextraction using a dodecylsulfate-doped polypyrrole film coupled to ion mobility spectrometry for the simultaneous determination of atrazine and ametryn in soil and water samples, Talanta 78 (2009) 1107-1114.

[37] P. Shahdousti, N. Alizadeh, Headspace-solid phase microextraction of selenium(IV) from human blood andwater samples using polypyrrole film and analysis with ion mobility spectrometry, Anal. Chim. Acta 684 (2011) 67-71.

[38] N. Alizadeh, A. Mohammadi, M. Tabrizchu, Rapid screening of methamphetamines in human serum by headspace solid-phase microextraction using a dodecylsulfate-doped polypyrrole film coupled to ion mobility spectrometry, J. Chromatogr. A 1183 (2008) 21-28.

[39] H. Kalhor, N. Alizadeh, Determining urea levels in dialysis human serum by means of headspace solid phase microextraction coupled with ion mobility spectrometry and on the basis of nanostructured polypyrrole film, Anal. Bional. Chem. 405 (2013) 5333-5339.

[40] A. Karimi, N. Alizadeh, Rapid analysis of captopril in human plasma and pharmaceutical preparations by headspace solid phase microextraction based on polypyrrole film coupled to ion mobility spectrometry, Talanta 79 (2009) 479-485.

[41] E. Aguilera-Herrador, R. Lucena, S. Cárdenas, M. Valcárcel, Ionic liquid-based single drop microextraction and room-temperature gas chromatography for on-site ion mobility spectrometric analysis, J. Chromatogr. A 1216 (2009) 5580-5587.

[42] R. H. Louis, W. F. Siems, H. H. Hill, Detection limits of an ion mobility detector after capillary gas chromatography, J. Microcol. Sep. 2 (1990) 138-145.

[43] A. B. Kanu, H. H. Herbert, Ion mobility spectrometry detection for gas chromatography, J. Chromatogr. A 1177 (2008) 12-27.

[44] S. P. Karasek, G. E. Spangler, Electron capture: theory and practice in chromatography. Elsevier, Amsterdam, 1981.

[45] Y. Lu, P. B. Harrington, Forensic application of gas chromatography-differential mobility spectrometry with two-way classification of ignitable liquids from fire debris, Anal. Chem. 79 (2007) 6752-6759.

[46] M. Basanta, D. Singh, S. Fowler, I. Wilson, R. Dennis, C. L. P. Thomas, Increasing analytical space in gas chromatography-differential mobility spectrometry with dispersion field amplitude programming, J. Chromatogr. A. 1173 (2007) 129-138.

[47] G. A. Eiceman, E. G. Nazarov, R. A. Miller, E. V. Krylov, A. M. Zapata, Micro-machined planar field asymmetric ion mobility spectrometer as a gas chromatographic detector, Analyst 127 (2002) 466-471.

[48] W. Vautz, R. Slodzynski, C. Hariharan, L. Seifert, J. Nolte, R. Fobbe, S. Sielemann, B. C. Lao, L. Hildebrand, Detection of metabolites of trapped humans using ion mobility spectrometry coupled with gas chromatography, Anal. Chem. 85 (2013) 2135-2142.

[49] S. Sielemann, J. I. Baumbach, P. Pilzecker, G. Walendzik, Detection of trans-1,2-dichloroethene, trichloroethene and tetrachloroethene using Multi-Capillary Columns Coupled to Ion Mobility Spectrometers with UV-Ionisation Sources, Int. J. Ion Mobil. Spectrom. 2 (1999) 15-21.

[50] J. Falchiwsky, M. Brodacki, J. Stach, Detection of DMS using hand-held IMS, Int. Soc. Ion Mobility Spectrom. 39 (2003) 42-45.

[51] W. Vautz, S. Sielemann, J. I. Baumbach, The influence of humidity on the determination of organic trace substances in ambient air using UV ion mobility spectrometry: alpha-and beta-pinene, 3-carene and limonene, Int. J. Ion Mobil. Spectrom. 6 (2003) 21-29.

[52] W. Vautz, J. I. Baumbach, E. Uhde, Detection of emissions from surfaces using ion mobility spectrometry, Anal. Bioanal. Chem. 384 (2006) 980-986.

[53] G. Walendzik, J. I. Baumbach, D. Klockow, Coupling of SPME with MCC/UV–IMS as a tool for rapid on-site detection of groundwater and surface water contamination, Anal. Bioanal. Chem. 382 (2005) 1842-1847.

[54] E. G. Nazarov, R. A. Miller, E. V. Krylov, J. A. Stone, G. A. Eiceman, Quantitative determination of n-alkanethiols in air and in a blended gas mixture of methane with air by gas chromatography/differential mobility spectrometry, Int. J. Ion Mobil. Spectrom. 12 (2009) 81-90.

[55] J. P. Bach, M. Gold, D. Mengel, A. Hattesohl, D. Lubbe, S. Schmid, B. Tackenberg, J. Rieke, S. Maddula, J. I. Baumbach, C. Nell, T. Boeselt, J. Michelis, J. Alferink, M. Heneka, W. Oertel, F. Jessen, S. Janciauskiene, C. Vogelmeier, R. Dodel, A. R. Koczulla, D. Blum, Measuring compounds in exhaled air to detect Alzheimer's disease and Parkinson's disease, PLoS ONE 10 (2015) 1-13.

[56] J. I. Baumbach, Ion mobility spectrometry coupled with multi-capillary columns for metabolic profiling of human breath, J. Breath. Res. 3 (2009) 1-16.

[57] V. Besa, H. Teschler, A. M. Khan, P. Zarogoulidis, J. I. Baumbach, U. Sommerwerck, L. Freitag, K. Darwiche, Exhaled volatile organic compounds discriminate patients with chronic obstructive pulmonary disease from healthy subjects, Int. J. Chron. Obstruct. Pulmon. Dis. 10 (2015) 399-406.

[58] K. Darwiche, J. I. Baumbach, U. Sommerwerck, H. Teschler, L. Freitag, Bronchoscopically obtained volatile biomarkers in lung cancer, Lung 189 (2011) 445-452.

[59] H. Handa, A. Usuba, S. Maddula, J. I. Baumbach, M. Mineshita, T. Miyazawa, Exhaled breath analysis for lung cancer detection using ion mobility spectrometry, PLoS ONE 9 (2014) 1-13.

[60] V. Ruzsanyi, J. I. Baumbach, S. Sielemann, P. Litterst, M. Westhoff, L. Freitag, Detection of human metabolites using multi-capillary columns coupled to ion mobility spectrometers., J. Chromatogr. A 1084 (2005) -145.

[61] A. Ulanowska, M. Ligor, A. Amann, B. Buszewski, Determination of volatile organic compounds in exhaled breath by ion mobility spectrometry, Chem. Anal (Warsow) 53 (2008) 953-965.

[62] W. Vautz, J. Nolte, R. Fobbe, J. I. Baumbach, Breath analysis—performance and potential of ion mobility spectrometry, J. Breath. Res. 3 (2009) 8.

[63] M. Westhoff, P. Litterst, L. Freitag, J. I. Baumbach, Ion mobility spectrometry in the diagnosis of sarcoidosis: results of a feasibility study , J. Physiol. Pharmacol. 58 (2007) 739-751.

[64] M. Westhoff, P. Litterst, L. Freitag, W. Urfer, S. Bader, J. I. Baumbach, Ion mobility spectrometry for the detection of volatile organic compounds in exhaled breath of patients with lung cancer: results of a pilot study., Thorax 64 (2009) 744-748.

[65] R. Cumeras, E. Figueras, C. E. Davis, J. I. Baumbach, I. Gràcia, Review on ion mobility spectrometry. Part 2: hyphenated methods and effects of experimental parameters, Analyst 140 (2014) 1391-1410.

[66] A. B. Kanu, P. Dwivedi, M. Tam, L. Matz, H. H. Hill, Ion mobility–mass spectrometry, J. Mass Spectrom. 43 (2008) 1-22.

[67] H. Borsdorf, G. A. Eiceman, Ion Mobility Spectrometry: Principles and Applications, Appl. Spectrosc. Rev. 41 (2006) 323-375.

[68] A. B. Kanu, C. Wu, H. H. Hill, Rapid preseparation of interferences for ion mobility spectrometry, Anal. Chim. Acta 610 (2008) 125-134.

[69] P. Dwivedi, A. J. Schultz, H. H. Hill, Metabolic Profiling of Human Blood by High Resolution Ion Mobility Mass Spectrometry (IM-MS)., Int. J. Mass Spectrom. 298 (2010) 78-90.

[70] M. M. Gaye, S. J. Valentine, Y. Hu, N. Mirjankar, Z. T. Hammoud, Y. Mechref, B. K. Lavine, D. E. Clemmer, Ion Mobility-Mass Spectrometry Analysis of Serum N-linked Glycans from Esophageal Adenocarcinoma Phenotypes, J. Proteome Res. 11 (2012) 6102-6110.

[71] K. Kaplan, P. Dwivedi, S. Davidson, Q. Yang, P. Tso, W. Siems, H. H. Hill, Monitoring dynamic changes in lymph metabolome of fasting and fed rats by electrospray ionization ion mobility mass spectrometry (ESI-IMMS), Anal. Chem. 81 (2009) 7944-7953.

[72] U. Dharmasiri, S. L. Isenberg, G. L. Glish, P. M. Armistead, Differential ion mobility spectrometry coupled to tandem mass spectrometry enables targeted leukemia antigen detection, J. Proteome Res. 13 (2014) 4356-4362.

[73] B. C. Bohrer, D. E. Clemmer, Shift reagents for IMS-IMS-MS analysis of complex peptide mixtures: evaluation of 18-crown-6 ether complexes, Anal. Chem. 83 (2011) 5377-5385.

[74] M. R. Menlyadiev, G. A. Eiceman, Tandem differential mobility spectrometry in purified air for high-speed selective vapor detection, Anal. Chem. 86 (2014) 2395-2402.

[75] S. I. Merenbloom, B. C. Bohrer, S. L. Koeniger, D. E. Clemmer, Assessing the Peak Capacity of IMS-IMS Separations of Tryptic Peptide Ions in He at 300 K, Anal. Chem. 79 (2007) 515-522.

[76] S. Armenta, M. Alcala, M. Blanco, A review of recent, unconventional applications of ion mobility, Anal. Chim. Acta 703 (2011) 114-123.

[77] I. Marquez-Sillero, E. Aguilera-Herrador, S. Cárdenas, Ion mobility spectrometry for environmental analysis, Trac-Trends in Anal. Chem. 30 (2011).

[78] T. Keller, A. Miki, P. Regenscheit, R. Dirnhofer, A. Schneider, H. Tsuchihashi, Detection of designer drugs in human hair by ion mobility spectrometry (IMS), Forensic Sci. Int. 94 (1998) 55-63.

[79] A. Sheibani, M. Tabrizchi, H. Ghaziaskar, Determination of methadone in human hair by headspace extraction and ion mobility spectrometry, Anal. lett. 44 (2011) 667-675.

[80] L. T. Demoranville, J. R. Verkouteren, Measurement of drug facilitated sexual assault agents in simulated sweat by ion mobility spectrometry, Talanta 106 (2013) 375-380.

[81] B. Baert, S. Vansteelandt, B. De Spiegeleer, Ion mobility spectrometry as a high-throughput technique for in vitro transdermal Franz diffusion cell experiments of ibuprofen, J. Pharm. Biomed. Anal. 55 (2011) 472-478.

[82] T. Perl, E. Carstens, A. Hirn, M. Quinerl, W. Vautz, J. Nolte, M. Jünger, Determination of serum propofol concentrations by breath analysis using ion mobility spectrometry, Anaesthesia 103 (2009) 822-827.

[83] Q. Zhou, E. Li, Z. Wang, Y. Gong, C. Wang, L. Guo, H. Li, Time-resolved dynamic dilution introduction for ion mobility spectrometry and its application in end-tidal propofol monitoring, J. Breath. Res. 9 (2015) 1-8.

[84] Y. Liu, Y. Gong, C. Wang, Q. Zhou, D. Wang, L. Guo, X. Pi, X. Zhang, S. Luo, H. Li, E. Li, Online breath analysis of propofol during anesthesia: Clinical application of membrane inlet-ion mobility spectrometry, Acta. Anaesthes. Scandinavica 59 (2015) 319-328.

[85] J. Mercer, D. Shakleya, S. Bell, Applications of ion mobility spectrometry (IMS) to the analysis of gamma hydroxibutyrate and gamma hydroxyvalerate in toxicological matrices, J. Anal. Toxicol. 30 (2006) 539-544.

[86] S. Armenta, M. De la Guardia, M. Alcalà, M. Blanco, Noninvasive double confirmation of cocaine abuse, Anal. Chem. 85 (2013) 11382-11390.

[87] S. Armenta, S. Garrigues, M. De la Guardia, J. Brassier, M. Alcalà, M. Blanco, Analysis of ecstasy in oral fluid by ion mobility spectrometry and infrared spectroscopy after liquid-liquid extraction, J. Chrom. A. 1384 (2015) 1-8.

[88] M. T. Jafari, M. Javaheri, Selective method based on negative electrospray ionization ion mobility spectrometry (ESI-IMS) for direct analysis of salivary thiocyanate, Anal. Chem. 82 (2010) 6721-6725.

[89] S. Soonberg, S. Armenta, S. Garrigues, M. De la Guardia, Detection of tetrahydrocannabinol residues on hands by ion-mobility spectrometry (IMS). Correlation of IMS data with saliva analysis, Anal. Bional. Chem. 407 (2015) 5999-6008.

[90] J. K. Lokhnauth, N. H. Snow, Solid phase micro-extraction coupled with ion mobility spectrometry for the analysis of ephedrine in urine, J. Sep. Sci. 28 (2005) 612-618.

[91] Y. Wang, S. Nacson, J. Pawliszyn, The coupling of solid-phase microextraction/surface enhanced laser desorption/ionization to ion mobility spectrometry for drug analysis, Anal. Chim. Acta 582 (2007) 50-54.

[92] M. T. Jafari, H. Saraji, H. Sherafatmand, Electrospray ionization-ion mobility spectrometry as a detection system for three-phase hollow fiber microextraction technique and simultaneous determination of trimipramine and desipramine in urine and plasma samples, Anal. Bional. Chem. 399 (2011) 3555-3564.

[93] M. T. Jafari, H. Saraji, A. H. Ameri, Coupling of solid phase microextraction with electrospray ionization ion mobility spectrometry and direct analysis of venlafaxine in human urine and plasma., Anal. Chim. Acta 853 (2015) 460-468.

[94] V. Ruzsanyi, P. Mochalski, A. Schmid, H. Wiesenhofer, M. Klieber, H. Hinterhuber, A. Amann, Ion mobility spectrometry for detection of skin volatiles, J. Chrom. B 911 (2012) 84-92.

[95] A. Ulanowska, M. Ligor, A. Amann, B. Buszewski, Determination of volatile organic compounds in exhaled breath by ion mobility spectrometry., Chem. Anal (Warsow) 53 (2008) 953-965.

[96] J. C. Reynolds, G. Blackburn, C. Guallar-Hoyas, V. H. Moll, V. Bocos-Bintitan, G. Kaur-Atwal, D. Howdle, E. L. Harry, L. J. Brown, C. S. Creaser, C. L. P. Thomas, Detection of Volatile Organic Compounds in Breath Using Thermal Desorption Electrospray Ionization-Ion Mobility-Mass Spectrometry, Anal. Chem. 82 (2010) 2139-2144.

[97] R. Purkhart, H. Köhler, E. Liebler-Tenorio, M. Meyer, G. Becher, A. Kikowatz, P. Reinhold, Chronic intestinal Mycobacteria infection: Discrimination via VOC analysis in exhaled breath and headspace of feces using differential ion mobility spectrometry, J. Breath. Res. 5 (2011).

[98] J. D. Sobel, Z. Karpas, A. Lorber, Diagnosing vaginal infections through measurement of biogenic amines by ion mobility spectrometry, Europ. J. Obstetr. Gynecol. Reprod. Biol. 163 (2012) 81-84.

[99] M. K. Bomers, F. P. Menke, R. S. Savage, C. M. J. E. Vandebroucke-Grauls, M. A. van Agmael, J. A. Covington, Y. M. Smulders, Rapid, Accurate, and on-site detection of C. Difficile in stool samples, Am. J. Gastroenterology 110 (2015) 588-594.

[100] A. Roine, T. Saviauk, P. Kumpulainen, M. Karjalainen, A. Tuokko, J. Aittoniemi, R. Vuento, J. Lekkala, T. Lehtimäki, T. L. Tammela, N. K. J. Oksala, Rapid and accurate detection of urinary pathogens by mobile IMS-based electronic nose: A proof-of-principle study, PLoS ONE 9 (2014) 1-11.

[101] R. P. Arasaradnam, E. Wstenbrink, M. J. McFarlane, R. Harbord, S. Chambers, N. O'Connell, C. Bailey, C. Nwokolo, K. Bardhan, R. Savage, J. A. Covington, Differentiating coeliac disease from irritable bowel syndrome by urinary volatile organic compound analysis - A pilot study, PLoS ONE 9 (2014) 1-9.

[102] R. P. Arasaradnam, M. J. McFarlane, C. Ryan-Fisher, E. Westenbrink, P. Hodges, M. G. Thomas, S. Chambers, N. O'Connell, C. Bailey, C. Harmston, C. Nwokolo, K. D. Bardan, J. A. Covington, Detection of Colorectal Cancer (CRC) by Urinary Volatile Organic Compound Analysis, PLoS ONE 9 (2014) 1-6.

[103] R.Garrido-Delgado, L.Arce, Pérez-Marín C.C, M.Valcárcel, Use of ion mobility spectroscopy with an ultraviolet ionization source as a vanguard screening system for the detection and determination of acetone in urine as a biomarker for cow and human diseases, Talanta 78 (2009) 863-868.

[104] H. Schimdt, J. I. Baumbach, D. Klockow, Detection of perfluorocarbons using ion mobility spectrometry, Anal. Chim. Acta 484 (2003) 63-74.

[105] R. Pozzi, P. Bocchini, F. Pinelli, G. C. Galletti, Rapid analysis of tile industry gaseous emissions by ion mobility spectrometry and comparison with solid phase micro-extraction/gas chromatography/mass spectrometry., J. Environ. Monit. 8 (2006) 1219-1226.

[106] G. A. Eiceman, M. R. Salazar, M. R. Rodriguez, T. F. Limero, S. W. Beck, J. H. Cross, R. Young, J. T. James, Ion mobility spectrometry of hydrazine, monomethylhydrazine, and ammonia in air with 5-nonanone reagent gas, Anal. Chem. 65 (1993) 1696-1702.

[107] C. Chen, C. Dong, Y. Du, S. Cheng, F. Han, L. Li, W. Wang, K. Hou, H. Li, Bipolar Ionization Source for Ion Mobility Spectrometry Based on Vacuum Ultraviolet Radiation Induced Photoemission and Photoionization, Anal. Chem. 82 (2010) 4151-4157.

[108] H. Borsdorf, A. Rämmler, Continuous on-line determination of methyl tert-butyl ether in water samples using ion mobility spectrometry, J. Chromatogr. A 1072 (2005) 45-54.

[109] Y. Du, W. Zhang, W. Whitten, H. Li, D. B. Watson, J. Xu, Membrane-Extraction Ion Mobility Spectrometry for in Situ Detection of Chlorinated Hydrocarbons in Water, Anal. Chem. 82 (2010) 4089-4096.

[110] P. Dwivedi, L. M. Matz, D. A. Atkinson, H. H. Hill, Electrospray ionization-ion mobility spectrometry: a rapid analytical method for aqueous nitrate and nitrite analysis, Analyst 129 (2004) 139-144.

[111] M. T. Jafari, M. Azimi, Analysis of Sevin, Amitraz, and Metalaxyl Pesticides Using Ion Mobility Spectrometry, Anal. lett. 39 (2006) 2061-2071.

[112] M. T. Jafari, Determination and identification of malathion, ethion and dichlorovos using ion mobility spectrometry, Talanta 69 (2006) 1054-1058.

[113] M. T. Jafari, T. Khayamian, Direct determination of ammoniacal nitrogen in water samples using corona discharge ion mobility spectrometry, Talanta 76 (2008) 1189-1193.

[114] M. Nousiainen, K. Peräkorpi, M. Sillanpää, Determination of gas-phase produced ethyl parathion and toluene 2,4-diisocyanate by ion mobility spectrometry, gas chromatography and liquid chromatography, Talanta 72 (2007) 984-990.

[115] F. K. Tadjimukhamedov, J. A. Stone, D. Papanastasiou, J. E. Rodriguez, W. Mueller, H. Sukumar, G. A. Eiceman, Liquid chromatography/electrospray ionization/ion mobility spectrometry of chlorophenols with full flow from large bore LC columns, Int. J. Ion Mobil. Spectrom. 11 (2008) 51-60.

[116] A. Ashori, A. Sheibani, Homogeneous liquid-liquid extraction coupled to ion mobility spectrometry for the determination of p-toluidine in water samples, Bull. Environ. Contam. Toxicol. 94 (2015) 474-478.

[117] P. B. Harrington, P. Rearden, Harr, Rapid screening of precursor and degradation products of chemical warfare agents in soil by solid-phase microextraction ion mobility spectrometry (SPME-IMS), Anal. Chim. Acta 545 (2005) 13-20.

[118] A. B. Kanu, P. E. Haigh, H. H. Hill, Surface detection of chemical warfare agent simulants and degradation products, Anal. Chim. Acta 553 (2005) 148-159.

[119] R. R. Kunz, F. L. Leibowitz, D. K. Downs, Ultraviolet photolytic vapor generation from particulate ensembles for detection of malathion residues in aerosols, Anal. Chim. Acta 531 (2005) 267-277.

[120] D. Sevier, M. Gribb, R. Walters, J. Imonigie, K. Ryan, A. Kanu, H. Hill, F. Hong, J. Baker, S. M. Loo, An in-situ ion mobility spectrometer sensor system for detecting gaseous VOCs in unsaturated soils, ASCE Conf. Proc. 1 (2006) 225-234.

[121] A. K. Viitanen, E. Saukko, A. Virtanen, P. Yli-Pirilä, J. N. Smith, J. Joutsensaari, J. M. Mäkelä, Ion Mobility Distributions during the Initial Stages of New Particle Formation by the Ozonolysis of a-Pinene, Environ. Sci. Technol. 44 (2010) 8917-8923

[122] A. B. Kanu, H. H. Hill, M. M. Gribb, R. N. Walters, A small subsurface ion mobility spectrometer sensor for detecting environmental soil-gas contaminants, J. Environ. Monit. 9 (2007) 51-60.

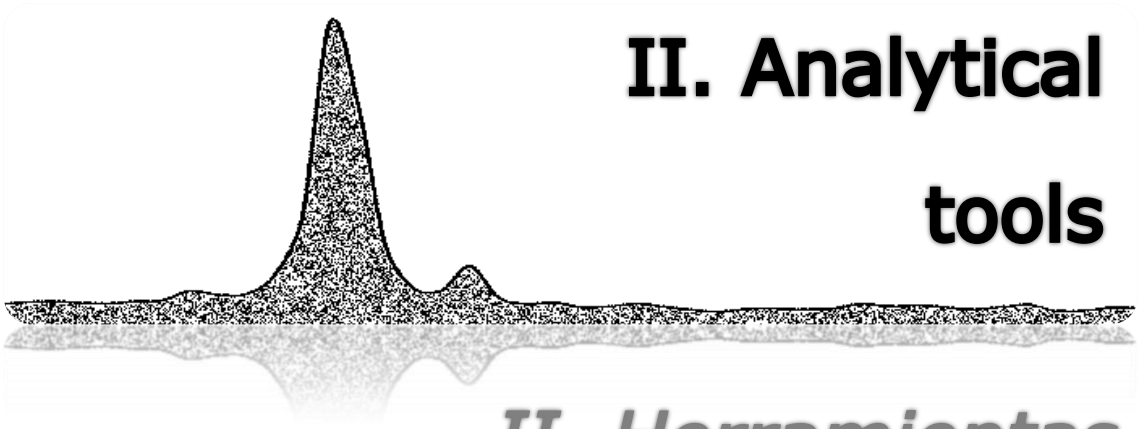

II. Analytical tools

II. Herramientas analíticas

The experimental work shown in this Thesis was carried out with several analytical tools such as standards, chemicals, samples, devices and analytical instruments of different characteristics. In this section of the Thesis are fully described.

II.1. Standards and chemicals

II.1.1. Analytes

In this part are summarized the analytical standards used in the experimental work which are classified by chemical groups. The standards and analytes used were of high purity and they were stored following advice of the supplier (Sigma-Aldrich, St. Louis, MO, USA).

- ✧ Alcohols: methanol, ethanol, ethylene glycol and propane-1, 2-diol.
- ✧ Aldehydes: butyraldehyde, benzaldehyde and tolualdehyde.
- ✧ Aromatic hydrocarbons: benzene, ethylbenzene, toluene, *m*-xylene, *o*-xylene y *p*-xylene, also called by the generic name of BTEX. Biphenyl, dibenzofuran, triphenylmethane.
- ✧ Carboxylic acids: butanoic acid, 4-hydroxy-acid, ammonium salt *γ*-hydroxybutyric (GHB) in methanol.
- ✧ Ethers: diphenyl ether.
- ✧ Ketones: acetone.
- ✧ Phenols: phenol.

II.1.2. Solvents and other chemicals

Other chemicals also used in the experimental work are summarized here:

- ✧ Sample gas and drift gas used for IMS instruments was nitrogen coming from cylinder with a purity of 6.0 and 5.0 supplied by Abelló Linde (Barcelona, Spain). In the work done

with the differential mobility spectrometer, nitrogen was also used, but in this case it was generated on site from a gas generator (model nk-10L-HP) from Peak Scientific (Renfrew, United Kingdom) this gas was purified by passing through a charcoal adsorbent-bed gas-purifier and a moisture filter from Varian (Crawley, United Kingdom) and a triple-bed gas purifier from Thames Restek (Saunderton, United Kingdom) all mounted in series.

- ✧ High purity helium (99.999 %) supplied by Praxair (Danbury, USA) was used as carrier gas in the gas chromatograph coupled to the differential mobility spectrometer.
- ✧ Synthetic air of high purity 5.0 was supplied by Carburos metálicos (Barcelona, Spain) and it was used as sample gas for the UV-ion mobility spectrometer.
- ✧ Water used as solvent to prepare standards was ultrapure water obtained by an on site purification set up from Milli-Q (Millipore, Bedford, MA, USA).
- ✧ Potassium chloride (99 %) was used as a solvent to dilute the initial concentration of analyte in saliva samples when using the differential mobility spectrometer.
- ✧ Anhydrous dichloromethane (≥99.8 %) was used to dilute HTF samples, and as extractant for phenol when using the SPE cartridges, as solvent to prepare standards. As well, it was used as solvent to prepare standards solutions of analytes and perform the calibration of the differential mobility spectrometer under optimized conditions.
- ✧ 1-chlorotetradecane GC grade (98 %) was used as internal standards in the GC-FID.
- ✧ Potassium bromide FT-IR grade (≥99 %) was used to build the IR pills with the samples of HTF as a pre-treatment step prior to the measurement by FT-MIR.
- ✧ Hydrochloric acid was used to acidify the pH of standards and samples.

- ✧ Sodium hydroxide was used to basify the pH of standards and samples.

II.1.3. Extraction and preconcentration systems used

Several materials were used to extract or preconcentrate analytes present in the samples prior to the introduction of volatiles to the IMS:

- ✧ 30 mg and 60 mg, 3 mL and 30 µm of pore size of polymeric reversed-phase sorbent HLB OASIS® cartridges were supplied from Waters (Milford, MA, USA).
- ✧ 60 mg, 3 mL and 30 µm of pore size of silica based sorbent C_{18} cartridges were acquired from Varian (Harbor City, CA, USA)
- ✧ 60 mg, 3 mL and 30 µm of pore size of a neutral resin comprised of divinylbenzene-based particle grafted with polyvinylpyrrolidone polymer SolEx HRPHs® cartridges from Thermo Fisher Scientific (Waltham, MA, EEUU) were also used.
- ✧ Multiwalled nanotubes (MWNTs) were used with a diameter of 5-20 nm and 1-10 µm of length, supplied by Bayer Material Science (Leverkusen, Germany).
- ✧ A titanium cylinder (6 mm long, 2 mm o.d. C-SPTD5-6MM from Markes International Ltd. (Llantrisant, United Kingdom) coated on the internal and external surface with polydimethylsiloxane (internal wall thickness 1 µm and external wall thickness 0.5 mm) was used to recover analytes from the saliva.
- ✧ Glass thermal desorption tube from Markes International Ltd. (Llantrisant, United Kingdom)
- ✧ 25 cm steel tube filled with 1 g TENAX TA porous polymer adsorbent, 60-80 mesh from Sigma-Aldrich (St. Louis, MO, USA). Glass wool was also used in the extreme to avoid the loss of the material.

II.1.4. Laboratory material

- ✧ Hamilton® glass micro syringes of 1 and 10 µL.
- ✧ Glassware of different volume as test tubes, pipettes, flasks, volumetric flasks, beakers and amber glass bottles.

- ✧ Glass vials of 10 and 20 mL.
- ✧ Chromatography vials of 2 mL.
- ✧ Dilution glass flasks of 100, 500 and 1000 mL.
- ✧ Micropipettes of 100, 1000 and 5000 µL.
- ✧ Magnetic caps with silicone septum.
- ✧ Disposable Nylon filters of 0.45 µm pore size and inner diameter of 25 mm.
- ✧ Teflon and steel tubes and connectors of 1/8'' and 1/4'' from Varian (Harbor City, CA, USA).
- ✧ Magnetic stirrer.
- ✧ Glass stirrer.
- ✧ Spatula.
- ✧ Tweezers.
- ✧ Staples.
- ✧ Parafilm® M.
- ✧ Latex gloves, security glasses and vapours mask.
- ✧ Milton® sterilising liquid (Suffolk, Reino Unido).
- ✧ Plastic containers of different sizes for the proper management of laboratory waste.

II.2. Samples

In the experimental work developed in this Thesis, different samples were analysed:

- ✧ Air: Campus Rabanales parking area, fume hood and chemicals room from the group FQM-215 laboratory, Department of Analytical Chemistry, University of Cordoba.
- ✧ Environmental waters: water sample form Guadalquivir River in the local area of Cordoba, water sample from Rabanales stream, affluent of Guadalquivir River, and water sample from

a well placed in private estate in the village of Nueva Carteya (Cordoba). They were stored in amber glass bottles at 4 ºC in the refrigerator before analysis.

- ✧ Gasoline: gasoline 95 octanes from Cepsa (Spain).
- ✧ Heat transfer fluid: HTF samples collected by the workers of the thermosolar plant "La Africana" (Cordoba). HTF samples produced at lab scale in a reactor in the laboratory.
- ✧ Saliva: saliva samples were given by adult volunteers which were healthy and who gave informed consent. Saliva from smokers was also collected. Participants were recruited from University of Cordoba and Loughborough University staff, students and their social networks. Participants were asked to only drink cold water, and refrain from flavored, caffeinated, or other drinks at least 1 hour before the saliva collection. Samples were stored at -18 ºC until their analysis.
- ✧ Soil: soil samples were collected from Campus Rabanales parking area, garden in the area of the train station and park in the city center (Cordoba, Spain).

II.3. Devices and small instruments

- ✧ Magnetic stirrer device from Velp Cientifica (Milan, Italy).
- ✧ Ultrasonic bath from PCE instruments (Meschede, Germany).
- ✧ Digital flow check HR™ meter from Chromatographie Service GmbH (Langerwehe, Germany) to control the gas flow for sample and drift gas of the IMS instruments.
- ✧ pHmeter Crison micropH 2000 from Crison (Barcelona, Spain).
- ✧ Precision balance OHAUS Explorer (Nänikon, Switzerland).
- ✧ Chromatographic oven HP 5890 from Agilent Technologies, (Palo Alto, CA, USA).
- ✧ Thermoreactor ECO 1G from Velp Scientific (Usmate, Italy).
- ✧ Two stainless-steel switching valves, Selectomite®-7177G2Y from Hoke Inc. (Spartanburg, SC, USA).
- ✧ Heater mantle from J. P. Selecta S.A. (Barcelona, Spain).

- ✧ Pump and flow controller PFC-6020 supplied by Ramen S.A. (Madrid, Spain).
- ✧ 1 L reactor with heater and pressure controller from Sanical Astur, S.L. (Oviedo, Spain).
- ✧ Pressure and temperature controller from Lascar electronics (Salisbury, United Kingdom).
- ✧ Peristaltic pump from J. P. Selecta S.A. (Barcelona, Spain).
- ✧ Portable hygrometer and temperature controller PCE-HT 71N LOG32 from PCE instruments (Meschede, Germany).
- ✧ The SPE procedure was performed on a Visiprep DL SPE Vacuum Manifold from Supelco (Bellafonte, PA, USA).
- ✧ Concentrator plus from Eppendorf Iberica S.L.U. (Madrid, Spain).
- ✧ Laboratory centrifuge Centronic-BL II from J. P. Selecta S.A. (Barcelona, Spain).

II.4. Analytical instruments

In this section are summarized the instruments that were used for the experimental work. Three of these instruments correspond to ion mobility spectrometers or instruments derived from this technology. Several sample introduction systems (SISs) were used such as headspace and exponential dilution; and also other system to facilitate the separation of analytes such as chromatographic systems. All of them are fully described in this section. In order to compare results obtained with the IMS instruments (vanguard techniques), other rutinary or rearguard instruments were also used such as gas chromatography mass spectrometry (GC-MS), gas chromatography flame ionization detection (GC-FID) and fourier transform medium infrared spectroscopy (FT-MIR) that are summarized in this part.

A) Ion mobility instruments

II.4.1. Ion mobility spectrometry with lineal drift tube and ultraviolet lamp as ionization source

The ion mobility spectrometry with lineal drift tube and ultraviolet lamp as ionization source (UV–IMS) instrument used, supplied by GAS (Dortmund, Germany), is depicted in **Figure 1**.

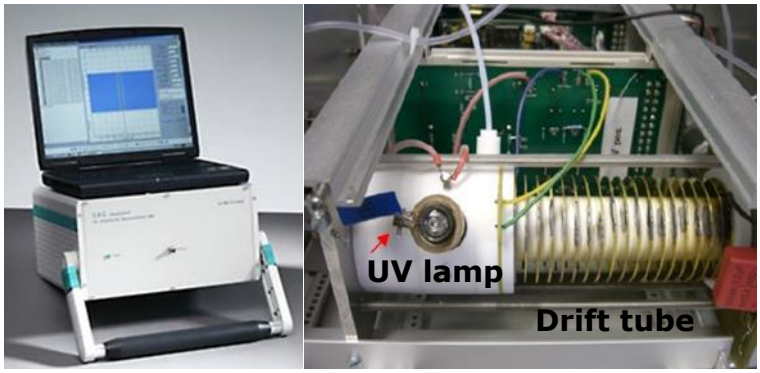

Fig. 1. Photo of the UV-IMS and detail of the UV lamp (signaled with an arrow) and the drift tube of the instrument.

The instrument is 350 × 350 × 150 mm in size, has a tube length of 12 cm, a weight of 5 kg, and uses a current supply of 230 V / 50–60 Hz and a constant voltage supply of 333 V cm^{-1}. The instrument works at room temperature and ambient pressure, being 297 K and 101 kPa respectively. The ion source used for the formation of positive ions was an ultraviolet lamp which provides and ionization energy of 10.6 eV. For the data acquisition GASpector software from GAS (Dortmund, Germany) in a laptop connected to the instrument for store and data processing was used. All spectra were recorded in the positive ion mode and each spectrum was obtained with the parameters shown in **Table 1**.

Table 1. UV-IMS operation parameters.

Parameters	Used values
Number of spectra	25, 50, 250, 300
Average	64
Trigger delay (ms)	0.4
Spectra length (points)	124
Grid pulse width (µs)	100, 500, 1000
Repetition rate (ms)	50
Sampling frequency (Hz)	30.000

- ✧ Number of spectra: the number of single spectra recorded during a measurement.
- ✧ Average: the number of "transient"/ volatile single spectra acquired and averaged to one "persistent"/ transferred single spectrum.
- ✧ Trigger delay: the time (in ms) acquisition "sleeps" after the shutter grid pulse
- ✧ Spectra length: the number of discrete samples taken for each single spectrum, e.g. 124; you may want to choose a sampling frequency (see below) and multiply it with the desired acquisition time (probably some milliseconds) to obtain this number.
- ✧ Grid pulse width: the width of the shutter grid pulse (in µs)
- ✧ Repetition rate: the time (in ms) between each grid pulse/ acquisition start for a "transient" spectrum.
- ✧ Sampling frequency: the frequency (in Hz) used for digitizing the signal.

The UV-IMS does not have a specific sample introduction system, so different systems were used to produce and extract the volatile compounds present in the sample and introduce them into the ion mobility spectrometer. SISs used in the experimental work are described below and summarized in **Table 2**.

Table 2. SISs operation parameters selected when using UV-IMS.

SISs experimental conditions	**Headspace**	**Exponential Dilution**	**Exponential dilution-membrane setup**	**Gas generator**	**Thermal desorption sorbent tube[5]**	**Aspiration pump Euphore chamber**
Volume of sample (µL)	100	1	1	[4]	-	[6]
Head space volume (mL)	10	1000	1000[3]	-	-	-
Heating time (min)	5	1	1	-	-	-
Temperature (ºC)	60 , 80 and 90[1]	Room temperature[2]	Room temperature[2]	35	60-220 ºC 15 ºC min^{-1}	Room temperature
Sample Gas ($mL\ min^{-1}$)	Synthetic air 2.2	Synthetic air 2.2	N_2 5.0	Synthetic air 2.2	N_2 5.0	Filtered air
	80	100	50	100	20	100
Drift gas ($mL\ min^{-1}$) N_2 5.0	140	150	150	150	100	150

[1]60 ºC for benzene, toluene, ethylbenzene and xylene isomers, 80 ºC for acetone and 90 ºC for ethanol. [2]Although the analytes were evaporated using a dryer, the flask was not heated during the measurement. [3]The sample flask was connected to the humidity flask of 500 mL filled with water to increase moisture in the sample gas. [4]Permeation tubes of 4 cm were filled with each liquid analyte and its weight was measured to calculate the permeation rate. [5]Conditions used for desorption step. A temperature ramp was applied to the column filled with sorbent material TENAX to elute the analytes that were transported with the sample gas to the UV-IMS. [6]Liquid pure standard of the analyte was injected to the chamber; concentration of the analyte in the volume of the chamber was calculated at each time.

✧ Static headspace: vials of 10 or 20 mL were used closed with caps with silicone septum in which the liquid sample is placed inside. During the volatilization step, the headspace from volatiles coming from the liquid sample is generated inside the vial during an optimized time and heated if necessary. In the injection step, two switching valves were actuated to have the headspace vapours formed in the vial swept out by the gas stream and transferred to the UV–IMS system for measurement as is shown in **Figure 2**. This system is shown in *Block III chapter 1 and Block IV chapter 4*.

Fig. 2. Photo of the headspace set-up coupled to the UV-IMS.

✧ Exponential dilution system: The exponential dilution procedure involves placing a pure liquid standard with an initial volume in a volumetric flask [e.g. 1 µL of liquid pure standard inside a 1000 mL flask], which is plotted in **Figure 3**. This system was studied in *Block III chapter 1, chapter 2 and 3*.

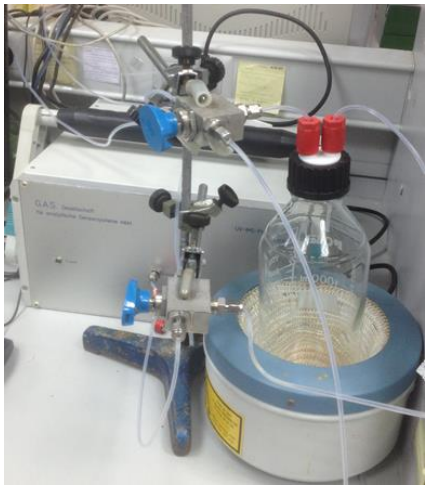

Fig. 3. Photo of the exponential dilution set-up coupled to the UV-IMS.

Evaporation is completed by heating the flask with a hot air gun at 300 ºC during 1 min. Based on the ideal gas law ($PV = nRT$), the number of

molecules of a gas is proportional to its volume; therefore, using the volume, density and concentration of the analyte, the flask volume, atmospheric pressure and room temperature as shown in equation (1):

$$Initial\ concentration(C_0) = \frac{\frac{density\ x\ volume}{molecular\ weight} x\ NA}{flask\ volume} \Big/ NA\ x\frac{1\ mol}{22.4\ L} x \frac{T\ (CN)}{T} x \frac{p\ (CN)}{p} \quad (1)$$

After applying this equation, an initial concentration (C_o) of gaseous standard in gas is obtained [e.g. 2064 $ppm_{(g)}$ for ethanol]. In order to reduce such a high initial concentration, pure gas (synthetic air or nitrogen) is passed through the volumetric flask during a specific time depending on the initial concentration of analyte [e.g. 20 min for ethanol] at a high flow rate (250 mL min^{-1}). The resulting final concentration, C_t ($ppm_{(g)}$), is calculated as follows:

$$C_t = C_o\, e^{(-Ft/V_f)} \quad (2)$$

Being C_o ($ppm_{(g)}$) the initial concentration, F (mL min^{-1}) the flow rate of the gas, t (min) time, V_f (mL) the volume of the dilution flask. The analyte concentration in the dilution flask is thus efficiently reduced [e.g. to 14 $ppm_{(g)}$ for ethanol] and the gaseous standard made ready for IMS measurement. The gas flow (e.g. F = 100 mL min^{-1}) allowed to achieve decreasing concentrations of analytes (C_t) and consequently decreasing signals (V) by diluting the initial concentration (C_o) of analyte in the gaseous sample during the measurement.

- ✧ Membrane set up coupled to an exponential dilution system: the membrane holder was made in steel and has a size of 85x78x35 mm, supplied by Ramem S.A. (Madrid, Spain). It is illustrated in **Figure 4**. Inside the membrane holder there is a cavity in which a commercial polydimethyl silicone membrane or PDMS (SSP-M823) of 16 mm of diameter and different thickness of 76.2 µm and 254 µm, acquired from Specialty Silicone Products (New York, USA) is placed. The membrane holder set-up can be heated by using a heater cord connected to a PID temperature controller also manufactured by

Ramem S.A. (Madrid, Spain). Membrane is cleaned passing through it clean synthetic air and being replaced periodically. This system is fully explained in Block III Chapter 2.

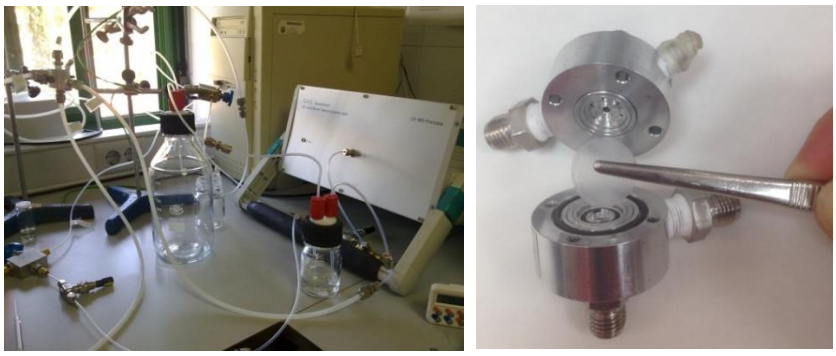

Fig. 4. Photo of the membrane set-up used from RAMEM S.A.

✧ Calibration gas generator: calibration gas generator called OVG-4® and individual permeation tubes already filled with each analyte were provided by Owlstone® (Cambridge, UK), which is illustrated in **Figure 5**. Each permeation tube was conditioned during two days at 35 ºC and passing a constant flow of 100 mL min^{-1} of synthetic air. Concentrations of gaseous standards provided by the gas calibration generator at each time were calculated taking into account the furnace temperature, permeation rate and the flow rate selected, using the software supplied by Owlstone®. This system is shown in *Block III Chapter 1*.

Fig. 5. Photo of the calibration gas generator from Owlstone® used.

- Thermal desorption from sorbent tube: During the adsorption step a steel tube filled with Tenax TA sorbent is connected to an extraction pump to sample air at ambient temperature. Analytes present in air are retained in the sorbent material. In the desorption step, the sorbent tube is connected to the UV-IMS and placed inside a GC oven. Then, a temperature ramp is applied to perform the thermal desorption. The sample gas transferred the analytes to the IMS instrument in order to start the measurement. The experimental set-up is shown in **Figure 6**. This system was used in the experimental work shown in *Block III chapter 3*.

Fig. 6. Photo of the adsorption step with the extraction pump and TENAX column and desorption step of TENAX column performed in a GC oven coupled to UV-IMS.

- Sampling from a Euphore chamber to UV-IMS and UV-DMA: experimental studies of this work were carried out in European Photoreactor (Euphore) located in Valencia (Spain), shown in **Figure 7**. These atmospheric simulators are based on two semi-spherical structures; each one is built with PTFE of 125 μm thick with a volume of 200 m^3. The inlet and outlet ports and other accessories are located in the floor. The air used in the chamber is previously passed through a purification system to reduce the water vapour, solid particles, NO_x and other components to traces levels. Integrated into the flanges there are ports for the injection of reactants and the

sampling lines for different analytical instruments. An extraction pump was connected from the sample lines to UV-IMS and UV-DMA instrument to transport the analytes. The results from these experiments are shown in the *Block VI Result and Discussion* section.

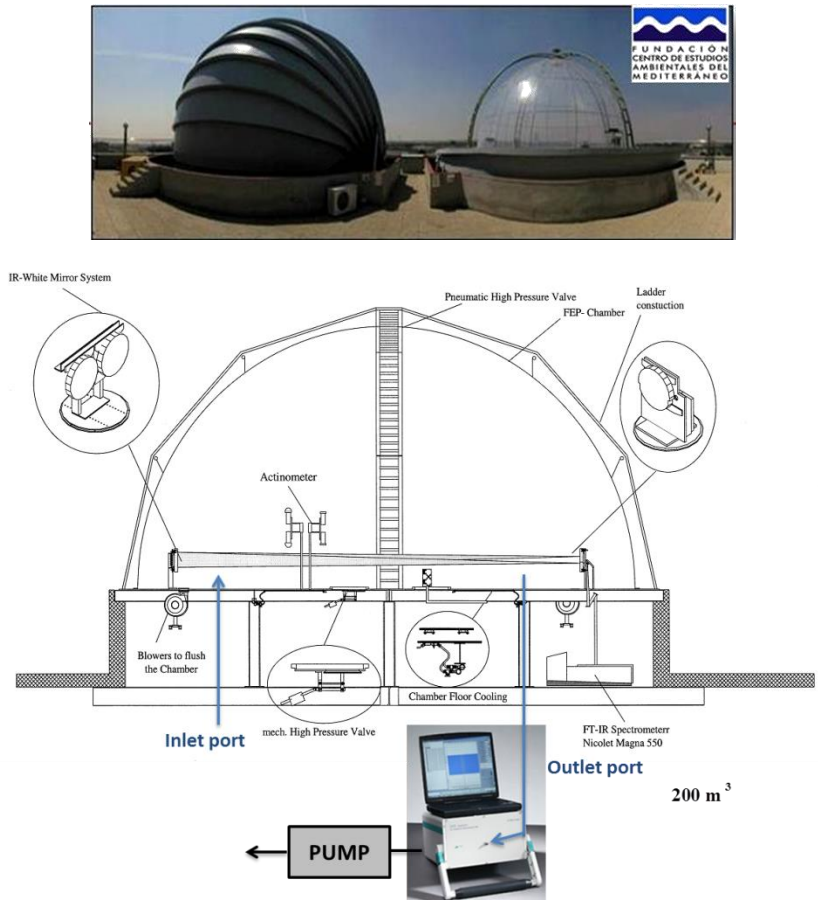

Fig. 7. Photo and schema of Euphore chamber and experimental set-up.

In **Figure 8** is shown as an example a topographic plot and a IMS spectrum obtained with the UV-IMS when using exponential dilution set-up to measure ethanol at 14 $ppm_{(g)}$. The topographic plot shows a collection of spectra obtained during a measurement. The GAS software used, allowed previewing a specific spectrum. Responses obtained can be characterized by its signal intensity in volts (y axis) and drift time in milliseconds (x axis).

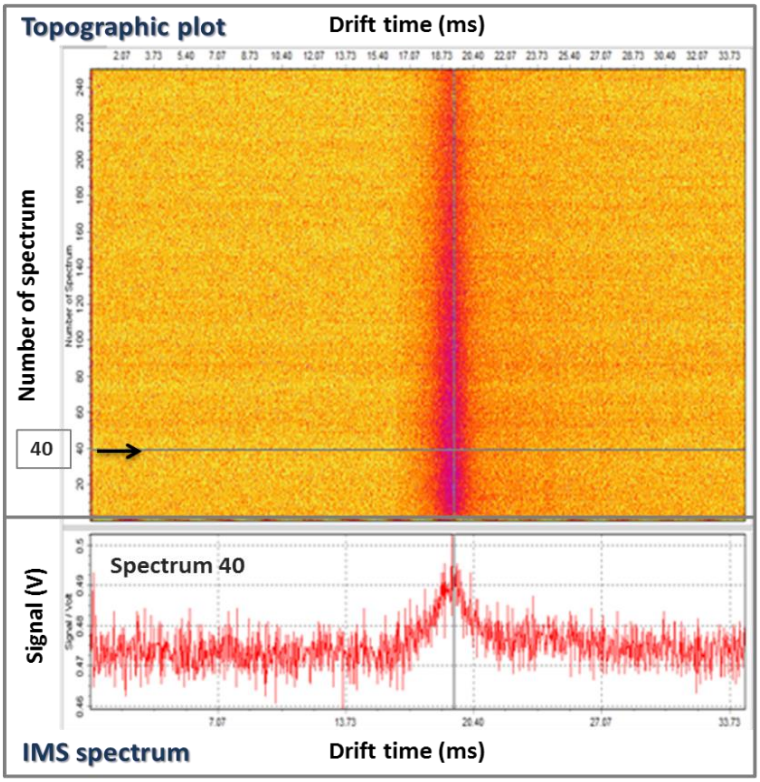

Fig. 8. Topographic plot and IMS spectrum 40 obtaining when a gaseous sample of 14 $ppm_{(g)}$ of ethanol was measured by UV-IMS.

II.4.2. Ion mobility spectrometry with lineal drift tube and tritium source as ionization source

A photo of the Ion mobility spectrometry with lineal drift tube and tritium source as ionization source (GC-^{3}H-IMS) instrument used, (FlavourSpec®, from G.A.S., Dortmund, Germany) is illustrated in in **Figure 9**. The GC–^{3}H–IMS instrument was equipped with a heated splitless injector for direct sampling of the headspace from the sample. For better reproducibility, the instrument was coupled to an autosampler from CTC Analytics AG (Zwingen, Switzerland). The device also presented a ^{3}H ionization source (St. Petersburg, Russia) with an activity of 300 MBq which is below the exemption limit of the EURATOM guideline (1 Gbq). The instrument operates in negative or positive ionization mode.

Fig. 9. Photo of the Flavourspec® used from GAS and internal detail of the instrument.

After incubation at a specific temperature and time, a volume of headspace was automatically injected by a heated syringe (80 ºC) into the GC–^{3}H–IMS equipment. After injection, the carrier gas (nitrogen) passing through the injector inserted the sample into the GC column heated at the optimized temperature for timely separation. The GC column used was 30 m long x 0.25 mm of ID CC filled with 0.5 µm film thickness of methyl, phenyl and vinylsiloxane in a 94:5:1 proportion from CS-Chromatographie Service GmbH (Dürem, Germany). Once ions are formed in the ionization chamber and are focused to a shutter grid, they start to move along the drift tube. The shutter opening time was set to 100 µs, allowing the ions to pass at short pulses towards the separation chamber. A summary of conditions used are shown in **Table 3**. This system is shown in *Block IV Chapter 4, 5 and 6; and Block V Chapter 8*.

Drift tube length was 5 cm which a potential difference of 400 V cm^{-1}. Another IMS device with a longer drift tube of 10 cm, which a potential difference of 500 V cm^{-1} was also used to study how to improve the resolution of the separation between benzene and the reactant ion peak (RIP) signal. Data were acquired by the integrated computer within the equipment, displayed on it and consecutively processed using the software

LAV version 2.0.0 from G.A.S. Library supplied by GAS was also used to identification purposes. All spectra were recorded in the positive ion mode.

Table 3. Experimental conditions followed when using Flavourspec®.

Experimental conditions	**Benzene and phenol in HTF**	**Phenol in environmental samples**	**Toxics in saliva**
	Block IV Chapter 4 and 5	*Block IV Chapter 6*	*Block V Chapter 8*
Pre-treatment			
	Direct measurement (1)	SPE	μSPE
Headspace a utosampler			
Sample volume (μL) or mass (mg)	100	1000	(2)
Vial volume (mL)	20	20	10
Heating time (min)	5	20	20
Heating temperature (ºC)	35	70	80
IMS			
Carrier gas flow (mL min^{-1}) N_2 5.0	10	10	5
Drift gas flow (mL min^{-1}) N_2 5.0	250(3)	250	250
Injector (ºC)	80	80	80
GC column (ºC)	40	40	40
Drift tube temperature (ºC)	65	65	75

(1) Concentrated degraded HTF samples were diluted with raw HTF. (2) Desorption of the μSPE device was performed in the vial. N_2 5.0 was used for carrier gas and drift gas. (3) The drift gas flow rate for IMS with 10 cm drift tube length was 150 mL min^{-1}.

II.4.3. Differential mobility spectrometer with niquel source as ionization source

The Differential mobility spectrometer with niquel foil tube source as ionization source (^{63}Ni-DMS) used in the study was a planar device (SDP-1

Sionex, MS USA) with a 0.5 mm gap between the two parallel electrodes and a 5 mCi (or 185 mBq) ^{63}Ni ionisation source illustrated in **Figure 10**.

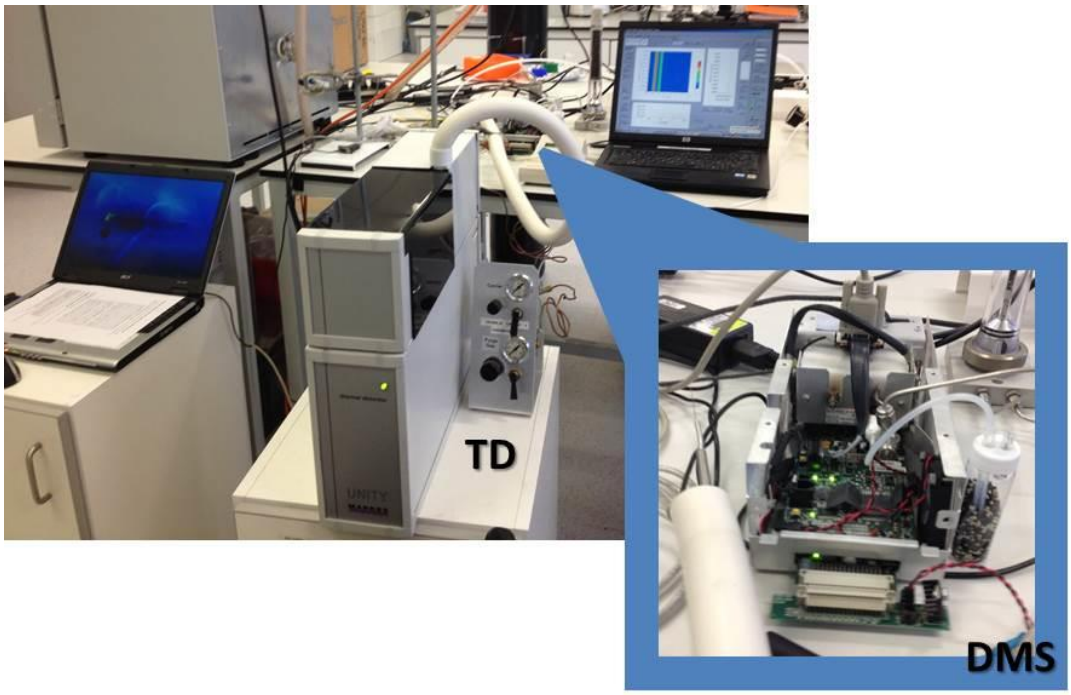

Fig. 10. Photo of the Ni^{63}-DMS used and detail of the thermo desorption unit used for saliva samples.

The DMS was controlled through a virtual instrument (Sionex DMx Expert, Version 2.4.0) run on the Dell laptop (Inspiron, 4000). This system is shown in *Block V Chapter 7.* The data were saved to a Microsoft Excel spreadsheet file for post-run processing. The transport gas was purified nitrogen with water concentrations maintained in the range 22.5 to 26.3 mg m^{-3} (Panametrics Series 35 hygrometer). Multi-linear regression was used to optimise the differential mobility spectrometer operating parameters of: dispersion-field; temperature; number of compensation-field steps; and compensation-field step duration (DOE PRO XL Software for Microsoft Excel, SigmaZone).

Two instrument configurations were used in this study. Method development and calibration were undertaken using liquid injections to a GC-DMS. Characterisation of the recovery of the analytes from spiked saliva samples was undertaken using a thermal desorption unit interfaced to the GC-DMS. For calibration purposes, the DMS described above was coupled to a GC. A 30 m long wall-coated open-tubular capillary GC column with an internal diameter of 0.32 mm and a 0.5 µm thick trifluoro propyl methyl polysiloxane stationary phase (Rtx-200MS, Restek, UK) was interfaced to a DMS with a heated transfer-line configured as a sheath flow interface made from a 20 cm length of ¼" stainless steel tubing with the GC-column axially aligned within the tube. The transfer-line was heat-traced with heating tape and maintained at 100°C.

For saliva analysis, a two-stage thermal desorption unit (Markes International Unity 2) as shown in **Figure 10** was used to recover VOC extracts from saliva samples with a cold trap for refocusing the recovered VOCs packed with a mixed bed of Tenax TA and Carbograph 1TD. The 1.5 m long transfer line to the GC-column was a deactivated methyl-capped capillary column (Restek, UK) with an internal diameter of 0.23 mm i.d. maintained at 110°C).

B) OTHERS INSTRUMENTS

II.4.5. Gas chromatography-Mass Spectrometry

Gas chromatography-Mass Spectrometry (GC–MS) analyses were performed on a Saturno 2200 instrument from Varian (Palo Alto, USA). HTF samples were diluted in dichloromethane (1 g/50 mL) and 1 µL aliquots injected at 265 ºC in the split mode (split ratio 1/50). The chromatographic column used (30 m, 0.25 mm i.d., 0.25 µm film thickness) was packed with 5% phenyl silicone from Agilent (Santa Clara, USA). Helium (99.999%) at a flow rate of 1 mL min^{-1} was used as carrier gas from Praxair (Danbury, USA). The temperature programme was as follows: 35 ºC (2 min) and 10

ºC/min ramp to 285 ºC (5 min). Ions were detected in the full scan mode (0.5 s/scan), using the *m*/*z* range 45–400.

II.4.6. Gas chromatography-flame ionization detector

Gas chromatography-flame ionization detector (GC-FID) analyses were carried out using a Varian CP 3800 fitted with a split/splitless injector and FID from Perkin Elmer (Massachusetts, USA). Helium (99.999%), from Praxair (Danbury, USA), was used as the carrier gas and was set at 1 mL min^{-1}. The separation was performed with a HP-1, fused silica capillary column, 30 m x 0.25 mm i.d. with 1.0 µm stationary film thickness of 100 % polydimethylsiloxane from Agilent (Santa Clara, USA). The column temperature was programmed as follows: initial oven temperature 33 °C for 4 min, increasing to 180 °C at 6 °C min^{-1}, then holding for 3 min and then directly to 300 °C at 15 °C min^{-1} and holding for 8 min. The injector temperature was set to 275 °C, with an injection volume of 1 µL, and desorption was carried out in the split mode (split 1/10). The detector temperature was held at 310 °C. For the analysis, 1-chlorotetradecane (10 mg mL^{-1}) was used as an internal standard.

II.4.7. Fourier transform medium infrared spectroscopy

Infrared spectra were obtained by transmission mode, using a Fourier transform medium infrared spectroscopy (FT-MIR), Tensor 27 spectrometer from Bruker Optik GmbH (Ettlingen, Germany) equipped with CsI beam splitters and a DTGS detector. Spectra were acquired by using the software OPUS v.6.5, also from Bruker. 200 scans for each measurement were recorded in the wavelength range of 4000-200 cm^{-1} with a resolution of 4 cm^{-1}. For analysis, a droplet (2 µL) of HTF sample was added to KBr to form a pellet that was then inserted into the instrument for measurement.

III. Potential of UV-Ion mobility spectrometry for environmental analysis

III. Potencial de la espectrometría de movilidad iónica UV para el análisis ambiental

IMS is a sensitive, quick and inexpensive technique; these advantages make it highly suitable for environmental analysis. In this *Block III*, different strategies to generate gaseous standards were tested to calibrate a portable UV-IMS. Problems detected using this instrument were overcome by using a membrane set-up to avoid humidity interference and a pre-separation step to improve selectivity.

Different alternatives to generate gaseous standards were tested in *Chapter 1*, in order to calibrate the UV-IMS prior to real sample analysis. Two home-made systems were presented. One of them is based on a static headspace system for measuring analytes present in liquid samples and the other was an exponential dilution set-up for measuring analytes in gaseous samples. Also a gas generator based on permeation tubes was used. These SISs were coupled to the UV-IMS for the analysis of standards. The analytical performance of the three systems was studied and the results obtained were compared.

The ion chemistry related to the formation of ion products in the drift tube of the UV-IMS can be affected by moisture. In *Chapter 2*, the changes on the IMS spectra with high humidity were described for BTEX compounds. As well, a membrane set-up was proposed as an alternative to avoid the entrance of humidity to the UV-IMS when measuring humid gaseous samples.

Finally, in order to improve low selectivity obtained with the UV-IMS, a Tenax TA trap was coupled to the IMS instrument as can be seen in *Chapter 3*. BTEX from gaseous samples were retained in this trap and then desorbed thermally for its analysis by UV-IMS. The method proposed was used for separate efficiently benzene and toluene from the rest of compounds present in the gaseous sample.

Chapter 1
Calibration of ion mobility spectrometer with gaseous standards

Capítulo 1

Calibración del equipo de movilidad iónica con estándares gaseosos

Talanta 111 (2013) 111–118

Contents lists available at SciVerse ScienceDirect

Talanta

journal homepage: www.elsevier.com/locate/talanta

A COMPARATIVE STUDY BETWEEN DIFFERENT ALTERNATIVES TO PREPARE GASEOUS STANDARDS FOR CALIBRATING UV-ION MOBILITY SPECTROMETERS

Laura Criado-García, Rocío Garrido-Delgado, Lourdes Arce, Miguel Valcárcel*

Department of Analytical Chemistry, Annex C-3 Building, Campus of Rabanales, Institute of Fine Chemistry and Nanochemistry, University of Córdoba, 14071 Córdoba, Spain

An UV-Ion Mobility Spectrometer is a simple, rapid, inexpensive instrument widely used in environmental analysis among other fields. The advantageous features of its underlying technology can be of great help towards developing reliable, economical methods for determining gaseous compounds from gaseous, liquid and solid samples. Developing an effective method using UV-Ion Mobility Spectrometry (UV-IMS) to determine volatile analytes entails using appropriate gaseous standards for calibrating the spectrometer. In this work, two home-made sample introduction systems (SISs) and a commercial gas generator were used to obtain such gaseous standards. The first home-made SIS used was a static headspace to measure compounds present in liquid samples and the other home-made system was an exponential dilution setup to measure compounds present in gaseous samples. Gaseous compounds generated by each method were determined on-line by UV-IMS. Target analytes chosen for this comparative study were ethanol, acetone, benzene, toluene, ethylbenzene and xylene isomers. The different alternatives were acceptable in terms of sensitivity, precision and selectivity.

Keywords: gaseous standards, head-space, exponential dilution, gas generator, calibration, UV–IMS.

© 2013 Elsevier B.V. All rights reserved

1. Introduction

Ion Mobility Spectrometry (IMS) is a useful technique for on-field analysis [1]. In fact, the expeditiousness, trace-level sensitivity and operational simplicity of IMS have aroused increasing interest in its use in a variety of areas including pharmaceutical, forensic, biomedical and environmental sciences. For example, the IMS technique has been successfully used for the environmental monitoring of hazardous compounds. Among other advantages, IMS uses an inexpensive equipment running under atmospheric pressure [2], which makes it highly portable and suitable for the on-line monitoring of volatile organic compounds (VOCs) such as benzene, toluene and xylene isomers [3, 4].

The operational principle behind IMS is very simple [5-10]. Thus, ions generated by an ionization source are driven to a Faraday plate (the detector) held in the end of the drift tube under a constant, uniform electric field, providing the number of ions detected a measure of the analyte concentration. The time each ion takes to travel the distance from the shutter grid to the detector, which is called the "drift time", depends on the ion mass, charge, shape and size. From the drift time and the instrumental parameters the reduced ion mobility, K_0 ($cm^2\ V^{-1}\ s^{-1}$), can be calculated considering the influence of ambient pressure (P) and temperature (T) as is showing in the Equation (1):

$$K_0 = \left(\frac{l}{tE}\right)\left(\frac{PT_0}{P_0T}\right) \qquad (1)$$

being l (cm) the length of the drift region, E ($V\ cm^{-1}$) the electric field strength, t (s) the drift time, P the atmospheric pressure (P_0 = 101325 Pa) and T the temperature of the drift gas (T_0 = 273 K).

The high operational flexibility of IMS facilitates the measurement of a variety of analytes in liquid, solid and gaseous samples; however, only gaseous samples can be directly introduced into an ion mobility

spectrometer, so analytes present in liquid and solid samples must be volatilized prior to introduction into the instrument. An efficient sample introduction system (SIS) is therefore essential for accurate measurements by IMS [11]. If the target analytes are inefficiently extracted or transferred to an IMS instrument, their measurements will hardly be representative of the analytical problem at hand. This shortcoming led us to develop efficient types of SISs according to the type of sample allowing preparing calibration gas standards and introducing real samples to be measured. Measuring gaseous analytes (e.g. ethanol, acetone, benzene, toluene, ethylbenzene and xylene isomers) in air or liquid samples by UV–IMS requires calibrating the instrument with an appropriate method. Some commercial gas generators can produce traceable, precise, repeatable and accurate concentrations of chemicals and calibration gas standards [12-14]. Otherwise, this type of generation of gaseous standards is usually highly time-consuming and expensive. These two features are the opposite of the main advantages of the UV-IMS (rapid and cheap technique). For this reason, two fast and inexpensive SISs as reliable as commercial gas generators were coupled to UV-IMS equipment to study their potential to produce standard gaseous compounds. The operational simplicity and relatively low cost make these alternatives very promising for calibrating IMS instruments. The aim of this work was to characterize their qualitative and quantitative response in the determination of VOCs gaseous standards by UV–IMS. The ion mobility spectra, reduced mobilities and analytical figures of merits of each analyte studied are also discussed.

2. Experimental

2.1. UV–Ion Mobility Spectrometer

The UV–IMS instrument used, supplied by Gesellschaft für Analytische Sensorsysteme (GAS, Dortmund, Germany), is depicted in **Figure 1**.

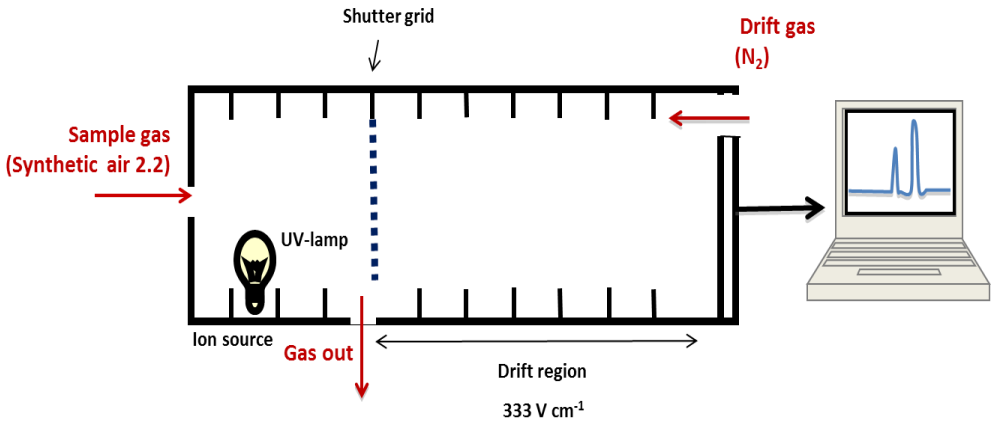

Fig. 1. Scheme of the UV-IMS instrument used.

The instrument is 350 × 350 × 150 mm in size, has a tube length of 12 cm, a weight of 5 kg, and uses a current supply of 230 V / 50–60 Hz and a constant voltage supply of 333 V cm^{-1}. All spectra were recorded in the positive ion mode and acquired under the conditions listed in **Table 1**. The temperature and pressure in the drift tube were at 297 K and 101 kPa, respectively.

Table 1. UV-IMS operational parameters used in this work.

Parameter	Value selected
Number of spectra	25 and 250
Average	64
Trigger delay (ms)	0.4
Spectra length (points)	1024
Grid pulse width (µs)	500
Repetition rate (ms)	50
Sampling frequency (Hz)	30000

2.2. Generation of gaseous standards

Obtaining gaseous standards is a much more difficult task than producing liquid standards. In fact, the production of gaseous standards is subject to some problems including the wall memory effect and instrument noise [15, 16]. This led us to study two home-made systems for obtaining

gaseous standards to determine analytes present in liquid and gaseous samples which are shown in **Figure 2A** and **2B**. The results obtained with the exponential dilution method were compared with the gaseous standards generated by a commercial system which is illustrated in **Figure 2C**. The operating conditions used are shown in **Table 2**.

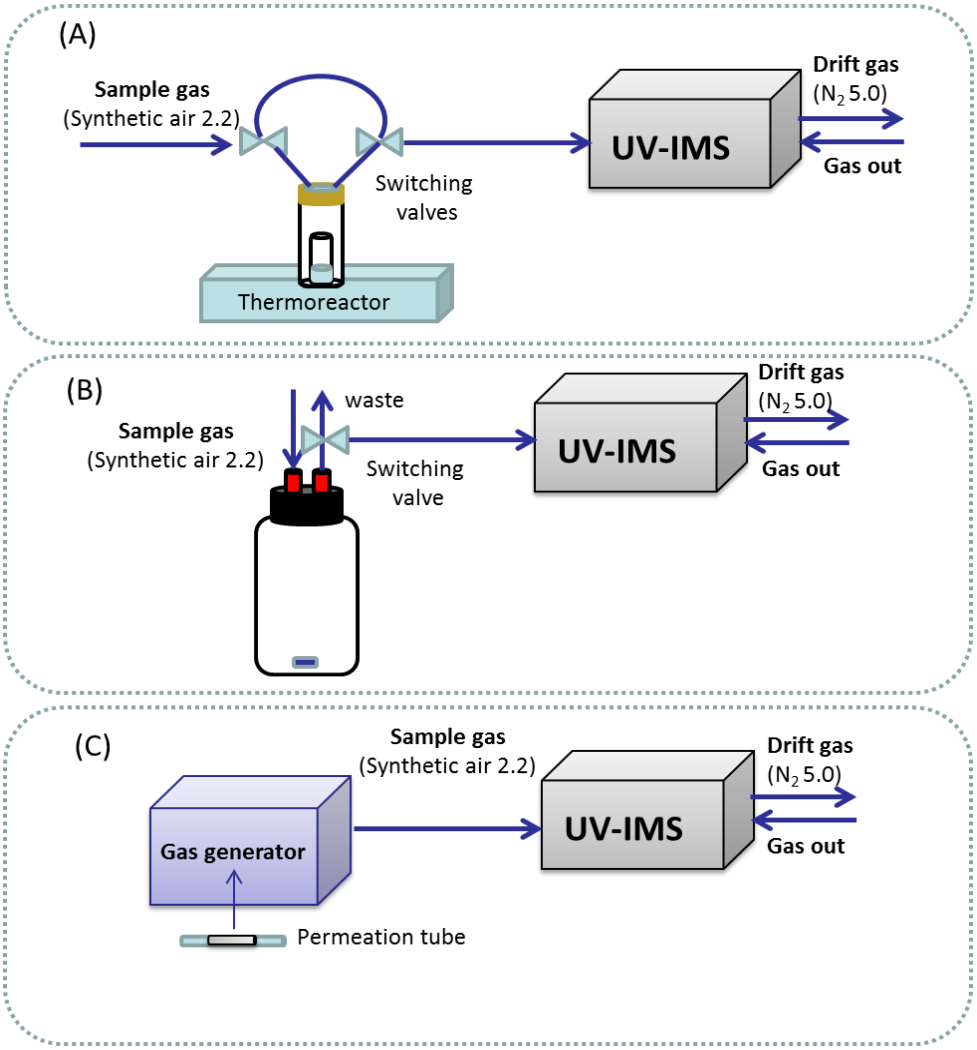

Fig. 2. Sample introduction system used to obtain gaseous standards from a head-space vial (A), an exponential dilution flask (B) or a calibration gas generator (C).

VOCs employed included ethanol, acetone, benzene, toluene, ethylbenzene, *o*-xylene, *m*-xylene and *p*-xylene, all supplied by SIGMA (St Louis, MO, USA). Their physical and chemical properties are summarized in

Table 3. These analytes were selected on the grounds of their belonging to representative families of VOCs.

Table 2. Operational conditions used to obtain gaseous standards by using the three proposed procedures.

Experimental conditions	Head-space method	Exponential dilution method	Gas Generator
Volume of sample (µL)	100	1	(3)
Head space volume (mL)	10	1000	-
Heating time (min)	5	1	-
Temperature (ºC)	60, 80 and 90(1)	Room temperature(2)	35
Sample gas (mL min^{-1}) Synthetic air 2.2	80	100	100
Drift gas (mL min^{-1}) N_2 5.0	140	150	150

(1) Different temperatures were chosen to generate the head-space vapors for each analyte: 60 ºC for benzene, toluene, ethylbenzene and xylene isomers, 80 ºC for acetone and 90 ºC for ethanol. (2) Although the analytes were evaporated using a dryer, the flask was not heated during the measurement. (3) Permeation tubes of 4 cm were filled with each liquid analyte and its weight was measured to calculate the permeation rate.

Table 3. Physical and chemical properties of VOCs measured by UV-IMS.

Family	IUPAC name	Molecular weight (g mol^{-1})	Density (g mL^{-1})	Boiling point (ºC)	Polarity	Ionization energy (eV)	Drift time obtained by exponential dilution (ms)
Ketones	Acetone	58.04	0.79	56.3	5.1	9.70	18.93
Alcohols	Ethanol	46.07	0.78	78	-	9.99	18.20
Aromatics	Benzene	78.11	0.87	80.05	2.4	9.24	15.83
	Ethylbenzene	106.17	0.86	136	-	8.77	17.63
	Toluene	92.14	0.86	110.8	2.4	8.83	16.69
	Xylene (*m*-, *o*-, *p*-)	106.16	0.86	138	2.5	8.44	17.43,17.38, 17.47

2.2.1. Generation of gaseous standards by static head-space system

Gaseous standards were prepared from liquid standards when performing the home-made head-space system shown in **Figure 2A**. This system could be suitable to determine analytes present in liquid samples (e.g. VOCs present in water samples). In each analysis, 100 µL of liquid standard was placed in a 1.5 mL glass vial which was in turn inserted into a 10 mL vial and tightly closed with a Teflon septum. Samples were heated in an Eco 1G Thermoreator (Velp Scientific) for 1 min (volatilization step) while a stream of synthetic air 2.2 from Carburos Metálicos (Barcelona, Spain) was passed through the UV–IMS equipment. The flow rates (80 mL min^{-1} for the sample gas and 140 mL min^{-1} for the drift gas) were controlled by an Altech Digital Flow Check HRTM device from Chromatographic Service GmbH. After 5 min heating, two stainless-steel switching valves (Selectomite®-7177G2Y, HOKE Incorporated, Spartanburg, SC) were actuated to have the head-space vapours formed in the vial swept out by the synthetic air stream and transferred to the UV–IMS system for measurement (injection step). Connections were made with 1/8-inch Teflon tubes obtained from Varian (Harbor City, Los Angeles, CA, USA) [17].

The calibration curves were obtained by preparing individual stock solutions of 100 mg L^{-1} for each analyte. Dilutions were made by placing 10, 50, 100, 200, 300, 400 or 500 µL of stock solutions in a 10 mL volumetric flask and making to volume with distilled water purified by passage through a Milli-Q system from Millipore (Bedford, MA, USA). These standard solutions were prepared on a daily basis and stored at ambient temperature until analysis.

2.2.2. Generation of gaseous standards by exponential dilution flask

Exponential dilution is a commonly used method for accurately delivering a range of concentrations to an IM spectrometer. This system could be used to determine analytes present in gaseous samples (e.g. VOCs in air samples).The home-made exponential dilution set-up of **Figure 2B** was used here to prepare gaseous standards.

Concentrations are given in parts-per-million in gas, $ppm_{(g)}$, which express the number of analyte molecules present in a million of molecules of air. Based on the ideal gas law ($PV = nRT$), the number of molecules of a gas is proportional to its volume; therefore, $ppm_{(g)}$ was calculated from this equation, using the volume, density and concentration of the analyte, the flask volume, atmospheric pressure and room temperature. The exponential dilution procedure involves placing a pure liquid standard with an initial volume of 1 µL in a 1000 mL (V_f) volumetric flask. Then, hot air is applied locally to the flask with a hot air gun to evaporate the little drop of 1 µL of analyte approximately at 300 ºC only during 1 min. It results in an initial concentration (C_o) of gaseous standard [e.g. 2064 $ppm_{(g)}$ for ethanol], usually in synthetic air. In order to reduce such a high initial concentration, synthetic air 2.2 is passed through the volumetric flask during a specific time depending on the initial concentration of analyte [e.g. 20 min for ethanol] at a high flow rate (250 mL min^{-1}). A magnetic stir bar is placed inside the flask to stir the gas at 900 rpm. The resulting final concentration, C_t ($ppm_{(g)}$), is calculated as follows:

$$C_t = C_o\, e^{(-Ft/V_f)} \qquad (2)$$

Being C_o ($ppm_{(g)}$) the initial concentration, F (mL min^{-1}) the flow rate of the gas, t (min) time, V_f (mL) the volume of the dilution flask.

The analyte concentration in the dilution flask is thus efficiently reduced [e.g. to 14 $ppm_{(g)}$ for ethanol] and the gaseous standard made ready for IMS measurement. The synthetic air 2.2 at a flow rate (F = 100 mL min^{-1}) allowed to achieve decreasing concentrations of analytes (C_t) by diluting the initial concentration (C_o) of analyte in the gaseous sample. Therefore, the analyte signal and concentration decreases during the measurement.

2.2.3. Generation of gaseous standards by a calibration gas generator

Finally, a calibration gas generator called OVG-4® from Owlstone® (Cambridge, UK) shown in **Figure 2C** was used to generate gaseous standards of acetone, benzene, ethylbenzene, toluene and p-xylene.

Individual permeation tubes already filled with each analyte were provided by Owlstone® (Cambridge, UK). Before starting the measurement of gaseous standards by UV-IMS, it was necessary to condition each permeation tube during two days heating at 35 ºC and passing a constant flow of 100 mL min^{-1} of synthetic air. Concentrations of gaseous standards provided by the gas calibration generator at each time were calculated taking into account the furnace temperature, permeation rate and the flow rate selected, using the software supplied by Owlstone®.

3. Results and discussion

Calibration standards must be prepared in a similar matrix or environment to that of the target analytes. This led us to propose different strategies to generate gaseous standards depending on whether the target analyte is present (in a liquid or gaseous sample). One home-made system based on head-space could be suitable to analyse VOCs present in liquid samples and another in which exponential dilution was performed to measure analytes present in gaseous samples. The results obtained from the gaseous home-made system performing exponential dilution method were also compared with the results provided by the commercial gas generator.

3.1. Evaluation of alternatives proposed to generate gaseous standards

3.1.1. Generation of gaseous standards by a static head-space system

The SIS previously reported by our research group [17], and others for the same purpose [5, 15], cannot be used to determine analytes present in aqueous samples (e.g. waste water from a petrol station) because the liquid sample tends to condensate in the Teflon tube connecting the SIS to the UV–IMS instrument, which can seriously damage the equipment. Additionally, placing liquid standards directly in the vial present another

problem; thus, the synthetic air stream drags the gaseous compounds formed in the vial, which leads to exceedingly strong signals and, occasionally, delays subsequent measurements owing to the need to clean the equipment. These problems were not initially observed by the authors [17] since the initial intended use of this SIS was to measure compounds present in non-aqueous, solid or even viscous samples (e.g. fat from pig or olive oil), these shortcomings led us to introduce a slightly modification in the SIS. In this work, the liquid standard was introduced in a little vial and it was placed in a bigger vial tightly closed. Such a simple modification prevented that the flow of gas fell on the standard liquid, allowing liquid standards to be measured without overload the IMS signal. In **Figure 3**, different systems tested to perform head-space method are shown, namely: placing a 1.5 mL vial inside a 10 mL vial (A); a 250 µL Eppendorf tube inside a 10 mL vial (B) and a 1.5 mL vial inside a 20 mL vial (C).

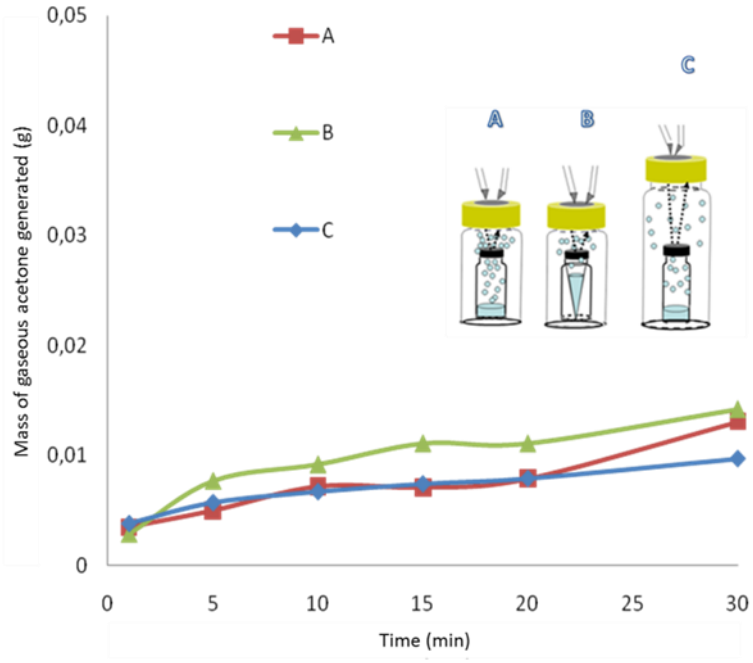

Fig. 3. SISs tested to perform head-space method.

In all systems, 100 µL of acetone was placed inside an opened vial which was in turn placed in a tightly closed vial. These vials were heated at 50 ºC during times from 1 up to 30 minutes. During these times, a loss weight of the liquid standard was observed due to the fact that liquid molecules of acetone passed to the gas phase in the head-space inside the bigger vials. As can be seen in **Figure 3**, an almost identical amount of gaseous acetone was produced in all systems used during the different heating times tested. For this reason, any of these devices could be used to measure VOCs present in liquid samples. In this work, the system A was selected.

Once the best SIS to perform the head-space method was chosen, sample volume, heating time, head-space volume, temperature, sample gas and drift gas were optimized with a view to maximizing repeatability and peak height of the ion mobility signal. The optimum values selected are summarized in **Table 2**.

3.1.2. Generation of gaseous standards by exponential dilution

Exponential dilution was carried out in a flask of 1 L using the experimental set-up shown in **Figure 2B**. The entire liquid standard (1 µL) deposited inside the flask was quickly evaporated with a hot air gun. Heating and stirring were assessed in this experimental set-up. Stirring was found to improve the analytical signals. Also, using two flasks in the sequence led to a slightly increased signal as seen in previous work [18]; however, it was obtained a worse reproducibility in the measurements. Heating the flask at 30 ºC under stirring also detracted from signal intensity. Finally, as recommended in a previous study [19] to enhance sensitivity, a single 1000 mL flask containing a magnetic stir bar was used in this work. Therefore, exponential dilution is an effective choice for calibrating UV–IMS device instruments for analytes present in air samples. This SIS affords a simple, inexpensive method suitable for on-site analysis.

3.2. Analytical features

Analytical features of each method proposed in this work are shown in this section. Different analytes were used for each method depending on their availability.

3.2.1. Calibration curves, Limits of Detection (LODs) and Limits of Quantification (LOQs)

The calibration curve, LODs and LOQs obtained for the head-space set-up are shown in **Table 4**. When the head-space method was used, the minimum concentration detected was much higher than the minimum concentration detected with exponential dilution set-up. The reason of this fact could be that when head-space method was performed, the liquid sample was heated to generate volatiles compounds which represent only a fraction of the total compounds present in liquid sample place inside the vial. Therefore, only the fraction of compounds passing to the gas phase was measured by UV-IMS. Moreover, the effect of moisture should be taken into account when the gaseous fraction is measured from a liquid sample since it might reduce the signal intensity. Notice that the UV-IMS device used in this work has not any membrane in the inlet port.

Table 4. Calibration curve, LOD and LOQ obtained with the head-space set-up.

	Regression equation				
Analyte	**Intercept ± S_a**	**Slope ± S_b**	**Regression coefficient (R^2)**	**LOD* (ppm)**	**LOQ* (ppm)**
Acetone	0.0018 ± 0.0043	0.0043 ± 0.0002	0.977	3.0	10.0
Ethylbenzene	0.011 ± 0.002	0.00174 ± 0.00008	0.983	3.4	11.5
Benzene	0.005 ± 0.004	0.0026 ± 0.0002	0.933	4.6	15.4
Toluene	0.014 ± 0.003	0.0025 ± 0.0001	0.963	3.6	11.8
m−Xylene	0.011 ± 0.003	0.0032 ± 0.0002	0.959	2.8	9.4
o−Xylene	0.012 ± 0.002	0.0026 ± 0.0001	0.969	2.3	7.7
p−Xylene	0.011 ± 0.003	0.0017 ± 0.0001	0.944	5.3	17.6

*LODs and LOQs were calculated as 3 and 10 times, respectively, the standard deviation of the intercept of the calibration curve divided by its slope.

On the other hand, the results obtained (LODs, LOQs and precision values) using the exponential dilution set-up proposed to calibrate the UV-IMS device when analytes are present in air samples have been compared with the values obtained with the calibration gas generator. The results are illustrated in **Table 5**.

LODs obtained with exponential dilution set-up were low [below 1 ppm (g)] for ethanol and acetone, but slightly higher for aromatics such as p-xylene and toluene [1.8 and 1.6 $ppm_{(g)}$] respectively. Obviously, LODs and LOQs were lower using the commercial gas generator due to the fact that major inaccuracies in the preparation of gaseous standards were avoided. This comparison was vital to assess the suitability of each methodology proposed in this work. While the exponential dilution method was a cheap and quick alternative to calibrate IMS device, the calibration gas generator was successfully used to prepare lower concentrations of analyte in a more precise way, but unavoidably investing more money and time.

The main difference between the methods proposed in this work is that head-space is used for measuring analytes present in liquid samples in a cheap and rapid way. On the other hand, exponential dilution set-up and generator gas calibrator device are used when analytes are present in gaseous samples. As a result, it is essential that these two methods: head-space and exponential dilution set-ups be used appropriately depending on the matrix in which is present the analyte.

3.2.2. Precision

Precision expressed as RSD (%), was assessed for target analytes performing head-space set-up, exponential dilution system and using the calibrator gas generator described in **Figure 2**. Intraday RSD values were lower for drift time in all cases studied.

Table 5. Values of LOD and LOQ obtained with the exponential dilution method and calibrator gas generator.

Analyte	Regression equation				LOD* ($ppm_{(g)}$)	LOQ* ($ppm_{(g)}$)
	Procedure	Intercept ± S_a	Slope ± S_b	Regression coefficient (R^2)		
Ethanol	Exponential dilution	0.041 ± 0.002	0.0079 ± 0.0002	0.989	0.8	2.5
Acetone	Exponential dilution	0.012 ± 0.003	0.0109 ± 0.0004	0.981	0.8	2.8
	Gas generator	0.160 ± 0.003	0.0245 ± 0.0005	0.967	0.4	1.2
Ethylbenzene	Exponential dilution	0.04 ± 0.01	0.027 ± 0.001	0.968	1.1	4.1
	Gas generator	0.049 ± 0.005	0.140 ± 0.005	0.955	0.1	0.4
Benzene	Exponential dilution	0.054 ± 0.010	0.027 ± 0.001	0.973	1.1	3.7
	Gas generator	0.010 ± 0.001	0.0094 ± 0.0004	0.984	0.3	1.1
Toluene	Exponential dilution	0.03 ± 0.02	0.035 ± 0.002	0.923	1.6	5.4
	Gas generator	0.083 ± 0.001	0.032 ± 0.001	0.992	0.1	0.3
m−Xylene	Exponential dilution	0.11 ± 0.02	0.041 ± 0.002	0.971	1.5	4.9
o−Xylene	Exponential dilution	0.11 ± 0.02	0.041 ± 0.002	0.964	1.5	4.9
p−Xylene	Exponential dilution	0.013 ± 0.002	0.0033 ±0.0002	0.939	1.8	6.1
	Gas generator	0.118 ± 0.002	0.078 ± 0.003	0.993	0.1	0.3

*LODs and LOQs were calculated as 3 and 10 times, respectively, the standard deviation of the intercept of the calibration curve divided by its slope.

Average values of RSD for head-space (3.57% for peak height and 0.40% for drift time) were slightly lower than the values obtained for exponential dilution set-up (10.46% for peak height and 0.54% for drift time). A reason of this fact could be the irreproducibility of preparing the gaseous samples in the dilution flask. On the other hand, the precision using the commercial gas generator have been also evaluated in a same day (0.30% for peak height and 0.22% for drift time).

Therefore, RSD values obtained using the calibration gas generator, were lower than the values obtained with both home-made methods. These values demonstrated the high precision of this commercial device to prepare individual standard solutions. With this study, it may seem that there is evidence of IMS repeatability when good practices are followed.

3.2.3. Selectivity

Selectivity was assessed by measuring 5, 10, 20 $ppm_{(g)}$ of a gaseous mixture containing five BTX (benzene, toluene, m-xylene, o-xylene and p-xylene) and measuring the head-space generated by heating at 60 ºC a liquid mixture containing 5, 10 and 20 ppm of the same analytes in water under the experimental conditions described in **Table 2** and in **Figure 2A** and **2B**, respectively.

Only one intense peak at 17.78 ms which could correspond to a monomer (M^+) and a little peak shoulder at 17.98 ms were obtained from a gaseous mixture of the analytes which is illustrated in **Figure 4A**; the peak increased from 5 to 20 $ppm_{(g)}$ keeping the same shape and decreasing slightly the little shoulder when the concentration was increased. The global signal of all analytes from a gaseous mixture appeared at a slightly longer drift time (17.78 ms) compare to the signal obtained for the individual analytes (benzene at 15.83 ms, toluene at 16.69 ms, m-xylene at 17.43 ms, o-xylene at 17.38 ms and p-xylene at 17.47 ms). These differences in drift times can be ascribed to ion-molecules reactions produced inside the UV-IMS device. So, when a gas mixture of different analytes is introduced in the UV-IMS device a cluster of higher molecular weight might be formed.

Therefore, more time is needed for this new ion to reach the end of the drift tube and be detected by the Faraday plate. In addition, this bigger ion cannot be resolved in the drift tube due to the structural similarities of the target analytes.

On the other hand, when vapours from the liquid sample from 5 to 20 ppm were measured, which is shown in **Figure 4B**, it could be assumed that the first peak obtained in the IMS spectrum correspond to a monomer ion (M^+ at 16.65 ms) and the second peak correspond to a dimmer ion (M^{2+} which appear later in the IMS spectrum at 17.61 ms).

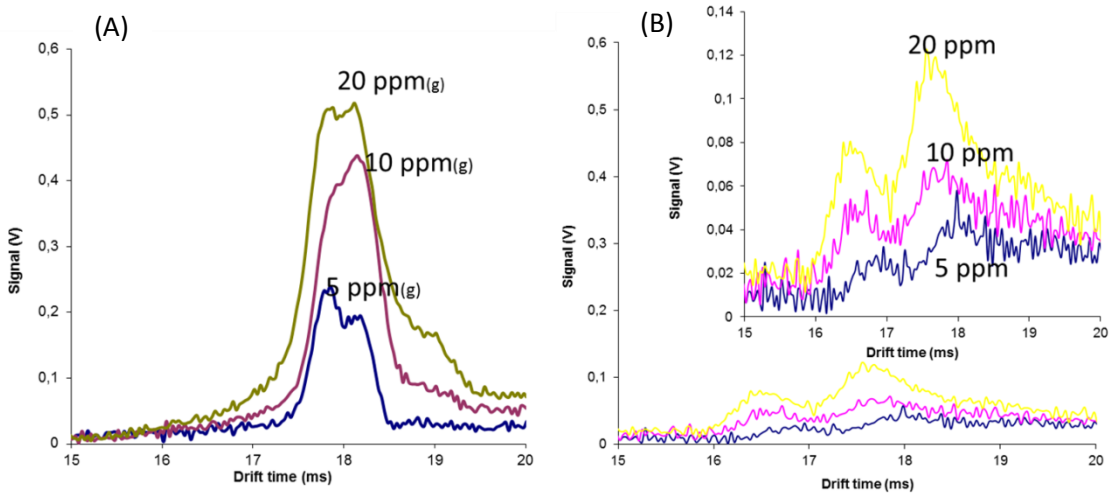

Fig. 4. UV-IMS spectrum for (A) a blended gaseous sample containing 5, 10 and 20 $ppm_{(g)}$ of benzene, toluene, m-xylene, o-xylene and p-xylene in a 1 L flask and (B) the vapours from the head-space generated by heating at 60 ºC a liquid mixture containing 5, 10 and 20 ppm of benzene, toluene, m-xylene, o-xylene and p-xylene in water.

The reason of the emergence of monomer and dimmer peaks in the IMS spectra could be associated with the fact that when the concentration of analyte molecules is increased further, the monomer may be clustered with an additional molecule, forming a dimmer [5]. This phenomenon is clearly distinguished in this case due to the small amount of volatile compounds produce after heating (during 5 minutes) 100 µL of liquid standard using the head-space method. Furthermore, when this method is

used, humidity could be other fact to be considerated in the apparition of monomer and dimmer in the IMS spectra. More molecules of water reach the IMS device when we are heating a liquid standard to produce volatiles analytes than when gaseous standards are introduced directly in the IMS by using the exponential dilution method.

From these results it can be concluded that, due to the similar molecular weights of compounds measured in this work prevent its separation by using only UV-IMS. Therefore, we recommend using a pre-column in order to accurately separate and identify each analyte present in the sample prior to its IM analysis. Furthermore, a membrane placed before the entrance of volatiles to the UV-IMS device would be highly recommended to avoid the humidity influence on the ion mobility signals.

Finally, some analytical properties of the three systems tested were compared in **Table 6**.

Table 6. Comparison of the three methods proposed in this work to prepare gaseous standards.

Analytical properties		**Head-space method**	**Exponential dilution method**	**Gas generator**
Sensitivity	LOD	2.3-4.6 ppm	0.8-1.8 $ppm_{(g)}$	0.1-0.4 $ppm_{(g)}$
	LOQ	7.7-17.6 ppm	2.5-6.1 $ppm_{(g)}$	0.3-1.2 $ppm_{(g)}$
Robustness		Medium	Medium	High
Time (1)		<10 min	<45 min	>48 h
Cost		Low	Low	High
Operation		Easy	Easy	Medium
Possibility to prepare blended gas mixtures		Yes	Yes	No

(1) Time needed for performing a complete set of concentrations to calibrate the UV-IMS device for each analyte.

The attractiveness of the home-made methods proposed for liquid and gaseous samples are mainly the speediness, low cost, simplicity and acceptable sensitivity values. The different optimized methods shown in this

work will be used in the future to measure analytes present in different samples from workplaces environment by using UV-IMS technology.

3.3. Reduced mobilities of compounds studied

Once studied the analytical features of the different experimental set-up to produce gaseous standards, the reduced mobility, K_0, has been calculated for each target analyte by using the different methods proposed in order to accurately identify analytes from the IM spectra. K_0 corrects operational and environmental deviations. K_0 values, which were calculated from equation (1), are compared with previously reported values in **Table 7**. In practice, K_0 does not always match reported values; the differences usually are ascribed to differences in the preparation of standards and the ionization source used. As can be seen from **Table 7**, the K_0 values obtained by other authors with an identical ionization source (a UV-lamp) were very similar, whereas those obtained by using a different (radioactive) source to measure ethanol, acetone, toluene, *m*-xylene and *p*-xylene were markedly different [4, 5, 20-24]. Variations in K_0 values have been also observed associated to the different methods used to generate gaseous standards.

Figure 5 shows the spectra for the individual analytes from a gaseous sample containing 50 $ppm_{(g)}$ measuring by using the exponential set-up already described. As can be seen in **Table 3**, despite benzene and toluene have a higher molecular weight than acetone and ethanol appeared first, at lower drift time in the IMS spectra. After them, the rest of BTX appeared and finally ethanol and acetone which have a lower molecular weight. The reason why it is easier for aromatics compounds to appear sooner in the IMS spectra could be attributed to the presence of delocalized electrons and the molecule conformation [25-27]. So, under constant electric field, aromatics compounds must move more easily along the IMS drift tube than other family of compounds. Therefore, they appear before in the IMS spectra than linear molecules such as acetone and ethanol.

Table 7. Reduced mobility of the target VOCs studied.

Compound	Method	Drift time (ms)	K_0 calculated (1)	IMS type	Method	K_0 reported	Ref
Acetone	Head-space	18.23 ± 0.04	1.830 ± 0.004	UV-IMS	Head-space	1.75	[20]
	Exponential dilution	18.93 ± 0.12	1.76 ± 0.01	Tritium (^{3}H) TOF-IMS	Exponential dilution	1.44	[23]
				HSCC-UV-IMS	Exponential dilution	1.74	[21]
	Gas generator	17.69 ± 0.03	1.880 ± 0.003	^{63}Ni-CF-IMS	Gas generator	2.32	[24]
Ethanol	Exponential dilution	18.20 ± 0.04	1.830 ± 0.004	UV-IMS	Exponential dilution	1.91	[5]
				Tritium (^{3}H) TOF-IMS	Exponential dilution	1.58	[23]
Ethylbenzene	Head- space	17.15 ± 0.02	1.94 ± 0.02	-			
	Exponential dilution	17.63 ± 0.04	1.89 ± 0.04	-			
	Gas generator	17.07 ± 0.02	1.950 ± 0.003	-			
Benzene	Head-space	17.10 ± 0.08	1.95 ± 0.01	-			
	Exponential dilution	15.83 ± 0.03	2.110 ± 0.005	MCC-UV-IMS	Exponential dilution	2.27	[4]
				HSCC-UV-IMS	Exponential dilution	2.01	[21]
	Gas generator	16.84 ± 0.03	1.980 ± 0.004	^{63}Ni-CF-IMS	Gas generator	2.31	[24]
Toluene	Head-space	17.13 ± 0.05	1.94 ± 0.01	-			
	Exponential dilution	16.69 ± 0.09	2.00 ± 0.01	MCC-UV-IMS	Exponential dilution	2.13	[4]
				HSCC-UV-IMS	Exponential dilution	1.91	[21]
	Gas generator	16.66 ± 0.03	2.00 ± 0.04				
m-Xylene	Head-space	15.98 ± 0.05	2.09 ± 0.01				
	Exponential dilution	17.43 ± 0.04	1.910 ± 0.004	MCC-UV-IMS	Exponential dilution	2.05	[4]
				HSCC-UV-IMS	Exponential dilution	1.83	[21]
o-Xylene	Head-space	15.69 ± 0.02	2.120 ± 0.003	-			
	Exponential dilution	17.38 ± 0.04	1.920 ± 0.005	-			
p-Xylene	Head-space	17.17 ± 0.02	1.940 ± 0.003	-			
	Exponential dilution	17.47 ± 0.06	1.910 ± 0.007	-			
	Gas generator	16.91± 0.02	1.970 ± 0.003	UV-hydrogen discharge lamp-IMS	Gas generator	1.83	[22]

(-) No reported values available. TOF: Time of flight; HSCC: high speed capillary column; CF: cross flow; MCC: multicapillary column.

Notice that lower signal intensity was obtained when ethanol was measured by UV-IMS compared with the signal intensity obtained with the others analytes analysed. A possible reason of this fact could be related to tendency of this molecule to be affected by the water molecules (5% RH approx.) present in the sample gas (synthetic air). Humidity could act as an interferent and consequently it might reduce the IMS signal as it has been studied for other authors [28-29].

On the other hand, the spectra for toluene, ethylbenzene and benzene were quite similar (an intense peak with different shoulders can be appreciated), signals appearing at about 17 ms. Xylene isomers, which belongs to the same compound family as benzene and toluene, exhibited a slightly different spectrum (only one intense peak without shoulders).

The spectra for the three isomers of xylene were quite similar, which made distinguishing their reduced mobilities rather difficult. The difficulty in identifying these compounds by direct UV–IMS (i.e. without a pre-separation column) arises from the similarities between the target analytes. Based on the foregoing, one can expect determining the studied analytes individually in a single sample to be rather a difficult task. However, the proposed method can be used effectively to screen air samples and determine these analytes by using a sorbent tramp column coupled to the UV–IMS in order to improve sensitivity and selectivity.

It should be noted that the K_0 values calculated in this work for some of the analytes tested are for the first time reported in the literature. These values are crucial towards their identification in air samples analysed by UV–IMS.

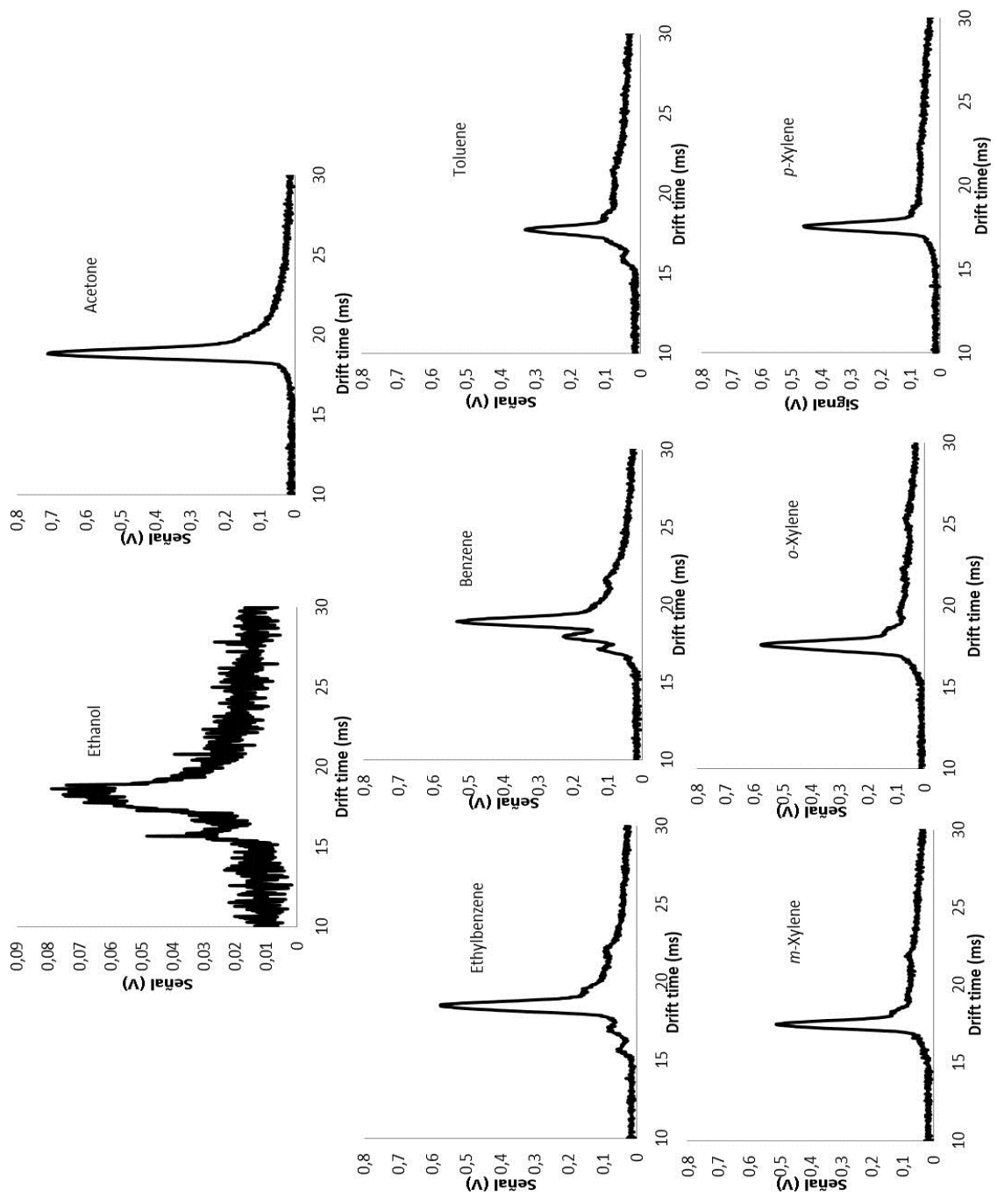

Fig. 5. UV-IMS spectra for 50 $ppm_{(g)}$ VOC gaseous standards obtained by exponential dilution as shown in Fig. 2B.

4. Conclusions

Based on the results of this work, using the proposed home-made SISs as well as the calibration gas generator for UV–IMS allows the reliable production of gaseous standards and calibration of IM equipment. The proposed home-made head-space SIS provided acceptable values of LOD and LOQ throughout the operational range studied for all compounds studied. The exponential dilution set-up used affords quick and sensitive measurements of the different concentrations of gaseous VOCs tested. All these results were comparable with the ones obtained with the calibration gas generator. The proposed calibration methods will be used in future work to determine the studied pollutants in liquid and air samples from workplaces such as gas stations and industries.

The IMS was not intended to replace traditional analytical instruments such as GC/MS, but rather to provide a rapid, inexpensive quantitative and qualitative method as a complement to other well-established methods. Its portability and rapid response make IMS a useful tool for on-line and in situ environmental analyses. The simplicity of use and relatively low cost of the equipment and the methods proposed makes IMS quite attractive and promising for general use in analytical practice in air quality control. Before using this device for field monitoring, a robust and reliable calibration method should be performed. In this work, UV-IMS equipment has been demonstrated to be able to be calibrated in a simpler manner by using different home-made systems depending if the analytical problem to be resolved is in aqueous or gaseous samples.

Acknowledgements

Funding from Spain's DGICyT (Grant CTQ2011-23790) is gratefully acknowledged. LCG wishes to thank the Spanish Ministry of Education, Culture and Sport for award of a pre-doctoral grant (AP2009-3528) as well as the Institute of Physics CSIC (Madrid, Spain) for the concession of calibration gas generator during the experimental work.

References

[1] J.I. Baumbach, Int. J. Ion Mobil. Spec. 11 (2008) 3-11.

[2] L. Arce, in R.A.Meyers (Editor), Encyclopedia of Analytical Chemistry. 2011, p. 333-350.

[3] G. Allison, Journal of Automatic Chemistry 20 (1998) 1-7.

[4] St. Sielemann, J.I.Baumbach, H.Schmidt, P.Pilzecker, Field Anal. Chem. Technol. 4 (2000) 157-169.

[5] G.A. Eiceman, Z. Karpas, Ion Mobility Spectrometry. Boca Raton, Fl 33487-2742, 2005.

[6] J.E. Roehl, Appl. Spectrosc. Rev. 26 (1991) 1-57.

[7] G. Walendzik, Anal. Bioanal. Chem. 382 (2005) 1842-1847

[8] A.B. Kanu, Hill Jr.H.H., J. of Chromatogr. A 1177 (2008) 12-27.

[9] D.C. Collins, M.L.Lee, Anal. Bioanal. Chem. 372 (2002) 66-73.

[10] G.A. Eiceman, L.G. Gonzalez, Y.F. Wang, B. Pittman, G.E. Burroughs, Talanta 39 (1992) 459-467.

[11] L. Arce, M. Menéndez, R. Garrido-Delgado, M. Valcárcel, Trac-Trends in Anal. Chem. 27 (2008) 139-150.

[12] www.hovacal.de (accessed 30 october 2012)

[13] www.owlstonenanotech.com (accessed 30 october 2012)

[14] www.vici.com (accessed 30 october 2012)

[15] A. Neganowska-Nowak, Critical Rev. Anal. Chem. 35 (2005) 31-55.

[16] P. Konieczka, Trac-Trends in Anal. Chem. 26 (2007) 744-751.

[17] R. Alonso, V. Rodríguez-Estevez, A. Domínguez-Vidal, M.J.Ayora-Cañada, L. Arce, M. Valcarcel, Talanta 76 (2008) 591-596.

[18] S. Greenhouse, Anal. Chim. Acta 236 (1990) 221-226.

[19] B. Borderie, D. Lavabre, G. Levy, J. Photochem. Photobiol. A: Chem. 56 (1991) 13-23.

[20] R. Garrido-Delgado, L. Arce, C.C. Pérez-Marín, M. Valcárcel, Talanta 78 (2009) 863-868.

[21] Z. Xie, S. Sielemann, H. Schmidt, F. Li, J.I. Baumbach, Anal. Bioanal. Chem. 372 (2002) 606-610.

[22] C.S. Leasure, M.E.Fleischer, G.K. Anderson, G.A. Eicemann, Anal. Chem. 58 (1986) 2142-2147.

[23] C. Tiebe, Anal. Bioanal. Chem. 395 (2009) 2313-2323.

[24] M. Zhang, S. Wexler, Int. J. Mass Spectrom. 258 (2006) 13-20.

[25] K.E. Peters, C.C. Walters, J.M. Moldowan, The Biomarker Guide: Biomarkers and Isotopes in the Environment and Human History. Cambridge University Press, 5 A.D.

[26] M. Meot-Ner, P. Hamlet, E.P. Hunter, F.H. Field, J. Am. Chem. Soc. 100 (1978) 5466-5471.

[27] E. Matito, M. Durán, M. Solà, J. Chem. Phys. 122 (2005) 14109-14117.

[28] W. Vautz, S.Sielemann, J.I. Baumbach, Anal. Chim. Acta 513 (2004) 393-399.

[29] M. Mäkinen, Talanta 84 (2011) 116-121.

Chapter 2
Membrane set-up to avoid humidity interference in ion mobility measurements

Capítulo 2

Sistema de membrana para evitar la interferencia de la humedad en las medidas de movilidad iónica

Submited to J. Chromatogr. A

MEMBRANE SET UP COMBINED WITH UV-IMS DEVICE TO IMPROVE ANALYTICAL PERFORMANCE AND AVOID HUMIDITY INTERFERENCE ON THE DETERMINATION OF BTX COMPOUNDS IN GASEOUS SAMPLES

L. Criado-García, L. Arce, M. Valcárcel

Department of Analytical Chemistry. Annex C-3 Building. Campus of Rabanales. Institute of Fine Chemistry and Nanochemistry. University of Cordoba. 14071 Córdoba, Spain.

UV-Ion Mobility Spectrometry (UV-IMS) is a reliable and inexpensive technique which allows efficient monitoring of BTX (benzene, toluene, m-xylene, o-xylene and p-xylene) in different air samples. Water molecules are unavoidably present in every on-field measurement affecting sensitivity and selectivity of the UV-IMS method. For this reason, the influence of humidity on the mobility spectra when measuring BTX is discussed here. Furthermore, in this work a PDMS membrane assembled on an ad-hoc designed membrane holder coupled to UV-IMS was proposed for online measurement of analytes in humidity gas-phase samples without sample preparation/pre-treatment steps. The use of this membrane prevents the humidity of the sample from entering into the IMS, and the consequent distortion of the signal due to humidity. Precision, LODs and LOQs average values were improved in 69, 70 and 70% respectively when the membrane was used coupled to the UV-IMS. Thus, BTX can be determined directly and quantified unequivocally with the membrane system in ambient air even at humid condition.

Keywords: BTX, humidity, ion mobility spectrometry, UV.

1. Introduction

A key advantage of ion mobility spectrometry (IMS) has been the ability to perform on-site measurements using portable instruments. They exhibit excellent detection limits for numerous chemical substances within few seconds response [1]. However, a general limitation in the on-field application is the varying measuring conditions at different sampling sites (e.g. humidity and temperature) [2] that can change the response characteristics of the detector. The importance of moisture was identified as one of the most significant influencing parameters [3]. Although humidity is a well-known problem in experimental work with IMS, it is not documented in some cases when measuring BTX by IMS with photoionization source.

Humidity effect on IMS signal has been reported in previous IMS works as is summarized in **Table 1**. The dependence of moisture in positive ion mobility spectra was extensively studied when radioactive ionization sources were used: tritium source (^{3}H) with linear IMS [2, 4, 5]; and nickel source (^{63}Ni) with DMS [6-9], with FAIMS [10] or with linear IMS [11-13]. However, less works in which moisture effect was studied with UV ionization source was found. Vautz et al. investigated terpenes using photoionization as ionization source in an IMS device and observed decreased signal intensities of positively charged ions with increasing carrier gas humidity [14-16]. The relative humidity may affect both the ion's chemistry and reduced mobility (K_0). Water may cause a shift in the drift time peaks of certain target ions as a result of the analyte clustering with water neutrals, effectively increasing the collisions-cross section of the ion [13]. The broadening or appearance of new peaks may also occur [15].

In the case of polar compounds of high proton affinity the increased humidity does not lead to the reduction of the sensitivity and can even results in increased separation power [17].

Table 1. Humidity interferences on IMS signal reported in previous works.

Compound	Instrument	Ionization source	Humidity range	Changes observed	Ref
Anilines, toluenes, chlorobenzenes and ketones	IMS	^{3}H	10-2000 ppm_v	shifting peak position, increment of detection limits	[2]
Volatiles from odor sources	IMS	^{3}H	On-field (30-100% RH)	lower intensity of peaks	[5]
Acetone, ethanol, acetaldehyde, methanol and dichloromethane	DMS	^{63}Ni	40% RH	shifting RIP and analyte peak position	[7]
BTEX, TMB, hexane and naphthalene	DMS	^{63}Ni	6.5-538 ppm_v	shifting peak position, lower intensity of peaks	[6]
Halogens (Br^-, I^-, Cl^-)	IMS	APCI	5-2000 ppm_v	shifting peak position, lower intensity of peaks	[18]
DMMP	IM-TOFMS	^{63}Ni	5-2000 ppm_v (4.3% RH)	increased clustering and cross section of the ion	[12]
Halogens (Br^-, I^-, Cl^-)	IMS	^{3}H	2-793 ppm_v	increased clustering, additional peaks formed, shifting peak position, lower sensitivity, peak shape (broadening)	[4]
MIBK	IMS	Corona	1-100 ppm_v	increased clustering	[20]
Malathion	IMS	^{63}Ni	-	additional peaks formed	[11]
Formaldehyde	DMS	^{63}Ni	42-900 ppm_v	shifting RIP and analyte peak position, lower intensity of peaks	[8]
TMA	IMS	^{63}Ni	10-16500 ppm_v (70% RH)	shifting RIP and analyte peak position and shape, sensitivity and selectivity decreased	[13]
Acetaldehyde, methanol, ethanol, propane, 2-propanol, 1-butanol, ethylacetate, dichloromethane, toluene, xylene, 2-butanone, hexane, benzene, octamethylcyclotetrasiloxane	DMS	^{63}Ni	50% RH	lower intensity of peaks	[9]
Alpha-pinene, beta-pinene, D,L-limonene, 3-carene	IMS	UV	0-100% RH	lower intensity of peaks, varied peak shape, additional peaks formed, sensitivity decreased	[14-16]
DMMP, TMP, DEMP, DEEP, DIMP, DEIP, TEP, TPP, DBBP, TBP	FAIMS	^{63}Ni	0-10000 ppm_v	shifting peak position, additional peaks formed	[10]

BTEX: benzene, toluene, ethylbenzene and xylene isomers; TMB: 1,2,4-trimethylbenzene; DMMP: dimethylphosphonate; MIBK: methyl isobutyl ketone; TMA: trimethylamine; TMP: trimethyl phosphate; DEMP: diethylmethyl phosphonate; DEEP: diethyl phosphonate; DIMP: diisoprophylmethyl phosphonate; DEIP: diethylisoprophyl phosphonate; TEP: triethyl phosphate; TPP: tripropyl phosphate: DBBP: dibutylbutyl phosphonate; TBP: tri-n-butyl phosphate; IMS: ion mobility spectrometer also called DTIMS: drift tube ion mobility spectrometer; DMS: differential mobility spectrometer; IM-TOFMS: ion mobility spectrometer time of flight mass spectrometer; FAIMS: field asymmetric ion mobility spectrometer; APCI: atmospheric pressure chemical ionization.

By contrast, all of the tested non-polar compounds demonstrated a decrease of the signal area with an increase of the humidity. So there is a clear dependence of signal intensity and peak position on the way in which the vaporized water was transported into the ion mobility spectrometer. Changes in signal intensity due to moisture dependence strongly rely on structural features of substances investigated and are therefore different for each compound [18]. Warneke et al. [19] have observed that the increased concentration of the water led to a significant reduction of benzene and toluene signal by proton-transfer-reaction mass spectrometry. The concentration of the hydrated monomer ions depends on the water partial pressure in the IMS cell as well as temperature, since the equilibrium constant are temperature dependent [20]. A higher degree of hydration can be observed with decreasing temperature and/or a humidity increase [18]. As well in the positive mode, compounds with higher proton affinity respond better but when moisture is present in the ionization region, simple hydrocarbons or aromatics with low proton affinities do not respond well in the IMS [21].

The effects that water has on mobility analysis can be alleviated by changing the reactant ion chemistry and removing water from the internal atmosphere of the instrument when using IMS with radioactive source. Ammonia dopant [22] and acetone [21] were added into the sample gas to control the ionization, and thus humidity does not affect the IMS response. A high speed capillary column [23] or a multicapillary column was also proved to avoid moisture interference and enhance sensitivity when using UV-IMS [15, 24]. Also the moisture can accurately be removed by using molecular sieve pack [9] or filters [25] or membrane inlets between the sample gas and the ionization region [21]. Polydimethyl siloxane or PDMS is among the more popular gas permeable materials available [26]. This type of material has the following characteristics: strength, stability and flexibility from the siloxane chain and inertness and water repellence from the attached methyl group [27]. The biocompatibility, chemical inertness, elasticity, gas permeability, and low-cost of this material have made it attractive for use in membrane technology, microfluidics, and bio-analytical

applications [28]. Gases permeate silicone by a solution/diffusion mechanism whereby the rate of gas permeation is directly proportional to the product of solubility of the gas, and the rate of diffusion of the dissolved gas in silicone [29].

For a careful validation of UV-IMS measurements and a reliable interpretation of the results obtained with this technology, it is necessary to know the basic influencing factors for qualitative and quantitative analysis. Using humid carrier gas causes reduced signal intensities. For this purpose, we have fully studied for first time the influence of moisture on the BTX signals using ion mobility spectrometry with an UV lamp as an ionization source. There are previous works in which BTX compounds have been previously measured by UV-IMS [23, 24, 30-32] but in any case the influence of humidity has been reported. Furthermore, a PDMS membrane in a home-made set-up, that can be easily connected when required, was implemented successfully in this work to avoid the effect of the humidity when using UV-IMS for on-field monitoring.

2. Experimental

2.1. Sample introduction set-up

The experimental set-up developed in this work is illustrated in **Figure 1**. It is integrated by a humidity flask (a 0.5 L flask filled with 0.5 L of water to generate humidity, working as a home-made humidifier) coupled to a sample flask (a 1 L flask in which gaseous standards were created). Synthetic air supplied by Carburos Metálicos (Barcelona, Spain) as the sample gas which first goes to the humidity flask in order to enrich the humidity in the air and then reaches the sample flask, in which 1µL of liquid standard is introduced and heated for 1 min to volatilize the analytes. Benzene, toluene, *m*-xylene, *o*-xylene and *p*-xylene were supplied from Sigma-Aldrich Chemical Co. (St Louis, MO, USA). The initial concentration is diluted with synthetic air during a fixed time by using the switching valve 1. In this way, different concentrations of gaseous compound are achieved

inside the sample flask using exponential dilution methodology; as was described in a previous work [33]. Then, this sample gas is flushed into the PDMS membrane system in which analytes diffused along it. Once there, the sample gas (with humidity content) goes to the membrane. The second gas flow, acting as carrier gas is also synthetic air which sweeps directly to the membrane from the opposite side to drag analytes which have permeated through the PDMS membrane conducting them to the UV-IMS for its analysis.

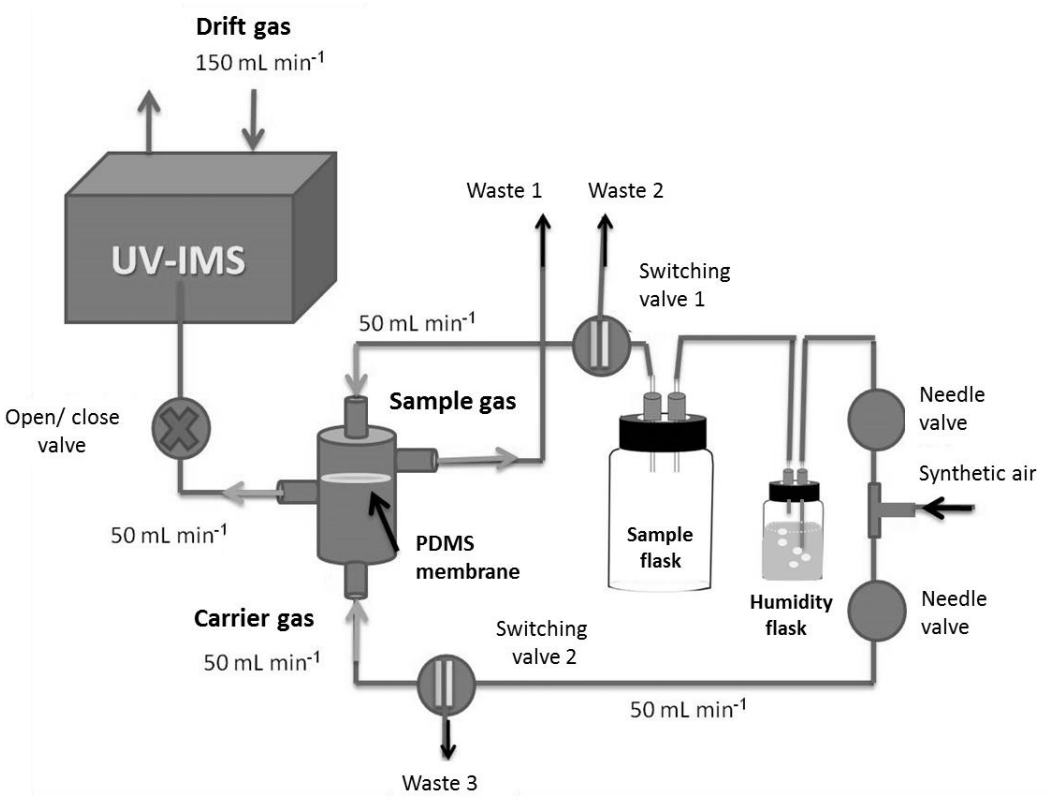

Fig. 1. Schematic diagrams of the liquid injection and thermal desorption instrumental configurations used in this work.

A, purified He supply; B, Nitrogen supply; C, Pressure gauge; D, flow control; E, split injection; F; gas chromatograph; G, heated transfer lines; H, sheath-flow inlet, I, differential mobility spectrometer; J, molecular sieve trap for exhaust gasses; K, thermal desorption unit; and L, data acquisition and processing.

2.2. Humidity monitoring

Humidity inside the sample flask was monitored by using a portable hygrometer and temperature controller PCE-HT 71 N LOG 32 from PCE instruments (Mesched, Germany) placed inside the sample flask. Humidity and temperature values were registered along each measurement. Humidity values used in this work ranged from 10% RH for the moisture content of synthetic air gas, 75% RH for synthetic air gas enriched after flowing through a 0.5 L flask filled with water at room temperature (24 ºC), and 85% RH for synthetic air gas enriched after flowing through a 0.5 L flask filled with ultrapure water and heated at 100 ºC.

2.3. Membrane set-up

The membrane holder was made in steel and has a size of 85x78x35 mm, supplied by Ramem S.A. (Madrid, Spain) illustrated in **Figure 2**.

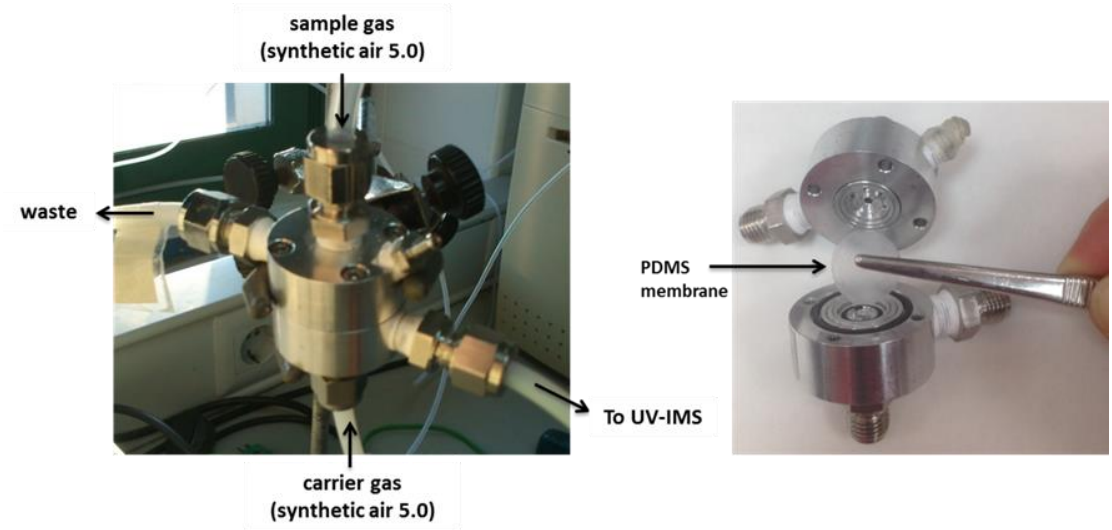

Fig. 2. Photo of the assembled membrane holder with its connections and the internal part in which membrane is placed.

Inside the membrane holder there is a cavity in which a commercial polydimethyl silicone membrane or PDMS (SSP-M823) of 16 mm of diameter acquired from Specialty Silicone Products (New York, USA) was placed. In this work two different thickness of membrane were used: 76.2

μm and 254 μm. This kind of membrane is 30 times more permeable than non-silicone stable polymers. The membrane holder set-up can be heated by using a heater cord connected to a PID temperature controller also manufactured by Ramem S.A. (Madrid, Spain). Membrane was cleaned passing through it clean synthetic air at 50 mL min^{-1} and replace periodically. Blanks were performed before each measurement.

2.4. UV-IMS

An instrument manufactured by Gesellschaft für Analytische Sensorsysteme (GAS, Dortmund, Germany), was used for the experiments reported here. It is equipped with a UV lamp. The instrument is 350×350×150 mm in size, has a drift tube length of 12 cm, a weight of 5 kg, and uses a current supply of 230 V/ 50–60 Hz and a constant voltage supply of 333 V cm^{-1}. The temperature and pressure in the drift tube were kept at room temperature and ambient pressure; 297.15 K and 101.3 kPa respectively. Signal acquisition parameters were as follows; 1024 points per spectrum, grid pulse width was set 100 μs to allow the ions to pass in short pulses into the separation chamber, sampling frequency 30.000, scan repetition rate 50 ms and 64 averages per scan. Nitrogen 5.0 supplied by Abelló Linde (Barcelona, Spain) was used as drift gas of the UV-IMS instrument to eliminate impurities and neutral ions which could remain inside the drift tube. Data were acquired in positive mode and processed by a computer running the software GASpector v.3.99.035 DSP from GAS.

3. Results and discussion

The competence to perform analysis with the proposed membrane set-up coupled to UV-IMS is here presented. This SIS offers a versatile, simple and inexpensive method suitable for on-site and direct analysis. The humidity influence of the BTX on the ion mobility spectra was also discussed in this section.

3.1. SIS parameters optimization

Sample and carrier gas flows, humidity generation method and thickness of the PDMS membrane were optimized.

Sample and drift gas flows

Synthetic air was chosen as sample and carrier gas to reproduce responses that will be obtained with real air samples in on-site monitoring. Gas flow values for sample and for carrier gas were 30, 50 and 100 mL min^{-1}. Finally equal flows (50 mL min^{-1}) were selected for both sample and drift gas flow due to higher intensities signal for 50 mg $L^{-1}_{(g)}$ BTX sample was reached at 10% RH. For the sample gas, this value was beneficial in order to give analytes present in the sample gas enough time to permeate through the membrane. Related to the carrier gas, it was suitable not to use higher flow values in order to avoid dilution of analytes and consequently signal losses. Therefore analytes could successfully permeate throw the membrane and be driven to the UV-IMS device by the carrier gas.

Humidity generation

Humidity that enriched the sample gas was generated using dilution flask filled with ultrapure water and connected to the sample flask in which analytes were injected. Three different designs were tested as shown in **Figure 3**. Humidity was measured inside the flask along time to check the relative humidity (%) achieved and the reproducibility of home-made humidifier. Design A gave an average value of 10% RH without using the humidity flask in this design, only the synthetic gas passed through the sample flask. The final RH% value obtained for design B (humidity flask filled with 100 mL of water at room temperature) and C (humidity flask filled with 500 mL of water at room temperature) was 75% RH after 30 min in both cases. Design B was discarded because with design C, 75% RH was reached quicker (20 min) and with less variation between the following times. Finally, in design D when the humidity flask filled with 500 mL of ultrapure water and it was heated at 100 ºC, the highest humidity level (85% RH) was obtained with the proposed system but this system was

discarded because at such extreme condition, water droplets appeared in the tube connections and irreproducibilities in the measurements were found. In any case, filter or sorbent material was used in order to retain moisture present in the gas cylinder before the introduction of the sample through the membrane set up coupled to the UV-IMS.

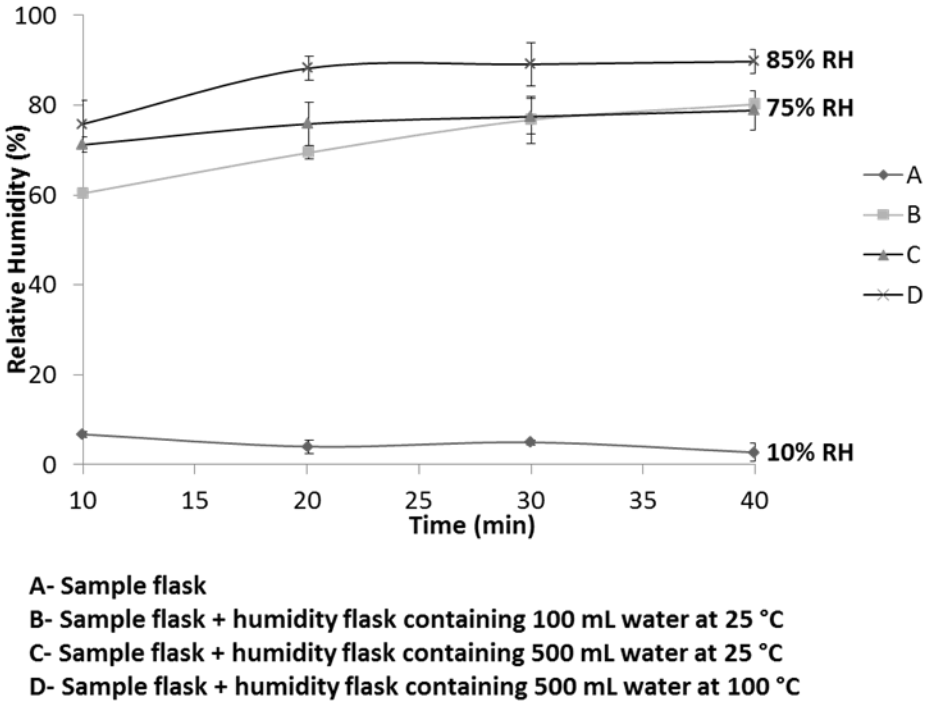

Fig. 3. Relative humidity achieved with the alternatives proposed for the generation of moisture placing water in the humidity flask at different conditions.

Membrane thickness

PDMS membranes of different thickness (76.2 μm and 254 μm) were tested. The peak height intensities obtained for 50 mg $L^{-1}_{(g)}$ of benzene, m-xylene and p-xylene at 75% RH measured by the membrane set up coupled to UV-IMS are plotted in **Figure 4**. IMS signal obtained without membrane and with 10% RH was assigned with 100% and the rest of signal values measured with the membrane set-up were calculated referring to this maximum value. Higher intensity values were obtained for all analytes when

76.2 µm PDMS membrane was used inside the membrane holder. Analyte permeation was enhanced and water permeation avoided with the thinner membrane. Consequently, 76.2 µm PDMS membrane was used for further experiments.

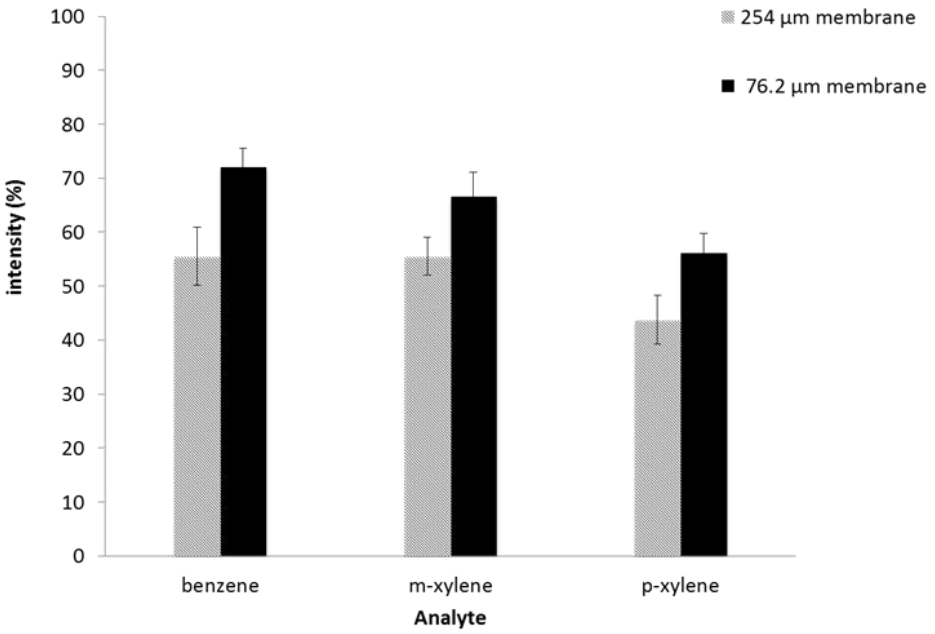

Fig. 4. Intensity of signal obtained with different thickness of membrane at 75% RH.

3.2. Influence of humidity on the ion mobility spectra of the BTX compounds measured by UV-IMS

The influence of humidity on the IMS signal of BTX compounds is illustrated in **Figure 5A** where a clear dependence between the moisture content in the sample gas and the IMS signal obtained was observed. The spectrum of each individual compound was obtained measuring 50 mg $L^{-1}_{(g)}$ of benzene, toluene, *m*-xylene, *o*-xylene and *p*-xylene by UV-IMS at 10% RH and 75% RH without the membrane set-up. Increasing humidity (% RH) of the sample gas caused decreasing of signal intensity of the main peaks of

all analytes, approx. 50.23% for benzene and toluene and 76.49% for xylene isomers as observed in **Figure 5A**.

Also the formation of new peaks (marked with asterisk) at approx. 21 ms for benzene, toluene, *m*-xylene and *o*-xylene and around 15 ms for m-xylene and *o*-xylene were observed. These additional peaks complicate the spectra and make even more difficult the identification of target analytes because the shape of the IMS spectra now depends on humidity [15]. In order to assess the identity of the ion, the reduced mobility constant (K_0) of peak was calculated equation (1). The velocity of an ion in a buffer gas under the influence of a homogeneous electric field is directly proportional to the electric field strength. The proportionality constant between the velocity of ions and the electric field strength known as the ion mobility constant (K), becomes a qualitative measure of the ion. Since the velocity of the ion is affected by both temperature (297.15 K) and pressure (101.3 KPa), measured mobility constants were corrected to standard temperature and pressure to produce a reduced mobility constant (K_0):

$$K_0 = K \frac{P}{760} \frac{273}{T} \quad (1)$$

The mobility of an ion K also depends on the collision cross section Ω and N, the number density of molecules per unit volume (2.47x1025 molecules m^{-3}) and according to the theory of Chapman-Enskog, Mason-Champ equation (2) can be obtained:

$$K = \frac{3}{16} \frac{q}{N} \left(\frac{2\pi}{\mu \, k_B T} \right)^{1/2} \frac{1}{\Omega} \quad (2)$$

where q is the elementary charge of electron (1.602 x 10^{-19} C), μ is the reduced mass of the pair of the diffusing ions and carrier gas molecules (uma), $\mu = mM\ (m + M)$, with respective masses of m, mass of the ion (analyte charged in the form of M^+), and M, mass of the buffer gas (synthetic air; 26.98 g mol^{-1}); kB is the Boltzmann constant (1.38065 x 10-23 J K^{-1}) and T is the gas temperature (297.15 K).

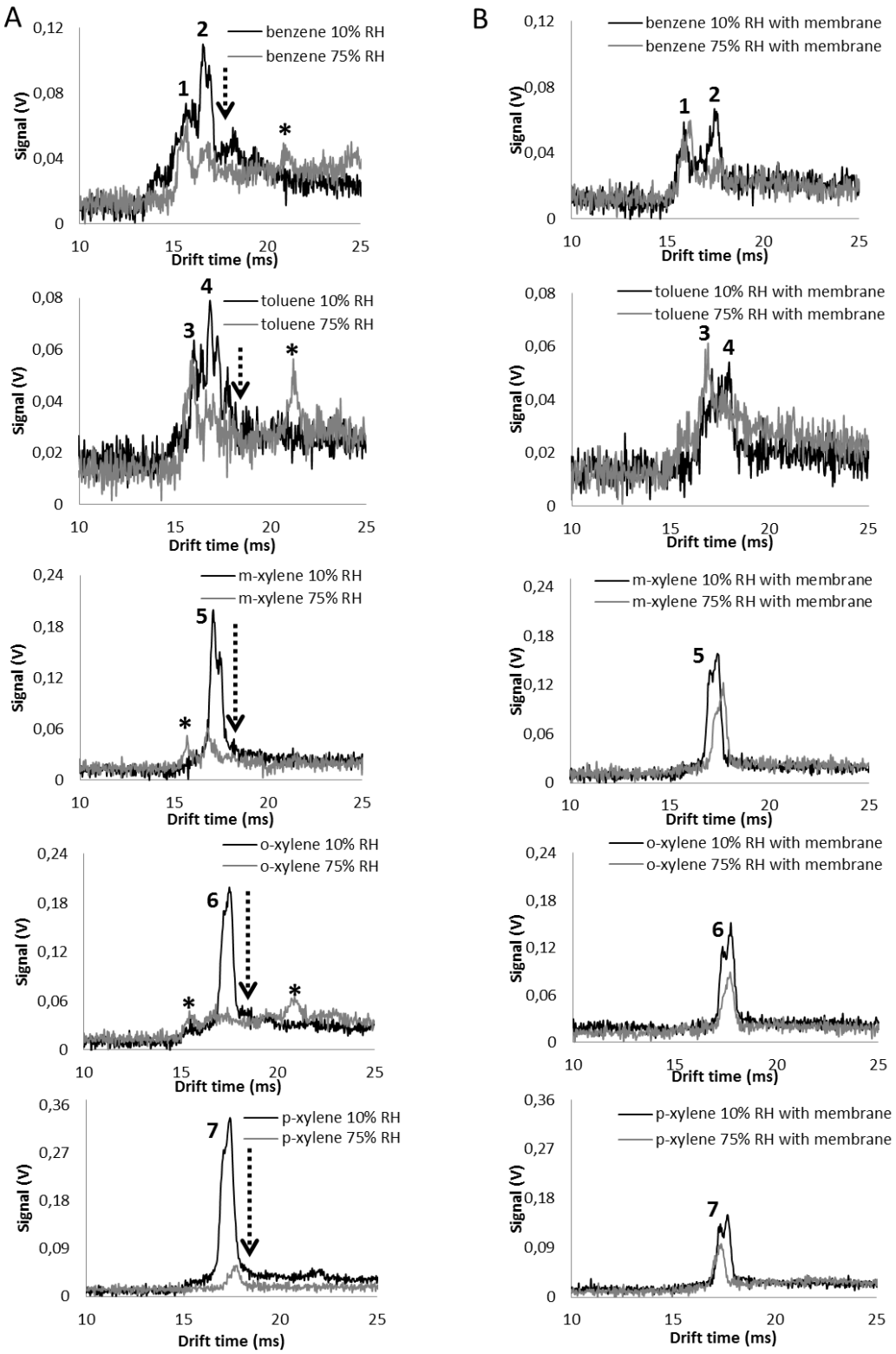

Fig. 5. Spectra of individual BTX obtained at 10 and 75 % RH without membrane (A) and with membrane set up (B) measured with UV-IMS.

In **Table 2** are summarized drift times, K_0 values and Ω calculated for all peaks of each compound that appeared in the IMS spectra. Slightly differences in drift times values (<1.26%) of more intense peaks were observed for all compounds when humidity is increased in the sample gas (75% RH). Therefore, moisture did not provoke an intense drift shifting in the characteristic peaks for the target analytes. K_0 value, which gives a characteristic value of each ion, was calculated for the peaks obtained (1-7); obtaining a correspondence in the range of values reported in a previous work [33]. Also, Ω values were reported for first time for the target analytes when using a UV-IMS.

Table 2. Drift time and corresponding reduced mobility of the major peaks found in the IMS spectra under the influence of humidity.

Compound	10% RH	75% RH	10% RH	75% RH	10% RH	75% RH
	Drift time (ms)		**K_0 (cm^2 V^{-1} s^{-1})**		**Ω (Å²)**	
Benzene	15.75(1)	15.65(1)	2.11(1)	2.12(1)	110.6(1)	109.9(1)
	16.58(2)	16.68(2)	2.00(2)	1.99(2)	116.5(2)	117.2(2)
		21.08*		1.58*		148.2*
Toluene	15.98(3)	15.91(3)	2.08(3)	2.09(3)	112.2(3)	111.7(3)
	16.81(4)	16.98(4)	1.98(4)	1.96(4)	117.9(4)	119.1(4)
		21.11*		1.57*		148.7*
m-Xylene	17.08(5)	16.78 (5)	1.95(5)	1.98(5)	120(5)	117.9(5)
		15.75*		2.11*		110.6*
o-Xylene	17.51(6)	17.41(6)	1.90(6)	1.91(6)	123(6)	122.3(6)
		15.40*		2.16*		108.2*
		20.83*		1.59*		146.4*
p-Xylene	17.41(7)	17.71(7)	1.91(7)	1.88(7)	122.3(7)	124.4(7)

* New peaks formed when increasing humidity in the measurement.

As can be seen in **Figure 5**, new peaks formed (*) presented a lower reduced mobility (1.57-1.59 cm^2 V^{-1} s^{-1}) and a higher size as indicated by its collision cross section values calculated (146.4-148.7 Å2) compared with characteristics peaks of each analyte (1-7). These clusters can be formed with analyte ions and water neutrals (n≥1) and could be the reason why these peaks appeared at longer drift times and K0 values decreased when water content is increased inside the IMS [13]. With an increase of water concentration the potential cluster size increase but the strength of the attachment decrease [10], so it can also occur that the big and thereby slow ions formed are partially lost on the walls of the drift tube or reach the

Faraday-plate too late for its detection [15], it could explain the instability of the formed large cluster and the reason why sometimes not observed as was the case of *p*-xylene. As well new peaks (*) were also detected before the expected peak from *m*-xylene and *o*-xylene around 15 ms. It can occur that lighter clusters probably formed with water molecules and impurities or fragments contained in the sample gas.

Moisture in the sample gas affected each analyte in a different way due to its structure and the reactivity of each analyte with water molecules. As consequence, UV-IMS cannot be used under humid condition with direct analyte introduction for the detection of BTX as others authors also signalled in a previous work for terpenes measurement [15]. There is a need of introducing previous step or treatment of the humid sample gas containing also the analyte prior to the introduction to the IMS device.

3.3 Membrane set-up coupled to UV-IMS to avoid the influence of moisture

In **Figure 5B** is shown the spectra obtained by using the membrane set up coupled to the UV-IMS at the same conditions that were acquired the spectra of **Figure 5A**. At lower humidity conditions (10% RH), the most intense peaks from BTX could be detected at their correspondent drift time without any shift in time. As well the appearance of secondary peaks related to humidity was avoided when using the membrane at the two selected humidities values 10 and 75% RH. The diffusion of the non-polar analytes through the non-porous PDMS membrane was demonstrated in this work, the permeation of volatile molecules occurs via a solution-diffusion mechanism. During permeation, gases and vapors absorb onto one surface of the membrane, diffuse across it, and desorb from the opposite surface [34]. However, it was noted a reduction of signal when using the membrane set up, most probably because the desorption take more time compared to the absorption and diffusion and the reactivity between the analyte and the membrane. IMS signal obtained without membrane at 10% RH was assigned with 100%. As can be expected the analyte losses were higher when humid gaseous samples (75% RH) were measured without membrane

(77-87%). When using 76.2 µm PDMS membrane (75% RH) signal losses were always below 43% for all cases.

A study of the sensitivity and the selectivity obtained with the analytical method proposed can highlight the ability of this technology to determine BTX in gaseous samples. Calibration curves were obtained with and without 76.2 µm PDMS membrane and under the effect of humidity (75% RH). As an example, m-xylene calibration curves obtained with the membrane set-up and without membrane at 75% RH are plotted in **Figure 6**. Topographic plot and individual spectra obtained at the highest and lowest concentration measured are also plotted in **Figure 6** for m-xylene. An exponential dilution experiment was performed in which concentration was decreased along time, explained in detail elsewhere [33].

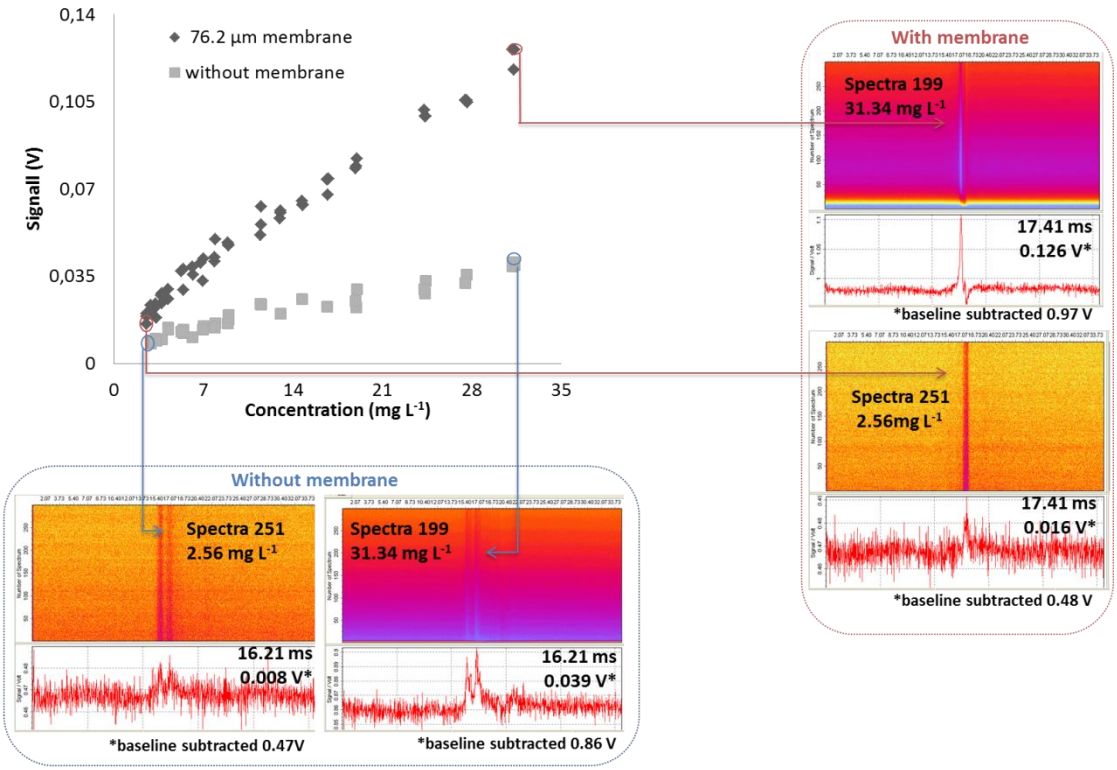

Fig. 6. Calibration curves obtained for *m*-xylene at 75% RH with and without membrane. Topographic plots and individual spectra at the lowest and maximum concentration as example to show how signals were extracted to build the calibration curve.

Signal intensities were extracted from the topographic plot at a specific spectra number and time. Taking into account the initial concentration (C_0), concentration at that time (C_t) can be calculated with the following equation (3):

$$C_t = C_o e^{(-Ft/V_f)} \quad (3)$$

Being C_0 (mg $L^{-1}_{(g)}$) the initial concentration, F (mL min^{-1}) the flow rate of the gas, t (min) time, V_f (mL) the volume of the dilution flask; explained in detail in a previous work [33]. As can be seen in the **Figure 6**, the humidity affected the slope of the calibration curve. The high humid condition caused a limited sensitivity when no membrane was used. Lower peaks intensities were observed when increasing humidity of the sample. The calibration equation was used to calculate LOD and LOQ values; these values were calculated to assess the sensitivity of the method, as three and ten times the standard deviation of the intercept, among the slope from the calibration curves. In **Table 3** are shown the LODs and LOQs calculated for each compound when 76.2 μm PDMS membrane was used at 75% RH. For quantification purpose it can be confirmed that the humidity also affected negatively when no membrane was used. It drastically increased LODs and LOQs values of analytes that can result in the wrong quantification as was experimentally observed in this work. LODs and LOQs values obtained here at 75% RH when membrane set up was used in combination with UV-IMS are in the same order of magnitude as shown in a previous publication when BTX were measured without humidity interference [33].

The precision study was carried out with 50.29 mg $L^{-1}_{(g)}$ of individual m-xylene when 76.2 μm PDMS membrane was used with a humidity content of 75% RH. These experiments were performed repeatedly in the same day (n= 6) while the reproducibility was carried out by analyzing the same samples for three consecutive days (n= 9); in all cases under the same experimental conditions. Precision values of the peak height and drift time were expressed as relative standard deviation (RSD). When membrane was used within-day RSD values were 1.1% for drift time and 12.0% for peak height; all values were obtained in the range of the RSD values

reported in a previous work [33]. RSD values were much higher without the membrane set up; 3.7% for drift time and for peak height 24.5%. As was expected between-day precision values were slightly higher than within-day RSD values. The humidity content in the sample gas contributed to increase irreproducibilities in the measurements related to peak position and intensity of the IMS signal. Humidity interference was reduced considerably when membrane was used. Consequently, precision was improved when using the membrane set up previous to UV-IMS measurement.

Table 3. Analytical figures of merit to the determination of *m*-xylene and a gaseous mixture of benzene, toluene, *m*-xylene, *o*-xylene and *p*-xylene (24 ºC, 75% RH) using PDMS membrane and without it coupled to UV-IMS.

Analyte	Regression equation			LOD ($mg\ L^{-1}_{(g)}$)	LOQ ($mg\ L^{-1}_{(g)}$)	Without membrane	
	Intercept ± S_a	Slope ± S_b	R^2			LOD ($mg\ L^{-1}_{(g)}$)	LOQ ($mg\ L^{-1}_{(g)}$)
Benzene	-0.0176 ± 0.0014	0.00535 ± 0.00006	0.995	0.77	2.56	2.77	9.25
Toluene	-0.0222 ± 0.0023	0.00580 ± 0.00010	0.994	1.21	4.03	2.12	7.07
m-Xylene	0.0136 ± 0.0008	0.00345 ± 0.00005	0.993	0.70	2.33	1.74	5.80
o-Xylene	0.0024 ± 0.0007	0.00199 ± 0.00005	0.989	1.09	3.65	2.29	7.65
p-Xylene	-0.0138 ± 0.0019	0.01143 ± 0.00010	0.998	0.49	1.63	1.05	3.52

4. Conclusion

Different behaviours were found when BTX were measured by UV-IMS in presence of humidity. The most relevant analytical consequences of moisture level inside the drift tube include changes in peak intensity, peak position shifts, peak shape and the formation of different ions depending on humidity values making difficult the correct identification and quantification of these compounds in gaseous samples. The results presented in this work demonstrate the importance of avoiding the moisture content in the analysis of BTX compounds with IMS with photoionization source. The PDMS membrane holder coupled to UV-IMS improved the precision, LOD and LOQ values when using the proposed membrane set up coupled to the UV-IMS. Further work will be done with other membrane materials to overcome analyte losses detected and enhance analytical performance of this

proposed set up. This work opens a new interface which extends the range and versatility of UV-IMS to determinate BTX, potentially present in workplace areas such as factories, gas station and garages, which are difficult to detect with UV-IMS at atmospheric air conditions due to interferents such as moisture.

Acknowledgements

Authors gratefully acknowledge the funding received from Spain's DGICyT (Grant CTQ2014-52939R). LCG wishes to thank the Spanish Ministry of Education, Culture and Sport for a pre-doctoral grant (AP 2009-3528). A special thanks to S. López-Vidal and the company RAMEN S.A., Madrid (Spain) for their support during the project.

The authors have declared no conflict of interest.

References

[1] H. Borsdorf, G. A. Eiceman, Ion mobility spectrometry: principles and application, Appl. Spectrosc. Rev. 41 (2006) 323-375.

[2] H. Borsdorf, P. Fiedler, T. Mayer, The effect of humidity on gas sensing with ion mobility spectrometry, Sensor Actuat. B 218 (2015) 184-190.

[3] G.A.Eiceman, Z.Karpas, H.H.Hill, Ion mobility spectrometry. 2013.

[4] T. Mayer, H. Borsdorf, Accuracy of ion mobility measurements dependent on the influence of humidity, Anal. Chem. 86 (2014) 5069-5076.

[5] H. Borsdorf, S. Badeweg, F. Löper, M. Höhnisch, R. Petrich, T. Mayer, The correlation of odors in the environment with ion mobility spectra patterns, Int. J. Ion Mobil. Spec. 18 (2015) 1-7.

[6] A. Kuklya, F. Uteschil, K. Kerpen, R. Marks, U. Telfgheder, Effect of humidity on analysis of aromatic compounds with planar differential ion mobility spectrometry, Int. J. Ion Mobil. Spec. 18 (2015) 67-75.

[7] T. Limero, E. Nazarov, M. Menlyadiev, G. A. Eiceman, Studies of the ionization chemistry in the re-circulation loop of the differential mobility spectrometer analyzer used to monitor air quality in the international space station, Int. J. Ion Mobil. Spec. 18 (2015) 77-86.

[8] T. N. Oboee, M. Piech, J. V. Mantese, S. Dardona, Effect of water vapor and formaldehyde detection with differential, Int. J. Ion Mobil. Spec. 15 (2012) 131-139.

[9] T. Limero, E. Reese, P. Cheng, J. Trowbridge, Preparation of a gas chromatograph-differential mobility spectrometer to measure target volatile organic compounds on the international space station, Int. J. Ion Mobil. Spec. 14 (2011) 81-91.

[10] N. Krylova, E. Krylov, G. A. Eiceman, Effect of moisture on the field dependence of mobility for gas-phase ions of organophosphorus compounds at atmospheric pressure with field asymmetric ion mobility spectrometry, J. Phys. Chem. A 107 (2003) 3648-3654.

[11] H. Cheng, J. Li, X. Gao, J. Jia, D. Zhang, D. Zhao, Malathion detection method using microhotplate-based preconcentrator and ion mobility spectrometry, Intern. J. Environ. Anal. Chem. 92 (2012) 279-288.

[12] B. C. Hauck, D. J. Davis, A. E. Clark, W. F. Siems, C. S. Harden, V. M. McHugh, H. H. Hill, Determining the water content of a drift gas using reduced ion mobility measurements, Int. J. Mass Spectrom. 368 (2014) 37-44.

[13] M. Mäkinen, M. Sillapää, A. K. Viitanen, A. Knap, J. Mäkela, J. Puton, The effect of humidity on sensitivity of amine detection in ion mobility spectrometry, Talanta 84 (2011) 116-121.

[14] W. Vautz, S. Sielemann, J. I. Baumbach, The influence of humidity on the determination of organic trace substances in ambient air using UV ion mobility spectrometry: alpha- and beta-pinene, 3-carene and limonene, Int. J. Ion Mobil. Spec. 1 (2003) 21-29.

[15] W. Vautz, S. Sielemann, J. I. Baumbach, Determination of terpenes in humid air using ultraviolet air using ultraviolet ion mobility spectrometry, Anal. Chim. Acta 513 (2004) 393-399.

[16] W. Vautz, V. Ruszani, S. Sielemann, J. I. Baumbach, Sensitive ion mobility spectrometry of humid ambient air using 10.6 eV UV-IMS, Int. J. Ion Mobil. Spec. 7 (2004) 3-8.

[17] A. Kuklya, F. Uteschil, K. Kerpen, R. Marks, U. Telgheder, Development of an electrospray 63Ni-differential ion mobility spectrometry for the analysis of aqueous samples , Talanta 120 (2014) 173-180.

[18] T. Mayer, H. Borsdorf, Which parameters influence the quantitative determination of halogenated substances? A summary of systematic investigations, Int. J. Ion Mobil. Spec. 18 (2015) 33-39.

[19] C. Warneke, C. van der Veen, S. Luxembourg, J. A. de Gouw, A. Kok, Measurements of benzene and toluene in ambient air using proton-transfer-reaction mass spectrometry: calibration, humidity dependence, and field intercomparison, Int. J. Mass Spectrom. 207 (2001) 167-182.

[20] Z. Izadi, M. Tabrizchi, H. Farrokhpour, Thermodynamic study of proton-bond dimers formation in atmospheric pressure: An experimental and theorical study, J. Chem. Thermodynamics 63 (2013) 17-23.

[21] H. H. Hill, G. Simpsons, Capabilities and limitations of ion mobility spectrometry for field screening applications, Field Anal. Chem. Technol. 1 (1997) 119-134.

[22] J. Puton, M. Nousiainen, M. Sillanpää, Ion mobility spectrometers with doped gases, Talanta 75 (2008) 978-987.

[23] Z. Xie, S. Sielemann, H. Schmidt, J. I. Baumbach, Determination of acetone, 2-butanone, diethyl ketone and BTX using HSCC-UV-IMS, Anal. Bional. Chem. 372 (2002) 606-610.

[24] S. Sielemann, J. I. Baumbach, H. Schmidt, P. Pilzecker, Quantitative analysis of benzene, toluene and m-xylene with the use of a UV-Ion mobility spectrometer, Field Anal. Chem. Technol. 4 (2000) 157-169.

[25] A. Kanu, H. H. Hill, Ion mobility spectrometry detection for gas chromatography, J .Chromatogr. A 1177 (2008) 12-27.

[26] Y. Du, W. Zhang, W. Whitten, H. Li, D. B. Watson, J. Xu, Membrane-extraction ion mobility spectrometry for in situ detection of chlorinated hydrocarbons in water, Anal. Bional. Chem. 82 (2010) 4089-4096.

[27] E. Boscani, M. L. Alexander, P. Prazellerm, T. D. Märk, Membrane inlet proton transfer reaction-mass spectrometry (EI-PTR-MS) for direct measurements of VOCs in water, Int. J. Mass Spectrom. 239 (2004) 179-186.

[28] A. S. Creba, A. N. E. Weissfloch, E. T. Krogh, C. G. Gill, A enzyme derivatized polydimethylsiloxane (PDMS) membrane for use in membrane introduction mass spectrometry (MIMS), J. Am. Soc. Mass Spetrom. 18 (2007) 973-979.

[29] J. P. Montoya, Medarray Inc., 2012. https://permselect.com/files/Using_Membranes_for_Gas_Exchange.pdf (accessed 29/09/15)

[30] J. W. Leonhardt, H. Bensch, M. Nolting, J. Baumbach, Determination of Benzene, Toluene, and Xylene by means of an ion mobility spectrometer device using photoionization, NASA Conf. Publ. 3301 (1995) 49-56.

[31] J. I. Baumbach, S. Sielemann, Z. Xie, H. Schmidt, Detection of the gasoline components methyl tert-butyl ether, benzene, toluene, and m-xylene using ion mobility spectrometers with a radioactive and UV ionization source, Anal. Chem. 75 (2003) 1483-1490.

[32] S. Sielemann, Z. Xie, H. Schmidt, J. I. Baumbach, Determination of MTBE next to Benzene, Toluene and Xylene within 90 s using GC/IMS with Multi-Capillary Column, Int. J. Ion Mobil. Spec. 4 (2001) 69-73.

[33] L. Criado-Garcia, R. Garrido-Delgado, L. Arce, M. Valcárcel, A comparative study between different alternatives to prepare gaseous standards for calibrating UV-Ion Mobility Spectrometers, Talanta 111 (2013) 111-118.

[34] C. Bothe Almquist, S. T. Hwang, The permeation of organophosphorus compounds in silicone rubber membranes, J. Membr. Sci. 153 (1999) 57-69.

Chapter 3
Tenax trap to enhance the selectivity of ion mobility measurements

Capítulo 3

Trampa TENAX para mejorar la selectividad de las medidas de movilidad iónica

In progress

TENAX TA COLUMN AS A CONVENIENT APPROACH TO IMPROVE SELECTIVITY OF UV-IMS WHEN MONITORING GASEOUS COMPOUNDS IN AIR SAMPLES

L. Criado-García, N. Almofti, L. Arce, M. Valcárcel*

Department of Analytical Chemistry, Annex C-3 Building, Campus of Rabanales. Institute of Fine Chemistry and Nanochemistry, University of Córdoba, 14071 Córdoba, Spain.

This study investigated the efficiency of coupling Tenax TA, as a pre-separation step, to overcome the low selectivity offered by UV-IMS when measuring gaseous compounds presents in air samples. Firstly, target analytes were trapped in a Tenax TA column at ambient temperature and then they were desorbed thermally in an oven and carried them to UV-IMS for their analysis. All parameters i.e. temperature ramp, sample gas flow rate, drift gas flow rate, adsorption time and adsorption flow rate were optimized to obtain high sensitivity. The proposed system was fully validated in terms of selectivity, sensitivity and precision. The system was calibrated with benzene and toluene standard gases generated in the exponential dilution flask. The limit of detection obtained was 0.54 and 0.57 mg m^{-3} for benzene and toluene, respectively. The developed method was successfully applied to identify these analytes in air samples close to a gasoline spillage.

Keywords: benzene, toluene, Tenax TA, ion mobility spectrometry, thermal desorption.

1. Introduction

Indoor and outdoor air monitoring and measurement of air pollutants are vital part in evaluating people public health and maintaining a healthful surrounding environment [1]. The development of a selective and sensitive analytical method to monitor volatile organic compounds (VOCs) in vulnerable areas with high level of VOCs is needed [2]. Benzene, toluene, ethylbenzene and xylene; known as BTEX, are belong to the aromatic carbonyl group of volatile organic compounds [3]. BTEX compounds are concentrated in outdoor environment near to industrial areas, next to petrochemical facilities [4] and in gas stations or parking areas [5]. BTEX are toxic compounds that even an exposure to small quantities may result in damage to human health [6]; diseases such as cancer and chronic respiratory disorders are reported [7]. Benzene and toluene are the two important compounds in this group, since benzene is classified in group 1 (human carcinogen) according to the International Agency on Research and Cancer (IARC) classification. Method 1501 of the National Institute for Occupational Safety and Health (NIOSH) stated that gas chromatography-flame ionization detector (GC-FID) is the official method to measure BTEX compounds from air samples. Therefore, most recent works use this technique for the determination of these volatile compounds, including BTEX in air [8, 9].

As it is well-known, Ion Mobility Spectrometry (IMS) is a powerful tool in air monitoring [10] both quantitatively and qualitatively. IMS with its advantages in operating under atmospheric pressure, its portability and detecting analytes presented in low concentration [11] along with performing relatively fast analysis make it a promising technique in the field of environmental analysis. By contrast, the main drawback of IMS is the low resolution [12] to identify individual signals for each component of a mixture. Selectivity can be enhanced by using a pre-separation step based on thermal desorption in order to resolve mixture components prior to IMS analysis [13].

In this work, Tenax TA, a widely used adsorbent for air analysis, was selected as a suitable alternative to improve the selectivity of the UV-IMS method. Target analytes in gaseous samples were retained in this sorbent and then thermal desorption was performed prior to its analysis by UV-IMS. The main advantage of this sorbent is that it has no chemical reaction with ozone thus is considered as inert to any sample compounds [23]. Tenax TA has been used previously as adsorbent trap combined with IMS; to retain pentan-2-one from liquid standards [14], aldehydes from olive oil [13], tert-butyl ether from water samples [15] and microbial biomarkers from air samples [16]. Also Tenax TA was used with Carbotrap in a sorbent mixture to determine cadaverine and putrescine from permeation tubes [17]. However, as far as we are concerned, this material has not been used before to retain *in situ* benzene and toluene present in air samples and determined them by UV-IMS.

For all of these reasons, the aim of this work was to show the potential of UV-IMS as a portable instrument to be used as a sensor which can give a quick and a global signal of BTEX present in gaseous samples. As well, when it is needed, the selectivity of the method can be improved by including a pre-separation step with Tenax TA to identify and quantify benzene and toluene in the gaseous samples.

2. Experimental

2.1. Chemicals and materials

Pure standard solutions for identification and quantification of compounds including; benzene, toluene, ethylbenzene and (*m-, p-* and *o-*) xylene, were all obtained from Sigma Aldrich (St Louis, MO, USA) with a purity of 99%. In **Table 1** are summarized the main physical and chemical properties of the target analytes. Methanol was used for cleaning the syringe. All BTEX standards were stored in a fridge at low temperature (4 $^{\circ}$C). The Tenax TA solid sorbent (2,6-diphenylene oxide) was purchased from Scientific Instrument Services (Ringoes, New Jersey, USA). An empty

stainless steel column (25 cm x 0.6 cm) was filled with 1 g of solid Tenax TA. Before used, Tenax TA column was activated in an oven by passing N_2 gas at a flow rate of 20 mL min^{-1} at 250 °C for 4 hours. Blanks (flushing nitrogen through an empty vial) were done before each measurement.

Table 1. Physical and chemical properties of BTEX compounds.

IUPAC name	Molecular weight (g mol^{-1})	Boiling point (ºC)	Ionization energy (eV)
Benzene	78.11	80.05	9.24
Ethylbenzene	106.17	136	8.77
Toluene	92.14	110.8	8.83
m-Xylene	106.16	139	8.44
o-Xylene	106.16	144.5	8.56
p-Xylene	106.16	138.2	8.44

2.2. Ion mobility spectrometer

The UV-IMS instrument used was supplied by Gesellschaft für Analytische Sensorsysteme (GAS, Dortmund, Germany). The instrument is 350 mm x 350 mm x 150 mm in size, with a tube length of 12 cm. The total weight of the instrument is 5 kg, and it uses a current supply of 230 V/50–60 Hz. The voltage applied is a constant voltage supply of 333 V cm^{-1}. The instrument is operated at ambient temperature and pressure. Purified nitrogen (N_2, 5.0) supplied by Abelló Linde (Barcelona, Spain) was used as sample and drift gas in this work. The heat unit was 5892A Chromatographic oven supplied by HP Hewlett Packard. Flow rates were controlled by using an Alltech Digital Flow Check HR™ instrument, supplied by the Chromatographie Service GmbH. Spectra were acquired in the positive ion mode. Data obtained was stored and treated with GASpector® software (Version 3.9.9.DSP from G.A.S.-Gesellschaft für Analytische Sensorsysteme, Dortmund, Germany). The length for each spectrum was 1024 points (each spectrum being formed with an average of 64 scans), the

grid pulse width 100 μs, the repetition rate 50 ms and the sampling frequency was 30 kHz. UV-IMS conditions are summarized in **Table 2**.

Table 2. The UV-IMS system conditions.

Parameter	**Value**
Pressure of drift tube	atmospheric
Temperature of drift tube	ambient
Drift and sample gas	N_2 (5.0)
Drift gas flow rate	100 mL min^{-1}
Sample gas flow rate	20 mL min^{-1}
Drift voltage polarity	Positive
Ionization source	UV lamp (10.6 eV)
Trigger delay	0.4 ms
Grid Pulse width	100 μs
Repetition rate	50 ms
Sampling frequency	30000 Hz
Electric field strength	333 V/cm
Length of the drift tube	12 cm

2.3. Experimental-set up

The sample introduction system (SISs) used in this study was an exponential dilution flask (EDF) and is illustrated in **Figure 1A**. A 1000 mL volumetric flask was used in which 1μL of each pure liquid standards is placed using a glass syringe. Then, volatilization of liquid standards drops was achieved by heating the flask for 1 min using a hot air gun. A heater mantle from J.P.Selecta (Barcelona, Spain) was used to maintain the temperature of EDF and ensure the homogeneity of the gases during the exponential step. In order to decrease the initial concentration, a flow of N_2 was passed through the EDF for a specific time. Following this procedure, different concentrations of gaseous standards in the EDF were obtained. Once reached the required initial concentration, the switching valve was

directed towards to the Tenax TA column to start the adsorption step. Then, the retained compounds on the Tenax TA were thermally desorbed and transferred to the UV-IMS to start the measurement as it is illustrated in **Figure 1B**. The direction of the analyte desorption was the same as the direction in which they have been adsorbed on the Tenax TA. The temperature program was as followed; initial temperature 60 °C for 1 min, a temperature ramp of 15 °C min^{-1} up to 220 °C held for 2 min. The sample gas flow rate was 20 mL min^{-1} and the drift gas was 100 mL min^{-1}. A blank analysis to test the column was processed after each measurement in order to avoid carry over between samples.

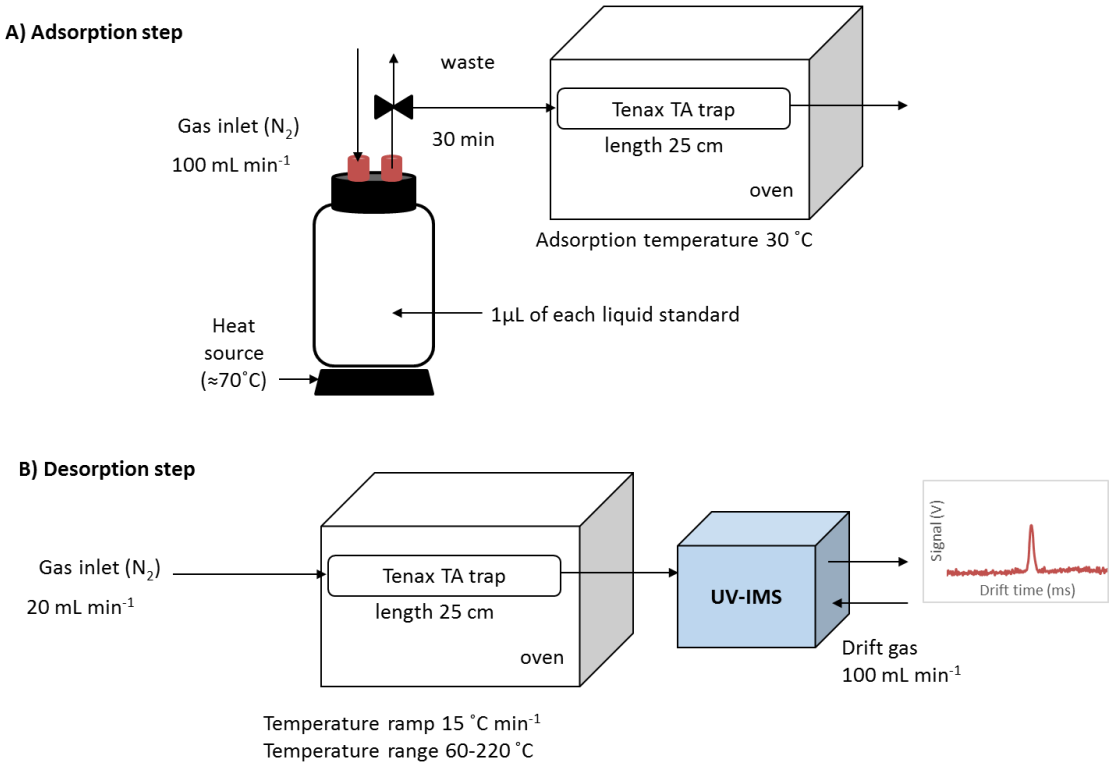

Fig. 1. (A) Exponential dilution used as sample introduction system to generate gaseous standards and (2) desorption step conditions.

2.4. On-field air sampling

The proposed method was tested for monitoring real air samples collected from Campus of Rabanales (University of Córdoba, Spain) car parking area, in which a gasoline spillage was reproduced. Sampling started at midday by pouring 5 mL of gasoline 95 on the pavement in a shaded area. Meteorological conditions were recorded at the sampling site for each sample. According to EPA, BTEX are presented with other components in gasoline. Five air samples were collected at different time interval by using Tenax TA column connected to a pump & flow controller PFC-6020 supplied by Ion Explorer by Ramem IONER (Madrid, Spain), operated at 100 mL min^{-1} for 30 min. Immediately, after sampling collection, the Tenax TA trap was introduced in the oven to start the desorption of the analytes retained in the column. In this step, the TENAX trap was connected to the UV-IMS for its analysis at the optimized conditions.

3. Results and discussion

In this study, a Tenax TA column coupled to UV-IMS instrument was optimized and then utilized to the determination of benzene and toluene in air. This combination along with the thermal desorption improves the two basic analytical properties; sensitivity and selectivity, of the method used with the UV-IMS. Ethylbenzene and xylene isomers were included during the optimization study of the proposed method. Although ethylbenzene and xylene isomers were not separated by using this method, they did not interfere with benzene and toluene signals.

3.1. Parameters optimization

Temperature program

Temperature ramp was firstly optimized. A gaseous sample of 42.60 mg m^{-3} for benzene, 42.11 mg m^{-3} for toluene, 42.11 mg m^{-3} for ethylbenzene and 42.11 mg m^{-3} for xylene isomers was used. Three temperature ramp levels (5, 15 and 20 ºC min^{-1}) were tested. The adsorption on Tenax TA column was performed at 30 ºC, recommended by the manufacturer of the Tenax TA. The desorption temperature range was set from 60 to 220 ºC with an initial time of 2 min at 60 ºC and a final time

of 5 min at 220 ºC. Finally 15 ºC min^{-1} was chosen for further experiments attending to the high intensity of peaks and the good resolution achieved. The same behaviour was also observed at lower concentrations.

Factorial design optimization for parameters that affect the adsorption and desorption steps

In **Table 3** are summarized the conditions studied and the value selected for each parameter. Each experiment was done by duplicate and the intensity for each peak appearing on topographic maps was recorded along with the drift time and spectra number. A gaseous sample containing initial concentrations of 5.76 mg m^{-3} for benzene, 5.69 mg m^{-3} for toluene, 5.69 mg m^{-3} for ethylbenzene and 5.70 mg m^{-3} for xylene isomers was used for optimization study. The exponential dilution flow rate was 200 mL min^{-1} and exponential time was 25 min. The optimum values were chosen attending to the highest signal obtained in the IMS spectra.

Table 3. Optimization of the operating condition of the proposed system.

Parameters	Units	Levels	Level 1	Level 2	Level 3	Optimum value
Adsorption step						
Adsorption time	min	3	5	15	30	30
Adsorption flow rate	mL min^{-1}	3	100	200	300	100
Desorption step						
Temperature ramp	°C min^{-1}	3	5	15	20	15
Sample gas flow rate	mL min^{-1}	3	20	30	40	20
Drift gas flow rate	mL min^{-1}	3	100	200	300	100

In the adsorption step, adsorption time and adsorption flow rate were optimized. The influence of the adsorption time was examined at three different levels 5, 15 and 30 min. Adsorption of targeted compounds on the trap increased with time during the first 30 min. The effect of the adsorption

flow rate was studied from 100 to 300 mL min^{-1}. Peak height increased when flow rate was at 100 mL min^{-1}, above which it decreases slightly.

For the desorption step, the sample gas and drift gas flow rates were also studied. It can be concluded that the maximum intensity for benzene and toluene was achieved by using sample gas flow rate of 20 mL min^{-1} and drift gas of 100 mL min^{-1}. In **Figure 2A** and **2B** are shown as an example the surface plots obtained for benzene obtained with Minitab 17 for adsorption time and flow rate, and for sample and drift gas flow rates used in the desorption step; respectively.

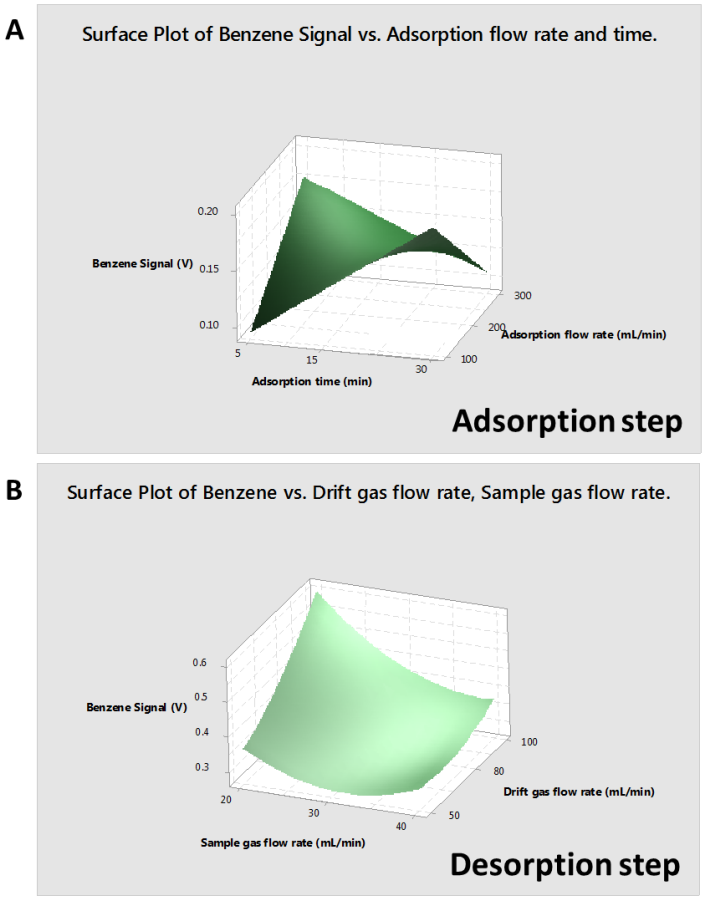

Fig. 2. Surface plots obtained for benzene optimization for (A) gas flow rate and time for the adsorption step and (B) sample gas flow rate drift gas flow rate used for the desorption step.

3.2. Analytical features of the proposed method

The proposed analytical method was validated in order to assess its suitability to identify and quantify benzene and toluene in gaseous air samples. The validation was performed by calculating limit of detection (LOD) and limit of quantification (LOQ). LOD and LOQ were calculated through dividing by three to ten times, respectively, the intercept standard error by the linear coefficients of the calibration curves (slope). Each measurement was performed by triplicate. In **Table 4** are shown the values obtained for LOD and LOQ.

Table 4. Regression coefficient, LOD and LOQ obtained.

Analyte	Calibration curve ($y= ax +b$)	R^2	Sa	Sb	LOD (mg m^{-3})	LOQ (mg m^{-3})
Benzene	y= 0.0438x +0.0544	0.958	0.008	0.003	0.54	1.79
Toluene	y= 0.0278x +0.0527	0.976	0.005	0.002	0.57	1.90

The precision study of the proposed method was assessed by using a standard gaseous of benzene and toluene at a concentration of 3.83 and 3.80 mg m^{-3}, respectively. The measurements were performed under the same experimental conditions. Precision study was carried out by performing repeatability and reproducibility studies as seen in **Table 5**. Repeatability was assessed by analyzing 6 replicates during one day in which the precision was lower than 1.34% for drift time and 0.81% for retention time. RSD values were higher for peak intensities (< 19.95%). This will indicate that the experiment is repeatable and precise enough for on-field analysis. On the other hand, reproducibility was evaluated by analyzing 9 replicates over three consecutive days. The high values of % RSD found in some cases can be referred to that the SIS is basically a home-made system, the system is not operated in an automated manner which in turn increases slightly the influence of personal errors in the preparation of standards.

Table 5. Precision study of the proposed method, values are presented as %RSD.

	Compounds	Intensity	Drift time	Retention time
Repeatability	Benzene	13.11	1.24	0.81
n=6	Toluene	19.95	0.98	0.74
Reproducibility	Benzene	12.71	1.43	0.78
n=9	Toluene	16.38	1.18	0.66

The selectivity of the method was assessed by measuring a gaseous sample mixture containing the 6 individual BTEX which were firstly added to the dilution flask and measured directly by UV-IMS. The initial concentrations were 25.81 mg m^{-3} for benzene, 25.51 mg m^{-3} for toluene, 25.53 mg m^{-3} for ethylbenzene and 25.53 mg m^{-3} for xylene isomers. Also the same experiment was performed with the developed methodology, using Tenax TA column to improve the UV-IMS selectivity. In **Figure 3A** is plotted the topographic plot when the gaseous sample was measured directly by UV-IMS. As can be seen, only a single peak was detected, tailing along the IMS topographic plot which is the sum of individual signals from the components in the mixture. The reason why this peak appeared at a longer drift time (19.81 ms) is related to the formation of a bigger cluster. Therefore, it took more time to reach the Faraday plate of the IMS compared with the drift times of individual analytes from the mixture, which were lower for all cases (<17 ms).

By contrast when the proposed methodology was used, pre-separation was achieved with the Tenax TA trap and consequently resolution of the UV-IMS was notoriously improved. As can be seen in **Figure 3B** the individual peaks from benzene and toluene were extracted from the topographic plot. Benzene appeared in the IMS spectra 130 (6.5 min approx.) and its IMS spectrum present a monomer peak (M^+) at 15.31 ms. Toluene was secondly eluted giving its signal in the spectra 150 (7.5

min approx.), its IMS spectrum presented also a monomer peak (M^+) at 15.91 ms.

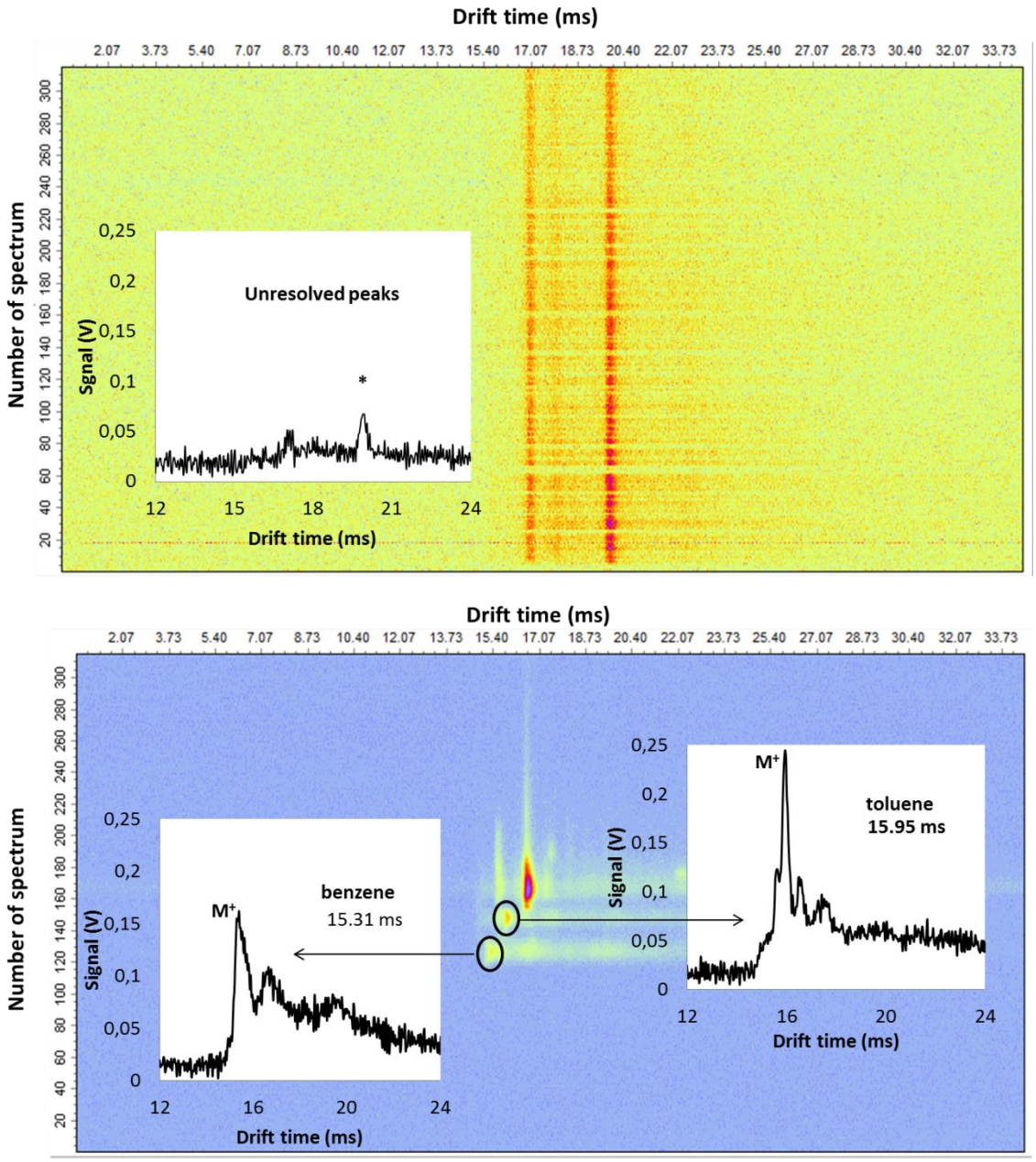

Fig. 3. Topographic plot of a mixture of BTEX at 25 mg m^{-3} (A) obtained by direct measurement with UV-IMS (spectra number 40 is plotted in which only one peak marked with an asterisk was observed) and, (B) by using the proposed methodology Tenax-UV-IMS. Extracted IMS spectrum for benzene and toluene are also plotted.

Better separation was achieved thanks to the use of Tenax TA column that allowed resolving some peaks from the BTEX mixture since they are eluted one by one by thermal desorption and they can be detected in the UV-IMS device.

3.3. Real samples analysis

The proposed method was tested to monitor real air samples of a gasoline spillage in a parking area following the methodology exposed in this work. Benzene and toluene in air sample was quantified in these air samples. As was expected the concentration of benzene and toluene decreased along time, as can be seen in **Figure 4**.

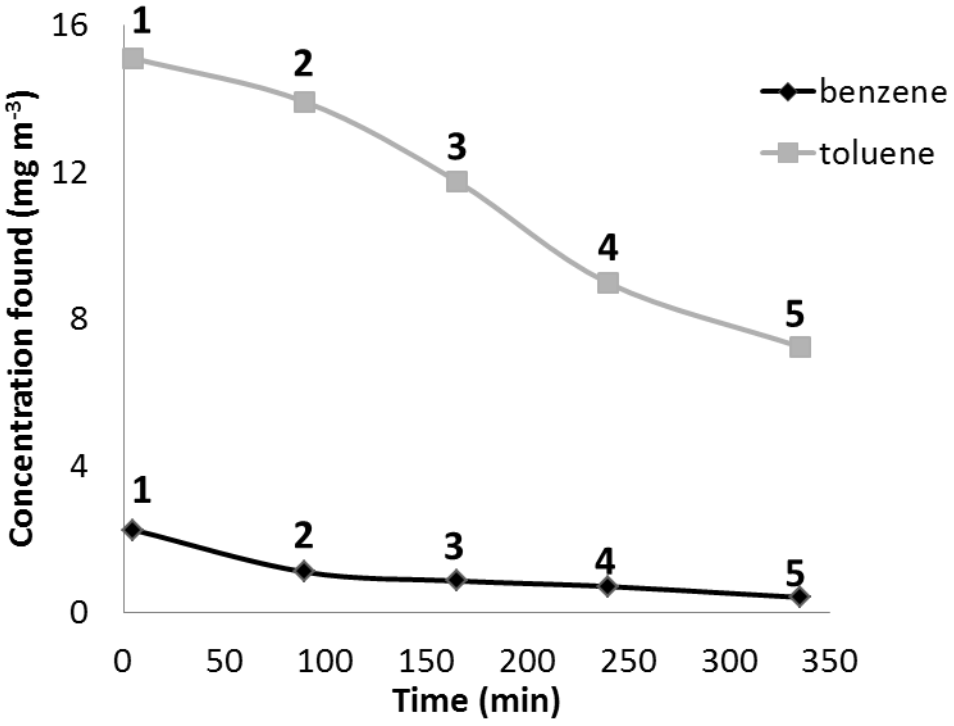

Fig. 4. Concentration of benzene and toluene in air samples (1-5) collected along time from the pavement of a parking area in which a gasoline spillage (5 mL) was simulated. The samples were measured with Tenax-UV-IMS.

As it is shown in **Table 6**, toluene was the compound which was presented at higher concentration (15.08 mg m^{-3}) in the analyzed sample. This value could be justified since toluene level in gasoline is doubled to the amount of benzene, according to the EPA.

Table 6. Concentrations obtained for benzene, toluene and ethylbenzene from gasoline spillage on pavement over time.

5 mL gasoline spillage on pavement	Elapsed time (min)	Concentration (mg m^{-3})	
		Benzene	Toluene
Sampling 1	5	2.24	15.08
Sampling 2	90	<LOQ	13.89
Sampling 3	165	<LOQ	11.73
Sampling 4	240	<LOQ	8.96
Sampling 5	335	<LOQ	7.23

In all cases concentrations for benzene and toluene found in the air in the point of the spillage on the pavement meet the short term exposure limit (STEL). Toluene was the only analyte that can be quantified in the five samples taken from the spillage. Also, the first measurement of benzene was above the LOQ and can be calculated using calibration curve. In the real sample, there was little bit increase in the drift time of the targeted compounds. This might be referred to the interaction of other components found in gasoline. Moreover, this increasing might be referred to the high concentration of gasoline used that interferes with Tenax TA and prevent the preferable adsorbent of compounds on the sorbent material.

4. Conclusion

In this work, it has been demonstrated the potential of Tenax TA column as a pre-separation step for the determination of benzene and toluene in air samples prior to the introduction of these compounds to UV-

IMS for analysis. This methodology was implemented successfully to identify and quantify benzene and toluene in real air samples close to a gasoline spillage source above the LOQ of 1.79 and 1.90 mg m^{-3}, respectively. The signals for other compounds present in the air sample did not interfere with benzene and toluene signals during the measurement. One limitation of the proposed methodology is that separation obtained with Tenax TA and UV-IMS was not enough to differentiate compounds with similar chemical properties such as xylene isomers and ethylbenzene that could be presented in the gaseous mixture. Other pre-separation method to improve resolution, e.g. multicapillary column (MCC) will be tested in future work. The Tenax-UV-IMS method offers a reliable, simple and inexpensive approach to enhance some basic analytical properties such as selectivity. This methodology could be used in the future in some gas stations and industrial working areas as an on-site air monitoring alarm for any sudden release of benzene and toluene or any other potential pollutant above a certain level.

Acknowledgments

The authors are grateful to Spain's DGICyT (Grant CTQ2014-52939R) for funding this work. L. Criado-García wishes to thank the Spanish Ministry of Education, Culture and Sport for award of a pre-doctoral grant (AP 2009-3528). Also N. Almofti wants to thanks for the Erasmus Mundus Master in Forensics Science grant, founded by the Education, Audiovisual and Culture Executive Agency (EACEA) of the European Commission.

The authors have declared no conflict of interest.

References

[1] C. Liadu, N. Nguyen, R. Nasreddine, S. Le Calvé, Experimental performances study of a transportable GC-PID and two thermo-desorption based methods coupled to FID and MS detection to assess BTEX exposure at sub-ppb level in air, Talanta 127 (2014) 33-42.

[2] M. Parra, D. Elustondo, R. Bermejo, J. Santamaría, Quantification of indoor and outdoor volatile organic compounds (VOCs) in pubs and cafés in Pamplona, Atmos. Environ. 42 (2008) 306-311.

[3] M. Caselli, G. de Gennaro, A. Marzocca, L. Trizio, M. Tutino, Assessment of the impact of the vehicular traffic on BTEX concentration in ring roads in urban areas of Bari (Italy), Chemosphere 81 (2010) 306-311.

[4] P. Baltrenas, E. Baltrenaite, V. Đerevièienë, P. Pereira, Atmospheric BTEX concentrations in the vicinity of the crude oil refinery of the Baltic region., Environ. monit. assess. 182 (2011) 115-127.

[5] A. Rezazadeh, Z. Naghavi, F. Zayeri, S. Selehpour, M. D. Seyedi, Occupational exposure of petroleum depot workers to BTEX compounds, Int. J. Occ. Med. I. T. 3 (2012) 39-44.

[6] Y. Zhou, J. Yu, Z. Yan, C. Zhang, Y. Xie, L. Ma, Q. Gu, F. Li, Application of portable gas chromatography-photo ionization detector combined with headspace sampling for field analysis of benzene, toluene, ethylbenzene, and xylene in soils, Environ. monit. assess. 185 (2012) 3037-3048.

[7] C. Vlachokostas, A. Michailodou, D. Spyridi, N. Moussiopoulos, Bridging the gap between traffic generated health stressors in urban areas: Predicting xylene levels in EU cities, Environ. pollut. 180 (2013) 251-258.

[8] K. Elke, E. Jermann, J. Begerow, L. Dunemann, Determination of benzene, toluene, ethylbenzene and xylenes in indoor air at

environmental levels using diffusive samplers in combination with headspace solid-phase microextraction and high-resolution gas chromatography–flame ionization detection, J. Chromatogr. A. 826 (1998) 191-200.

[9] R. Maghsoodi, A. Bahrami, F. Ghorbani, H. Mahjub, D. Malaki, Investigation of qualitative and quantitative of volatile organic compounds of ambient air in the mahshahr petrochemical complex in 2009, J. Res. Health Sci. 13 (2013) 69-74.

[10] I. Marquez-Sillero, E. Aguilera-Herrador, S. Cárdenas, Ion mobility spectrometry for environmental analysis, Trac-Trends in Anal. Chem. 30 (2011).

[11] S. Hajialogol, S. Ghorasi, A. Alinoori, A. Torabpour, M. Azimi, Thermal Solid Sample Introduction–Fast Gas Chromatography–Low Flow Ion Mobility Spectrometry as a field screening detection system., J. Chromatogr. A. 1268 (2012) 123-129.

[12] C. G. Fraga, D. R. Kerr, D. A. Atkinson, Improved quantitative analysis of ion mobility spectrometry by chemometric multivariate calibration, Analyst 134 (2009) 2329-2337.

[13] R. Garrido-Delgado, F. Mercader-Trejo, L. Arce, M. Valcárcel, Enhancing sensitivity and selectivity in the determination of aldehydes in olive oil by use of a Tenax TA trap coupled to a UV-ion mobility spectrometer, J. Chromatogr. A 1218 (2011) 7543-7549.

[14] M. E. Huxham, C. L. P. Thomas, Cold vapour desorption of volatile organic compounds from an adsorbent trap, Anal. Commun. 36 (1999) 317-320.

[15] R. Pozzi, F. Pinelli, P. Bocchini, G. C. Galletti, Rapid determination of methyl tert-butyl ether using dynamic headspace/ ion mobility spectrometry, Anal. Chim. Acta. 504 (2004) 313-317.

[16] R. M. Räsänen, M. Hakansson, M. Viljanen, Differentiation of air samples with and without microbial volatile organic compounds by aspiration ion mobility spectrometry and semiconductor sensors, Build Environ. (2010).

[17] M. A. Awan, I. Fleet, C. L. P. Thomas, Optimising cell temperature and dispersion field strength for the screening for putrescine and cadaverine with thermal-desorption-gas chromatography-differential mobility spectrometry, Anal. Chim. Acta. 611 (2008) 226-232.

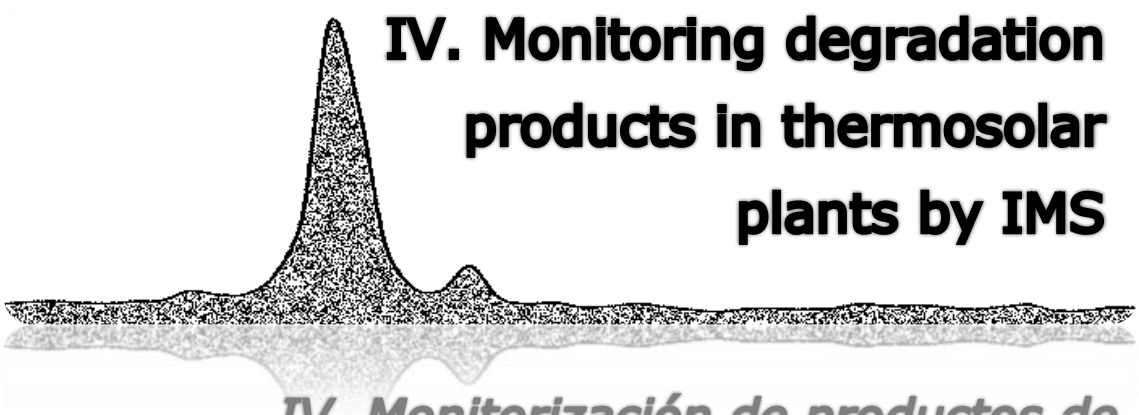

IV. Monitoring degradation products in thermosolar plants by IMS

IV. Monitorización de productos de degradación en las plantas termosolares mediante IMS

Renewable energy is widely spread in our society. In the case of thermosolar plants the energy is taken from the sun to be transformed later in electricity. The pipes of the thermosolar plant with parabolic design to concentrate sunlight are filled with thermosolar oil, which is exposed at high temperatures and high pressures. This fluid can be toxic for workers and dangerous for the environment due to the products that can be generated during its working life. A method for the rapid assessment of HTF quality and for the quantification of toxic products is needed to be implemented in the thermosolar plant as was exposed in *Block IV*.

In *Chapter 4*, two IMS instruments were used to measure HTF samples. On one hand, UV-IMS demonstrated its potential to give fingerprints which allowed the differentiation of HTF samples. In that sense we could differentiate between HTF samples exposed at high temperatures and pressures. On the other hand, ^{3}H-GC-IMS allowed us to detect selectively benzene and phenol in the HTF samples. These results were compared with GC-MS and FT-MIR.

A methodology based on headspace ^{3}H-GC-IMS was optimized and fully validated to measure benzene and phenol in HTF samples that were generated by a lab scale reactor that reproduced conditions at which HTF is exposed in the thermosolar plant as was exposed in *Chapter 5*. This method did not need pre-treatment step. Only the headspace of a volume of 100 μL of HTF is injected in the IMS. Therefore, this method developed can be easily automatized for its implementation in the thermosolar for periodical monitoring of HTF. Results obtained were compared with GC-FID.

Finally, in order to improve low sensitivity obtained with direct headspace for trace analysis a pre-treatment step based on SPE was included for its use in combination with ^{3}H-GC-IMS for determination of low concentrations of phenol in environmental samples as can be seen in *Chapter 6*.

Chapter 4
Potential of IMS to monitor heat transfer fluid

Capítulo 5

Potencial de IMS para monitorear aceite termosolar

Microchemical Journal 121 (2015) 163–171

Contents lists available at ScienceDirect

Microchemical Journal

journal homepage: www.elsevier.com/locate/microc

POTENTIAL OF ION MOBILITY SPECTROMETRY VERSUS FT-MIR AND GC-MS TO STUDY THE EVOLUTION OF A HEAT TRANSFER FLUID AFTER ITS HEATING PROCESS IN A THERMOSOLAR PLANT

Laura Criado-García, Rocío Garrido-Delgado, Lourdes Arce, Francisco López, Rogelio Peón, Miguel Valcárcel*

(1) Department of Analytical Chemistry, Annex C-3 Building, Campus of Rabanales, Institute of Fine Chemistry and Nanochemistry, University of Córdoba, 14071 Córdoba, Spain
(2) Magtel S.A., Gabriel Ramos Bejarano 114, P. I. Las Quemadas, 14014 Córdoba, Spain.
(3) TSK electrónica y electricidad S.A., Avda. Byron 220, P. C. Tecnológico, 33203 Gijón, Spain.

Heat Transfer Fluid (HTF) is commonly used in heat transfer industrial processes such as those performed in thermosolar plants. Although HTF is thermally stable, the high temperatures used in such plants (around 400 ºC) and overheating in continuous cycles can alter its composition. The potential changes in its initial composition (biphenyl and diphenyl ether), and the likely production of new compounds, such as benzene and phenol, require using fast-response portable instruments for on-site quality control at thermosolar plants. In this work, the degradation profile of HTF heated for a variable time was for the first time characterized by using two different Ion Mobility Spectrometry (IMS) instruments. The simple one used a UV lamp as ionization source (UV-IMS) whereas the other included a chromatographic column coupled to a tritium source (GC-^{3}H-IMS). Other analytical techniques such as Fourier Transform-Mid Infrared Spectroscopy (FT-MIR) and Gas Chromatography–Mass Spectrometry (GC-MS) were also used for the same purpose. Based on the results, both IMS instruments can be useful for on-line quality control of HTF in a thermosolar plant. Thus, the UV-IMS instrument can be used for screening purposes and the GC-^{3}H-IMS instrument for selective detection of benzene and phenol as degradation products.

Keywords: heat transfer fluid, thermosolar plant, ion mobility spectrometry, fourier transform-medium infrared spectrometry, gas chromatography-mass spectrometry.

© 2015 Elsevier B.V. All rights reserved

1. Introduction

Solar energy is by far the most abundant of all renewable forms of energy. Also, parabolic troughs constitute the best established and most widely used technology for concentrating solar energy at present [1]. Thermosolar plants based on parabolic troughs consist of large fields of collectors and use Heat Transfer Fluid (HTF) [2] since they offer exceptional high thermal and oxidation stability. Present-generation commercial HTFs are largely synthetic organic oils. The HTF used in this work was a eutectic mixture of diphenyl ether and biphenyl [3]. This type of HTF has a wide liquid temperature range, a high heat capacity and density, an also high thermal and chemical stability, and a low vapour pressure [4, 5]. Also, it currently offers the best combination of freezing point (12 ºC) and upper temperature limit (393 ºC) [6]. However, HTF can be toxic and highly flammable, and hence hazardous to plant operators. In addition, HTF efficiency in a thermosolar plant is limited by degradation at heating temperatures above 400 ºC.

One of the difficulties in assessing HTF usefulness in thermosolar plants is predicting its durability as an effective energy carrier. Until now, no large-scale studies of HTF lifetime or HTF degradation products resulting from repeated cyclic overheating at temperatures above 400 ºC in a thermosolar plant have been conducted. A method for rapid assessment of HTF quality is therefore much needed, and so is some means of monitoring degradation products potentially hazardous to workers and the environment in order to set off an alarm in the event of leakage from a thermal circuit at a thermosolar plant.

Ion Mobility Spectrometry (IMS) is a rapid, accurate technique widely used for the analysis of explosives, illicit drugs and chemical warfare agents, among other products, and available in dedicated commercial equipment. The analytical potential of IMS, particularly as regards operational speed and sensitivity, has extended its scope to pharmaceutical, food, feed, clinical, polymer, petrochemical and environmental analyses [7,

8]. In this work, IMS was used for the first time to examine the profile of HTF exposed at the heating process in a thermosolar plant. Technically, IMS involves converting sample vapour into ions by means of an ionization source operating at atmospheric pressure and characterizing such ions by their gas-phase mobility in a weak electric field [9].

IMS can use different types of ionization sources, the most effective choice in each case depending on the particular analyte to be determined. In this work, we used a radioactive tritium source and a UV lamp. Tritium (^{3}H) possesses a radioactive activity of 300 MBq, which is below the exemption limit in the EURATOM guideline (1 GBq). In a previous work, ^{3}H was used as an ionization source in the environmental monitoring of part-per-billion levels of toxic compounds in ambient air [10]. Other authors used UV lamp as ionization source to determine benzene, toluene and xylene among other compounds [11-13]; also, UV leads to comparatively simple responses and large scales of quantitative responses [8].

Benzene and phenol had never before been determined simultaneously in a similar matrix by IMS. Benzene was indeed measured individually by IMS with radioactive and UV ionization in a gasoline sample [11]. Also, benzene gaseous standard was measured by UV–IMS with various sample introduction systems [14], exponential dilution [13] and permeation tubes [12]. Phenol was also determined individually by IMS in combination with MS [15, 16]. The main purpose of this work was to develop an effective method for discriminating between raw and degraded HTF, and for simultaneously determining benzene and phenol in degraded HTF by ion mobility techniques. The results were compared with those provided by classical techniques such as Fourier Transform-Mid Infrared Spectroscopy (FT-MIR) and Gas Chromatography–Mass Spectrometry (GC–MS) in order to highlight the advantages of the proposed methods.

2. Experimental

2.1. HTF samples and laboratory-scale reactor

HTF was supplied by DOW® (Edegem, Belgium). Biphenyl, diphenyl ether, phenol, benzene and dichloromethane were purchased from Sigma–Aldrich (St. Louis, MA, USA). **Table 1** summarizes the chemical properties of the target compounds.

Table 1. Chemical properties of the compounds initially present in the HTF and of their degradation products.

	Compound	Ionization energy (eV)	Proton affinity[(1)] (kJ mol^{-1})	Boiling point (ºC)	Molecular structure
Initial compounds	Biphenyl	7.95	813.6	255	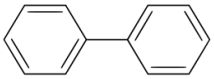
	Diphenyl ether	8.09	n.a.	258	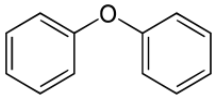
Degradation products	Benzene	9.28	750.4	80.1	
	Phenol	8.5	817.3	181.7	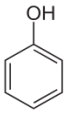
	Dibenzofuran	8.77	n.a.	285	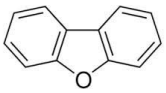
	Triphenylmethane	8.34	n.a.	359	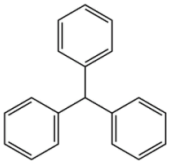

n.a.: not available. [(1)]Proton affinity of water = 691 KJ mol^{-1}.

The degradation process occurring in a thermosolar plant was simulated in the laboratory by placing approximately 180 mL of raw HTF in a 1 L reactor manufactured by Sanical Astur, S.L. (Oviedo, Spain). The reactor was purged with pure nitrogen (99.999 %) from Abelló Linde, S.A. (Barcelona, Spain) before heating in order to maintain an inert environment inside. The reactor pressure and temperature were checked by means of an automatic controller supplied by Lascar electronics (Salisbury, UK). Raw HTF

sample was heated at about 400 ºC in heating–cooling cycles and an aliquot of 10 mL of heated HTF sample was collected periodically from the reactor once the temperature decreased from 400 ºC to room temperature (20 ºC) after approximately 5 hours. The first aliquot of HTF sample was collected after 51 h of heating in the reactor. This period can be compared with the time that the HTF is exposed to high temperatures in a thermosolar plant along a year. Then the temperature was again increased up to 400 ºC to keep heating the rest of the HTF sample of the inside the reactor until it was stopped to take the second aliquot of HTF sample. This procedure was repeatedly throughout the rest of the heating process (462 h).

Degraded HTF samples were withdrawn by using a peristaltic pump from Gilson (Villiers, France) and Teflon tubing from Sigma–Aldrich (St. Louis, USA). **Figure 1** depicts the reactor and a set of degraded samples in the lab. A degraded HTF sample from a thermosolar plant supplied by Magtel S.L. (Córdoba, Spain) was also analysed.

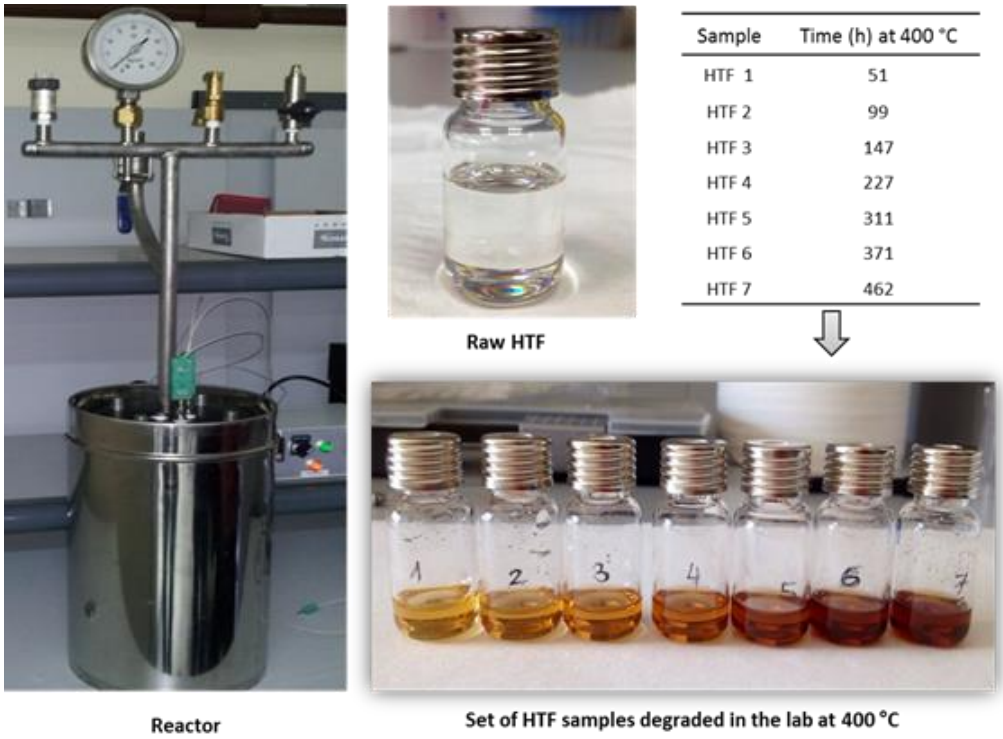

Fig. 1. Sample of raw HTF, a whole set of degraded HTF samples 1-7 and the lab-scale reactor.

All HTF samples were stored in air-tight glass vials at room temperature (23–25 ºC) in dark until analysis.

2.2. Equipment and methods

2.2.1. Ion mobility instruments

Both ion mobility instruments used in this work (UV–IMS and GC–^{3}H–IMS) were supplied by G.A.S. mbH (Dortmund, Germany).

The experimental set-up used with the portable, UV–IMS instrument is depicted in **Figure 2A**. The procedure involved placing 100 µL of HTF sample in a 10 mL vial that was then sealed with a Teflon septum and heated at 30 ºC for 5 min. Next, two switching valves were actuated to have the vapor phase from the vial headspace transferred into the UV-IMS equipment by the carrier gas (100 mL min^{-1}). The headspace was injected over the first 20 spectra (1 min) and a total of 50 spectra (2.5 min) were recorded.

The selectivity of the UV–IMS determination was improved by using an alternative device consisting of a gas chromatographic column coupled to an ion mobility spectrometer (GC–^{3}H–IMS). It was equipped with a heated splitless injector for direct sampling of the headspace from the HTF samples. For better reproducibility, the instrument was coupled to an autosampler from CTC Analytics AG (Zwingen, Switzerland). The analytical system was equipped with a ^{3}H ionization source (St. Petersburg, Russia) with an activity of 300 MBq. The instrument operates in negative or positive ionization mode. The experimental set-up is depicted in **Figure 2B**. For analysis, a volume of 100 µL of sample was placed in a 20 mL vial that was then closed with magnetic caps and a teflon septum. After 5 min incubation at 35 ºC, 200 µL of sample headspace was automatically injected by a heated syringe (80 ºC) into the GC–^{3}H–IMS equipment. After injection, the carrier gas (nitrogen) passing through the injector inserted the sample into the GC column heated at 40 ºC for timely separation. The GC column used was 30 m long x 0.25 mm of ID CC filled with 0.5 µm film thickness of methyl, phenyl and vinylsiloxane in a 94:5:1 proportion from CS-

Chromatographie Service GmbH (Dürem, Germany). Then, the analytes were eluted and driven into the ionization chamber prior to detection at the IM spectrometer heated at 65 ºC.

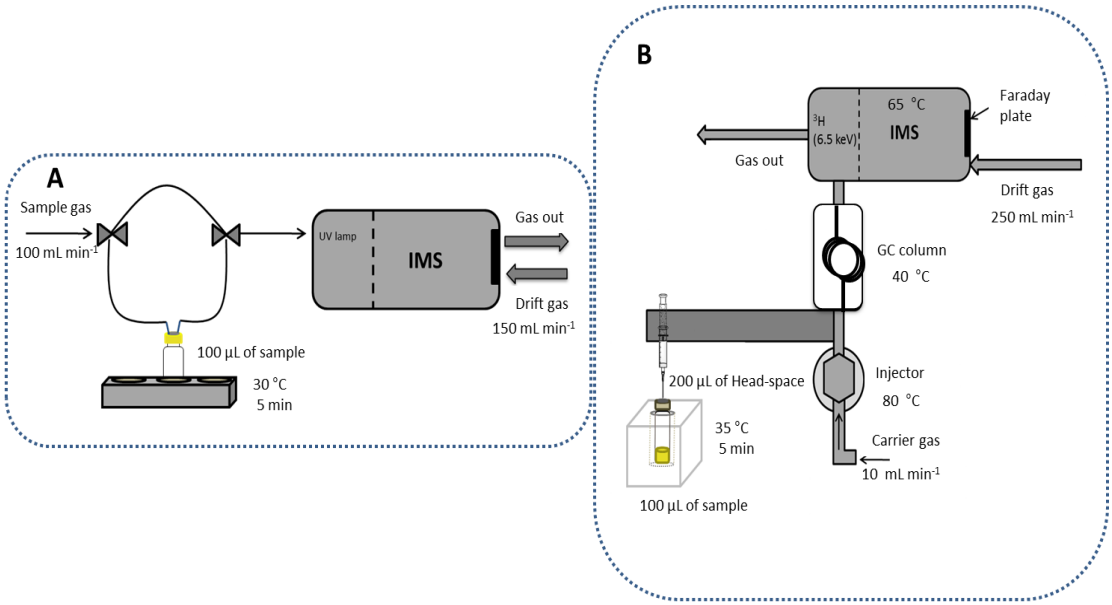

Fig. 2. Scheme of the experimental set-up for the UV–IMS instrument (A) and GC-^{3}H-IMS instrument (B).

The UV–IMS and GC–^{3}H–IMS instruments were based on the same operational principle. Thus, once ions formed in the ionization chamber and were focused on a shutter grid, they started to move along a drift tube. The shutter opening time was set at 100 µs for GC–^{3}H–IMS and 500 µs for UV–IMS in order to allow the ions to pass in short pulses into the separation chamber. The length of the drift tube was 10 cm for UV–IMS and 5 cm for GC–^{3}H–IMS.

A nitrogen stream was passed in the opposite direction of the drifting ions in order to prevent non-ionized impurities from entering the separation chamber. Nitrogen 5.0 supplied by Abelló Linde, S.A. (Barcelona, Spain) was used as sample and drift gas. Ions differing in mobility were separated under a constant electrical field of 333 V cm^{-1} for UV-IMS and 400 V cm^{-1} for GC–^{3}H–IMS. The drift tube for UV-IMS was kept under atmospheric

conditions (25 ºC and 101 kPa, respectively), whereas that for GC–^{3}H–IMS was heated at 65 ºC. As separated ions reached a Faraday plate, data were acquired and processed by a computer running the software GASpector v.3.99.035 DSP for UV-IMS and for GC–^{3}H–IMS, spectra were acquired and displayed by the integrated computer within the instrument and data was processed by using the software LAV v. 2.0.0, both from G.A.S (Dortmund, Germany). All spectra were recorded in the positive ion mode.

2.2.2. Infrared spectrometer

Infrared spectra were obtained in the transmission mode, using an FT-MIR Tensor 27 spectrometer from Bruker Optik GmbH (Ettlingen, Germany) equipped with CsI beam splitters and a DTGS detector. Spectra were acquired by using the software OPUS v.6.5, also from Bruker. For analysis, a droplet (2 µL) of HTF sample was added to KBr to form a pellet that was then inserted into the instrument for measurement.

2.2.3. Gas chromatograph–mass spectrometer

GC–MS analyses were performed on a Saturno 2200 instrument from Varian (Palo Alto, USA). HTF samples were diluted in dichloromethane (1 g/50 mL) and 1 µL aliquots injected at 265 ºC in the split mode (split ratio 1/50). The chromatographic column used (30 m, 0.25 mm i.d., 0.25 µm film thickness) was packed with 5% phenyl silicone from Agilent (Santa Clara, USA). Helium (99.999%) at a flow rate of 1 mL min^{-1} was used as carrier gas from Praxair (Danbury, USA). The temperature programme was as follows: 35 ºC (2 min) and 10 ºC/ min ramp to 285 ºC (5 min). Ions were detected in the full scan mode (0.5 s/scan), using the *m*/*z* range 45–400.

3. Results and discussion

As shown here by comparison with others two analytical instruments, IMS is an effective choice for characterizing the degradation profile of HTF.

3.1. Qualitative analysis by IMS

The first objective of this work was to demonstrate the ability of IMS to distinguish raw and degraded HTF which required optimizing the operational parameters of this technique. **Figure 3** shows the spectra for raw and degraded HTF samples obtained with the UV–IMS instrument. As can be seen, two common peaks were identified in the spectra from both samples, namely: *peak 1* at 20.9 ms and *peak 2* at 21.9 ms. However, only degraded HTF gave a third one: *peak 3* at 20.1 ms.

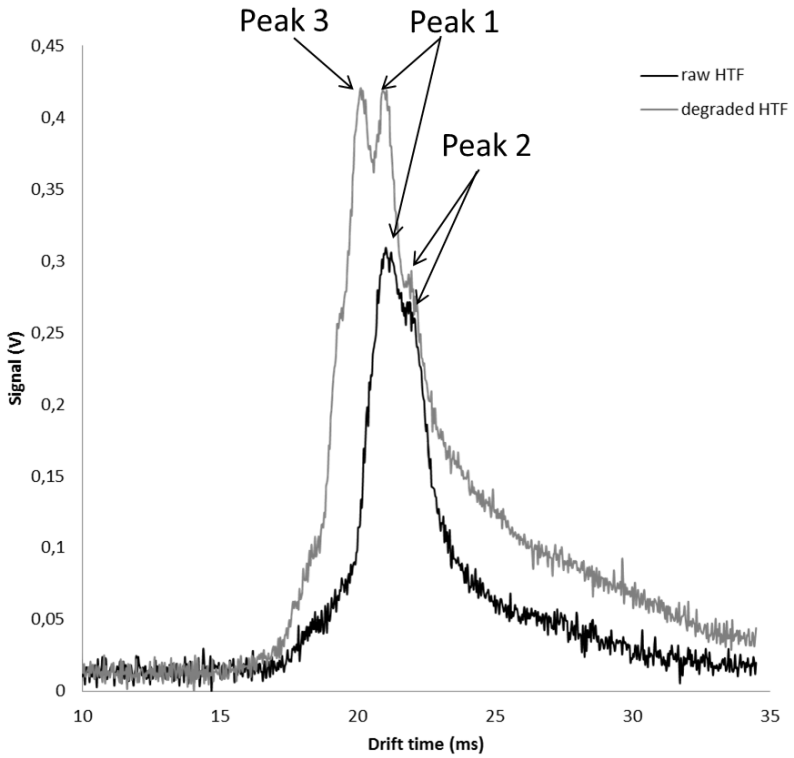

Fig. 3. Spectra for raw and degraded HTF sample as obtained with the UV-IMS instrument.

The intensity of the peaks for degraded HTF was presumably increased by the presence of degradation products such as benzene and phenol formed by effect of exposure to high temperatures for long times. This assumption was confirmed by analysing a raw HTF sample spiked with variable concentrations of benzene and phenol. Thus, *peak 1* increased with

increasing added concentration of phenol and benzene, and exhibited the same trend as in the degraded HTF samples. The photoionization energy of the UV lamp (10.6 eV) was high enough to ionize benzene (9.28 eV) and phenol (8.50 eV) through direct reaction of the analyte molecules (M) with photons (*hv*) to form positive ions (M^+) [11, 17]. Unfortunately, the resulting ions co-emigrated and no individual ion response for each compound in the mixture could be obtained.

A whole set of degraded HTF samples were also measured by UV–IMS. **Figure 4A** shows the ion mobility spectra for samples 1, 3 and 7 of degraded HTF, and one of raw HTF, as obtained with the UV–IMS instrument. As can be seen, the raw HTF sample and sample 1 of degraded HTF (51 h heating) gave *peak 1* and *peak 2*, albeit with different intensities. On the other hand, *peak 3* appeared first in sample 3 of degraded HTF (147 h heating) and in the sequence up to sample 7 of degraded HTF (462 h heating). *Peak 1* was the only one appearing in the spectra for all samples measured by UV–IMS. Therefore, the monitoring of HTF samples was carried out through the peak 1 signal. As can be seen from **Figure 4B**, its intensity increased with increasing degradation (i.e., increasing heating time) from sample 1 (51 h) to 4 (227 h) of degraded HTF as a result of the also increasing formation of degradation products. Notice that concentration found in the degraded HTF 1 sample (generated in the reactor at lab scale) and the degraded HTF sample collected from thermosolar plant was lower than 0.5 g kg^{-1} for benzene and 0.25 g kg^{-1} for phenol in both samples. These values were supplied by an external laboratory. So, a higher concentration of degradation compounds: benzene and phenol is expected along increased heating times.

Further heating after a certain time resulted in no more increase in IMS signal in the more degraded HTF samples 5 (311 h), 6 (462 h) and 7 (462 h) since saturation of the UV–IMS signal could be taking place.

Based on the foregoing, raw and degraded HTF can be distinguished by UV–IMS but no degradation compounds can be selectively identified by direct analysis of the headspace because the UV-IMS instrument has a

limited ability to separate ions. The required selectivity was obtained by using a GC column as a pre-separation step prior to IMS (GC–^{3}H–IMS).

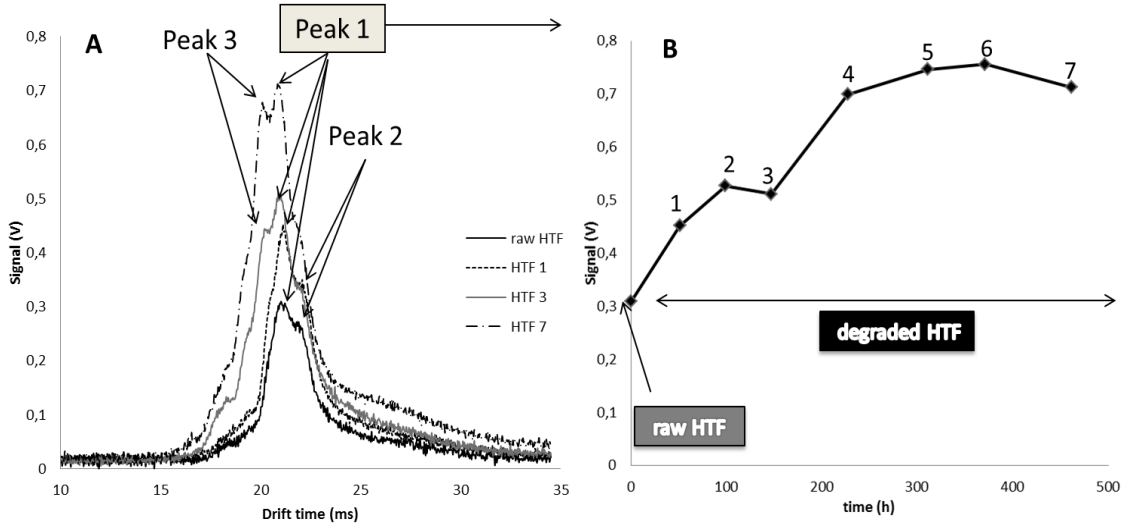

Fig. 4. Spectra for raw and degraded HTF samples 1, 3 and 7 (A) and degradation curve for *peak 1* (B) in raw HTF and in variably degraded HTF samples 1-7 as obtained with the UV–IMS instrument.

Figure 5A shows the topographic plot obtained from raw and degraded HTF samples measured by GC–^{3}H–IMS. Unlike the raw HTF sample, the degraded HTF sample exhibited two new, strong peaks presumably corresponding to two degradation compounds: benzene and phenol. This assumption was confirmed by analysing a raw HTF sample spiked with benzene and phenol at variable concentration levels. The drift and retention times for the spiked raw sample were quite similar to those for the degraded HTF sample. As expected, benzene was the first compound to appear in the chromatogram (56 s) due to its low boiling point (80.1 ºC). Benzene is a non-polar compound with a low proton affinity (750.4 KJ mol^{-1}), but higher than the water value (691 KJ mol^{-1}); therefore, it can be ionized by a tritium source. In fact, when a tritium source is used proton transfer from the reactant ion (H_3O^+), charge transfer with NO^+ or association of NO^+ could take place [18]. Notice that the reactant ion peak

(RIP), represent the total of all ions available in the ionization chamber described as $H^+(H_2O)_n$ when nitrogen is used as the carrier gas. Under the IMS conditions used in this work, benzene ions appeared a few milliseconds before the RIP in the spectrum (see **Figure 5B**). Thus, the benzene ions detected probably resulted from a charge transfer reaction with NO^+. Nevertheless, phenol (817.3 KJ mol^{-1}) ions seem to react with the RIP as its signal appears after the RIP with a drift time of 7.01 ms (see **Figure 5C**).

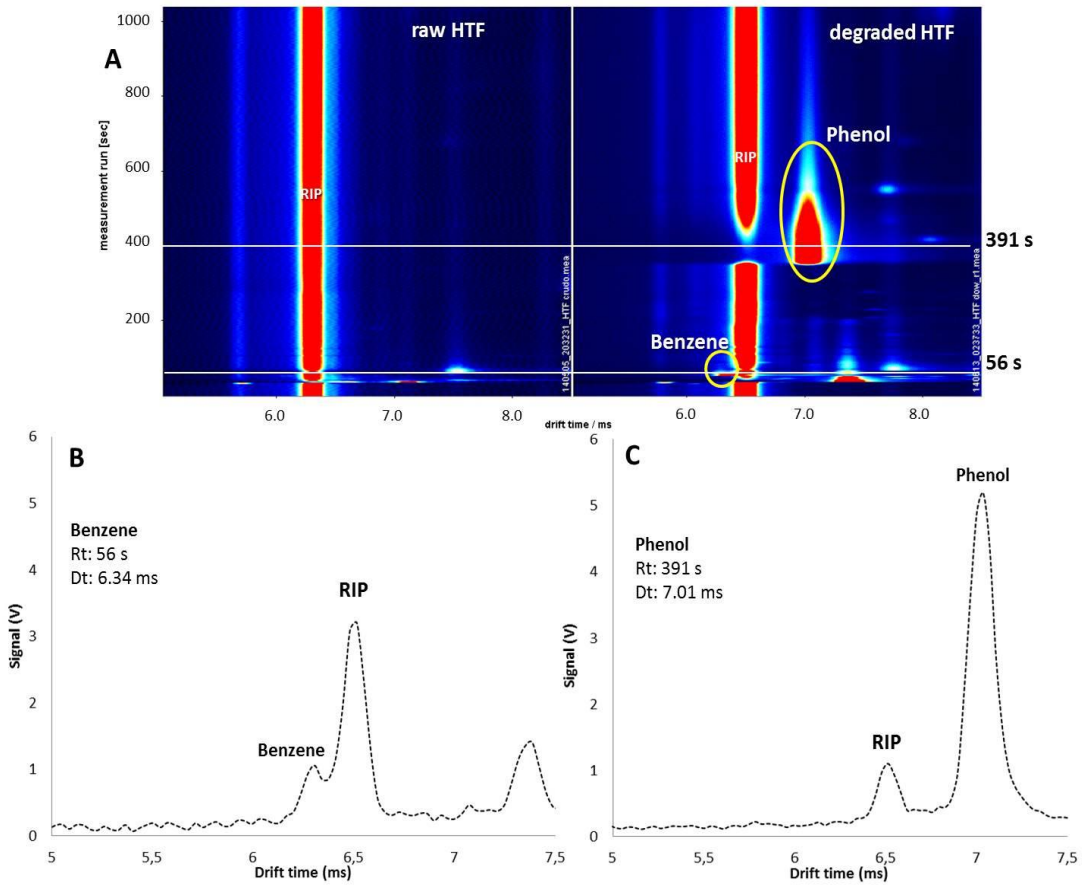

Fig. 5. Spectra for raw and degraded HTF samples 1, 3 and 7 (A) and degradation curve for *peak 1* (B) in raw HTF and in variably degraded HTF samples 1-7 as obtained with the UV–IMS instrument.

The retention time of phenol (391 s) was much higher than benzene (56 s) by a virtue of its higher boiling point (181.7 ºC) compared with benzene (80.1 ºC). **Figure 6A** shows the curves for benzene and phenol as

obtained from a whole set of degraded HTF samples measured by GC–^{3}H–IMS. As can be seen, the peak height for benzene (**Figure 6B**) and phenol (**Figure 6C**) increased for more degraded HTF samples, those in which exposition time at 400 ºC was higher.

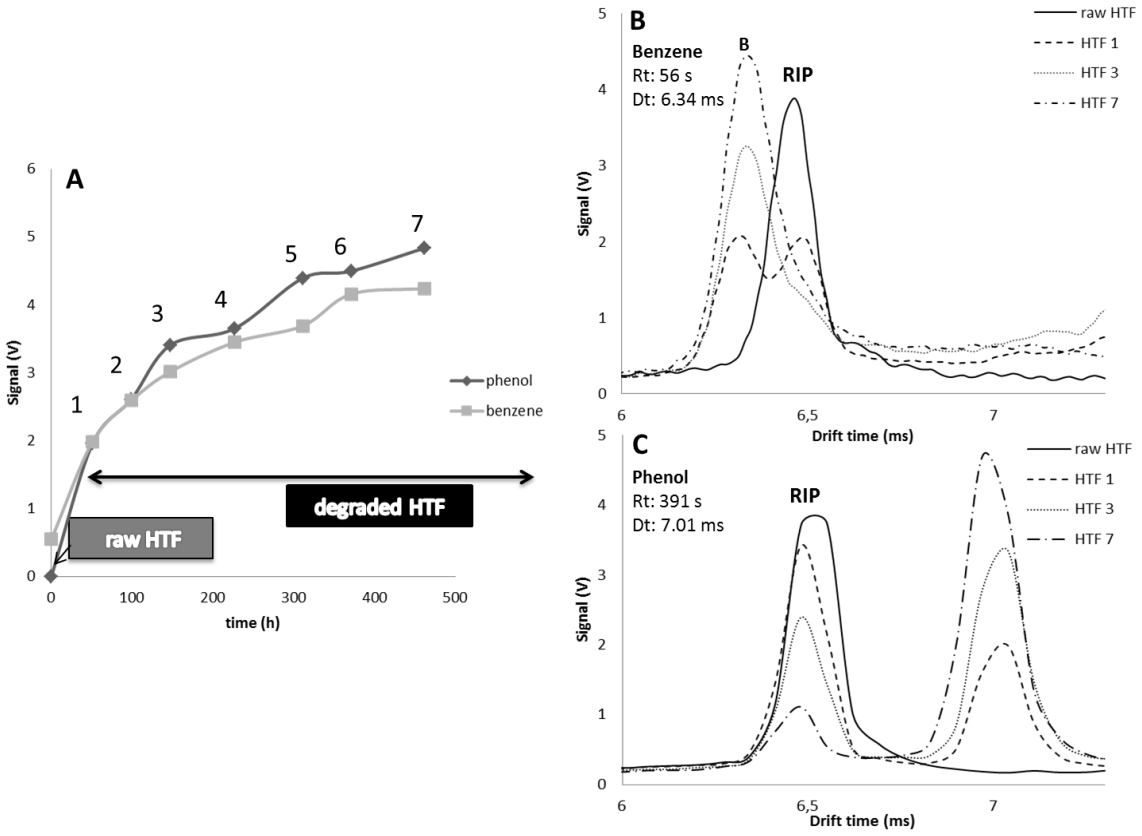

Fig. 6. Degradation curve for the benzene and phenol in raw and degraded HTF samples 1-7 (A) as obtained with the GC-^{3}H-IMS instrument. IMS spectra for benzene (B) and phenol (C) in raw and degraded HTF samples 1, 3 and 7.

Further evidence that the peaks for benzene and phenol were accurately assigned was provided by the fact that, as expected, both signals were higher with increasing heating time of HTF samples. As well it was observed how the phenol and benzene peaks increased whereas the RIP decreased or even suppressed. At low concentrations, protons from the

reactant ion are consumed proportionally to the density of neutral molecules in the sample vapor. At high concentrations, however, the reservoir of reactant ion charge is completely consumed [19].

In IMS, each ion has a characteristic reduced mobility (K_0) that can be highly useful for identification purposes. The K_0 values obtained for the benzene and phenol ion peaks are 1.94 and 1.75 $cm^2\ V^{-1}\ s^{-1}$, respectively. Similar values for benzene K_0 were found in the literature, 1.95 $cm^2\ V^{-1}\ s^{-1}$ [13] and 2.01 $cm^2\ V^{-1}\ s^{-1}$ [14]. Unfortunately, no phenol K_0 values previously determined in the positive mode by IMS were available for comparison. As stated above, however, phenol could be unequivocally identified in the ion mobility spectra from spiked samples.

The precision of the proposed method was assessed by analysing a sample of degraded HTF from a thermosolar plant. The precision values obtained with UV–IMS and GC–^{3}H–IMS are expressed as relative standard deviation (RSD) in **Table 2**.

Table 2. Precision, as relative standard deviation (RSD), in drift time, peak height and retention time as obtained with the UV-IMS and ^{3}H-GC–IMS instruments.

Degraded HTF	**UV-IMS**		**^{3}H-GC–IMS**					
	Peak 1		*Benzene peak*			*Phenol peak*		
	Drift time	Peak height	Drift time	Peak height	Retention time	Drift time	Peak height	Retention time
Repeatability (% RSD)	0.5	2.6	3.3	0.1	0.6	3.0	0.07	1.2
Reproducibility (% RSD)	1.8	4.7	4.4	0.07	1.0	3.5	0.15	1.7

Repeatability was assessed by analysing the same sample six times (n= 6) under identical experimental conditions on the same day, and reproducibility by analysing the same sample three times (n= 3) on three consecutive days. Repeatability and reproducibility in drift time were both lower with UV–IMS (0.5% and 1.8% respectively); on the other hand, RSD

in peak height was lower with ^{3}H-GC–IMS. It can be concluded that both UV–IMS and GC–^{3}H–IMS are suitable for analysing HTF samples with precision (RSD< 5%). Selectivity was better with GC–^{3}H–IMS than with UV–IMS by effect of the former allowing benzene and phenol to be detected without signal saturation in highly degraded HTF samples. Higher increments of the IMS signal from raw HTF to degraded HTF 4 sample (227 hours of heating) were observed with both IMS instruments. However, a saturation effect from degraded HTF 5 sample to degraded HTF 7 sample was observed with UV-IMS while a slightly increment for benzene and phenol signals was observed when using GC–^{3}H–IMS. In conclusion, during the first years of HTF heating in a termosolar plant (from 51 h up to 227 h of heating inside the lab-scale reactor) the chemical composition of HTF changed sharply due to the generation of degradation products (benzene and phenol) and consequently its thermal efficiency could be affected. The proposed IMS method for characterizing the degradation profile of HTF in thermosolar plants was also compared in terms of performance with two classical analytical techniques (FT-MIR and GC–MS) by analysing the same HTF samples.

3.2. Qualitative analysis by FT-MIR and GC–MS

This study involved using FT-MIR to characterize HTF samples. Firstly, raw and degraded HTF samples were measured (**Figure 7A**); then a whole set of degraded HTF samples (**Figure 7B**). A similar IR spectrum containing the typical absorbance bands for the initial HTF components and their degradation products was obtained in all cases. The bands included one at 3100 cm^{-1} corresponding to C–H bond vibrations, and several others at 1400–1600 cm^{-1} associated to C=C bonds in aromatic rings. The region from 1000 to 400 cm^{-1} contained several additional bands known as "aromatic fingerprints" and potentially highly useful for identifying the specific compounds present in HTF. There was, however, one other band at 1700 cm^{-1} possibly due to the increase in concentration of phenol and other degradation products present in degraded HTF. This band appeared in the spectra for samples 3–7 of degraded HTF. No differences between bands

were observed in less degraded samples, however. Also, increased transmittance values for aromatic compounds (bands from 1400 to 1600 cm^{-1}) were observed in the FT-MIR spectra for the more degraded HTF samples.

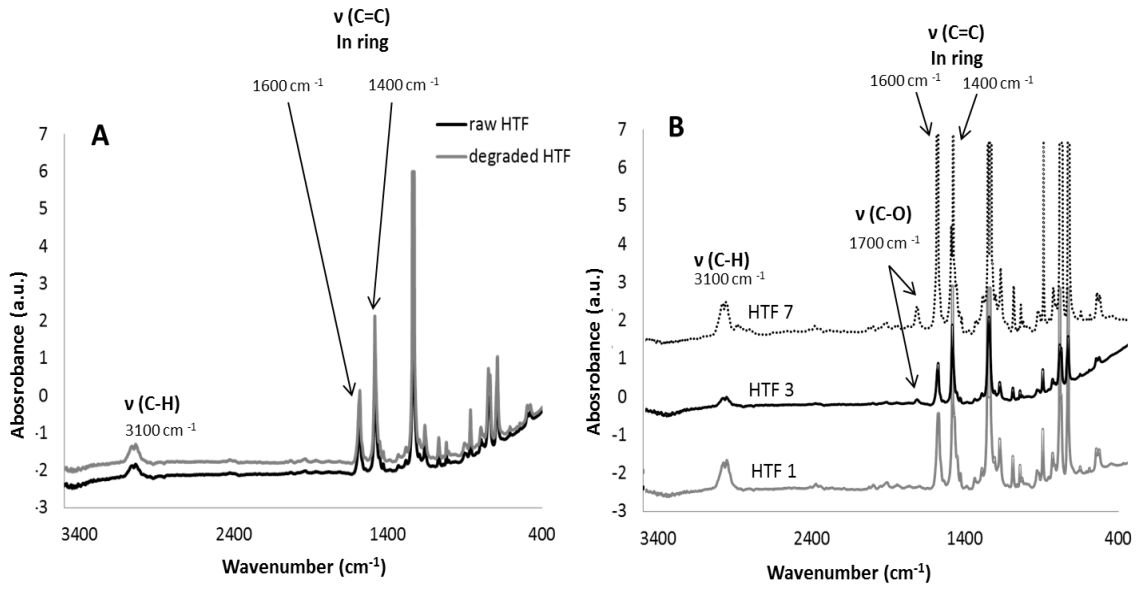

Fig. 7. Degradation curve for the benzene and phenol in raw and degraded HTF samples 1-7 (A) as obtained with the GC-^{3}H-IMS instrument. IMS spectra for benzene (B) and phenol (C) in raw and degraded HTF samples 1, 3 and 7.

Therefore, FT-MIR measurements can be useful to obtain global information about the compounds present in degraded HTF. However, the degradation products formed in raw HTF belong to the same family as the original compounds and are thus highly difficult to identify since they exhibit the same, typical bands of aromatics. In addition, FT-MIR measurements in this instrument require preparing KBr pellets with the samples prior to analysis; so it cannot be used for on-line analysis.

GC–MS was also chosen for identifying the compounds present in the HTF samples. The initial components of HTF (biphenyl and diphenyl ether) were detected in all degraded HTF samples (see **Figure 8**) since its

high concentration. Also, degradation products (benzene and phenol) appeared in sample 5 of degraded HTF, which was heated at about 400 ºC for 311 h, and in those heated for an even longer time. Other degradation compounds with a higher boiling point than benzene and phenol, dibenzofuran and triphenylmethane, also appeared in the chromatograms for samples 5 to 7 of degraded HTF. As can be seen from the chromatogram of Figure 8, all degradation products were clearly identified in degraded HTF sample 7. A magnified view of the chromatogram is also shown where phenol and benzene are well resolved from the solvent (dichloromethane).

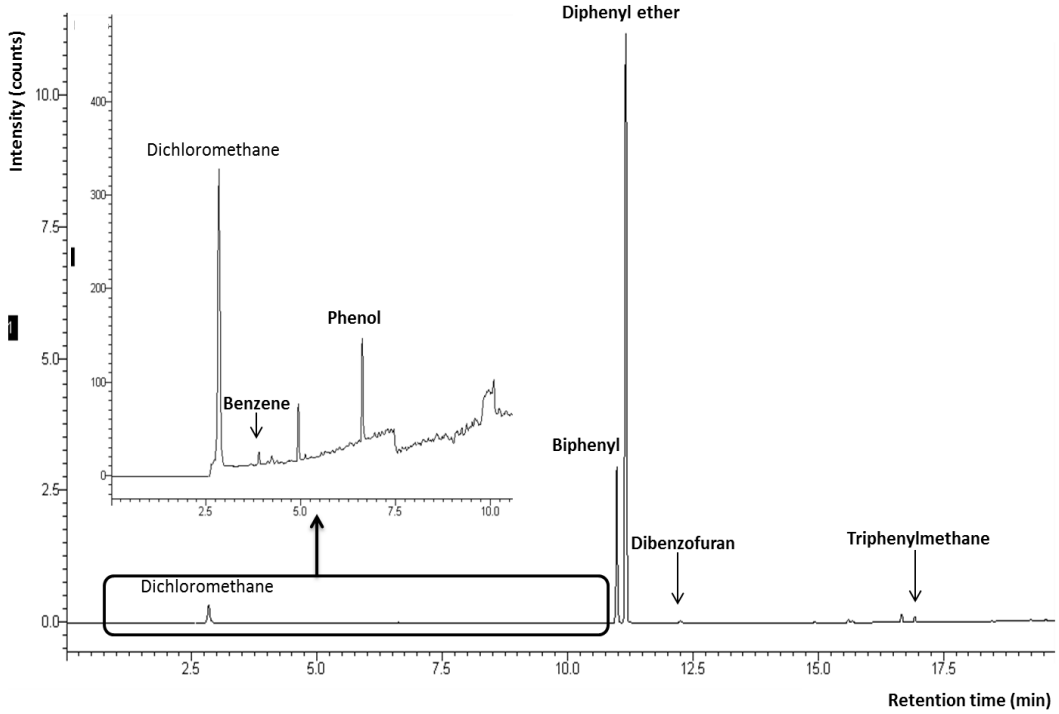

Fig. 8. Chromatogram of degraded HTF sample 7 as obtained by GC–MS.

Based on these results, GC–MS provides a powerful tool for identifying the components of degraded HTF. Although some degradation compounds such as benzene and phenol were also present in the less

degraded samples (1–4), they were undetected because the HTF samples were diluted to avoid contamination of the GC–MS with the main components of HTF (biphenyl and diphenyl ether). Therefore, one major disadvantage of using GC–MS to check HTF degradation is that the less concentrated compounds (benzene and phenol) cannot be detected jointly with the more concentrated compounds (diphenyl ether and biphenyl) without saturating the MS detector. Also, the GC–MS technique cannot be implemented in portable equipment for on-line use at a thermosolar plant.

3.3. Analytical performance of IMS versus FT-MIR and GC–MS

The techniques used to characterize the degradation profile of HTF are compared in terms of performance in **Table 3**. IMS can be quite effective for this purpose on account of its versatility and low cost. Thus, a global signal or fingerprint from HTF samples to distinguish raw and degraded HTF samples can be obtained with UV-IMS in a quick analysis (< 5 min). Also, the GC–^{3}H-IMS allows specific compounds to be identified by direct analysis of head-space from a HTF sample in 20 min of analysis. The precision is high with both IMS methodologies as was aforementioned. Moreover, expeditiousness and portability of IMS can be exploited for on-line measurements at thermosolar plants.

Table 3. Analytical performance of the instruments used to analyse HTF.

Analytical feature	**IMS instruments**		**Other instruments**	
	UV-IMS	GC–^{3}H-IMS	FT-MIRS	GC–MS
Precision	High	High	Low	High
Time per analysis	< 5 min	20 min	15 min	32 min
Cost	Low	Medium	Medium	Medium/High
Sample pretreatment	No	No	Yes[(1)]	Yes[(2)]
Portability	Yes	Yes	No	No

[(1)]KBr pellets were used for sample analysis. (2) Samples were diluted in dichloromethane.

The FT-MIR technique provides a global signal suitable for the rapid characterization of HTF samples, but fails to distinguish between degraded HTF samples. In addition, differences between bands for variably degraded samples are small. This instrument requires a sample preparation step and precision is not good enough compared with the others analytical instrument used.

Finally, GC–MS offers comprehensive information about the composition of HTF including compounds with too high a boiling point to be determined by IMS. However, its operational requirements make it unsuitable for on-site monitoring of HTF at a thermosolar plant; and its cost is much higher than IMS instruments.

4. Conclusions

In this work, degraded HTF samples were obtained at laboratory scale by using a reactor reproducing the high temperatures and pressures to which HTF is exposed in a thermosolar plant. Two new analytical methods based on the IMS technology were developed for monitoring HTF in a thermosolar plant with two different instruments. The UV–IMS instrument proved useful for the rapid monitoring of HTF degradation from a global IMS response. The GC–^{3}H–IMS instrument additionally afforded the identification of degradation products such as phenol and benzene in degraded HTF. IMS results were also compared with two classical analytical techniques. FT-MIR spectra provide little information to distinguish between variably degraded HTF samples. By contrast, the GC–MS technique allows most HTF components —some with high boiling points included— to be detected. However, GC–MS cannot be used on-line at a thermosolar plant.

Based on the foregoing, IMS was the analytical instrument that provided us with different fingerprints of raw and degraded HTF. It allows distinguishing HTF samples depending of its heating exposition. So IMS is an accurate and fast choice for analysing HTF in a thermosolar plant. Thus,

the methodologies here optimized will be essential to assess HTF efficiency as an effective energy carrier with its time of use in a thermosolar plant. The GC–^{3}H–IMS technology will be also powerful to check if the toxics compounds generated could put in risk workers and the environment. The next step in this project will be to carry out a fully validation of the methodology which will allow a quantitative study of the new products present in the HTF used in thermosolar plants.

Acknowledgements

The authors are grateful to Spain's DGICyT (Grant CTQ2011-23790), Magtel, S.A. and TSK Electrónica y Electricidad, S.A. for funding this work. LCG wishes to thank the Spanish Ministry of Education, Culture and Sport for award of a pre-doctoral grant (AP 2009-3528).

The authors have declared no conflict of interest.

References

[1] D. López-González, J. L. Valverde, P. Sánchez and L. Sánchez-Silva, Energy 54 (2013) 240-250.

[2] H. Price, E. Lüpfert, D. Kearney, E. Zarza, G. Cohen and R. Gee, J. Solar Energy Eng. 124 (2002) 25-109.

[3] M.E.V. Valkenburg, R. L. Vaughn, M. Williams and J. S. Wilkes, Thermochim. Acta 425 (2005) 8-181.

[4] D.M.L. Blake, M.J. Hale, H. Price, D. Kearney and U. Hermann, 11th SolarPACES International Symposium On concentrating Solar Power and Chemical Energy Technologies, Zurich, 2002.

[5] B. Wu, R. G. Reddy and R. D. Rogers, Proceedings of Solar Forum 2001 Solar Energy: The Power to Choose, Washington D.C, 2001.

[6] R. W. Bradshaw, J. G. Cordaro and N. P. Siegel, Proceedings of the ASME International Conference on Energy Sustainability, San Francisco, 2009.

[7] S. Armenta, M. Alcalá and M. Blanco, Anal. Chim. Acta 703 (2011) 114-123.

[8] I. Márquez-Sillero, E. Aguilera and M. Valcárcel, Trac-Trends Anal. Chem. 30 (2011) 677-690.

[9] R.G. Ewing, D. A. Atkinson, G. A. Eiceman and G. J. Ewing, Talanta 54 (2001) 515-529.

[10] J.W. Leonhardt, J. Radional. Nucl. Chem. 206 (1996) 333-339.

[11] J.I. Baumbach, St. Sielemann, Z. Xie and H. Schmidt, Anal. Chem. 75 (2003) 1483-1490.

[12] S. Sielemann, J.I. Baumbach, H. Schmidt and P. Pielzecker, Field Anal. Chem. Technol. 4 (2000) 157-169.

[13] Z. Xie, S. Sielemann, H. Schmidt and J.I. Baumbach, Anal. Bional. Chem. 372 (2000) 606-610.

[14] L. Criado-Garcia, R. Garrido-Delgado, L. Arce and M. Valcárcel, Talanta 111 (2013) 111-118.

[15] J. Laakia, C. Pedersen, A. Adamov, J. Viidanoja, A. Sysoev and T. Kotiaho, Rapid Commun. Mass Spectrom, 23 (2009) 3069-3076.

[16] G. A. Eiceman, J. F. Bergloff, J. E. Rodriguez, W. Munro and Z. Karpas, J.A. Soc. Mass Spectrom. 10 (1999) 1157-1165.

[17] D. Young, K. M. Douglas, G. A. Eiceman, D. A. Lake and M. V. Johnston, Anal. Chim. Acta 453 (2002) 231-243.

[18] J. Langejuergen, M. Allers, J. Oermann, A. T. Kirk and S. Zimmermann, Anal.Chem. 86 (2014) 7023-7032.

[19] G.A. Eiceman and Z. Karpas, Ion Mobility Spectrometry, 2nd ed., CRC press, Boca Raton, 2005.

Chapter 5
Quantification of benzene and phenol in in heat transfer fluid by IMS

Capítulo 5

Cuantificación de benceno y fenol en muestras de aceite termosolar mediante IMS

Talanta 144 (2015) 944–952

Contents lists available at ScienceDirect

Talanta

journal homepage: www.elsevier.com/locate/talanta

SIMULTANEOUS DETERMINATION OF BENZENE AND PHENOL IN HEAT TRANSFER FLUID BY HEAD-SPACE GAS CHROMATOGRAPHY HYPHENATED WITH ION MOBILITY SPECTROMETRY

Laura Criado-García, Rocío Garrido-Delgado, Lourdes Arce, Francisco López, Rogelio Peón, Miguel Valcárcel*

(1) Department of Analytical Chemistry, Annex C-3 Building, Campus of Rabanales, Institute of Fine Chemistry and Nanochemistry, University of Córdoba, 14071 Córdoba, Spain

(2) Magtel S.A., Gabriel Ramos Bejarano 114, P. I. Las Quemadas, 14014 Córdoba, Spain.

(3) TSK electrónica y electricidad S.A., Avda. Byron 220, P. C. Tecnológico, 33203 Gijón, Spain.

The quantitative determination of some compounds such as benzene and phenol in a complex matrix by ion mobility spectrometry (IMS) can be a difficult task, due to the influence of other components present in the matrix and the chemical properties of both compounds, such as their high volatility and low proton affinity. Monitoring of these compounds in a heat transfer fluid (HTF) is essential to check the correct working of a thermosolar plant and for safety and enviromental reasons. Benzene and phenol, among other compounds, are produced when HTF is exposed to high temperatures in continuous cycles and their presence can decrease the efficiency of HTF. For the first time, a headspace module coupled to a gas chromatography column in combination with an IMS (with a tritium ionization source) has been optimized and fully validated to simultaneously quantify benzene and phenol in HTF. The limit of detection (LOD) and limit of quantification (LOQ) achieved with the method proposed were 0.011 and 0.038 g L^{-1} and 0.004 and 0.014 g L^{-1} for benzene and phenol respectively. The precision of the method was evaluated in terms of repeatability and reproducibility with all values lower than 9.2 % and 13.3 %, respectively. Results demonstrated that benzene and phenol were

generated in the HTF heating process, and its concentration increased with heating time (approx. 483 h). The average concentration values for benzene and phenol in degraded HTF samples were not significantly different to values obtained using a gas chromatography-flame ionization detector instrument. Therefore, IMS is a promising technique for in-field quality control of HTF in a thermosolar plant due to its speed, versatility, sensitivity and selectivity to quantify these degradation compounds.

Keywords: benzene, phenol, heat transfer fluid, ion mobility spectrometry.

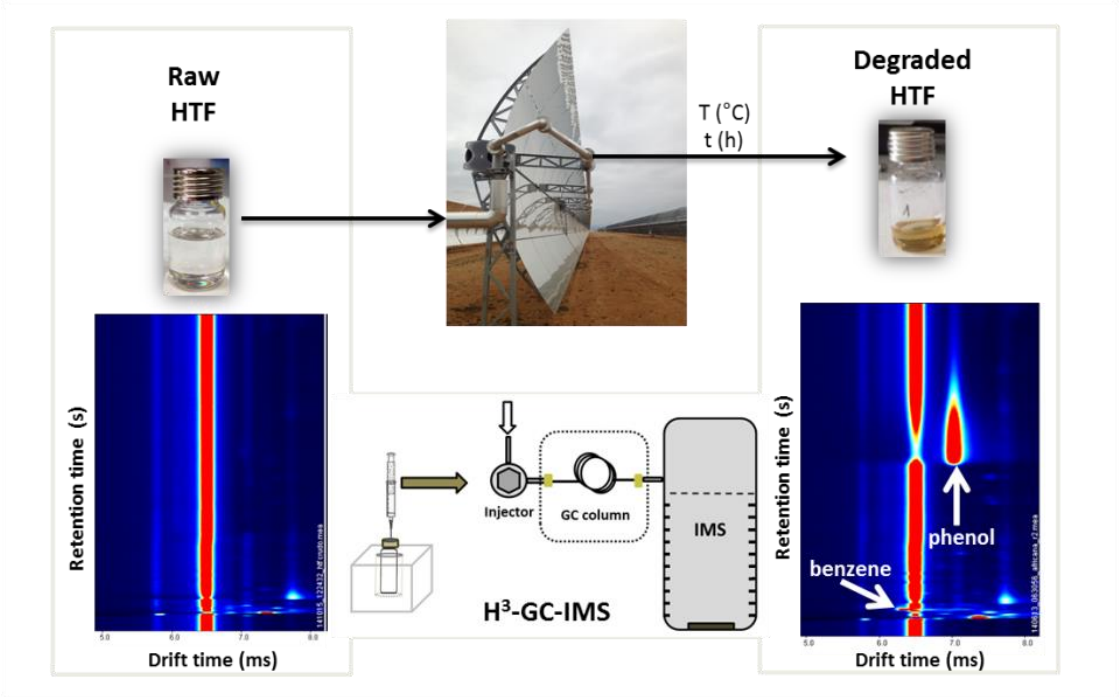

Graphical abstract

© 2015 Elsevier B.V. All rights reserved

1. Introduction

Heat transfer fluid (HTF) is a eutectic mixture composed of diphenyl ether and biphenyl [1]. This fluid has important uses in industry including uses in chemical processing equipment and open bath systems requiring fluid temperatures of up to 260 ºC. In some thermosolar plants with parabolic configuration, there are pipes filled with HTF which is heated to 394-400 °C due to concentrated sunlight [2]. Solar collectors transform solar radiation into heat which is transferred to the HTF [3]; it is possible due to the high heat capacity of HTF [4]. HTF also offers exceptional thermal and oxidation stability [5]. However, degradation compounds from HTF can be generated due to the fragmentation of the initial ingredients (biphenyl and diphenyl ether), or from other reactions that take place when heating HTF at high temperatures in a thermosolar plant. Degradation products are classified as lower boilers (benzene and phenol) or higher boilers (biphenyl, phenyl ether isomers and triphenylmethane, amongst others) as shown in **Figure 1**. High concentrations of degradation compounds in HTF can reduce the high heat transfer capacity of the fluid.

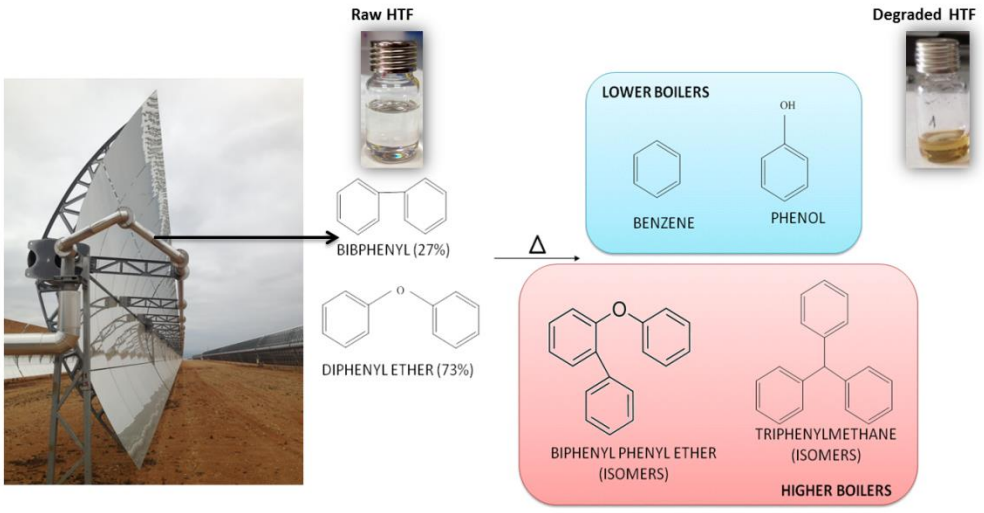

Fig. 1. Initial composition of HTF used in the thermosolar plant and its degradation compounds divided into high boilers and low boilers.

A 55 MW thermosolar plant with six hours of storage would require in the order of 8 million kg of HTF [6]. Replacing HTF in a thermosolar plant is expensive so it is essential to periodically check the HTF composition and study any possible changes. Currently, HTF samples are collected periodically from pipes to analyze its composition in an external laboratory. The sampling procedure can be dangerous to workers due to the toxicity and volatility of the degradation compounds, especially benzene and phenol. Therefore, a fast and sensitive method to determine the concentration of benzene and phenol in HTF samples in-situ at the thermosolar plant is needed.

In this work, we propose the use of ion mobility spectrometry (IMS) to quantify benzene and phenol in HTF samples. The selection of this technique was based on the several advantages of IMS for field application over other analytical techniques [7-9] such as its compact design, high sensitivity and rapid analysis. However a stand-alone IMS instrument would be unable to simultaneously monitor all the constituents of a complex mixture such as HTF [10]. IMS detection of benzene in the presence of other compounds with a higher proton affinity, such as phenol, is difficult since chemical ionization at atmospheric pressure leads to competing gas phase reactions in favour of other compounds [11]. One solution to improve IMS selectivity is to use a gas chromatography (GC) column [12] prior to the IMS device. The interface between GC and IMS can be easily achieved because the IMS is operated at ambient pressure, which alleviates the demands of interfacing between a vacuum and ambient pressure (as found in gas chromatography-mass spectrometry (GC-MS) instruments) [10]. When pre-separation is achieved in the GC column, the ion chemistry in the IMS device is simplified and demands on ion separations in the drift tube are reduced [13]. In this project, for the first time, benzene and phenol found in HTF samples were successfully quantified by coupling a GC column with IMS.

A recent study [14] found that the configuration of headspace (HS) coupled to GC-IMS, with a tritium ionization source (^{3}H), was the most

suitable to simultaneously detect benzene and phenol in HTF samples (mainly due to the incorporation of a GC column). The aim of this current study was to optimize and validate a new IMS method to quantify degradation products of a set of degraded HTF samples (produced in a lab-scale reactor which simulated thermosolar plant conditions). The results obtained with HS-GC-^{3}H-IMS were compared with the ones provided by GC coupled to a flame ionization detector (FID) having as a reference the official method (ISO 9377) to determine the composition of mineral oils.

2. Experimental

2.1. Reagents and samples

HTF was supplied by DOW® (Edegem, Belgium). Biphenyl, diphenyl ether, phenol, benzene and dichloromethane were purchased from Sigma–Aldrich (St. Louis, MA, USA). **Table 1** summarizes the chemical properties of the target compounds.

Table 1. Physico-chemical features of raw HTF supplied by Dow®.

Parameter	Value
Colour	Colourless to yellow
Odour	Aromatic
Freezing point (ºC)	12
Boiling point (ºC)	257
Flash point (closed cup) (ºC)	113
Vapour pressure (mm Hg at 25 ºC)	0.025
Solubility in water (% at 15.6 ºC)	0.001
Autoignition (ºC)	599
Thermal stability (ºC at 10.6 bar)	15-400
Density (kg m^{-3} at 25 ºC)	1056

2.2. Lab-scale HTF degradation process

The degradation process of HTF was carried out in continuous cycles in a reactor simulating the highest temperature (approx. 400 °C) the fluid is exposed to in a thermosolar plant, following the procedure previously described [14]. Approximately 180 mL of raw HTF was placed in a 1 L reactor manufactured by Sanical Astur, S.L. (Oviedo, Spain). The reactor was purged with pure nitrogen (99.999 %), from Abelló Linde, S.A. (Barcelona, Spain), in order to maintain an inert environment inside. The pressure and temperature of the reactor were controlled by means of an automatic controller supplied by Lascar electronics (Salisbury, UK) to heat HTF to approx. 400 ºC and 10 bar. An experimental correlation between HTF heating time in the reactor and in a thermosolar plant was made to collect a representative number of samples. These estimations were done by engineers working in a thermosolar plant who took into account the total volume of HTF used in the plant (2.6 x 106 kg) and its working time (3000 h $year^{-1}$). The engineers found that the thermosolar plant is only working at 34% of the total hours per year and only 2.1% of the total volume of HTF is at high temperatures. Therefore, heating HTF inside the reactor for 64 h is equivalent to heating for 1 year in the thermosolar plant. Following that estimation, the first sample containing 10 mL of degraded HTF was collected after heating the sample for 64 h in the reactor, by using a peristaltic pump from Gilson (Villiers, France) and Teflon tubing from Sigma–Aldrich (St. Louis, USA). The remaining volume of the HTF sample was heated again (following the same aforementioned procedure). The process was repeated 6 times until the fluid was heated for almost 483 h (equivalent to 7.5 years in the thermosolar plant). All HTF samples were stored in air-tight glass vials at room temperature (23–25 ºC) in darkness until analysis.

2.3. Equipment

2.3.1. HS-GC-^{3}H-IMS

A schematic diagram of the HS-GC-^{3}H-IMS instrument used (FlavourSpec®, from G.A.S., Dortmund, Germany) is illustrated in in

Figure 2. It was equipped with a heated splitless injector, which enabled direct sampling of the headspace from the HTF samples via an automatic sampler unit (CTC-PAL, CTC Analytics AG, Zwingen, Switzerland). The device is equipped with a ^{3}H ionization source (St. Petersburg, Russia) with an activity of 300 MBq which is below the exemption limit of the EURATOM guideline (1 Gbq). This instrument can be operated in negative or positive ionization mode. For analysis, a volume of 100 µL of sample was placed in a 20 mL vial that was closed with magnetic caps and a silicone septum. After 5 min incubation at 35 ºC, 200 µL of sample headspace was automatically injected by a heated syringe (80 ºC) into the GC–IMS equipment. Sample and drift gas used was pure nitrogen (99.999 %) supplied by Abelló Linde S.A. (Barcelona, Spain). After injection, the nitrogen carrier gas passing through the injector inserted the sample into the GC column which was 30 m long with an internal diameter (i.d.) of 0.25 mm and a 0.5 µm film thickness, consisting of methyl, phenyl and vinylsiloxane, from CS-Chromatographie Service GmbH (Dürem, Germany), in a 94:5:1 proportion.

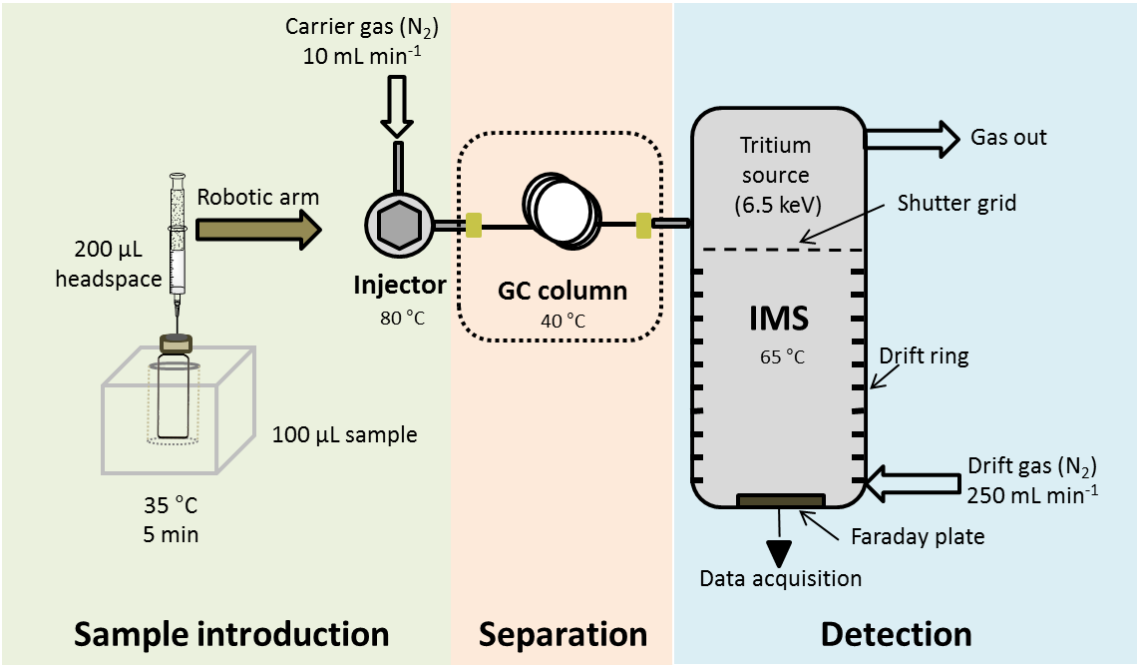

Fig. 2. Experimental set-up schematic used in this work.

The GC column was heated and maintained at 40 ºC for timely separation. The analytes were eluted from the GC column and driven into the ionization chamber. Once ions are formed they are focused to a shutter grid (BN gate), prior to the 5 cm long drift tube. Another device with a longer drift tube (10 cm) was employed to study how to improve the resolution of the separation between benzene and the reactant ion peak (RIP) signal. The BN gate opening time was set to 100 µs, allowing the ions to pass towards the separation chamber where ions differing in mobility were separated under a constant electrical field of 400 V cm^{-1} (5 cm drift tuve) and 500 V cm^{-1} (10 cm drift tube) . The IMS drift tube was kept under atmospheric pressure (101 kPa) and heated at 65 °C. The data were acquired and displayed by the integrated computer within the equipment, and processed using the software LAV version 2.0.0 from G.A.S. All spectra were recorded in the positive ion mode.

2.3.2 GC-FID

GC-FID analyses were carried out using a Varian CP 3800 fitted with a split/splitless injector and FID from Perkin Elmer (Massachusetts, USA). Helium (99.999%), from Praxair (Danbury, USA), was used as the carrier gas and was set at 1 mL min^{-1}. The separation was performed with a HP-1, fused silica capillary column, 30 m x 0.25 mm i.d. with 1.0 µm stationary film thickness of 100 % polydimethylsiloxane from Agilent (Santa Clara, USA). The column temperature was programmed as follows: initial oven temperature 33 °C for 4 min, increasing to 180 °C at 6 °C min^{-1}, then holding for 3 min and then directly to 300 °C at 15 °C min^{-1} and holding for 8 min. The injector temperature was set to 275 °C, with an injection volume of 1 µL, and desorption was carried out in the split mode (split 1/10). The detector temperature was held at 310 °C. For the analysis, 190 µL of HTF sample was diluted in 25 mL dichloromethane with 0.5 mL of 1-chlorotetradecane (10 mg mL^{-1}) added, to be used as an internal standard.

3. Results and discussion

A detailed optimization and validation of the HS-GC-^{3}H-IMS method was carried out in order to accurately quantify benzene and phenol in HTF. Quantification of these compounds was essential in order to check the stability of HTF (it was checked in terms of production of benzene and phenol) in a thermosolar plant and protect workers and the environment of the harmful effect of these toxic compounds. Results obtained with the proposed methodology were compared with results obtained using a GC-FID method.

3.1. Benzene and phenol peaks identification

Degraded HTF sample analysis by HS-GC-^{3}H-IMS resulted in two intense peaks which corresponded to benzene and phenol. To confirm the identification of these compounds, raw HTF was spiked with benzene and phenol at different concentrations and analysed using HS-GC-^{3}H-IMS. Benzene and phenol signals were identified according to both their retention and drift times in the topographic plot. The IMS spectra in **Figure 3A** and **3B** correspond to the benzene and phenol signals which appear at 55 s and 395 s (retention time) and at 6.3 ms and 7 ms (drift time) respectively.

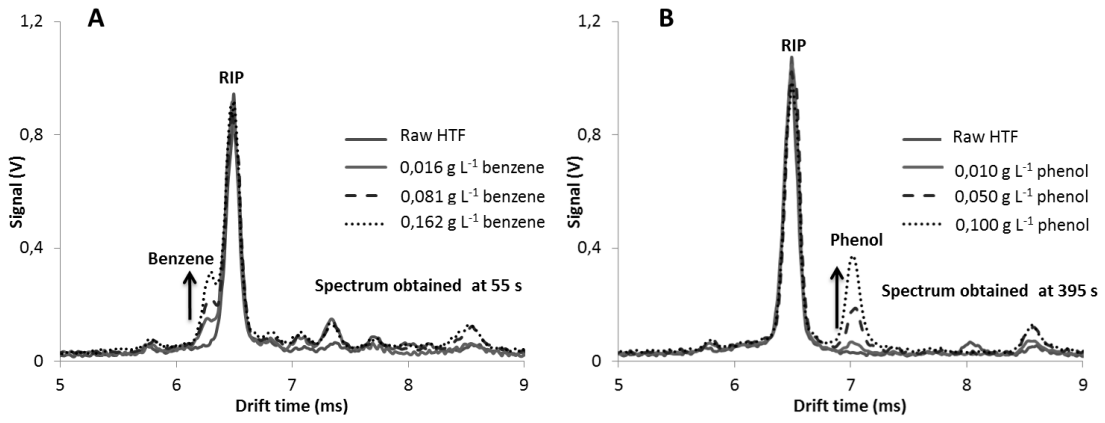

Fig. 3. IMS spectra of (A) benzene and (B) phenol signals in raw HTF samples spiked at different concentration levels.

Figure 4 shows the topographic plot of a raw HTF sample spiked with 0.100 g L^{-1} of phenol and 0.164 g L^{-1} of benzene. The RIP was observed at a drift time of 6.5 ms and its signal intensity decreased (see Figure 4B and 4C) when a compound with a higher proton affinity than water (697 kJ mol^{-1}), was introduced into the reaction chamber (proton affinity for benzene is 750.4 kJ mol^{-1} and for phenol 817.3 kJ mol^{-1}). A suppression of the RIP occurred at 45 s due to the appearance of other compounds in the IMS spectra, related with the injection of the headspace (signaled in **Figure 4C** with an asterisk).

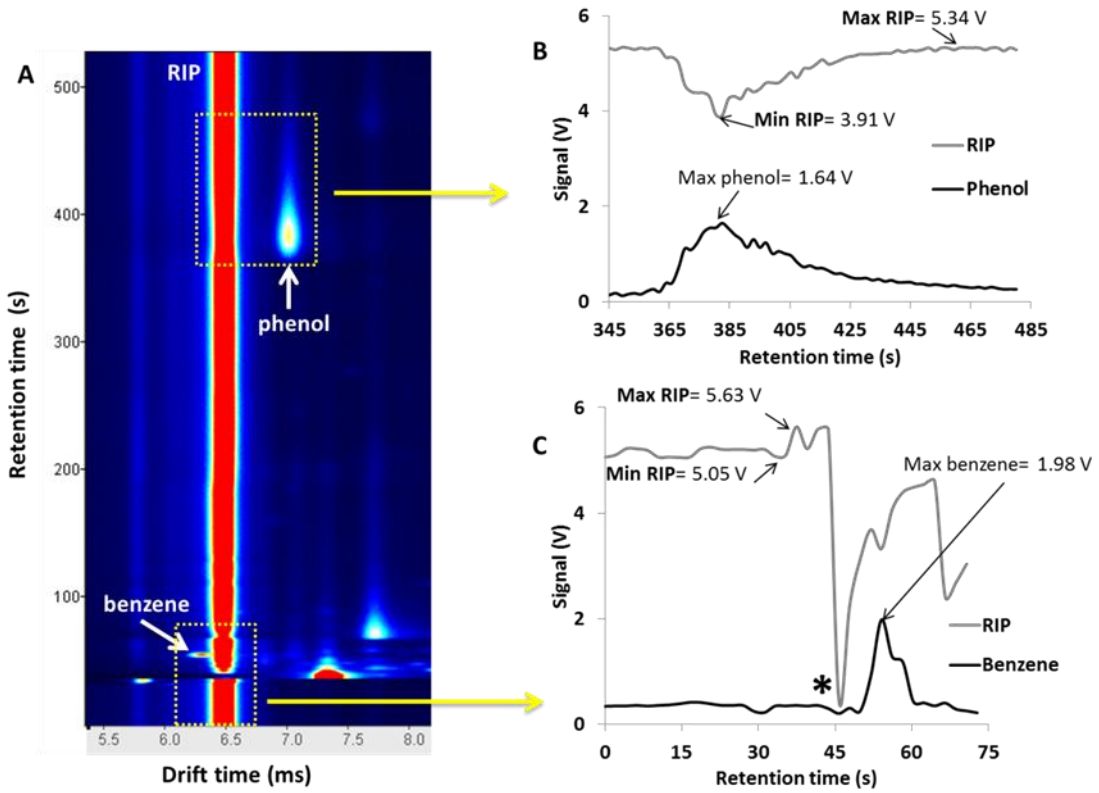

*shows the suppression of the RIP due to the presence of unknown compounds present in the headspace system from an empty vial.

Fig. 4. (A) Topographic plot of a sample of raw HTF spiked at 0.100 g L^{-1} of benzene and 0.164 g L^{-1} of phenol; Evolution of (B) phenol, (C) benzene and RIP signals obtained along the topographic plot.

The reduced mobility constant (K_0) of each compound was calculated in order to assess the identity of the ion. The velocity of an ion in a buffer gas under the influence of a homogeneous electric field is directly proportional to the electric field strength. The proportionality constant between the velocity of ions and the electric field strength, known as the ion mobility constant (K), becomes a qualitative measure of the ion:

$$K = \frac{v}{E} \quad (1)$$

where v is the velocity of the ion in cm s^{-1} and E the electric field strength in the drift region in V cm^{-1}. Since the velocity of the ion is affected by both temperature and pressure, measured mobility constants were corrected to standard temperature and pressure to produce a reduced mobility constant (K_0) [10]:

$$K_0 = K \frac{P}{760} \frac{273}{T} \quad (2)$$

where P is the pressure in the drift region in Torr and T is the buffer gas temperature in Kelvin. K_0 values were 1.94 $cm^2\ V^{-1}\ s^{-1}$ for benzene, 1.75 $cm^2\ V^{-1}\ s^{-1}$ for phenol, and 1.88 $cm^2\ V^{-1}\ s^{-1}$ for the RIP. The highest ion mobility value for the benzene ion, whose signal on the left of the RIP position using a radioactive ionization source, was also reported by Zimmermann et al. [11]. The benzene ion formed has an ion mobility higher than the cluster ion $H^+(H_2O)_n$ whose size is governed by a constant equilibrium (for clustering and declustering reactions), water concentration and drift gas temperature. At low water vapor concentration, the main proton carrier is $H^+(H_2O)$ which has a proton affinity of 697 kJ mol^{-1}. In the case where the water vapor concentration increases, the main proton carrier was found to be $H^+(H_2O)_2$ which has a higher proton affinity (808 kJ mol^{-1}) [20]. Due to the lower proton affinity of benzene (750.4 kJ mol^{-1}) its ionization can be problematic [20]. For all of these reasons, the benzene ions detected probably resulted from a charge transfer reaction with NO^+. This hypothesis is confirmed according to previous work, where in the presence of nitrogen as the working gas, the detection of M^+ ions were observed from aromatic compounds such as benzene by coupling corona

discharge-IMS with orthogonal acceleration time of flight mass spectrometry [7]. Moreover, the same benzene K_0 value obtained in this work was previously reported in other papers (1.94 $cm^2\ V^{-1}\ s^{-1}$ [15] and 1.95 $cm^2\ V^{-1}\ s^{-1}$ [16]). In general, published K_0 values are considered to match one another if their uncertainties are within 2 % (~0.02 $cm^2\ V^{-1}\ s^{-1}$) [17]. It is also important to take into account that the formation of the product ions depends on the physical and chemical properties of each specific compound, their concentration and the experimental design of the IMS device [18]. In the case of phenol, an easier ionization reaction occurred due to its higher proton affinity where the MH^+ ion was formed by a proton transfer reaction.

3.2. Instrumental parameters optimization

The main aims of the optimization procedure were to improve the selectivity of the method whilst avoiding contamination from the matrix in order to correctly identify benzene and phenol in the HTF samples. The parameters that were most influential during optimization (those that could enhance selectivity and reduce contamination) for HTF were: sample volume, heating temperature, heating time, injection volume, gas column temperature, IMS drift tube temperature, carrier gas flow and cleaning time. The range of values studied and those chosen as the working values for the proposed methodology are shown in **Table 2**.

Biphenyl and diphenyl ether, the initial compounds of HTF, could be strongly retained in the GC column and difficult to desorb, resulting in contamination in the following analyses due to their high concentration and high vapour pressure. Cross-contamination between samples was avoided by introducing a smaller volume of the sample headspace, created in the vial after a smooth heating of the sample, into the IMS device. Sample volume and heating temperature were studied first; the optimization found that 100 µL of HTF (placed into the sample vial) and heating to 35 ºC for 5 min, was sufficient to produce a significant signal to determine benzene and phenol, with an injection volume of 200 µL of the HS. Using these conditions no contamination of biphenyl and diphenyl ether was observed between analyses.

Table 2. Experimental conditions optimised to analyse HTF samples by HS-GC-^{3}H-IMS.

Experimental parameter	Studied range	Working values
Sample volume (μL)	50-1000	100
Carrier gas flow (mL min^{-1})	5-15	10
Drift gas flow (mL min^{-1})	-	250
Heating temperature (ºC)	30-80	35
Heating time (min)	5-30	5
Injection volume (μL)	100-1000	200
Analysis time (min)	-	20
Gas column temperature (ºC)	40-70	40
Drift tube temperature (ºC)	45-75	65
Cleaning carrier flow (mL min^{-1})	-	25
Cleaning time (min)	-	55

The GC column temperature was set at 40 ºC in order to guarantee the retention of the compounds in the column (mainly benzene). IMS drift tube temperature optimization found that higher temperatures along the drift tube reduced moisture considerably [19], which is of importance as benzene, which has a lower proton affinity, can be strongly affected by humidity [20]. Therefore, the drift tube temperature was set at 65 ºC to decrease moisture and to enhance ionization and signal intensity. Finally, cleaning time between samples was crucial to avoid any carry over between analyses. After 20 min of analysis, the carrier gas flow was increased from 10 mL min^{-1} up to 25 mL min^{-1} for 55 min. These optimized parameters were used for further experiments.

3.3. Validation of the method

The analytical method proposed in this work was validated to demonstrate its suitability to quantify benzene and phenol in degraded HTF samples during the heating process in the thermosolar plant. In the following section, the results obtained in terms of precision, sensitivity, accuracy and resolution are shown.

3.3.1. Precision

The precision study was carried out using a raw HTF sample spiked with 0.15 g L^{-1} of benzene and 0.11 g L^{-1} of phenol and a degraded HTF sample from a thermosolar plant. Precision values of the peak height, drift time and retention time expressed as relative standard deviation (RSD) are shown in **Table 3**. The same sample was analyzed (n=6) in the same day and under the same experimental conditions, while the reproducibility was carried out by analysing the sample for three consecutive days (n=9).

Table 3. Precision study of the methodology used in this work.

Precision values		**Raw HTF spiked with benzene and phenol**			**Degraded HTF samples**		
		Peak height	Drift time	Retention time	Peak height	Drift time	Retention time
Repeatability	Benzene	9.2	0.3	2.0	3.3	0.1	0.6
n=6	Phenol	5.2	0.2	1.2	2.9	0.1	1.2
(% RSD)							
Reproducibility	Benzene	13.3	0.3	5.4	4.5	0.03	1.0
n=9	Phenol	4.9	0.1	3.9	3.5	0.1	1.7
(% RSD)							

The optimized method is very precise because values lower than 4.5 % were obtained in all cases when the same degraded HTF sample was analysed. The RSD values obtained for the raw HTF with spiked standards of benzene and phenol were slightly higher due to experimental error in the preparation of the standard. Moreover, in both cases the method is more precise for the determination of phenol; which could be due to the higher volatility of benzene compared with phenol.

3.3.2. Calibration curves and linear range study

The influence of the benzene and phenol signal with the concentration was studied in HTF matrix. The final concentration ranges chosen were 0.005-1.000 g L^{-1} for benzene and 0.003-0.616 g L^{-1} for phenol because the polynomial tendency was lost above these ranges. A calibration curve was built for each compound using a second order polynomial equation, shown

in **Table 4** and **Figure 5A** and **5B**. The peak heights for benzene and phenol were normalized with the maximum intensity value for RIP, found in the spectra obtained between 1 to 45 seconds of each analysis; the RIP evolution during the IMS analysis is shown in **Figure 4**, where the maximum RIP intensity observed was 5.63 V.

Table 4. Calibration equations (2nd order polynomial and linear) and regression coefficients calculated for benzene and phenol.

Compound	Concentration range (g L^{-1})	Calibration equation	Sa	Sb	R^2	LOD* (g L^{-1})	LOQ* (g L^{-1})
		y=ax²+bx+c					
Benzene	0.005-1.000	$y=-1\cdot10^{-6}x^2+0.0017x+0.1590$	-	-	0.984	-	-
Phenol	0.003-0.616	$y=-2\cdot10^{-6}x^2+0.0021x+0.0523$	-	-	0.996	-	-
		y=ax+b					
Benzene	0.005-0.200	y=0.0018x+0.1387	0.007	$6.51*10^{-5}$	0.991	0.011	0.038
Phenol	0.003-0.123	y=0.0021x+0.0465	0.003	$4.76*10^{-5}$	0.993	0.004	0.014

*LOD and LOQ values were calculated from linear range as three and ten times, respectively, the intercept error divided by the slope of the calibration equation.

Table 4 shows the calibration curves obtained for the benzene and phenol, as well as their corresponding correlation coefficients. The variation of the signal with the concentration was adjusted for benzene and phenol, with a good regression to a polynomial equation of second order in the range of concentration studied (**Figure 5A** and **5B** and **Table 4**). A linear tendency was observed at lower concentration levels within the range of concentrations studied (see **Figure 5C** and **5D**). The linear range was approximately 2 orders of magnitude and for quantitative analysis of benzene and phenol in HTF samples, the linear range of each calibration curve was used (**Table 4**).

3.3.3. Limits of detection and quantification

The calibration equation from the linear range was used to calculate LOD and LOQ values; these were calculated to assess the sensitivity of the method, as three and ten times the standard deviation of the intercept, among the slope from the calibration curves in **Figure 5C** and **5D**. The LOD

and LOQ were 0.011 and 0.038 g L^{-1} for benzene and 0.004 and 0.014 g L^{-1} for phenol. The LOD for benzene was higher because its signal appeared jointly to the RIP signal which made its quantification challenging.

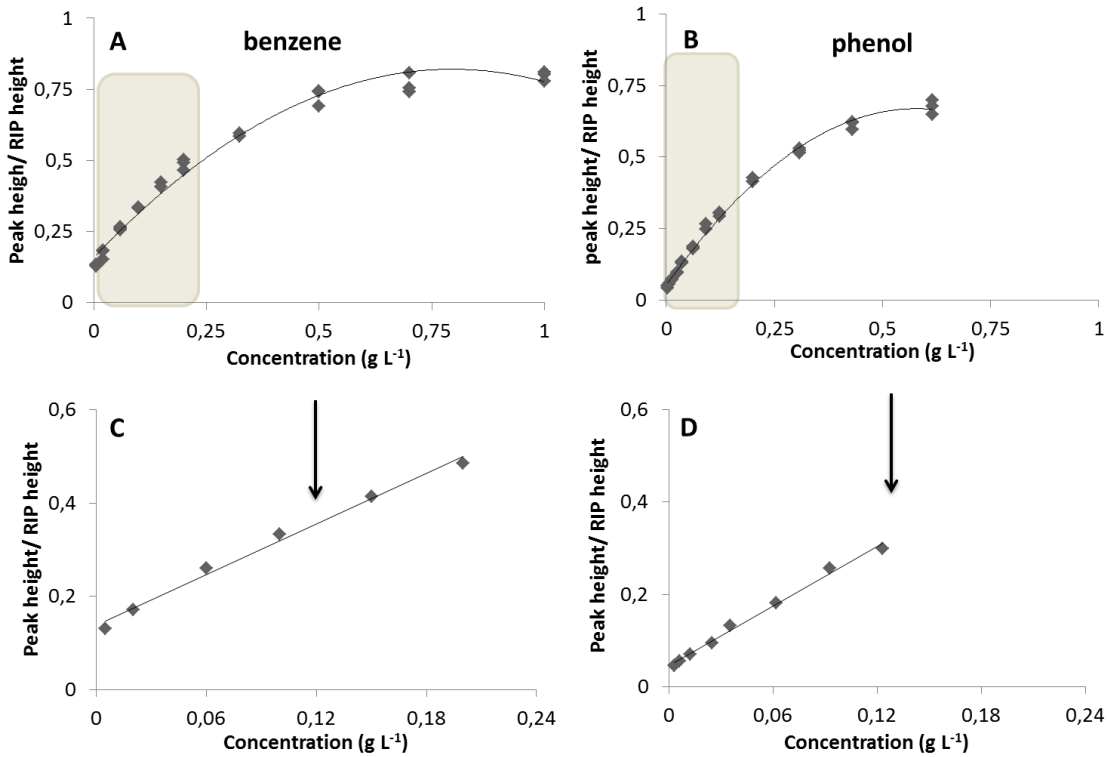

Fig. 5. Second order polynomial calibration curve for (A) benzene and (B) phenol; Linear calibration curves for (C) benzene and (D) phenol.

3.3.4. Accuracy

The accuracy of the method was calculated through a recovery study. A degraded HTF sample was spiked with benzene and phenol at three different concentrations (0.2, 1.0 and 4.0 g L^{-1}). The samples were diluted with raw HTF at different values, depending on the initial benzene and phenol concentration, to have a final concentration within the linear range of the calibration curve. The recovery values were between 59 % and 76 % for benzene and between 83 % and 108 % for phenol. Based on the results obtained, the method was more accurate for the determination of phenol

because recovery values were close to 100 %. The recovery values for benzene were lower due to the benzene peak appearing next to RIP, making its quantification difficult. Another reason for lower recovery values obtained for benzene could be its high volatility, which could affect the standards stability.

3.3.5 Improvement of the resolution

The resolution of this instrument cannot be improved since the drift tube is not a part of a commercial device which can be easily changed. However, results obtained were compared with another IMS instrument with a longer drift tube (10 cm). Two samples of raw HTF were spiked with 0.081 g L^{-1} and 0.162 g L^{-1} of benzene. These two spiked samples were analysed using both instruments. **Figure 6** shows the separation of the benzene peak from the RIP signal could be improved using this longer 10 cm drift tube rather than the 5 cm drift tube used for analysis.

Also, narrower peaks were obtained when the 10 cm drift tube was used. Moreover, the resolution of the IMS was studied in this work calculating resolving power (Rp), which is defined as the drift time (td) of the ion divided by the peak width at half-height ($w_{0.5}$) [21-22]. Rp values obtained for benzene peaks were 63 for the 12 cm drift tube and 47 for the 5 cm drift tube. Therefore the resolution for the benzene using the longer drift tube (10 cm) was slightly improved.

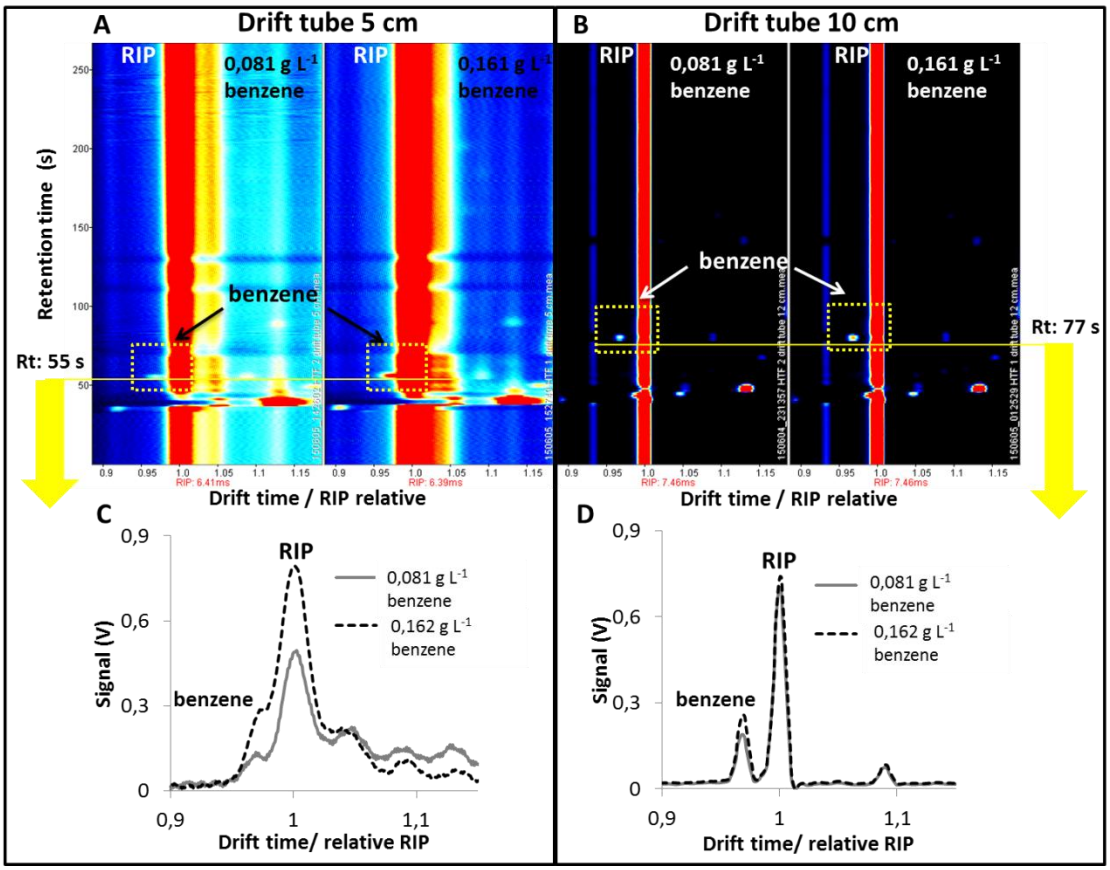

Fig. 6. Topographic plots of benzene spiked in raw HTF at two concentration levels (0.081 g L^{-1} and 0.162 g L^{-1}) and measured with two IMS instruments with drift tubes of (A) 5 and (B) 10 cm. Extracted IMS spectra of benzene using (C) 5 cm and (D) 10 cm drift tube length.

3.4. Analysis of lab-scale degraded HTF samples

When using HS-GC-3H-IMS, degraded HTF samples were diluted with raw HTF in order to have a lower concentration of benzene and phenol in the HTF sample (within the linear range of the calibration curve). So, the least degraded HTF samples were diluted ten times (1:10), medium degraded were diluted fifty times (1:50) and the most degraded HTF sample was diluted a hundred times (1:100).

Benzene and phenol from degraded HTF samples, produced in the lab-scale reactor, were quantified by HS-GC-^{3}H-IMS. The results obtained

were compared with ones obtained using a GC-FID instrument to demonstrate the capability of the proposed method. The figures in **Table 5** show how the concentrations of benzene and phenol increase as the heating time increases.

Higher concentrations were found for benzene than for phenol in the HTF samples. Benzene concentration increased from 0.50 g L^{-1} to 15.35 g L^{-1} along the sequence of degraded HTF samples. The concentration of phenol remained nearly constant in most of the degraded HTF samples analysed, reaching a maximum concentration found of 0.25 g L^{-1} using HS-GC-^{3}H-IMS analysis.

A significant statistical test, *t student test*, was applied to compare the analytical results (benzene and phenol average concentrations) obtained on the same degraded HTF samples using two different methods (HS-^{3}H-GC-IMS and GC-FID, see **Table 5**) with a predefined confidence limit at 95%. The null hypothesis (H_0) stated that concentration average for benzene and phenol in the degraded HTF samples (1-5) are the same for both methods.

Table 5. Concentration of benzene and phenol found in lab-scale degraded HTF samples by HS-GC-^{3}H-IMS and GC-FID methods.

Sample	Dilution	Heating time (h)	HS-GC-^{3}H-IMS		GC-FID	
			Benzene	Phenol	Benzene	Phenol
			Found±SD	Found±SD	Found±SD	Found±SD
1	1:10	68	0.50±0.03	0.172±0.005	0.22±0.07	0.12±0.01
2	1:10	259	0.7±0.1	0.25±0.02	0.53±0.04	0.26±0.05
3	1:10	292	1.5±0.1	0.25±0.01	1.47±0.13	0.30±0.03
4	1:50	343	1.35±0.08	0.21±0.06	1.86±0.26	0.23±0.01
5	1:100	483	15.35±0.6	0.25±0.02	7.63±2.01	0.43±0.05

Concentration found expressed in g L^{-1}. Three replicates for HS-GC-^{3}H-IMS and two replicates for GC-FID were done per sample. Benzene concentration found for degraded HTF samples 1 and 5 were the only values that showed statistical differences between both methodologies.

After applying the test, it could be concluded that both methods did not provide significant differences of concentration average for benzene and phenol in all degraded HTF samples analyzed at a confidence level of 95%. Therefore, the differences observed in the samples were due to random errors. However, two exceptions were observed in the benzene value (degraded HTF sample 1 and 5). In these cases, there were statistical differences that can be attributed to an error in the measurement of benzene due to the low separation between benzene peak and the RIP signal when using the 5 cm IMS drift tube.

Matrix effects posed by HTF samples on IMS signal were also investigated. As can be seen in **Figure 7**, raw and degraded HTF samples were analysed and only minor interference signals in the topographic plot were observed.

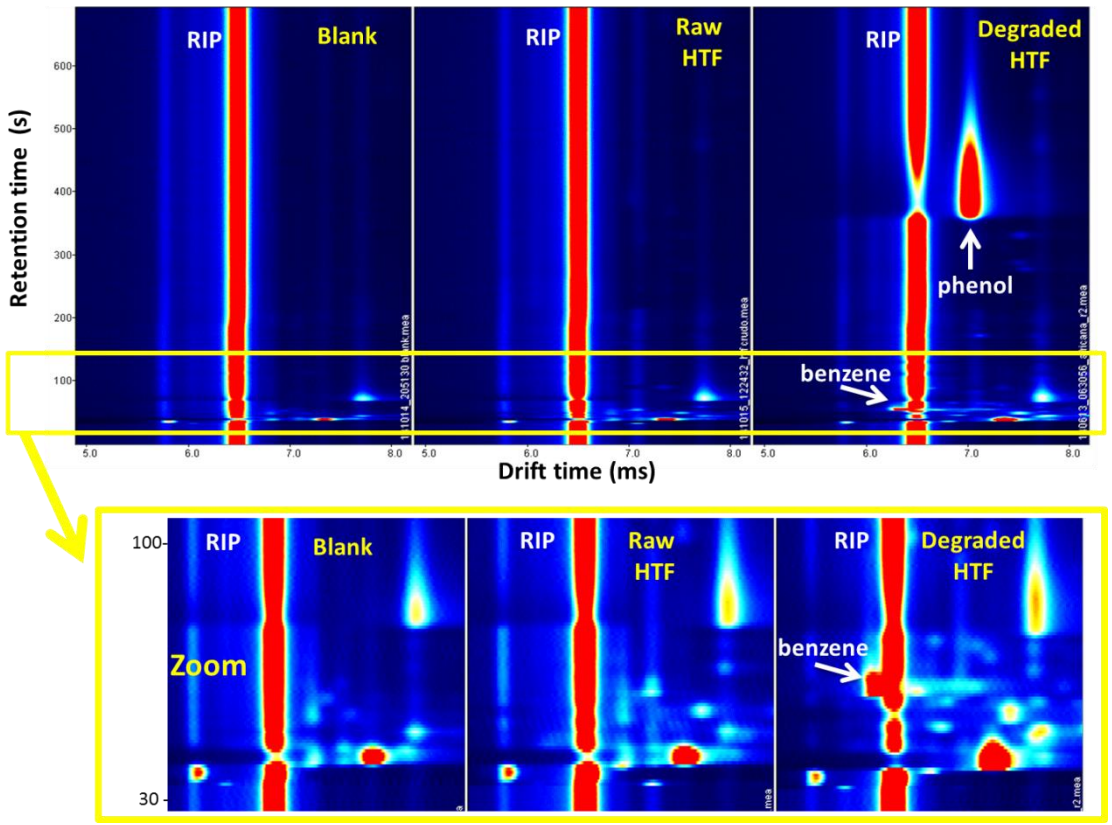

Fig. 7. Topographic plot of a blank (empty vial), raw HTF and degraded HTF. Zoom of the topographic plot from 30 to 100 s.

These observations evidently showed that the optimized parameters of the fully validated method were suitable against potentially adverse interferences in complex samples. Nevertheless, it is worthwhile to mention that benzene and phenol retention times, drift times and peak intensities were not affected by other compounds present in the HTF.

Therefore, it could be confirmed that IMS is a suitable technique to periodically monitor the concentration of benzene and phenol in HTF. Moreover, results obtained by GC-FID show a slight decrease in the concentration of the HTF main ingredients (14.76% for byphenyl and 0.54% for diphenyl ether) compared with its high initial concentration (261.3 g kg^{-1} for byphenyl and 716.6 g kg^{-1}) when the sample was heated for 483 hours. At that state, the high heat transfer capacity of HTF is expected to not be reduced further. However, the presence of lower boilers in the HTF can alter its diffusion through pipes and affect the operation of individual components in the thermosolar plant, so it is essential to monitor the presence of benzene and phenol in the HTF. The validated method here could be used as a routine method to monitor the quality of the HTF used in a thermosolar plant.

4. Conclusions

The methodology proposed in this work using HS-GC-^{3}H-IMS was used successfully for the first time to quantify benzene and phenol in HTF samples. The method does not require a sample preparation step. Direct headspace analysis was performed with only 100 µL of HTF sample. Precision, sensitivity, selectivity and accuracy were all strengths demonstrated in this method. The results obtained by HS-GC-^{3}H-IMS instrument showed no significant difference to those obtained by GC-FID revealed by using *t student test.* GC-IMS allowed two-dimensional separation (based on the retention time and drift time information) and quantification of lower boilers present in the HTF sample, not reported

before. In conclusion, IMS is a reliable and a quick technique feasible for quality control in the thermosolar industry.

Acknowledgements

Authors gratefully acknowledge the funding received from Spain's DGICyT (Grant CTQ2011-23790). LCG wishes to thank the Spanish Ministry of Education, Culture and Sport for a pre-doctoral grant (AP 2009-3528).

References

[1] M.E.V. Valkenburg, R.L. Vaughn, M. Williams, J.S. Wilkes, Thermochemistry of ionic liquid heat-transfer fluids, Thermochim. Acta 425 (2005) 8-181.

[2] M. Balghouthi, M.H. Chahbani, A. Guizani, Investigation of a solar cooling installation in Tunisia, Appl. Energ. 98 (2012) 138-148.

[3] L.A. Chidambaram, A.S. Ramana, G. Kamaraj, R. Velraj, Review of solar cooling methods and thermal storage options, Renew. Sust.Energ. Rev. 15 (2011) 3220-3228.

[4] R.W. Bradshaw, J.G. Cordaro, N. P. Siegel, Molten nitrate salt development for thermal energy storage in parabolic trough solar power systems in Proceedings of the ASME International Conference on Energy Sustainability, San Francisco, 2009.

[5] D. Valverde, J.L. López-González, P. Sánchez, L. Sánchez-Silva, Characterization of different heat transfer fluids and degradation study by using a pilot plant device operating at real conditions, Energy 54 (2013) 240-250.

[6] D.M.L. Blake, M.J. Hale, H. Price, D. Kearney, U. Hermann, New heat transfer and storage fluids for parabolic trough solar thermal electric plants in proceedings of the 11th Solar PACES International Symposium on concentrating Solar Power and Chemical Energy Technologies, Zurich, 2002.

[7] M. Sabo, S. Matejcik, Corona discharge ion mobility spectrometry with orthogonal acceleration time of flight mass spectrometry for monitoring organic compounds, Anal. Chem. 84 (2012) 5327-5334.

[8] Q. Meng, Z. Karpas, G.A. Eiceman, Monitoring indoor ambient atmospheres for VOCs using an ion mobility analyzer array with selective chemical ionization, Int. J. Environ. Anal. Chem. 61 (1995) 81-94.

[9] G.A. Eiceman, E.G. Nazaroz, B. Tadjikov, R.A. Miller, Monitoring volatile organic compounds in ambient air inside and outside buildings with the use of a radio-frequency-based ion-mobility

analyzer with a micromachined drift tube, Field Anal. Chem. Tech. 4 (2001) 297-308.

[10] G.A. Eiceman, Z. Karpas, Ion Mobility Spectrometry, 2nd edition, CRS Press, Boca Raton, 2005.

[11] S. Zimmermann, F. Gunzer, Simultaneous detection of benzene and toluene using a pulsed ion mobility spectrometer, Sensor Actuat. B-Chem. 188 (2013) 106-110.

[12] D.M. Davis, C.S. Harden, D.B. Shoff, S.E. Bell, G.A. Eiceman, R.G. Ewing, Analysis of ion mobility spectra for mixed vapors using Gaussian deconvolution, Anal. Chim. Acta 289 (1994) 263-272.

[13] A. Kanu, H.H. Hill, Ion mobility spectrometry detection for gas chromatography, J. Chromatogr. A 1177 (2008) 12-27.

[14] L. Criado-García, R. Garrido-Delgado, L. Arce, F. López, R. Peón, M. Valcárcel, Potential of Ion Mobility Spectrometry versus FT-MIR and GC-MS to study the evolution of a Heat Transfer Fluid after its heating process in a thermosolar plant, Microchem. J. 121 (2015) 163-171.

[15] H. Borsdof, H. Schelhorn, J. Falchowsky, H. R. Döring, J. Stach, Corona discharge ion mobility spectrometry of aliphatic and aromatic hydrocarbons, Anal. Chim. Acta 403 (2014) 235-242.

[16] L. Criado-Garcia, R. Garrido-Delgado, L. Arce, M. Valcárcel, A comparative study between different alternatives to prepare gaseous standards for calibrating UV-ion mobility spectrometers, Talanta 111 (2013) 111–118.

[17] R. Fernández-Maestre, C.S. Harden, R.G. Ewing, H.H. Hill, Chemical standards in ion mobility spectrometry, Analyst 135 (2010) 1433-1442.

[18] M. Jünger, B. Bödejer, J.I. Baumbach, Peak assignment in multi-capillary column-ion mobility spectrometry using comparative studies with gas chromatography-mass spectrometry for VOC analysis, Anal. Bioanal. Chem. 396 (2010) 471-482.

[19] T. Mayer; H. Borsdorf, Accuracy of ion mobility measuraments dependent on the influence of humidity, Anal. Chem. 86 (2014) 5069-5076.

[20] A. Kuklya, F. Uteschil, K. Kerpen, R. Marks, U. Telgheder, Effect of humidity on analysis of aromatics compounds with planar differential mobility spectrometry, Int. J. Ion Mobil.Spec (2014) *in press*. DOI: 10.1007/s12127-014-0162-8.

[21] W.F.Siems, C. Wu, E.E. Tarver, H.H. Hill, Measuring the resolving power of ion mobility spectrometers, Anal. Chem. 64 (1994) 4195-4201.

[22] S. Sielemann, J.I. Baumbach, H. Schmidt, P. Pielzecker, Quantitative analysis of benzene, toluene and m-xylene with the use of UV-Ion Mobility Spectrometer, Field Anal. Chem. Tech. 4 (2000) 157-169.

Chapter 6
Solid phase extraction as an approach to improve sensitivity of the headspace analysis-IMS

Capítulo 6

Extracción en fase sólida como aproximación para mejorar la sensibilidad en el análisis de espacio de cabeza-IMS

Submited to Anal. Methods

SOLID PHASE EXTRACTION TO ENHANCE SENSITIVITY WHEN HEADSPACE-GAS CHROMATOGRAPHY-ION MOBILITY SPECTROMETER IS USED

Laura Criado-García, Lourdes Arce, Miguel Valcárcel*

Department of Analytical Chemistry, Annex C-3 Building, Campus of Rabanales, Institute of Fine Chemistry and Nanochemistry, University of Córdoba, 14071 Córdoba, Spain

Ion mobility spectrometry (IMS) provides quick and reliable responses when this technology is applied in the environmental field. However, when headspace (HS) is selected as sample introduction system, there is a need to preconcentrate the sample in some cases because of the low efficiency of HS. This article discusses the parameters that affect the HS and the potential of combining solid phase extraction (SPE) before HS-IMS to improve the sensitivity of the method. The determination of phenol when it is presented in water or soil samples was selected as a case of study, obtaining a limit of detection of 0.94 μg mL-1 and 0.14 μg mL-1, respectively when direct analysis by HS-IMS was used. The methodology developed based on SPE prior to HS-IMS analysis is suitable to detect phenol at 0.05 μg mL-1 when 15 mL of water sample was passed through HLB 60 mg SPE cartridge and eluted with 1 mL of dichloromethane. The HS-IMS analysis of the eluent in which phenol was present was carried out without any interference from the solvent.

Keywords: headspace analysis, solid phase extraction, ion mobility spectrometry, phenol.

1. Introduction

Ion mobility spectrometry (IMS) has been widely used in environmental analysis [1]. It has been successfully applied to detect contaminants in soil [2] and aqueous media to prevent environmental accidents [3, 4]. From all alternatives to introduce volatiles inside the IMS, headspace analysis (HS) is one of most used. HS sampling offers several advantages such as the absence or lower volume of organic solvents needed, it does not require complicated instrument and matrix interferences can be minimized [5]. However, a number of operational parameters must be optimized including extraction temperature, time needed to achieve equilibrium between the sample and the headspace, and the headspace ratio in the headspace vial. All of them can exert effects on the HS analysis [6]. An important disadvantage of using HS is that the limits of detection (LOD) obtained can be higher than the ones required in environmental trace analysis.

Preconcentration step should be included before HS sampling, combining effective sampling with rapid detection while enhancing the sensitivity and selectivity of ion mobility techniques in the analysis of complex matrices [7, 8]. Previous works suggests that solid phase microextraction (SPME) [9-12] and membrane approaches [13, 14] are all appropriated for environmental applications with IMS. SPE can be a good alternative to increase the sensitivity of an IMS method due to its quick extraction of analytes and reliability to preconcentrate them [15]. However, SPE conditions should be studied carefully; mainly solvent used as eluent to guarantee an efficient elution from the sorbent and avoiding interferences in the IMS analysis. In previous works SPE was used for clean-up prior to the IMS analysis to detect and identify trace levels of explosives in war areas [16]. In the clinical field, molecularly imprinted SPE and corona discharge IMS were used to determine testosterone in urine [17]. However, no previous works have been reported in which SPE was used to

preconcentrate analytes in environmental samples and analyzing its extract by HS-IMS.

As a case of study, phenol, which is an analyte not very studied by IMS, was selected to demonstrate the potential of using SPE before IMS. In fact, only four works were found in the literature in which phenol was determined in chemical [18, 19], biological [20] and environmental samples [12]. Because of its high toxicity even at low concentrations, phenol is one of the most hazardous organic pollutants in wastewaters of various industries such as refineries [11], thermosolar plant [21, 22] and chemicals used in agriculture [23]. Moreover, it can reach the water environment through domestic wastes and treated sewage discharges [24]. Phenol also has an unpleasantly sharp, burning taste, which taints drinking water [25] at concentrations as low as 0.15 μg mL^{-1} [26]. The adult oral tolerable daily intake (TDI oral) for phenol from food and water combined is approximately 0.75 mg bw (body weight) day^{-1} [26]. The maximum allowable concentration of phenol for human consumption regulated by EPA is 2 μg mL^{-1} in drinking water [27]. Legal limits of phenol in soil are less restrictive. Phenol concentration found in soils must not exceed of 100 μg g^{-1}, 70 μg g^{-1} and 7 μg g^{-1} for industrial, urban and other uses areas; respectively (Spanish Government RD 9/2005). The standard EPA method is based on a concentrating liquid-liquid extraction followed by derivatization and GC analysis with electron capture detection.

The aim of the present work was to study how to maximize signal obtained when HS is used as a sample introduction system with IMS. SPE was incorporated as a pre-treatment step to improve the sensitivity when HS is used with IMS. Critical parameters affecting the extraction efficiency of SPE and analytical properties of the HS-IMS methodology were studied and optimized. The results demonstrated that the procedure developed (SPE combined with HS-IMS) has great potential for environmental applications.

2. Experimental

2.1. Reagents and samples

Phenol, methanol, acetonitrile and dichloromethane (DCM) were purchased by Sigma-Aldrich (St. Louis, USA). The stock solutions of these compounds were prepared at 1 g L^{-1} in purified water by passage through a Milli-Q apparatus from Millipore (Bedford, MA, USA). These stock standard solutions were diluted with purified water to prepare mixed standards concentrations in the range of 0.5 µg mL^{-1}-10 µg mL^{-1}. Environmental water samples were collected from river Guadalquivir, Rabanales stream and a local well (Córdoba, Spain). They were spiked at different concentration levels for precision and recovery studies. Stock, working standard solutions and water samples were stored at 4 ºC in the refrigerator before analysis. Soil samples were collected from Rabanales campus parking area, train station and park in the city centre (Córdoba, Spain). Spiked samples were prepared by adding volumes in the range of 10 to 60 µL of a standard solution of 25 mg L^{-1} prepared in Milli Q ultrapure water, corresponding to concentrations in the range of 0.25-1.5 µg g^{-1} of analyte spiked in 1 g of soil.

2.2. Equipment

Analyses were performed on a gas chromatograph column coupled to ion mobility spectrometer (FlavourSpec®) from G.A.S., Dortmund, Germany. The instrument was coupled to an automatic sampler unit (CTC-PAL, CTC Analytics AG, Zwingen, Switzerland). It was equipped with a heated splitless injector, which enabled direct sampling of the headspace from the samples. The device has a tritium ionization source (St. Petersburg, Russia) with an activity of 300 MBq which is below the exemption limit of the EURATOM guideline (1 Gbq). For analysis, a volume of 1 mL of liquid sample or 1 g of soil sample was placed in a 20 mL vial that was closed with magnetic caps and silicone septum. After 20 min incubation at 70 ºC with shaking, 200 µL of sample headspace was automatically injected by a heated syringe (80 ºC) into the IMS equipment.

After injection, the carrier gas (N_2 5.0, 10 mL min^{-1}) supplied by Abelló Linde S.A. (Barcelona, Spain) passing through the injector inserted the sample into the GC column which was 30 m long x 0.25 mm of ID CC filled with 0.5 μm film thickness of methyl, phenyl and vinylsiloxane from CS-Chromatographie Service GmbH (Dürem, Germany) in a 94:5:1 proportion, heated at 40 ºC for timely separation. Then, the analytes were eluted and driven into the ionization chamber for ionization, prior to detection by the IM spectrometer. A flow of nitrogen 5.0 at 250 mL min^{-1} supplied by Abelló Linde S.A. (Barcelona, Spain) in the opposite direction of the ions was employed as drift gas in order to prevent non-ionized impurities from entering the ionization chamber. Once ions are formed in the ionization chamber and are focused to a shutter grid (BN gate, grid pulse width 100 μs), they start to move along the drift tube of 5 cm length maintained at 65 ºC, under a constant electrical field of 400 Vcm^{-1}. The separated ions reach the detector (Faraday plate). Data were acquired and recorded during 30 min of analysis by the integrated computer within the equipment, displayed on it and consecutively processed using the software LAV version 2.0.0 from G.A.S. All spectra were recorded in the positive ion mode.

2.3. SPE procedure

Different commercial SPE cartridges were tested to preconcentrate phenol, namely (i) 30 mg and 60 mg of polymeric reversed-phase sorbent HLB OASIS (Waters, Milford, MA, USA), (ii) 60 mg of silica based sorbent C18 (Varian Harbor City, CA, USA) and (iii) 60 mg of a neutral resin comprised of divinylbenzene-based particle grafted with a polyvinylpyrrolidone polymer SolEx HRPHs (Thermo Fisher Scientific, Waltham, MA, USA). The SPE procedure was performed on a Visiprep DL SPE Vacuum Manifold from Supelco (Bellafonte, PA, USA). The pH of the samples was adjusted to pH 3 with 2 M HCl solution prepared from concentrated HCl supplied by Sigma-Aldrich (St. Louis, USA) and using MicropH 2000 meter from Crison (Barcelona, Spain). River, stream and well samples were filtered using a nylon membrane 0.45 μm pore size (Sartorius, Goettingen, Germany). In order to evaluate the effectiveness of

the SPE cartridges, they were conditioned with 5 mL of methanol and 5 mL of water at that sequence. Then, 15 mL of environmental water sample was passed through the SPE cartridge. This was followed by elution with 1 mL of dichloromethane (DCM) and introduced in the autosampler of the IMS instrument for its analysis.

3. Result and discussion

3.1. Direct HS-IMS optimization

In headspace sampling, the vapour phase is directly above and in contact with a liquid or solid sample in a sealed vial. Only an aliquot of the headspace is transferred to the IMS instrument for analysis. In **Figure 1** is shown a schematic diagram of the headspace which is thoroughly described in [28-30] coupled to the IMS instrument used in this work which has integrated a GC column as was fully described in the experimental section. Equilibrium between both phases must be generated.

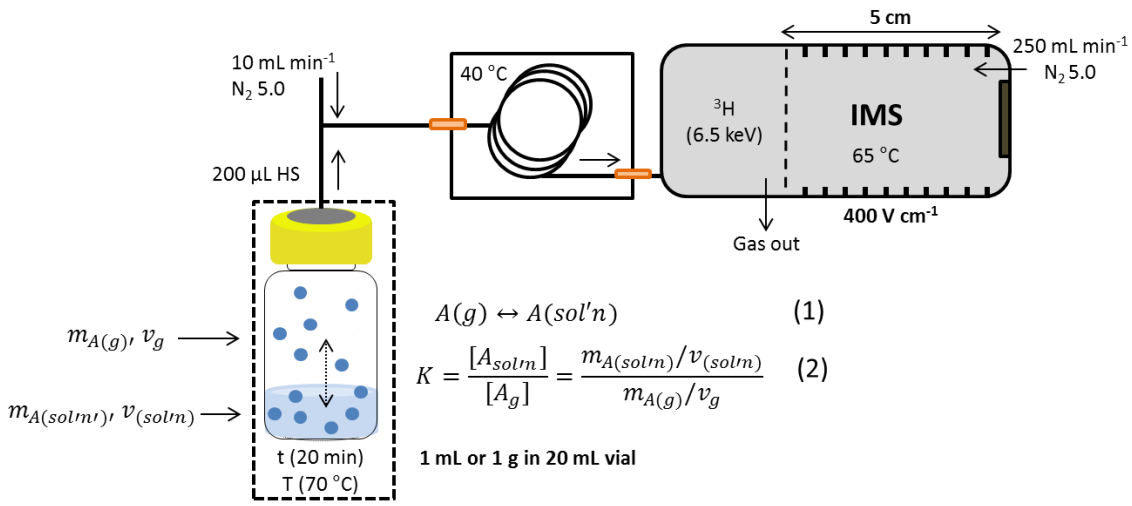

Fig. 1. Schema of headspace vial coupled to the IMS instrument used. In the equation (1) is shown the equilibrium constant expression and in the equation (2) the partitioning between gas phase and sample phase in concentration (expressed as mass or volume).

The variable A refers to the analyte, in this case phenol, and *K* refers to the concentration equilibrium constant for that analyte portioning between the solution (liquid or solid sample) and vapor phase. That equilibrium is reached within the vial prior to the removal of volume of the vapor phase for analysis. Also the detector response in static headspace can be increased by increasing vapor pressure of the analyte from matrix components [31]. Parameters that increase vapor pressure and affect the efficiency of headspace extraction: heating temperature and time, sample mass and volume (related to the headspace ratio), volume of headspace injected and instrumental parameters of IMS were carefully studied and controlled in order to improve the analytical performance of the HS sampling and therefore sensitivity, reproducibility and instrument response. In **Table 1** are shown the optimum values for the parameters optimized using the experimental set-up based on HS-IMS. A standard solution prepared in Milli-Q ultrapure water containing phenol at 5 μg mL^{-1} and soil sample spiked at 1 μg g^{-1} were used for optimization purposes. All analyses were made by triplicate.

Table 1. Experimental conditions for HS-GC-IMS used in this work.

Experimental parameter	Studied range	Optimum condition
Sample volume (mL) (1)	0.1-8	1
Sample mass (g) (2)	0.1-8	1
Vial volume (mL)	10 or 20	20
Carrier gas flow (mL min^{1})	5-15	10
Drift gas flow (mL min^{-1})	-	250
Heating temperature (ºC)	30-80	70
Heating time (min)	5-30	20
Injection volume (μL)	200-1000	200
Analysis time (min)	-	30
Gas column temperature (ºC)	40-70	40
Drift tube temperature (ºC)	45-75	65

(1) Sample volume used for water samples.
(2) Sample mass used for soil samples.

Sample heating temperature and time

In head-space sampling, heating temperature and time of the sample can accelerate the mass transfer of volatile analytes through the aqueous matrix for reaching equilibrium and acquiring the maximum signal. Heating temperatures in the range of 30 to 80 ºC during 5 to 30 min were tested. As it is plotted in **Figure 2**, a higher peak from phenol was achieved when 70 ºC was applied for 20 min. Heating at 70 ºC for 30 min resulted in not much change in the phenol peak height.

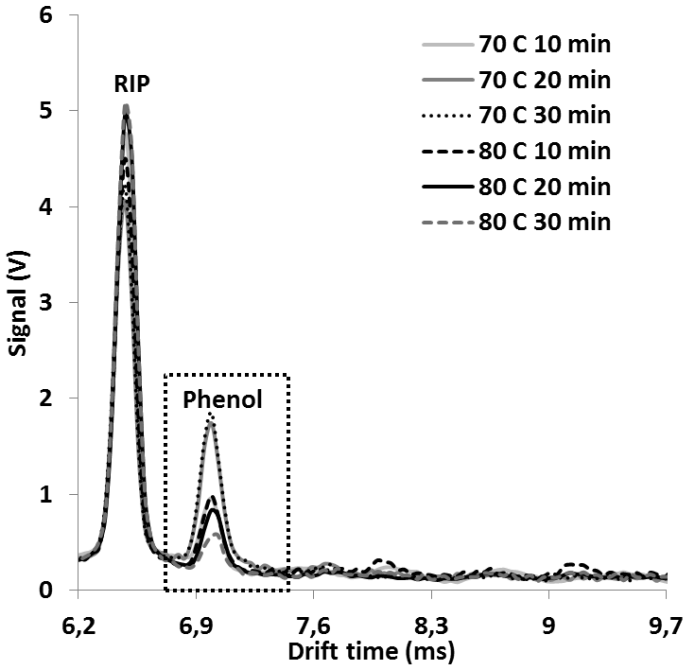

Fig. 2. IMS spectra of water sample spiked with phenol at 5 µg mL^{-1} extracted from liquid samples obtained when heating them at 70 and 80 ºC during 10, 20 and 30 min by HS-IMS.

This experiment proved that the equilibrium between liquid-gas phase was reached and the maximum volatile molecules were transferred from the liquid or solid sample to the headspace after 20 min. An increase in temperature may be used to decrease the partition coefficient of phenol by increasing vapor pressure in the vial from 0.452 mm Hg (20 ºC) to 7.52 mm Hg (70 °C) and increasing concentration in the gas phase as stated by

Henry's law (data calculated from NIST website). However this can be problematic if the solvent is also volatile [31]; like is the case of water. When the water sample was heated at 80 ºC the signal obtained for phenol was lower than the one obtained when heating at 70 ºC because more vapour water molecules are generated and they could interfere decreasing the peak height of phenol. Note that in the case of water samples the humidity content is much higher than in soil samples and moisture can interfere more in the IMS signal when increasing vapor pressure (increasing heating time and temperature). An intense signal was also observed for soil samples using these optimum values (70 ºC for 20 min). The same experiment was repeated at the LOQ concentration found for water (3 μg mL^{-1}) and soil samples (0.5 μg g^{-1}). Maximum signals were in accordance with the values chosen in the optimization process using 5 μg mL^{-1} and 1 μg g^{-1} of phenol spiked in water and soil samples respectively.

Sample volume and mass

Headspace volume ratio (sample volume divided by vial volume (10 or 20 mL)) has also an influence on the sensitivity of the method. Sample volumes and mass weights of 0.1, 0.25, 0.5, 1, 3 and 5 mL or g were added to a 10 mL vial and 0.1, 0.25, 0.5, 1, 5 and 8 mL or g to a 20 mL vial, respectively for water or soil samples. As shown in **Figure 3** when increasing sample volume in the range of 0.1-1 mL in 10 or 20 mL vial, higher concentrations were found in the headspace of the vial and consequently greater signal intensities. At higher volumes (> 1 mL) the headspace created is saturated and there was not increment in the IMS signal because the equilibrium of diffusion between liquid and gas phase in the headspace vial was reached and no more molecules from liquid phase could transfer to gas phase. Also when working with higher sample volumes we are contributing to increase the moisture in the headspace and consequently decreasing the signal in the IMS [32]. Some differences in signal intensities were appreciated in soil samples, when 1 g of sample was placed in 20 mL vial (0.89 V) or in 10 mL vial (0.75 V) obtaining the higher signal with 20 mL vial. As well, when more sample mass was placed in the

20 mL vial greater signals were obtained: 5 g (0.91 V) and 8 g (0.94 V); but as well an increment of RSD values was detected at higher mass values. In order to maximize sensitivity and precision, 1 mL of water and 1 g of soil samples was chosen for further analysis using a 20 mL vial for both.

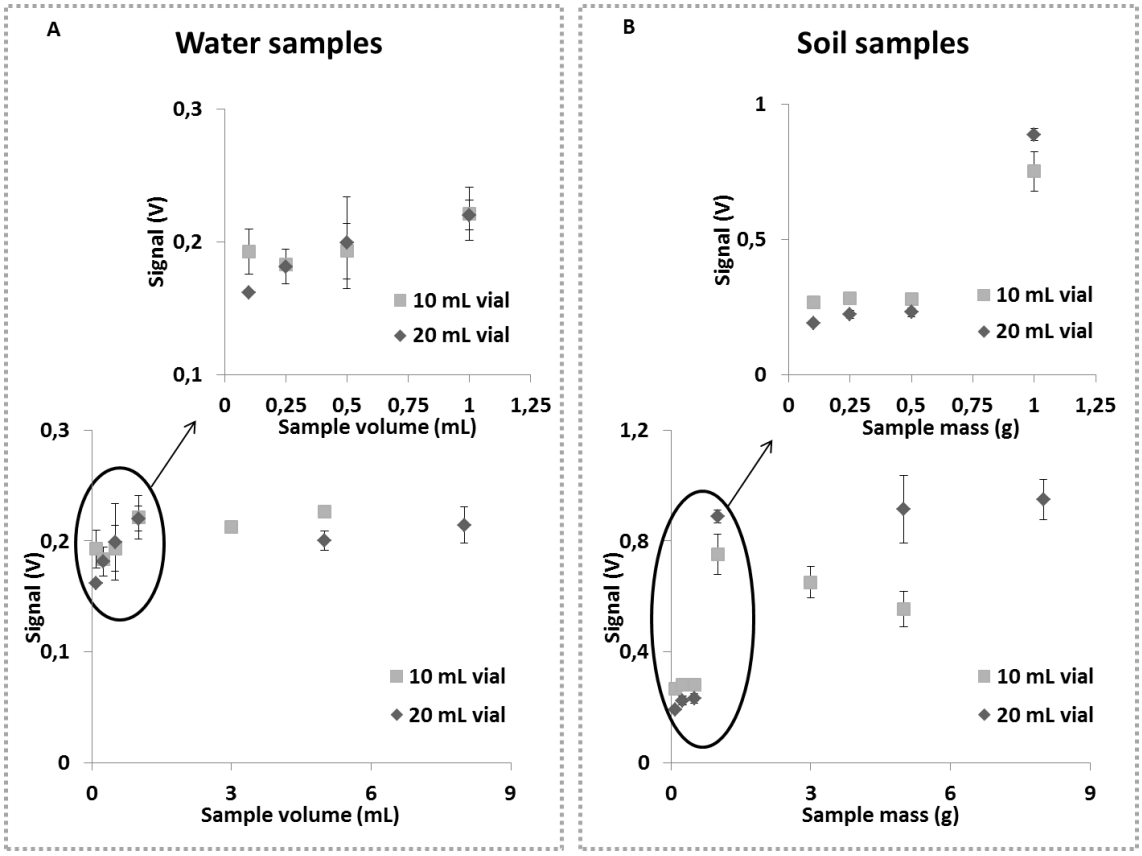

Fig. 3. IMS signal obtained for phenol spiked at (A) 5 µg mL^{-1} in water samples and (B) 1 µg mL^{-1} in soil samples in which different sample volumes and weight values were tested to generate the headspace in 10 and 20 mL vial.

Headspace volume injected

This parameter was studied in the range of 200-1000 µL using 5 µg mL-1 and 1 µg g^{-1} of phenol spiked in ultrapure water and soil sample respectively, and also with spiked samples at the LOQ values obtained. 1 mL was the maximum volume of the headspace syringe used. Results obtained for phenol spiked in water (3 µg mL^{-1}) and soil samples (0.5 µg g^{-1}) are shown in the **Figure 4 A** and **4B**. The highest signal for phenol was

obtained when 200 µL of headspace was injected to the IMS for analysis for both water and soil samples. As can be seen in **Figure 4C** the reactant ion peak (RIP) and phenol peak decreased when higher HS volumes were used. When higher values for HS volumes were tested, more molecules of analyte accompanied with more volatiles from the matrix and vapor molecules generated in the headspace were introduced, increasing the clustering in the ionization region of the IMS. Big clusters of water with phenol molecules and matrix compounds could form [33] and appeared at longer drift time (8.8-12.5 ms, marked with an asterisk) taking the charge of the RIP, competing with phenol ion (7.0 ms) and consequently decreasing its signal.

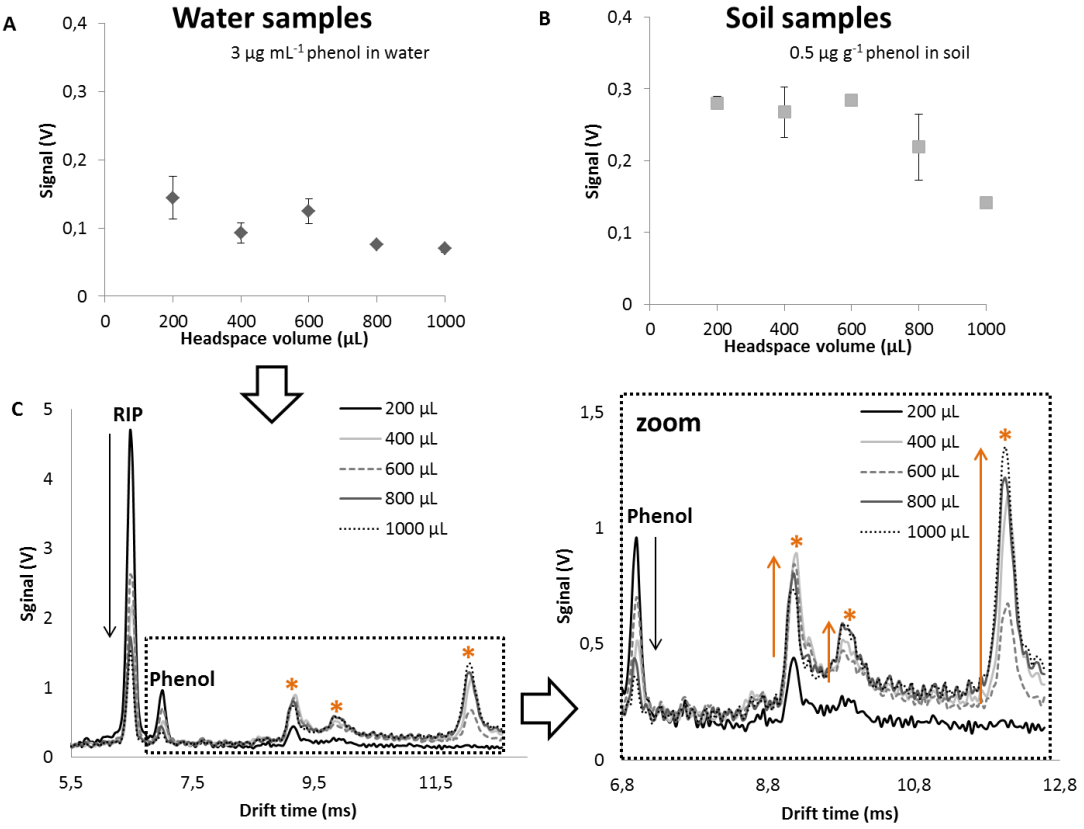

Fig. 4. Effect of headspace volume injected on the IMS for phenol spiked at (A) 3 µg mL^{-1} in water samples and (B) 0.5 µg mL^{-1} in soil samples. (C) IMS spectra obtained at the different HS volumes tested for water samples and a detailed zoom of the previous IMS spectra. *unknown signals related with clusters formation.

Instrumental parameters of IMS

IMS parameters that affect IMS response were also evaluated; optimum condition values are summarized in **Table 1**. The optimum carrier gas flow was 10 mL min-1 and drift gas flow at 250 mL min^{-1} based on the intense signal response obtained from the analyte at that condition. Gas column temperature was studied in the range of 40-70 ºC. It was set at 40 ºC to guarantee the retention of phenol in the GC column. Drift tube temperature was studied in the range of 45-75 ºC and set at 65 ºC because at that value was obtained the highest signal of phenol. Elevated temperatures resulted essential for drift tube in order to decrease moisture along the drift tube [34] and enhance the signal obtained from the target analyte.

3.2. Solid phase extraction optimization

Parameters were studied using a standard solution prepared in ultrapure water containing the analyte at 0.25 µg mL^{-1}. In **Table 2** are shown the optimum values for the SPE procedure. The eluent was analysed by HS-IMS method using the same optimized values as summarized in **Table 1**. All analyses were made by triplicate.

Table 2. Experimental conditions for SPE used in this work to measure phenol in environmental samples.

Experimental parameter	Studied range	Optimum condition
Type of SPE cartridge	C_{18}, HRPHS and HLB	HLB
Amount of sorbent (mg)	30, 50, 60	60
Sample volume (mL)	5-100	15
Sample pH	3-9	3
Elution solvent	Methanol, acetonitrile and dichloromethane	dichloromethane
Elution volumen (mL)	1 or 2	1

SPE cartridge

Cartridges that are widely used for phenols and trace analysis were tested namely C18 50 mg, HLB 30 mg and 60 mg, and SolEx HRPHs 60 mg. The highest sensitivity was achieved using HLB 60 mg cartridges. In all cases, 1 mL of solvent to extract analyte retained in the cartridge was used. Copolymer sorbent (HLB) cartridge resulted to be the most suitable sorbent to retain polar analytes such as phenol due to its hydrophilic part in its structure [15].

Sample volume and pH

The sample volume was optimized attending to the highest signal and recovery obtained to enhance sensitivity. The influence of sample volume was studied by passing volumes from 5 to 100 mL through SPE. From 5 to 15 mL, higher intensities of the peak were observed. Larger volume (up to 100 mL) led to moderately greater analytical signals but entailing a worse reproducibility (higher RSD values) probably because too high volume of sample could overload the cartridge and make difficult its elution, causing poor reproducibility and accuracy in the measurement. 15 mL of sample volume was chosen for all subsequent analyses as a compromise to achieve high sensitivity, good reproducibility and short analysis time. In the case that further sensitivity is required, volume higher than 15 mL can be used. The effect of the sample pH on the SPE performance was also studied; since it determines the state of the analyte in its ionic or molecular form and consequently, affects its interaction with the sorbent and the extraction efficiency. The extraction efficiency of HLB cartridge was higher when sample was acidified with 2 M HCl solution; adding 100 µL to stocks standards and 300 µL to river water samples in order to reach pH 3 in both cases. Phenol is a weak acid (pH= 5-6) and the retention of phenol in the HLB cartridge was favoured when the pH was decreased, below its pKa= 10. It was observed by other authors that the –OH group of phenol is stable, in its molecular form, in aqueous medium at lower pH [35]. Experimentally a more intense peak of phenol was obtained when the sample was set at pH 3 because the extraction efficiency was enhanced at acidic pH.

Eluent

When working with IMS, solvents should be carefully studied taking into account that they not produce ions that can interfere in the signal obtained from the target analyte as well that provide efficient elution in SPE. Methanol and acetonitrile are appropriated solvent to elute phenol [15] from the chosen SPE cartridge; but when analyzing by IMS the headspace of the analyte dissolved in methanol or acetonitrile an intense and tailing peak was observed in the IMS spectra and consequently interfering in the phenol signal acquired in the positive mode. By contrast, dichloromethane is also an adequate solvent, it was also ionized but it only yielded negative ions [36], so it did not interfere in the IMS signal in positive mode. Then, it was selected as eluent in the SPE procedure. Evaporation to dryness under nitrogen stream and reconstitution in water was also tested but discarded due to lower IMS signals obtained compared with direct analysis of the headspace eluent using DCM.

3.3. Analytical performance of SPE prior to HS-IMS

Prior to the analysis of environmental samples, the method was analytically characterized in terms of sensitivity, precision and recovery. Concentration range used for the calibration was in the range of 1-10 μg mL^{-1} when direct headspace analysis was used and 0.1-1 μg mL^{-1} for method developed based on SPE. **Table 3** shows the analytical figures of merit of the proposed method by using HS-IMS and SPE-HS-IMS. Calibration curves were obtained by plotting peak intensities versus concentrations. Measurements were done by triplicate. LODs and LOQs were calculated as three and ten times respectively, the intercept deviation (Sb) divided by the slope. More sensitivity was obtained for soil samples compared to water samples. The high humid condition created in the headspace of the water samples lately introduced into the IMS device caused a limited sensitivity, increasing LODs and LOQs obtained as it can be observed in **Table 3**. This could be alleviated by using a membrane or a sorbent to retain moisture. The determination of phenol in water samples by SPE-HS-IMS provided LODs and LOQs one order of magnitude lower (LOD=

0.05 μg mL^{-1} and LOQ= 0.18 μg mL^{-1}). In this case, preconcentration of the phenol present in water samples was successfully achieved by the use of an appropriated SPE procedure.

Table 3. Calibration curve and statistical figures of merit for the determination of phenol by HS-IMS and SPE combined with HS-IMS.

Method	Matrix	Calibration curve (*y= ax+b*)	R^2	$S_{x/y}$	Sa	Sb	LOD (μg mL^{-1})	LOQ (μg g^{-1})
HS-IMS	Water	y= 0.033x + 0.056	0.974	0.020	0.010	0.002	0.94	3.13
	Soil	y= 0.283x + 0.033	0.984	0.018	0.013	0.014	0.14	0.45
SPE-HS-IMS	Water	y= 0.056x + 0.037	0.995	0.002	0.001	0.002	0.05	0.18

The precision of the proposed method was assessed in terms of within-day and between-day precision, both expressed as RSD %, shown in Table 4. Direct headspace analysis was performed with spiked soil samples at 1 μg g^{-1} and river samples at 4 μg mL^{-1} and the SPE procedure was performed with spiked river samples at 0.5 μg mL^{-1} as can be seen in **Table 4**. Within-day precision was assessed by applying the procedure six times on the same day and between-day precision by analysing three times the sample over three consecutive days. Precision values for drift time and retention time were in all cases lower than 1.9%. Higher values for RSD were obtained for intensity peak height (RSD< 15%). It could occur that the experimental conditions chosen to generate the headspace (70 ºC for 20 min) led to volatilize other compounds coming from the matrix as it was observed by other authors [37]; affecting mainly phenol intensity signal.

The efficiency of SPE cartridge to retain analyte was assessed by conducting recovery test involving triplicate in river and local well samples spiked with phenol at 0.5 mg L^{-1} ranged from 90 to 98 % and confirmed that HLB 60 mg was an effective sorbent material for extracting lower concentrations of phenol from environmental water samples, especially suitable for trace analysis.

Table 4. Precision values for the determination of phenol by HS-GC-IMS and SPE combined with HS-GC-IMS.

Precision values	Matrix	HS-IMS				SPE and HS-IMS			
		Concentration Added	Peak height	Drift time	Retention time	Concentration added	Peak height	Drift time	Retention time
Within-day precision (% RSD, *n*= 6)	Water	4 µg L^{-1}	5.5	0.2	0.2	0.5 µg L^{-1}	7.7	0.3	0.5
	Soil	1 µg g^{-1}	2.2	0.3	0.9				
Between-day precision (% RSD, *n*= 9)	Water	4 µg L^{-1}	6.7	0.3	1.6	0.5 µg L^{-1}	15.5	0.7	1.9
	Soil	1 µg g^{-1}	10.1	0.4	1.2				

Analysis of environmental samples

The proposed method was successfully applied to the analysis of different environmental samples, three natural water and three soils, necessarily spiked with a standard of phenol because no positive samples were found. IMS topographic plots of well water sample (**Figure 5A**) and 4 µg mL^{-1} spiked well water sample (**Figure 5B**); soil sample (**Figure 5C**) and 0.5 µg g^{-1} spiked soil sample (**Figure 5D**) are shown. As can be seen phenol peak was successfully identified in the spectra from the spiked samples by HS-IMS. Other signals found in these analyses are discussed in the next section.

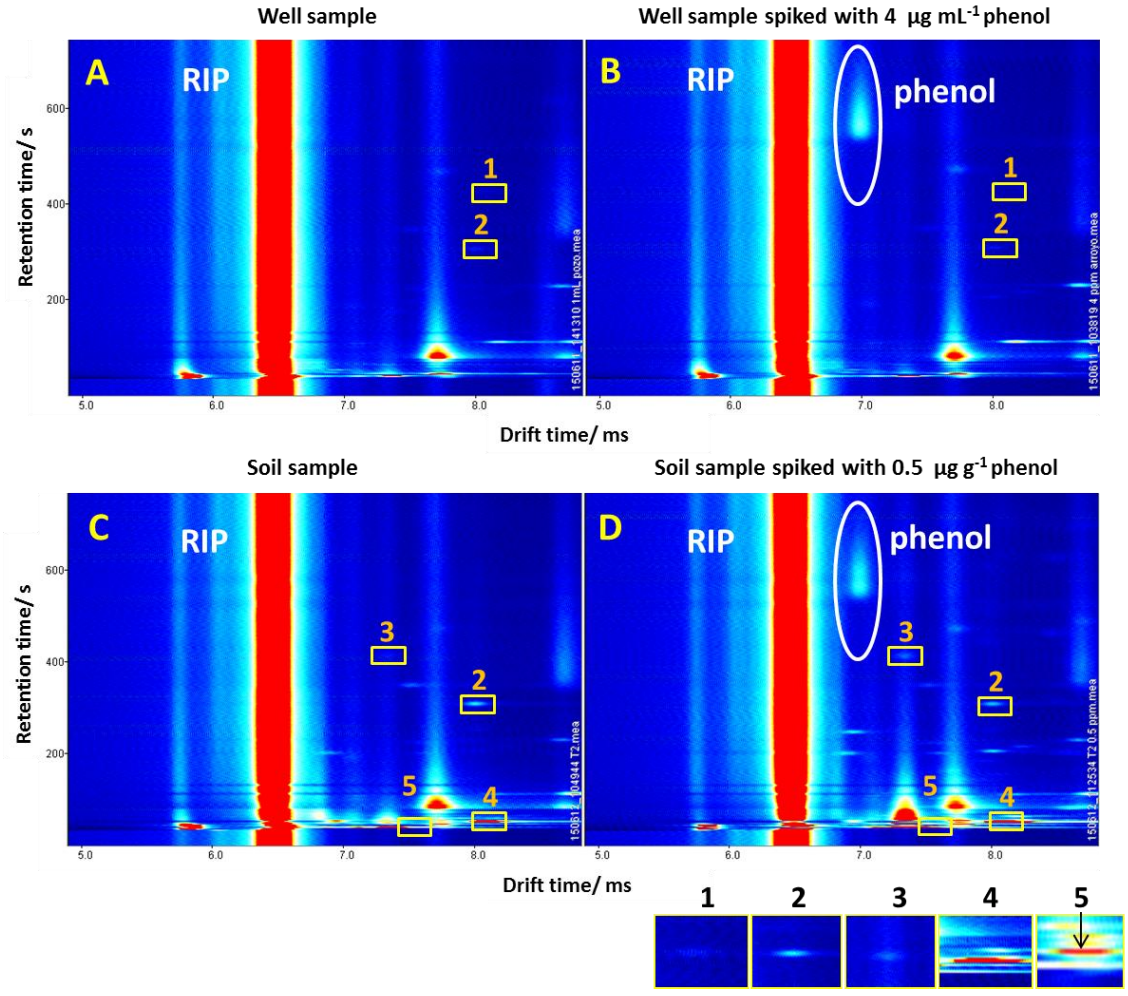

Fig. 5. IMS topographic plot obtained from (A) well sample, (B) well sample spiked at 0.5 µg mL^{-1}, (C) soil sample and (D) soil sample spiked at 0.5 µg g^{-1} by HS-IMS.

Study of possible interferences

In **Figure 6** are plotted the topographic plots obtained for DCM used as eluent in the SPE procedure and the river sample analyzed by HS-IMS and the same river sample spiked at 0.5 μg mL^{-1} by SPE and HS-IMS.

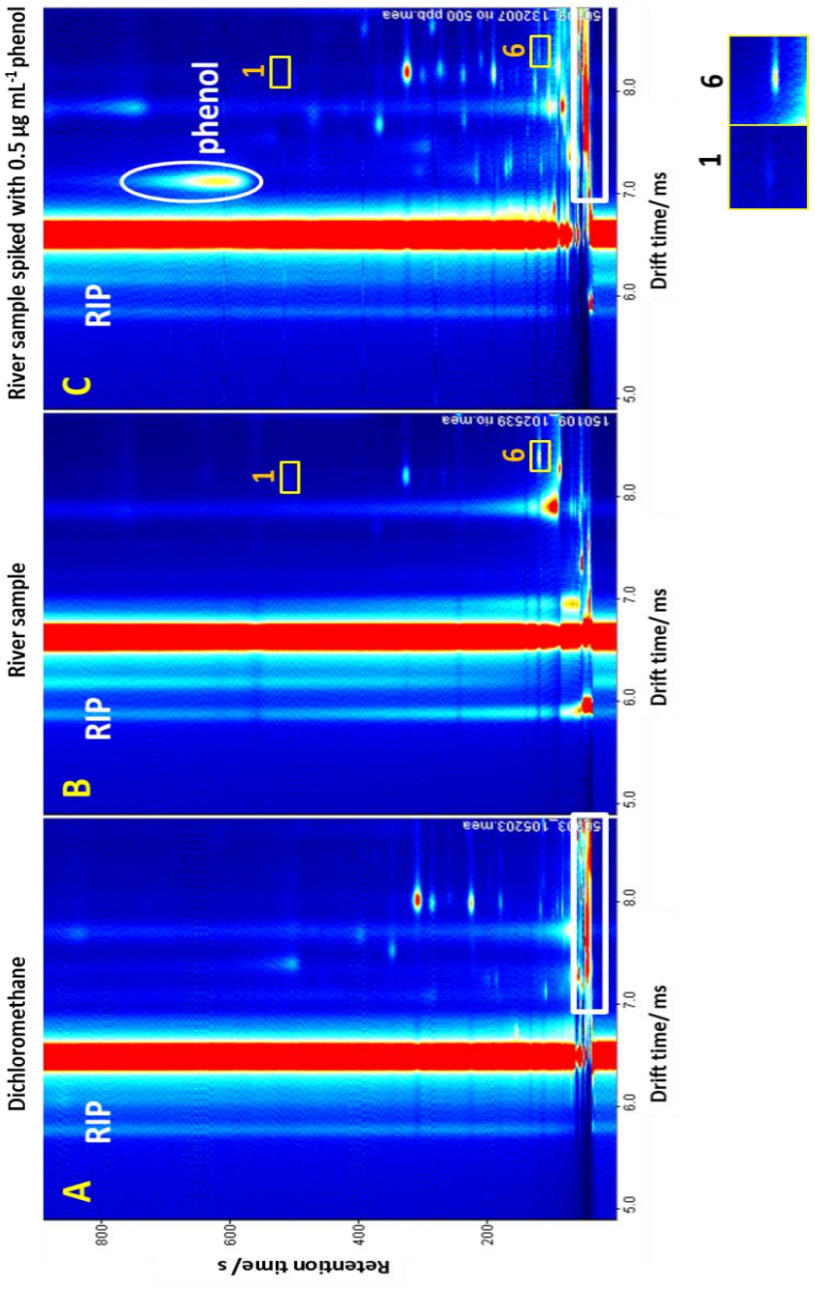

Fig. 6. IMS topographic plot obtained from (A) dichloromethane and (B) river sample by HS-IMS and (C) river sample spiked at 0.5 μg mL^{-1} by SPE and HS-IMS.

As can be seen, phenol peak was successfully identified in the spectra in an area free of interferences by the proposed SPE prior to HS-IMS method. DCM did not produce any signal that could interfere with the target analyte. However, it can be appreciated how some peaks related to impurities of the dichloromethane appeared in the topographic plot, especially in the first 60 seconds of the measurement, signalled with a white rectangle in Figure 6A and C. The potential of the method to identify more signals can also be demonstrated identifying other components present in the samples analyzed by using the GCxIMS library search tool provide by GAS. Note that these IMS signals that appeared in the topographic plots did not overlapped with the ion product observed for phenol at a drift time of 7 ms (spectrum 823, retention time 577 s). Six different signals were matched with 6 different compounds by using the information including in the GCxIMS library database: 1,8-cineole (1) in well and river water sample (**Figures 5A, 5B, 6B** and **6C**), 1-octen-3ol (2) in well water sample and soil sample (**Figure 5A, 5B, 5C** and **5D**); trans-limonene oxide (3), aryphyllene (4) and α-terpineol (5) in soil samples (**Figure 5C** and **5D**); and pyridine (6) in river samples (**Figure 6B** and **6C**). Further studies should be carried out, including standard addition to confirm the right assignment of these peaks. In any case, their signals obtained in the IMS spectra interfered in the correct identification and quantification of phenol in the environmental samples measured by the proposed methodology.

4. Conclusion

When headspace is used as sample introduction system to the IMS, special attention should be given to experimental parameters namely heating temperature, volume and mass of the sample, container vial, and headspace volume among others that affect enormously the headspace generation; as was demonstrated in this work. In case that the sensitivity obtained is not enough to determine low concentrations, SPE can be used combined with HS-IMS analysis. This approach proved effective extraction of phenol in environmental water samples. LODs and LOQs were reduced

considerably in one order of magnitude, 0.05 μg mL^{-1} and 0.18 μg mL^{-1}, respectively. The SPE eluent (dichloromethane) does not affect the correct identification and quantification of phenol in the HS-IMS measurement. Other peaks obtained in the analysis of environmental samples did not interfere with the correct identification and quantification of phenol. The main drawback of the pre-treatment proposed in this work is that automatization is difficult to be implemented. Validation of the methodology in terms of sensitivity, precision and recovery demonstrated its effectiveness in the environmental field for trace analysis.

Acknowledgements

The authors are grateful to Spain's DGICyT (Grant CTQ2014-52939R) for funding this work. LCG wishes to thank the Spanish Ministry of Education, Culture and Sport for award of a pre-doctoral grant (AP 2009-3528).

The authors have declared no conflict of interest.

References

[1] G. A. Eiceman, Ion mobility spectrometry as a fast monitor of chemical composition, *Trac-Trends Anal. Chem*., 2002, **21**, 259.

[2] A. B. Kanu, H. H. Hill, M. M. Gribb, R. N. Walters, A small subsurface ion mobility spectrometer sensor for detecting environmental soil-gas contaminants, *J. Environm. Monit.,* 2006, **9**, 51.

[3] S. Armenta, M. Alcala, M. Blanco, A review of recent, unconventional applications of ion mobility spectrometry (IMS), *Anal. Chim. Acta,* 2011, **703**, 114.

[4] J. I. Baumbach, Process analysis using ion mobility spectrometry, *Anal. Bional. Chem.*, 2006, **384**, 1059-1070.

[5] Y. Y. Zhou, J. F. Yu, Z. G. Yan, C. Y. Zhang, Y. B. Xie, L. Q. Ma, Q. B. Gu, F. S. Li, Application of portable gas chromatographt photo inonization detector combined with headspace sampling for field analysis of benzene, toluene, ethylbenzene and xylene in soils, *Environm. Monit. Assess*., 2013, **185**, 3037.

[6] J. C. Flórze-Méndez, M. L. Fernández-Sánchez, J. E. Sánche-Uría, E. Fernández-Martínez, A. Sanz-Medel, Static headspace, solid-phase microextraction and headspace solid-phase microextraction for BTEX determination in aqueous samples by gas chromatography, *Anal. Chim. Acta,* 2000, **415**, 9.

[7] R. Lu, R. M. O' Donnell, P. B. Harrington, Detection of cocaine and its metabolites in urine using solid phase microextraction ion mobility spectrometry with alternating least squares, *Forensic Sci. Int.*, 2009, **189**, 54.

[8] H. Borsdorf, T. Mayer, M. Zarejousheghani, G. A. Eiceman, Recent development in Ion Mobility Spectrometry, *Appl. Spectrosc. Rev.*, 2011, **46**, 472.

[9] G. Walendizk, J. I. Baumbach, D. lockow, Coupling SPME with MCC/UV-IMS as a tool for rapid on-site detection of groundwater and surface water contamination, *Anal. Bional. Chem.* 2005, **385**, 1842.

[10] P. Rearden, P. B. Harrington, Rapid screening of precursor and degradation products of chemicals warfare agents in solid by solid phase microextraction ion mobility spectrometry (SPME-IMS), *Anal. Chim. Acta*, 2015, **545,** 13.

[11] S. Mohammadi, A. Kargari, H. Sanaeepur, K. Abbassian, A. Najafi, E. Mofarrah, Phenol removal from industrial wastewaters: a short review, *Desalination and water treat*., 2015, **53**, 2215.

[12] S. Holopainen, V. Luukkonen, M. Nousiainen, M. Sillanpää, Determination of chlorophenols in water by headspace solid phase microextraction ion mobility spectrometry (HS-SPME-IMS), *Talanta*, 2013, **114**, 176.

[13] A. B. Kanu, C. L. P. Thomas, The presumptive detection of benzene in water in the presence of phenol with an active membrane-UV phto-ionisation differential mobility spectrometer, *Analyst*, 2006, **131**, 990.

[14] C. J. Koester, A. Moulik, Trends in environmental analysis, *Anal. Chem.*, 2005, **77**, 3737.

[15] I. Rodriguez, M. P. Llompart, R. Cela, Solid phase extraction of phenols, *J. Chromatogr. A*, 2000, **885**, 291.

[16] F. Garofolo, V. Migiozzi, B. Rojo, Application of ion mobility spectrometry to the identification of trace levels of explosives in the presence of complex matrices, *R. Com. Mass Spectrom.*, 1994, **8**, 527.

[17] S. Mirmahdieh, A. Mardihallaj, Z. Hashemian, J. Razavizadeh, H. Ghaziaskar, T. Khayamian, Analysis of testosterone in human urine

using molecularly imprinted solid-phase extraction and corona discharge ion mobility spectrometry, *J. Sep. Sci.*, 2011, **34**, 107.

[18] J. Laakia, C. S. Pedersen, A. Adamov, J. Vildanoja, A. Sysoev, T. Kotiaho, Sterically hindered phenols in negative ion mobility spectrometry-mass spectrometry, *R. Com. Mass Spectrom*., 2009, **23**, 3069.

[19] G. A. Eiceman, J. F. Bergloff, J. E. Rodriguez, W. Munro, Z. Karpas, Atmospheric pressure chemical ionization of fluorinated phenols in atmospheric pressure chemical ionization mass spectrometry, tandem mass spectrometry, and ion mobility spectrometry, *J. Am. Soc. Mass Spec.* 1999, **10**, 1157.

[20] G. B. Smith, G. A. Eiceman, M. K. Walsh, S. A. Critz, E. Andaloza, E. Ortega, F. Cadena, Detection of Salmonella typhimurium by hand-held ion mobility spectrometer: A quantitative assessment of response characteristics, *Field. Anal. Chem. Tech.*, 1997, **1**, 213.

[21] L. Criado-García, R. Garrido-Delgado, L. Arce, F. López, R. Peón, M. Valcárcel, Potential of ionmobility spectrometry versus FT-MIR and GC-MS to study the evolution of a heat transfer fluid after its heating process in a thermosolar plant, *Microchem. J.*, 2015, **121**, 163.

[22] L. Criado-García, R. Garrido-Delgado, L. Arce, F. López, R. Peón, M. Valcárcel, Simoultaneously determination of benzene and phenol in heat transfer fluid by head-space gas chromatography hyphenated with ion mobility spectrometry, *Talanta,* 2015, **144**, 944.

[23] S. Lacorte, D. Barcelo, Rapid degradation of fenitrothion in estuarine waters, *Environ. Sci. Technol*,. 1994, **28**, 1159.

[24] L. M. Davì, F. Gnudi, Phenolic compounds in surface water, *Water. Res.*, 1999, **33**, 3213.

[25] European Union Risk Assessment Report. Phenol., 2015, http://ecb.jrc.ec.europa.eu/documents/Existing-Chemicals/RISK_ASSESSMENT/REPORT (accessed 14-10-0015)

[26] Science Report SC050021 / Phenol SGV, 2009, https://www.gov.uk/government/uploads/system/uploads/attachment_data/file/313901/SCHO0709BQRN-e-e.pdf (accessed 14-10-0015)

[27] Public health statement of phenol. ATSDR ToxProfiles, 2009, http://www.atsdr.cdc.gov/toxprofiles/tp115-c1.pdf (accessed 14-10-0015)

[28] H. Hachenberg, A. P. Schimidt, Gas Chromatography Headspace Analysis. Hayden and Son, 1977.

[29] B. V. Ioffe, A. G. Vitenberg, Head-Space Analysis and Related Methods in Gas Chromatography. John Wiley and Sons, 1984.

[30] B. Kolb, L. S. Ettre, Static Headspace-Gas Chromatography Theory and Practice. John Wiley and Sons, 2006.

[31] N. H. Snow, G. P. Bullock, Novel techniques for enhancing sensitivity in static headspace extraction-gas chromatography, *J. Chromatogr. A*, 2010, **1217**, 2726.

[32] H. Borsdorf, S. Baldeweg, F. Löper, M. Höhnisch, R. Petrich, T. Mayer, The correlation of odors in the environment with ion mobility spectra patterns, *Int. J. Ion Mobil. Spec.*, 2014, **18**, 1.

[33] M. Mäkinen, M. Sillapää, A. K. Viitanen, A. Knap, J. Mäkela, J. Puton, The effect of humidity on sensitivity of amine detection in ion mobility spectrometry, *Talanta*, 2011, **84**, 116.

[34] T. Mayer, H. Borsdorf, Accuracy of Ion mobility measuraments dependent on the influence of humidity, *Anal. Chem.* 2014, **86**, 5069.

[35] A. P. Wilkinson, K. Wahala, G. Williamson, Identification and quantification of polyphenol phytoestrogens in foods and human biological fluids., *J. Chromatogr. B*, 2002, **777**, 93.

[36] Z. Karpas, A. V. Guamán, D. Calvo, A. Pardo, S. Marco, The potential of ion mobility spectrometry (IMS) for detection of 2,46-trichloroanisole (2,4,6-TCA) in wine, *Talanta*, 2012, **93**, 200.

[37] C. J. Denawaka, I. A. Fowlis, J. R. Dean, Evaluation and application of static headspace-multicapillary colum-gas chromatography-ion mobility spectrometrt for complex sample analysis, *J. Chromatogr. A*, 2014, **1338**, 136.

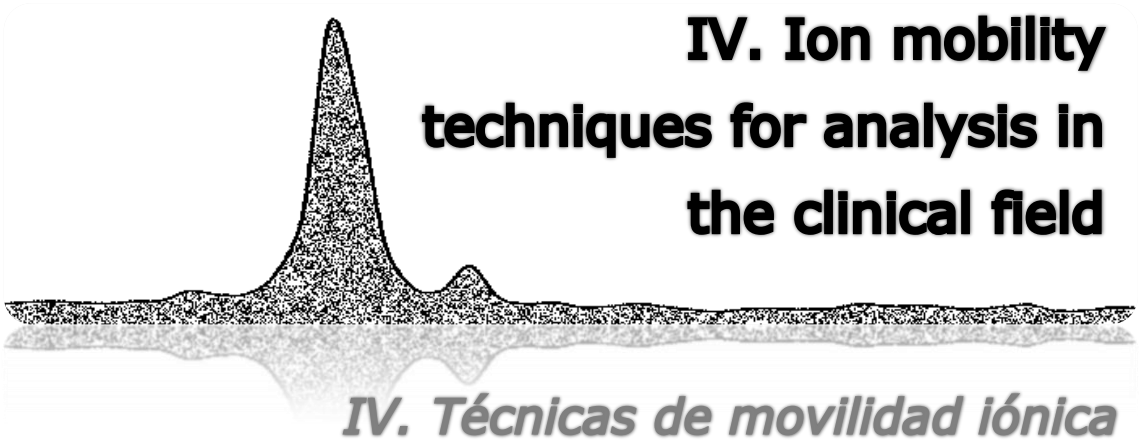

IV. Ion mobility techniques for analysis in the clinical field

IV. Técnicas de movilidad iónica para análisis en el ámbito clínico

Within the clinical field, rapid and sensitive methodologies are needed as was exposed in *Block V*. As well non-invasive analyses are more demanded nowadays in emergency rooms. Saliva is a recommended biological fluid due to the high information that can be extracted in a simple analysis. IMS techniques are versatile and offer a quick response in comparison with classical analytical techniques.

Intoxication from alcohols poisoning and drugs is an important problem which demand an efficient methodology to detect selectively these compounds from a quick analysis. In the *Chapter 7*, toxics compounds that can be present in adulterated alcoholic drinks and sedative were identified in saliva samples by thermal desorption-gas chromatography-differential mobility spectrometry. With the methodology proposed these compounds can be quantified at the toxicological rates in saliva samples. As well, differential mobility responses related to ion products and possible fragments from target analytes were also discussed.

Finally, in *Chapter 8* is shown a pre-treatment method based on a home-made μSPE device applied to extract selectively analytes of different nature from saliva samples. Humidity and interferences from the matrix were avoided with this low cost and simple approach. The desorption of analytes retained in the packed sorbent was carried out in the autosampler for its late analysis by ^{3}H-GC-IMS instrument.

Chapter 7
Determination of toxic compounds in saliva samples by differential mobility spectrometry

Capítulo 7

Determinación de compuestos tóxicos en muestras de saliva mediante espectrometría de movilidad diferencial

Accepted in J. Breath Res.

RAPID AND NON-INVASIVE METHOD TO DETERMINE TOXIC LEVELS OF ALCOHOLS AND γ-HYDROXIBUTYRIC ACID IN SALIVA SAMPLES BY GAS CHROMATOGRAPHY-DIFFERENTIAL MOBILITY SPECTROMETRY

L. Criado-García[(1)], D.M. Ruszkiewicz[(2)], G.A. Eiceman[(2)], C.L.P. Thomas[(2)*]

(1) Department of Analytical Chemistry. Annex C-3 Building. Campus of Rabanales. Institute of Fine Chemistry and Nanochemistry. University of Cordoba. 14071 Córdoba, Spain.

(2) Centre for Analytical Science, Department of Chemistry, Loughborough University. Loughborough, LE11 3TU, UK. *E-mail: C.L.P.Thomas@lboro.ac.uk

A polydimethylsilicone oral sampler was used to extract methanol, ethanol, ethylene glycol, 1,3-propandiol and γ-hydroxybutyric acid from samples of human saliva obtained using a passive-drool approach. The extracted compounds were recovered by thermal desorption, isolated by gas chromatography and detected with differential mobility spectrometry, operating with a programmed dispersion field.

Complex signal behaviours were also observed that were consistent with hitherto unobserved fragmentation behaviours in differential mobility spectrometry. These yielded high-mobility fragments obscured within the envelope of the water-based reactant ion peak. Further, compensation field maxima shifts were also observed attributable to transport gas modification phenomena. Nevertheless, the responses obtained indicated that in-vivo saliva sampling with thermal desorption gas chromatography may be used to provide a semi-quantitative diagnostic screen over the toxicity threshold concentration ranges of 100 $mg.dm^{-3}$ to 3 $g.dm^{-3}$. A candidate method suitable for use in low resource settings for the non-invasive screening of patients intoxicated by alcohols and volatile sedatives has been demonstrated.

Keywords: methanol, ethanol, ethylene glycol, propylene glycol, γ-hydroxybutyric acid, saliva, thermal desorption gas chromatography differential mobility spectrometry.

1. Introduction

Treatment of poisoning from the consumption of ethanol and the management of the intoxicated patient represents a significant burden on many health services. Further, poisoning from the consumption of other alcohols notably methanol and ethylene glycol occurs sporadically and from time-to-time outbreaks occur where food, drink or medicines are contaminated, resulting in significant mortality [1]. The essence of diagnosis is speed, and even in well–resourced health-care settings the collection of blood samples for remote analysis may introduce delays that prevent effective treatment. In communities and regions without recourse to gold-standard pathology services, or in cases where the numbers of patients runs into the hundreds [2] clinical teams may be forced to treat their patients symptomatically without recourse to reliable diagnosis. Other complications arise when intoxication from sedatives, such as γ-hydroxybutyric acid (GHB) taken intentionally or through malicious administration, is mistaken for ethanol abuse, or more seriously is masked by ethanol consumption. Consequently it would appear there is a need, across all scales of health services, for faster point-of-care toxicity screening for methanol, ethanol, ethylene-glycol and propylene glycol. It would also be helpful to be able to screen simultaneously for the presence of sedatives such GHB, and more recently, γ-butyrolactone.

Ethylene glycol and propylene glycol are highly soluble in aqueous media with Henry's Law constants of $4x10^{6}$ $mol.kg^{-1}.bar^{-1}$ and 910,000 $mol.kg^{-1}.bar^{-1}$ respectively making headspace analysis and, by implication, exhaled breath analysis unlikely to be practicable; note that in comparison the Henry's Law constants for methanol and ethanol are 230 $mol.kg^{-1}.bar^{-1}$ and 190 $mol.kg^{-1}.bar^{-1}$ respectively.

The utility of using saliva analysis for profiling methanol intoxication was proposed in 2009 [3] and subsequently an active membrane [4 and 5] was used to recover and analyse methanol and ethanol from human saliva with determination by thermal desorption gas chromatography differential

mobility spectrometry (TD-GC-DMS) across the concentration range 30 $mg.dm^{-3}$ to 500 $mg.dm^{-3}$ [6]. At that time the possible utility of extending the approach to glycols was noted. In saliva fluids, drugs of abuse have been reported to be detectable for between 5 and 48 hr in the $ng.cm^{-3}$ range [7] supporting the proposition of the development of saliva based screens. Indeed, methanol and ethanol present in saliva samples has been previously determined by GC-FID, with the proposition for extending the approach from confirmatory analyses to routine application in toxicology laboratories [8].

This research focussed on methanol, ethanol, ethylene glycol, propylene glycol and GHB. Ethanol toxicity is dependent on individual tolerance and use, although levels greater than 3 $g.dm^{-3}$ to 4 $g.dm^{-3}$ may be fatal due to respiratory depression and blood ethanol concentrations between 500 $mg.dm^{-3}$ and 700 $mg.dm^{-3}$ may be considered to be the highest that may be tolerated without neurological effects [9]. Methanol may cause metabolic acidosis, neurologic injuries, and death when ingested and blood-serum methanol levels greater than 200 $mg.dm^{-3}$ correlate with ocular injury, while the minimal lethal dose of methanol in adults is believed to be 340 mg. kg^{-1} of body weight [10]. Ethylene glycol is moderately toxic and its toxic by-products first affect the central nervous system, then the heart, and finally the kidneys. Current recommendations are that treatment with Fomepizole is initiated immediately if serum concentrations of methanol or ethylene glycol exceed 200 $mg.dm^{-3}$. In contrast, ingestion of propylene glycol is not as serious and large quantities are required to cause perceptible health damage in humans with blood-plasma concentrations over 4 $g.dm^{-3}$ associated with serious harm [11]. GHB has useful therapeutic uses such as treating narcolepsy; it is also a drug of abuse and is associated with assault. The therapeutic range is narrow and accidental overdosing is a common cause of injury with potentially fatal outcomes, normally associated with cardiorespiratory arrest [12].

The current work sought to extend the earlier TD-GC-DMS study to include a semi-quantitative diagnostic screen of alcohol toxicants and GHB

based on a non-invasive saliva sampling methodology and establish if direct extraction from saliva to a polydimethylsilicone coupon [13] with recovery and analysis by TD-GC-DMS was feasible. The DMS platform was chosen as this technique has been demonstrated to be effective for the rapid, robust and sensitive detection and quantitation of alcohols in low resource settings [14].

2. Experimental

2.1. Ethics, participant preparation and saliva sampling

It is helpful to note at the outset that the volunteers who participated in this research were not exposed to any chemical hazard(s). The study was conducted in accordance with the ethical principles of Good Clinical Practice and the Declaration of Helsinki. The local ethics committee (Ethical Advisory Committee, Loughborough University, Loughborough, LE11 2DT) approved the studies (References G10-P23 and G10-P24). Three healthy adult male non-smokers volunteered to participate in this study and gave written informed consent. The participants were recruited from Loughborough University staff, students and their social networks. Each participant provided two samples throughout the experimental campaign.

On the morning of their study visit participants were asked not to: brush their teeth; use any personal care products, or eat breakfast. Participants were also asked to only drink cold water, and refrain from flavoured, caffeinated, or drinks containing fruit juice(s). All saliva samples were taken in an in-vivo sample station located in a small internal room, where privacy was ensured, at the Centre for Analytical Science at the Chemistry Department of Loughborough University. A chaperone, of the same gender as the participant, was present during sample collection and access was restricted to only those researchers and participants involved in the sampling process. After an introduction to the study the participants were familiarised with the passive drool approach that was used to obtain a sample of their saliva [13], before proceeding to provide approximately 10

cm^3 of saliva. The participants sat with their head tilted forward to cause saliva to pool at the front of their mouth and then drain from their lips into a glass collection vial. On completion of sampling the vial was sealed promptly with a Teflon™ faced screw-top cap. Immediately after sampling the saliva was transferred to the laboratory where a 1.8 cm^3 aliquot of the saliva sample was pipetted into to a 2 cm^3 chromatography vial, and sealed immediately with a screw cap fitted with a silicone septum. These saliva aliquots were used immediately, within 3 hr of collection and maintained at ambient temperature (20 °C ± 2 °C) until disposal. Saliva residues were disposed immediately after use by diluting with a disinfectant solution and rinsed down a sink with a copious flow of running water. No cells or DNA were retained or stored.

2.2. Chemicals

Ethanol, methanol, ethylene glycol, propylene glycol, sodium chloride (purity of these compounds ≥99.8%) and butanoic acid, 4-hydroxy-, ammonium salt (GHB) in methanol (1 $mg.cm^{-3}$) were obtained from Sigma Aldrich; see **Table 1**. The carrier gas was obtained from BOC, UK, and purified by passing through two triple-bed gas purifiers mounted in series (Thames Restek). Nitrogen was generated on site (PEAK Scientific, UK, model nk-10L-HP) and purified by passing through a charcoal adsorbent-bed gas-purifier (Varian), a moisture filter (Varian), and a triple-bed gas purifier (Thames Restek), all mounted in series. Water (>18MΩ) was generated on site.

Table 1. Summary of chemicals used in the experimental procedure.

Compound	*IE*/ eV	*PA*/ $kJ.mol^{-1}$	T_{Bp}/ °C	CAS	Formula
Methanol	10.84	754.3	64.7	67-56-1	CH_3OH
Ethanol	10.48	776	72.6	64-17-5	C_2H_5OH
Ethylene glycol	10.55	815	197.3	107-21-1	$C_2H_6O_2$
Propylene glycol	10.80	876.2	182.2	57-55-6	$C_3H_8O_2$
(1)GHB	n.f.	n.f.	295.6	591-81-1	$\{C_4H_7O_3\}^-\{NH_4\}^+$

IE: ionization energy, *PA*: proton affinity, T_{Bp}: boiling point. n.f.: data not found. (1) Obtained as a methanolic solution of concentration 1 $mg.cm^{-3}$ in CH_3OH.

2.3. PDMS saliva sampler

A titanium cylinder (6 mm long, 2 mm o.d. C-SPTD5-6MM Markes International Ltd) coated on the internal and external surfaces with polydimethylsiloxane (internal wall thickness 1 μm and external wall thickness 0.5 mm) was used to recover VOCs from the saliva. This approach has been described previously for the in-vivo sampling of Saliva VOCs [13]. The saliva sampler was prepared by cleaning with Milton® sterilising liquid (Suffolk, UK) and then rinsing with deionised water before conditioning under vacuum at 190 °C for 15 hr. Once conditioned the PDMS rods were inserted into a cleaned and conditioned glass thermal desorption tube and thermally desorbed for 10 min at 190 °C; the resultant GC-MS trace provided verification that the PDMS sampling media was free of contamination. On removal from the thermal desorption unit the thermal desorption tube containing the PDMS coated titanium cylinder was immediately capped, sealed and stored at 4 °C. Before use the saliva-samplers were thermally desorbed again under the conditions in **Table 3** to remove any traces of possible VOC contamination that may have occurred during storage and to provide further verification that the sampler was free of contamination.

2.3. Instrumentation

Two instrument configurations were used in this study. Method development and calibration were undertaken using liquid injections to a GC-DMS. Characterisation of the recovery of the analytes from spiked saliva samples was undertaken using a thermal desorption unit interfaced to the GC-MS (**Figure 1**). Multi-linear regression was used to optimise the differential mobility spectrometer operating parameters of: dispersion-field; temperature; number of compensation-field steps; and compensation-field step duration (DOE PRO XL Software for Microsoft Excel, SigmaZone). Data were generated from a central composite design (CCD) with each of the 4 factors at 4 levels with replicates at five different concentrations; **see Table 2** [15]. The DMS parameters were optimised for maximum sensitivity while

maintaining "satisfactory" resolution between the ion clusters generated within the ^{63}Ni ionisation source see **Table 3**, and **Figures 2**, **3** and **4**.

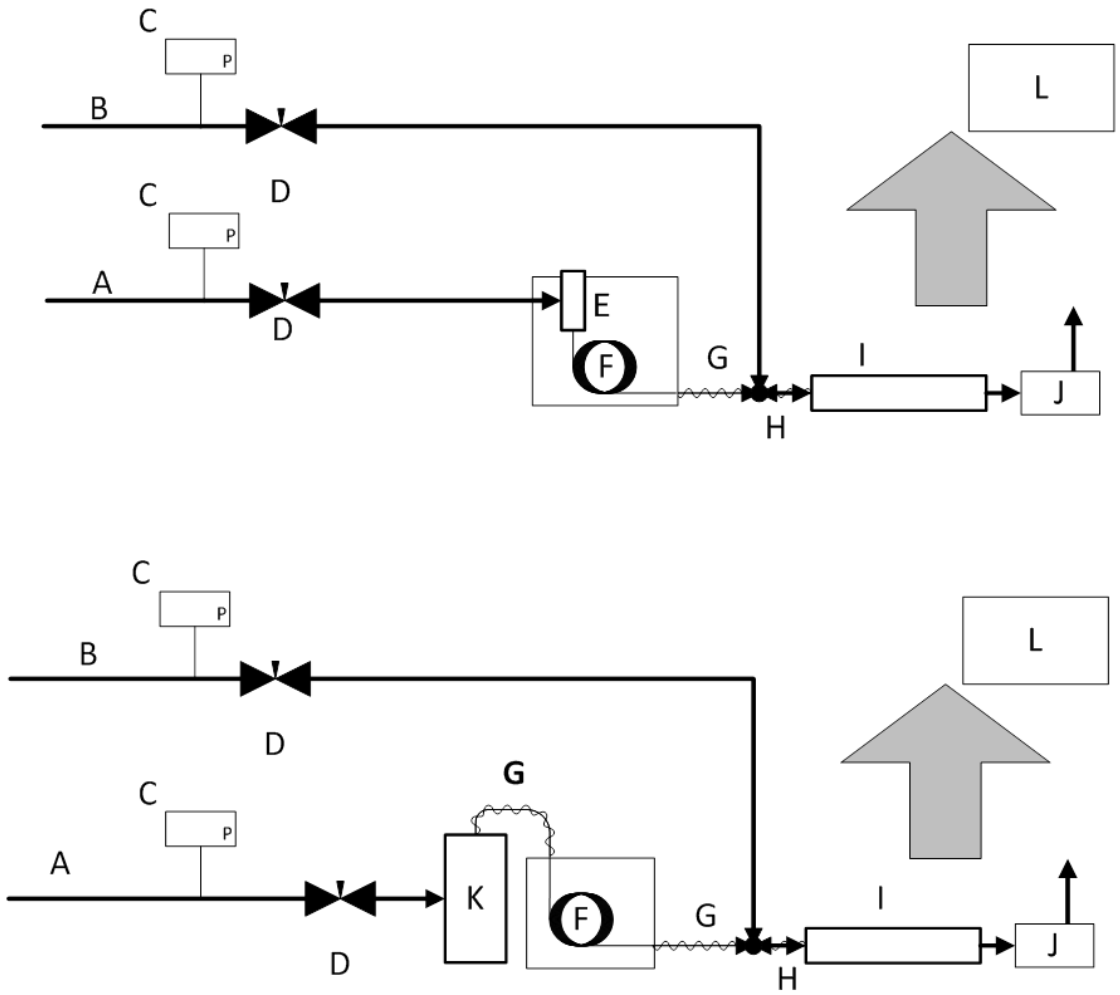

Fig. 1. Schematic diagrams of the liquid injection and thermal desorption instrumental configurations used in this work.

A, purified He supply; B, Nitrogen supply; C, Pressure gauge; D, flow control; E, split injection; F; gas chromatograph; G, heated transfer lines; H, sheath-flow inlet, I, differential mobility spectrometer; J, molecular sieve trap for exhaust gasses; K, thermal desorption unit; and L, data acquisition and processing.

Calibration of the DMS under optimised conditions was undertaken using gas chromatography to introduce known on-column masses of the analytes injected in a solution of dichloromethane, **Figure 1** and **Table 3**. A

30 m long wall-coated open-tubular capillary GC column with an internal diameter of 0.32 mm and a 0.5 µm thick trifluoropropylmethylpolysiloxane stationary phase (Rtx-200MS, Restek, UK) was interfaced to a DMS with a heated transfer-line configured as a sheath flow interface [16] made from a 20 cm length of ¼" stainless steel tubing with the GC-column axially aligned within the tube. The transfer-line was heat-traced with heating tape and maintained at 100 °C.

Table 2. Top: DMS factor levels selected for response optimisation study. Bottom operational parameters selected (predicted from multiple linear regression).

E_d/kV.cm^{-1}	T/℃	N	δt/ms	Ref	E_d/kV.cm^{-1}	T/℃	N	δt/ms
20	80	50	10	14	25	120	50	50
20	80	50	50	15	25	120	100	10
20	80	100	10	16	25	120	100	50
20	80	100	50	17	22.5	100	75	30
20	120	50	10	18	22.5	100	75	30
20	120	50	50	19	20	100	75	30
20	120	100	10	20	25	100	75	30
20	120	100	50	21	22.5	80	75	30
25	80	50	10	22	22.5	120	75	30
25	80	50	50	23	22.5	100	50	30
25	80	100	10	24	22.5	100	100	30
25	80	100	50	25	22.5	100	75	10
25	120	50	10	26	22.5	100	75	50

Compound	E_d/kV.cm^{-1}	T/℃	N	δt/ms
Methanol	25	100 (108)	110 (60)	10 (48)
Ethanol	18	100 (80)	110 (60)	10 (50)
Ethylene glycol	23	100 (100)	110 (75)	10 (10)
Propylene glycol	23	100 (120)	110 (75)	10 (30)
GHB	21	100	110	10

E_d is the dispersion field (Some instruments use the term Radiofrequency Voltage.); T is the gas temperature within the ion filter, sometimes referred to as "cell" temperature; N is the number of steps in the differential mobility compensation field scan (defining the fidelity of the spectral features); and, δt is the dwell time for each step in the compensation field scan (defining the sensitivity of the response). The combination of N and δt defines the chromatographic performance of the system.

The heating and cooling rates of the DMS cell were too slow to enable multiple levels to be selected within a single chromatographic run. Further, switching the number of steps and step duration in the DMS spectra during a chromatographic run was not possible. Consequently mid-range levels were used.

Table 2. Instrument parameters.

Parameter	GC-DMS	TD-GC-DMS	Units
Gas chromatograph conditions			
Carrier gas	He	He	
Injection temperature	200		°C
Split flow	10.2	see below	$cm^3.min^{-1}$
Carrier gas flow	1.5	1.5	$cm^3.min^{-1}$
Carrier gas pressure	172	172	kPa
Phase	trifluoropropylmethylpolysiloxane		
Column length	30	30	m
Column diameter	0.32	0.32	mm
Phase thickness	0.5	0.5	µm
Temperature start	30	30	°C
Hold-time start	1.5	1.5	min
Temperature ramp-1	6	6	°C. min^{-1}
End temperature-1	60	60	°C
Hold-time-1	2	2	min
Temperature ramp-2	20	20	°C. min^{-1}
Temperature final	180	180	°C
Hold time final	2	10	min
Differential mobility spectrometry			
Transport gas	N_2	N_2	
Dispersion field frequency	1.2	1.2	MHz
Dispersion field mark space ratio	1:3	1:3	
[H2O] in transport gas	22.5 to 26.3	22.5 to 26.3	$mg.m^{-3}$
Transport gas flow rate	300	300	$cm^3.min^{-1}$
DMS cell temperature	100	100	°C
Compensation field scan range	-500 to 100	-500 to 100	$V.cm^{-1}$
Compensation field scan increment	109.1	109.1	$V.cm^{-1}$
Compensation field scan dwell-time	10	10	ms
Dispersion field start	25	25	$kV.cm^{-1}$
Dispersion field start hold time	0 to 125	0 to 125	s
Dispersion field step-1	18	18	$kV.cm^{-1}$
Dispersion field step-1 hold time	125 to 185	125 to 185	s
Dispersion field step-2	23	23	$kV.cm^{-1}$
Dispersion field step-2 hold time.	185 to 600	185 to 600	min
Thermal Desorption			
Tube purge duration		1	min
Tube purge flow		32	$cm^3.min^{-1}$
Tube purge temperature		35	°C
Primary desorption temperature		180	°C
Primary desorption split		0	$cm^3.min^{-1}$
Primary desorption time		5	min
Cold trap low temperature		0	°C
Secondary desorption temperature		300	°C
Secondary desorption split		12	$cm^3.min^{-1}$
Secondary desorption time		5	min

The DMS used in the study was a planar device (SDP-1 Sionex, MS USA) with a 0.5 mm gap between the two parallel electrodes and a 5.9 MBq ^{63}Ni ionisation source. The DMS was controlled through a virtual instrument (Sionex DMx Expert, Version 2.4.0) run on the Dell laptop (Inspiron, 4000). The data were saved to a Microsoft Excel spreadsheet file for post-run processing. The transport gas was purified nitrogen with water concentrations maintained in the range 22.5 to 26.3 $mg.m^{-3}$ (Panametrics Series 35 hygrometer).

A two-stage thermal desorption unit (Markes International Unity 2,) was used to recover VOC extracts from saliva samples with a cold trap for refocusing the recovered VOCs packed with a mixed bed of Tenax TA and Carbograph 1TD. The 1.5 m long transfer line to the GC-column was a deactivated methyl-capped capillary column (Restek, UK) with an internal diameter of 0.23 mm i.d. maintained at 110°C).

2.4. Characterisation of spiked saliva samples

The concentration ranges used in this study are summarised in **Table 4**. A 100 $mg.cm^{-3}$ aqueous stock solution of ethanol, methanol, ethylene glycol, and propylene glycol was prepared and aliquots of the volumes required to generate the required concentrations were spiked into the saliva samples within three hours of the saliva being collected. To account for the lower concentration of the GHB standard, and to maintain a constant saliva background in the GHB characterisation experiments a different approach was adopted. Here 0.9 cm^3 of the saliva was used, and spiked with the required aliquot volume of the 1 mg. cm^{-3} GHB methanolic solution, before the volume was made up to 1.8 cm^3 with physiological saline ($NaCl_{(aq)}$ 8.5 $g.dm^{-3}$). The ammonia present in the saliva and the GHB salt co-eluted with methanol and suppressed the formation of methanolic product ions (ammonia has a higher proton affinity than methanol). This interference was eliminated by the addition of 150 µL of 8 % HCL solution into the saliva samples before the sampling rod was placed into the vial.

Once the analytes had been added the saliva standards were homogenised. Immediately this had been done a PDMS coated titanium cartridge was removed from its sealed thermal desorption tube and placed into the vial, which was then sealed immediately. It was important that this procedure was undertaken in a fast and reproducible manner to minimise the effects of evaporative losses in the study. The sealed vial was then placed into a heating-block, maintained at 37 °C for 10 minutes. At the end of the extraction-time the vial was uncapped and the PDMS coated titanium cartridge was removed with stainless steel tweezers and excess fluid removed by gently wiping it with a lint-free wipe ('Kimcare' Kimberly-Clark Professional, UK). The PDMS coated titanium cartridge was then placed immediately into its glass thermal desorption tube and analysed. Cross-contamination checks were run by taking blank runs between every measurement.

3. Results and discussion

3.1 Evaluation of responses

Figure 2 shows the GC-DMS response surfaces from methanol (A), ethanol (B), ethylene glycol (C), propylene glycol (D) and GHB (E) at three levels of column-loading that span the ranges of analyte concentrations associated with the physiological thresholds of these compounds. The four dispersion-field levels used (**Table 3**) enabled analytical responses to be resolved.

Figure 3 shows background subtracted differential mobility spectra obtained from the responses shown in **Figure 2** for methanol (A), ethanol (B) and ethylene glycol (C), while **Figure 4** compares the responses for propylene glycol (D) and GHB (E). The dotted lines in these figures indicate the boundary of the reactant ion peak that was removed by the background subtraction in the data processing.

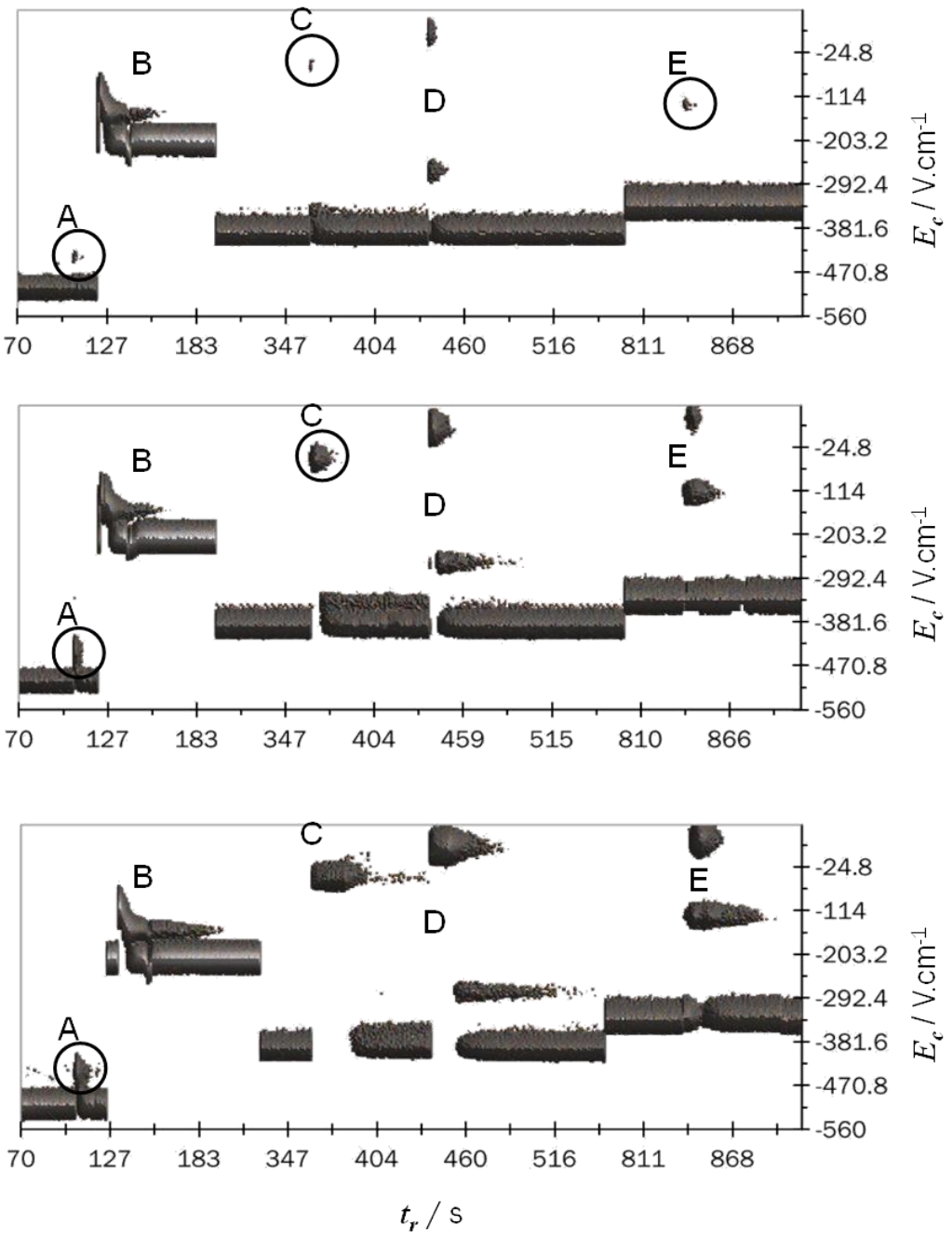

Fig. 2. GC-DMS response surfaces from methanol (A), ethanol (B), ethylene glycol (C), propylene glycol (D) and GHB (E) under optimized conditions at representative sample masses. Note the shifting position of the reactant ion peak as the dispersion field was switched. Top: responses produced from 200 pg , 5.1 ng, 2.9 ng, 2.7 ng and 510 pg of methanol, ethanol, ethylene glycol, propylene glycol and GHB respectively. Similarly the middle surface shows responses for 2.0 ng, 15.3 ng, 14.3 ng, 13.4 ng and 1.9 ng, while the bottom trace shows responses for 10.2 ng, 40.7 ng , 81 ng, 80.4 ng, 12.9 ng

The observed responses were complicated with shifts in compensation-field maxima with increasing concentration, and the generation of features embedded within the reactant ion peak that were only discernible after background subtraction. Such phenomena were indicative of the formation of fragment ions and, or, "auto-modification" of the alpha functions of the product ion.

With a dispersion-field of 25 $kV.cm^{-1}$ and a column-loading of 10.2 ng, methanol yielded two peaks attributed to a hydrated protonated monomer cluster ion at a compensation-field of -511 $V.cm^{-1}$, that was obscured within the reactant ion peak, and a hydrated proton-bound dimer ion at -439.6 $V.cm^{-1}$. Reducing the column-loading to 2.0 ng resulted in a compensation-field shift for the hydrated protonated monomer cluster ion to -502 $V.cm^{-1}$ accompanied by a hydrated proton-bound dimer response at between–444 $cm.V^{-1}$ and -439.6 $V.cm^{-1}$.

At a lower limit of a 200 pg column-loading, only one peak was observed at -439.6 $V.cm^{-1}$. These observations are consistent with an increase in the alpha-function [17] of a hydrated protonated methanol cluster ion with increasing methanol concentration [18] (modification of the transport gas) accompanied by the formation of a proton-bound dimer with increasing methanol concentration; albeit observed at the same compensation-field as the unmodified hydrated protonated monomer cluster ion response observed at concentrations below the threshold at which proton-bound dimers form.

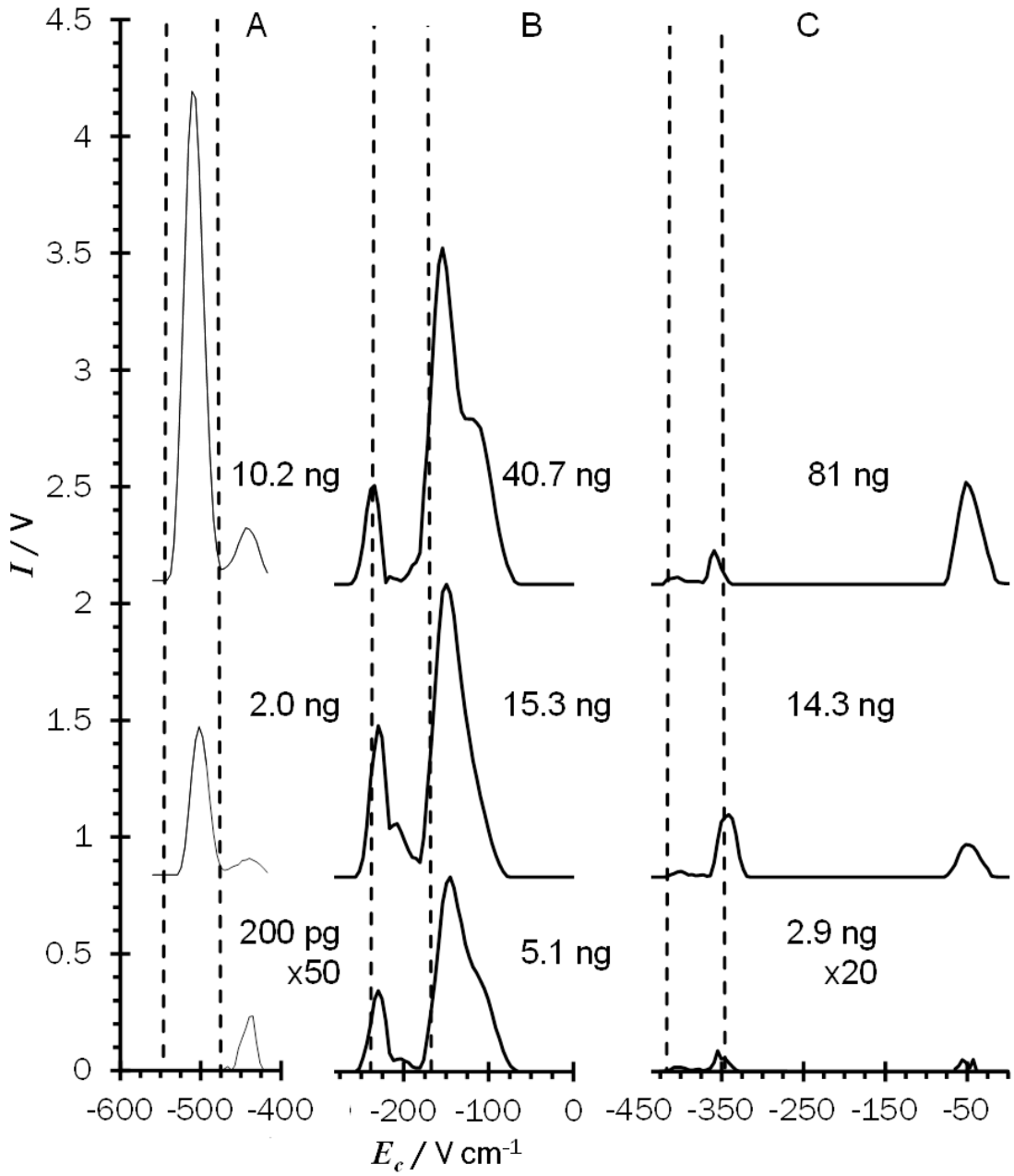

Fig. 3. Background subtracted differential mobility spectra extracted from the GC-DMS response surface shown in **Figure 2** for methanol (A), ethanol (B), ethylene glycol (C) (under optimized conditions at representative sample masses. The dotted lines indicate the position of the reactant ion peak in the spectrum (hydrated proton clusters).

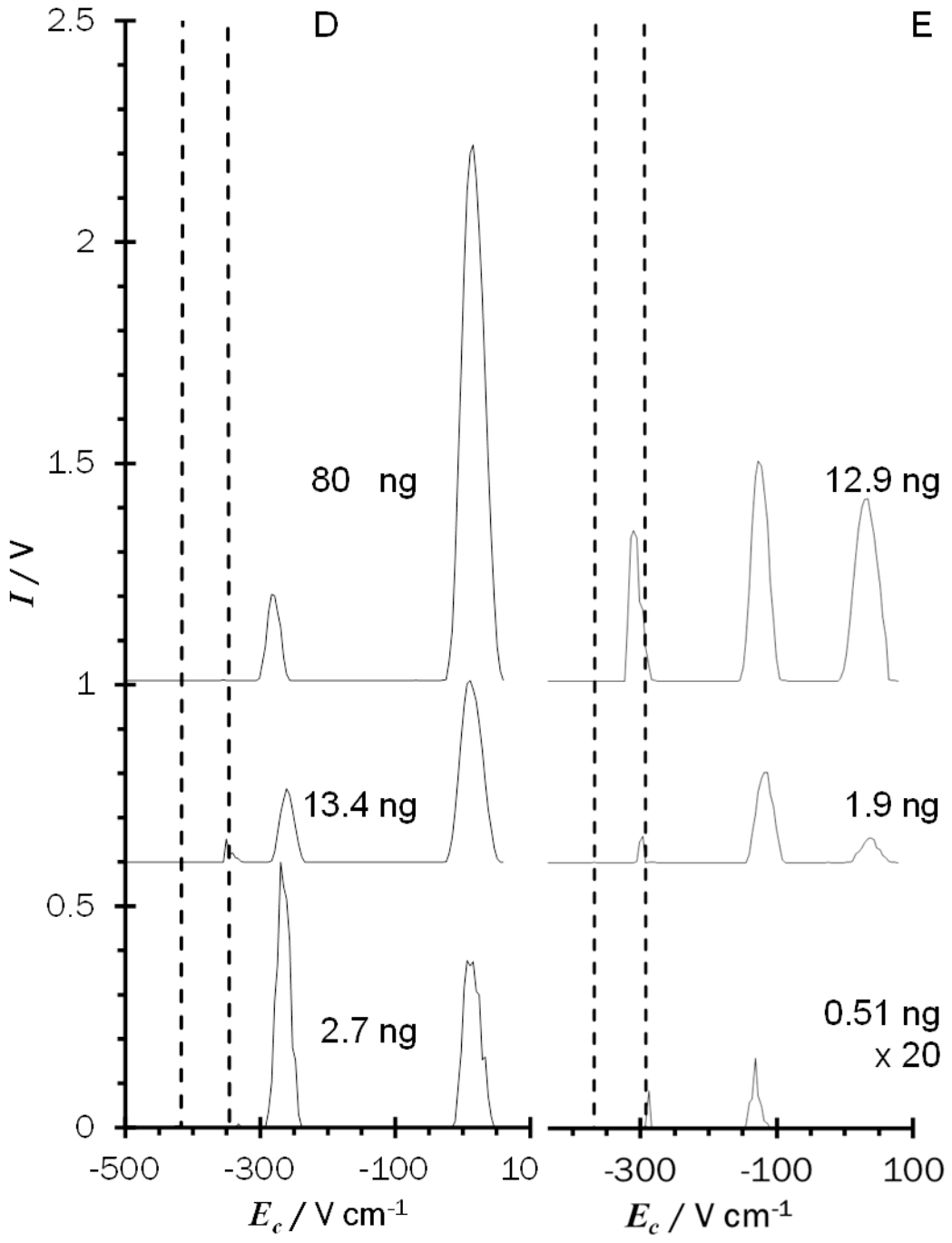

Fig. 4. Background subtracted differential mobility spectra extracted from the GC-DMS response surface shown in **Figure 2** for propylene glycol (D) and GHB (E) under optimized conditions at representative sample masses. The dotted lines indicate the position of the reactant ion peak in the spectrum (hydrated proton clusters).

At a dispersion-field of (18 $kV.cm^{-1}$) ethanol also yielded a complicated response with features consistent with the generation of fragment ions overlaid with unresolved hydrated protonated monomer cluster ions, and hydrated proton-bound cluster ions, observed to fall at approximately -154.2 $V.cm^{-1}$ for the hydrated protonated monomer cluster-ion and -122.8 $V.cm^{-1}$ for the proton-bound dimer cluster ion. Two features attributed to fragment ions were observed to be obscured within the reactant ion peak. One was at a compensation-field of -238 $V.cm^{-1}$ at a column-loading 40.7 ng and -230 $V.cm^{-1}$ at column-loadings of 15.3 ng and 5.1 ng. The other was present at -216.6 $V.cm^{-1}$ at 40.7 ng, shifting to -207.6$V.cm^{-1}$ at 15.3 ng and 5.1 ng.

At a dispersion-field of 22 $kV.cm^{-1}$ ethylene glycol produced a clearly resolved feature at -51.6 $V.cm^{-1}$, attributed to a proton-bound dimer cluster ion, along with two features obscured by the reactant ion peak. The weakest of these features, completely obscured by the reactant ion peak was observed at a compensation-field of -403.8 $V.cm^{-1}$ across the range of column-loadings with no indication of auto-modification observed. However, the other feature, partially obscured by the reactant ion peak, was observed to shift from a compensation-field of -359.2 $V.cm^{-1}$, with a column-loading of 81 ng, to -337 $V.cm^{-1}$ with a column loading of 14.3 ng. The lowest column loading applied generated a low intensity split peak that straddled -337.4 $V.cm^{-1}$. At the same dispersion-field (22 $kV.cm^{-1}$) propylene glycol yielded two features, both resolved from the reactant ion peak. The peak at a compensation-field of 15.4 $V.cm^{-1}$ was attributed to a proton bound dimer ion cluster. The feature attributed to a hydrated monomer-ion cluster was observed to shift to more negative compensation-fields with increasing column-loading. At 80 ng the peak maximum was at a compensation-field of -283.4 $V.cm^{-1}$, shifting to -261.2 $V.cm^{-1}$ when the column-loading was reduced to 2.7 ng.

GHB also showed complex behaviour with a dispersion-field of 23 $kV.cm^{-1}$. In addition to well-resolved hydrated protonated monomer cluster ions and proton-bound dimer cluster ions, fragment ions obscured within

the RIP envelope were also evident, and the compensation-field maxima of these fragment ions shifted with increasing column-loading of GHB. Hydrated protonated monomer cluster ions had a compensation field peak maximum at –131.8 $V.cm^{-1}$ and the proton-bound dimer compensation-field maxima was observed at 33.2 $V.cm^{-1}$. No discernible trend in a shift in compensation-field maxima was observed with column loading for the hydrated protonated monomer cluster ion, and the proton-bound dimer was not formed at the lowest column loading of 510 pg. At a column loading of 12.9 ng two unresolved fragment ions were discernible within the RIP envelope. The most intense feature was at 310.2 $V.cm^{-1}$ with a shoulder at -296.8 $V.cm^{-1}$. Reducing the column loading to 1.9 ng resulted in a single fragment ion with a compensation-field peak maximum at -301.2 $V.cm^{-1}$ and at a column loading of 510 pg the fragment ion was still observable with a compensation-field peak maximum of -288 $V.cm^{-1}$.

Despite the complexity of the responses it was possible to generate well resolved and analytically useful chromatographic peaks, see **Figure 5**. The chromatograms for ethylene glycol, 1,3-propandiol and GHB were generated by integration of the differential mobility spectra across the proton-bound dimer ion features and the hydrated protonated monomer responses, and these are shown as discrete traces in **Figure 5** overlaid with the summed chromatographic response, for ethanol and methanol the chromatograms were generated by integration of the complicated features that contained hydrated protonated monomers and proton-bound dimer ions. **Figure 5** shows the intensities of the peaks reflecting the differences in the ionisation efficiencies as well as the column-loadings of the five compounds. Of particular note was the behaviour of ethylene glycol with a peak shape that indicated a saturated response with significantly lower sensitivity compared to the other four compounds.

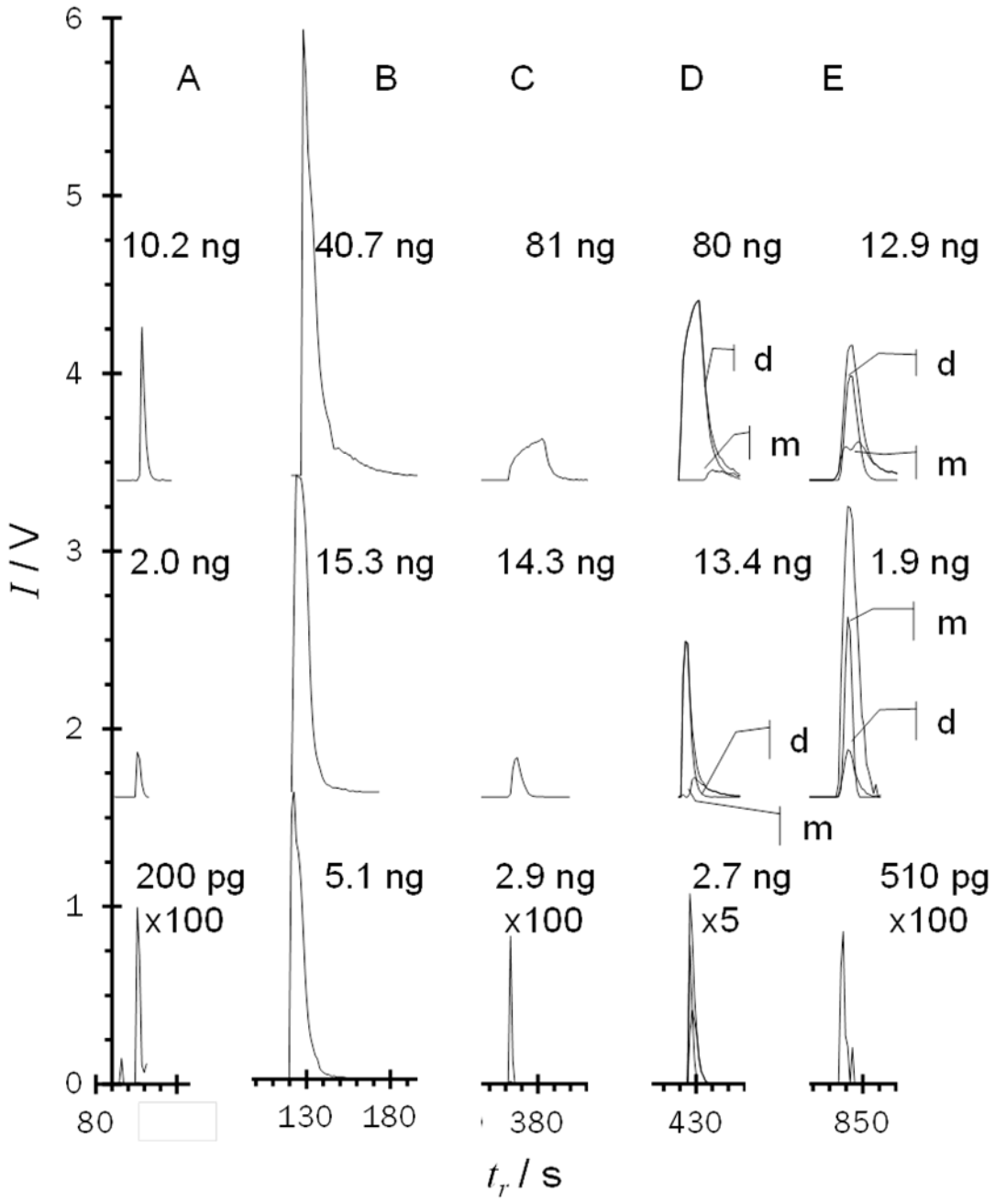

Fig. 5. Selected differential mobility chromatography for methanol (A), ethanol (B), ethylene glycol (C), propylene glycol (D) and GHB (E) under optimized conditions at representative sample masses. Protonated monomer (m) and proton bound dimer (d) responses are shown for propylene glycol and GHB as well as the total ion responses, see **Figures 2** and **4**. The responses shown for methanol, ethanol and ethylene glycol are the total ion responses, see **Figure 3**.

3.2. Calibration

Calibration of the differential mobility spectrometer was based on the peak volumes for the proton-bound dimer ion responses for the two glycols and GHB. The ethanol calibration was based on the integration of the complicated feature containing unresolved hydrated protonated monomers ion clusters and proton-bound dimer ions while the methanol calibration peak volume was taken from the proton-bound dimer ion response and at low concentrations the hydrated-protonated monomer cluster ion with the same value for the compensation-field maximum. **Table 4** summarises the calibration parameters data.

Table 4. Summary of the concentration ranges selected for the calibration of the DMS ([i](liq)) and the subsequent aliquot volumes (V(S)) and the concentrations of the spiked saliva standards [i](s) used to characterise the recovery of the analytes from by TD-GC-IMS.

Compound	$[i]_{(liq)}$ / mg.dm^{-3}	B_0 / V.s	B_1/V.s.ng^{-1}	LoD*/ng	R^2
Methanol	10 to 250	-0.02	0.27	0.42	0.994
Ethanol	250 to 1000	-8.22	0.28	4.62	0.983
Ethylene glycol	100 to 500	-0.02	0.27	0.52	0.994
Propylene glycol	100 to 500	-0.48	0.30	1.42	0.997
GHB	20 to 500	-0.18	0.31	0.63	0.995

Note: these ranges relate to the linear portion of the calibration range where the integrated peak volume (I) was given by:

$$I(\mathrm{V.s}) = B_0(\mathrm{V.s}) + B_1(\mathrm{V.s.ng^{-1}})$$

*, estimated from linear regression.

3.3. Saliva analysis

The responses obtained from saliva spiked with a range of concentrations of the analytes are summarised in **Figure 6** and **Figure 7**. The chromatography contained substantial numbers of recovered compounds from the saliva sample, nevertheless it was possible to identify the analytes reliably based on their compensation field and retention times.

The intensities of the responses observed reflected the combined interactions of: the adsorption/absorption behaviour of the analytes onto/into the PDMS sampler medium; the product ion dynamics noted above of the five compounds; and interactions with the saliva matrix. Matrix interactions in drooled saliva are problematic in that microbiological activity and stability of the analytes are likely to be related to the analyte's concentration and will have a time dependent element. Further the physical chemical properties of the saliva may also vary between samples. The previous study with this sampler contrasted the responses obtained from drooled saliva samples against those obtained by sampling directly in the mouth, under the tongue next to the salivary glands. Sampling in the mouth was found to be more sensitive and more reproducible than adopting a passive drool approach. Further, obtaining a passive drool sample requires significantly more patient/participant training and compliance than placing a small rod under their tongue and as such is likely to be a more practical approach to working with patients/participants who may have analytes at levels high enough to be a cause of concern for their safety and welfare [13]. Nevertheless the adoption of a passive drooled-saliva approach enabled a matrix that approximated the intended sampling conditions to be acquired safely and practicably. Finally, the loss of the more volatile methanol and ethanol to the saliva headspace and hence from the experiment also needs to be acknowledged as a methodological weakness.

The fragmentation behaviour observed during the method development stage with liquid injections was not observed in the saliva studies. The presence of other closely eluting components within the chromatogram made background subtraction problematic and subsequently it was not possible to investigate fragment ion artefacts with confidence. The on-column masses of methanol recovered were estimated to fall in the range 350 pg to 3 ng over the range 100 $mg.dm^{-3}$ to 2 $g.dm^{-3}$, and similarly for ethanol the on-column masses were estimated to fall in the range 29 ng to 42ng. Recoveries for ethylene glycol fell were lower with up to 7 ng obtained at high saliva loadings of 3 $g.dm^{-3}$, contrasted with propylene glycol recoveries of up to 22 ng at the same level. GHB was the most

efficiently recovered from saliva with 10 ng recovered at 100 mg.dm^{-3} increasing to an estimated on-column mass of 34 ng at 400 mg.dm^{-3}.

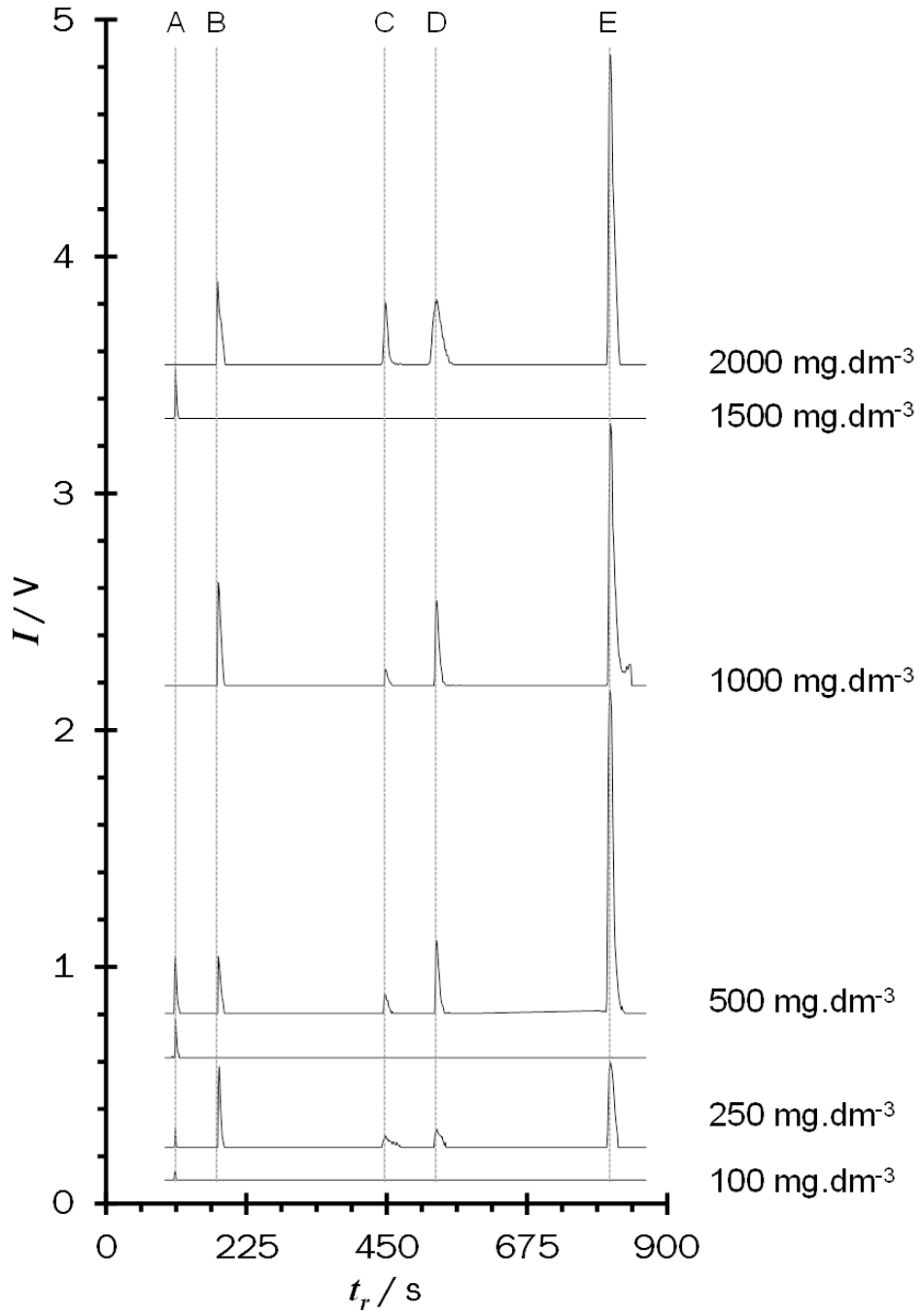

Fig. 6. Selective compensation field gas chromatographic traces obtained by thermal desorption gas chromatography differential mobility spectrometry for the five analytes at the concentration ranges studied. See Table 3 for the instrumentation parameters. Note that the chromatography has been aligned during post-processing.

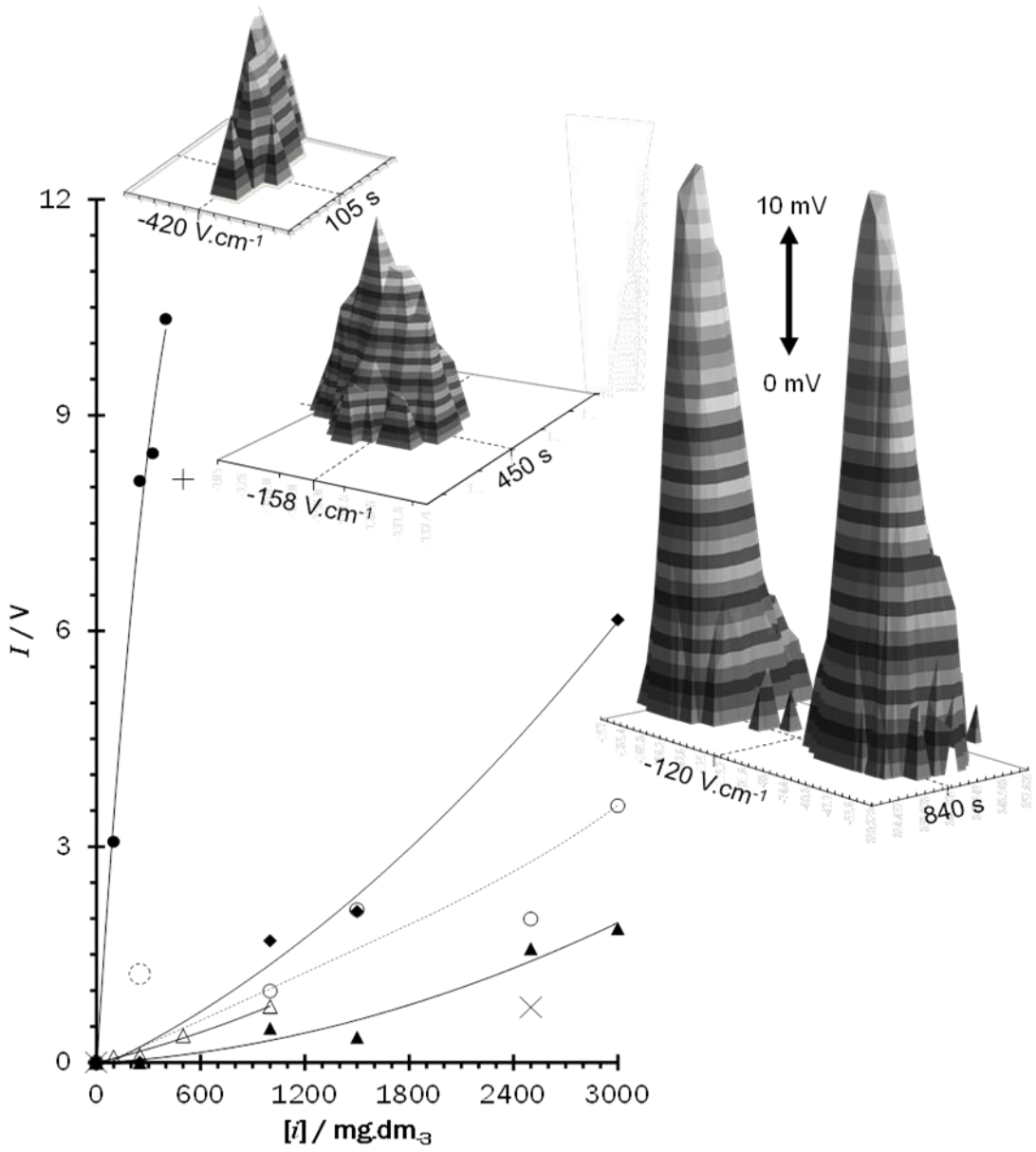

Fig. 7. Integrated responses for a range of spiked saliva concentrations for methanol (open triangles), ethanol (open circles), ethylene glycol (solid triangles), propylene glycol (solid diamonds) and GHB (solid circles). Three outliers are shown. A Dotted circle, cross and plus symbols for outliers observed with ethanol, 1,3-propandiol and GHB respectively. See text for details of signal features used for calibration.

The three inserts are extracted signals for analytes of most concern with respect to toxicity: top, methanol at 100 mg.dm^{-3}; middle, the monomer signal for ethylene glycol at 250 mg.dm^{-3}; and bottom, the monomer and proton bound dimer signals for GHB at 250 mg.dm^{-3}.

4. Conclusion

This pilot study demonstrates the effective recovery, detection and semi-quantitative estimation of all the analytes of interest to this work. This represents a potentially useful methodological advance in the rapid assessment of alcohol toxicity and embodied within a TD-GC-DMS or a TD-GC-IMS for it provides a fieldable approach for a rapid screen and evaluation protocol for alcohols present at toxic levels from a single non-invasive sample. This has not been possible previously and has the potential for the development of point-of-care toxicity assessment in emergency room settings. Indeed this study, in concert with others, is developing the concept of extending volatile biomarker measurement from breath to a range of excretory routes. There are instances when breath sampling might be problematic (a propensity for an inebriated patient to vomit for instance) and as such skin and saliva offer alternative routes and techniques for studying and exploiting the tissue/blood/breath-skin-saliva excretion mechanics for non-invasive diagnostics [19].

The apparently simplicity of the analytes belies significant complexity in the ion chemistries associated with their detection using ambient ionisation or radioactive ionisation approaches. Earlier mass spectrometric studies with alcohols have identified the formation of fragment ions associated with proton transfer ionisation approaches [20, 21 and 22]. The presence of signals due to product ion fragmentation would not appear to be without precedent. The alcohol product ions, and their fragment ions, are highly mobile and therefore are associated closely with the water-based reactant ion signals. Increasing resolution between the reactant ion signal and analyte signals by increasing the dispersion field strength has the combined effect of reducing the analytical sensitivity by reducing the analytical area of the ion filter while at the same time promoting fragmentation reactions [23 and 24]. The possible ion fragmentation of GHB has not been reported previously.

Compensation field maximum shifts attributable to the auto-modification of the transport gas by analyte neutrals was also observed and

this is an area that will require further investigation to characterise it completely.

The study of fragmentation mechanisms, products and their ramifications for alcohol determination by differential mobility spectrometry along with the development of detection and signal processing algorithms to enable peak-shift from auto-modification of the differential mobility transport gas to be handled efficiently are logical next steps in the development of this area. In parallel to such a study will be the refinement of the methodology to reduce the chromatographic run time to less than 300 s, and the continued development of the sampling approach to reduce the sampling time so that a total analytical run time of 600s might be achieved. This would to enable the delivery of a clinical pilot study within an appropriate poisons unit to assess the efficacy of this approach in patients, benchmarked to current gold-standard toxicity screens.

Acknowledgement

The Authors wish to thank the Spanish Ministry of Education, Culture and Sport for the pre-doctoral grant (AP 2009-3528) for the support of L. Criado-García and the Engineering and Physical Science Research Council alongside John Hoggs Technical Solutions for the support of D.M. Ruszkiewicz through an Industrial Case Studentship Award. The authors also acknowledge and thank the volunteers who participated in this research.

References

[1] Zhang G. Crews K. Wiseman H. Bates N. Hovda K.E. Archer J.R.H. and Dargan P. I. 2012 Application to Include Fomepizole on the WHO Model List of Essential Medicines URL: http://www.who.int/selection_medicines/committees/expert/19/applications/Fomepizole_4_2_AC_Ad.pdf, visited 21 September 2015.

[2] BBC News 2015 India alcohol poisoning: Mumbai death toll tops 100, URL: http://www.bbc.co.uk/news/world-asia-india-33224514, visited 21 September 2015.

[3] Heberlein A. Lenz B. Degner D. Hornhuber J. Hillemacher T. and Bleich S. 2009 Methanol Levels in Saliva—A Non-Invasive Parameter That May Be Useful in Detection of Alcohol Intoxication. Alcohol and alcoholism **45** 126-127.

[4] Rezgui N.D. Kanu A.B. Waters K.E. Grant B.M.B. Reader A.J. and Thomas C.L.P. 2005 Separation and preconcentration phenomena in internally heated poly(dimethylsilicone) capillaries: preliminary modelling and demonstration studies Analyst, **130** 755-762.

[5] Kanu A.B and Thomas C.L.P. 2006 The presumptive detection of benzene in water in the presence of phenol with an active membrane-UV ionisation differential mobility spectrometer Analyst **131** 990-999.

[6] Bocos-Bintintan V. Moll V.H. Flanagan R. J. and Thomas C. L. P. 2010 Rapid determination of alcohols in human saliva by gas chromatography differential mobility spectrometry following selective membrane extraction Int. J. Ion Mob. Spec. **13** 55-63.

[7] Verstraete, A. 2004 Detection Times of Drugs of Abuse in Blood, Urine and Oral Fluid. Ther. Drug. Monit. **26** 200-205.

[8] Mergen G. Kayaalti Z. Dural E. Aliyev V. Kaya S. Yalcin S. Karakus A. and Soylemezoglu T. 2011 Simultaneous Headspace-GC-FID Analysis for Methanol and Ethanol in Blood Saliva and Urine: Validation of Method and Comparison of Specimens LC GC EUROPE **24** 292-297.

[9] Jones A.W. 1993 Pharmacokinetics of ethanol in Saliva: Comparison with Blood and Breath Alcohol Profiles, Subjective Feelings of Intoxication, and Diminished Performance. Clin. Chem. **39** 1837-1844.

[10] Finkelstein Y. and Vardi J. 2002 Progressive parkinsonism in a young experimental physicist following long-term exposure to methanol Neurotoxicology **23** 521-525.

[11] Flanagan R. J. Braithwaite R. A. Brown S. S. Widdop B. and de Wolff F. A. 1995 The International Programme on Chemical Safety: Basic Analytical Toxicology Publ. World Health Organisation Geneva.

[12] Zvosec D.L. Smith S.W. Porrata T. Strobl A.Q. and Dyer J.E. 2011 Case series of 226 γ-hydroxybutyrate-associated deaths: lethal toxicity and trauma Am. J. Emerg. Med. **29** 319–332.

[13] Martin H. J. Riazanskaia S. and Thomas C. L. P. 2012 Sampling and characterisation of volatile organic compound profiles in human saliva using a polydimethylsiloxane coupon placed within the oral cavity Analyst **137** 3627-3634.

[14] Limero T. Reese E. Wallace W.T Cheng P. and Trowbridge J. 2012 Results from the air quality monitor (gas chromatograph-differential mobility spectrometer) experiment on board the international space station Int. J. Ion Mobil. Spec. **15** 189–198.

[15] Ali Awan M. Fleet I. and Thomas C. L. P. 2008 Optimising cell-temperature and dispersion-field strength for the screening for putrescine and cadaverine with thermal desorption gas chromatography differential mobility spectrometry Anal. Chim. Acta **611** 226-232.

[16] Young D. Thomas C. L. P. Breech J. Brittain A. H. and Eiceman G. A. 1999 Extending the concentration and linear dynamic range of ion mobility spectrometry with a sheath flow inlet Anal. Chim. Acta **381** 69-83.

[17] Eiceman G. A. Krylov E. V. Tadjikov Ewing R. G. Nazarov E. G. and Miller R. A. 2004 Differential mobility spectrometry of

chlorocarbons with a micro-fabricated drift tube Analyst **129** 297–304.

[18] Schneider B. B. Nazarov E. G. and Cove T. R. 2012 Peak capacity in differential mobility spectrometry: effects of transport gas and gas modifiers Int. J. Ion Mobil. Spec. **15** 141–150.

[19] Friedman L. Long F.A. and Wolfsberg M. 1957 Study of Mass Spectra of Lower Aliphatic Alcohols J. Chem. Phys. **27** 613–622.

[20] Smith S.C. McEwan M.J. Giles K. Smith D. Adams N.G. 1990 Unimolecular decomposition of a polyatomic ion a variable temperature selected ion flow drift tube: experiment and theoretical interpretation. Int. J. Mass Spectrom. and Ion Process. **96** 77-96.

[21] Karpas Z. Eiceman G.A. Ewing R.G. Harden C.S. 1994 Collision induced dissociation studies of protonated alcohol and alcohol-water clusters by atmospheric pressure ionization tandem mass spectrometry. Part 2. Ethanol, propanol and butanol Int. J. Mass Spectrom. and Ion Process. **133** 47-58.

[22] Eiceman G.A. Karpas Z. Hill H.H. 2013 Ion mobility spectrometry 3rd Ed. Publ. CRC Press ISBN 9781439859971.

[23] Shvartsburg A. 2008 Differential Ion Mobility Spectrometry Publ. CRC Press ISBN 9781420051063

[24] Shvartsburg A. 2008 Differential Ion Mobility Spectrometry Publ. CRC Press ISBN 9781420051063

Chapter 8

Micro-solid phase extraction and IMS as an approach to determine toxic compounds in saliva samples

Capítulo 8

La extracción en fase micro-sólida como aproximación para determinar compuestos tóxicos en muestras de saliva

In progress

EXTRACTION OF TOXIC COMPOUNDS FROM SALIVA BY MAGNETIC STIRRING ASSISTED MICRO-SOLID PHASE EXTRACTION STEP FOLLOWED BY HEADSPACE-GAS CHROMATOGRAPHY-ION MOBILITY SPECTROMETRY

L. Criado-García, L. Arce, M. Valcárcel*

Department of Analytical Chemistry. Annex C-3 Building. Campus of Rabanales. Institute of Fine Chemistry and Nanochemistry. University of Cordoba. 14071 Córdoba, Spain.

Saliva samples are an attractive alternative to blood and urine samples for profiling and screening human subjects due to the non-invasive nature and the accessibility of this sample. Ion mobility Spectrometry (IMS) is a sensitive technique which has been shown as a high selectivity technique for the determination of explosive and chemical agent and more recently it has been widely used in the clinical and biomedical field. Taking into account that it is always essential to provide fast and reliable responses to specific real problems in the clinical field, methods which offers these requirements are needed. In this work, a new method based on micro-solid phase extraction (μSPE) using a mixture of sorbents of different polarities (polymeric reversed-phase sorbent HLB, silica based sorbent C_{18} and multiwalled carbon nanotubes (MWCNTs)) was applied to extract benzene, toluene, butyraldehyde, benzaldehyde and tolualdehyde present in saliva to avoid the interferences from moisture and matrix components and enhance sensitivity and selectivity of the IMS methodology propose. The extraction of target analytes from saliva samples by using μSPE were followed by the desorption step carried out in a headspace vial in the autosampler. Then, 200 μL of headspace was injected into the GC column coupled to the IMS for its analysis. The method was fully validated in terms of sensitivity, precision and recovery. The LODs and LOQs were in the range of 0.27-0.38 and 0.91-1.66 μg mL^{-1}, respectively. The relative standard deviations were <3.5% for retention time and drift time values. The recovery values (79-

100%) indicate that the proposed method can be applied to determine toxic compounds in saliva samples.

Keywords: saliva, toxics compounds, micro-solid phase extraction, ion mobility spectrometry.

1. Introduction

Oral fluid or saliva is quite an interesting biological sample due to its non-invasive, easy, rapid and low-cost sampling [1]. Note that for many toxics and drugs a correlation between the blood and saliva concentration levels exist [2]. This fact opens the possibility of using saliva analysis to obtain bioanalytical information. As well, advantages that offer ion mobility spectrometry (IMS) technique such as high operational speed, sensitivity, simplicity, and portability [3] fit with the essence of a rapid diagnosis needed in the clinical field. The usefulness of IMS as a screening methodology for the on-site analysis of saliva has been critically demonstrated [4-6].

Although direct analysis of biological samples is possible in some cases [7], in most of the situations a previous sample treatment is required due to the complex biological matrices [8]. Ion mobility spectra for complex biological samples such as saliva typically consist of a number of signals and product ions [9] that can hinder the determination of target analytes. Besides, moisture introduced to the IMS coming from the sample can affect the ionization chemistry and producing changes in the spectra [10, 11]. A pretreatment based on solid-phase extraction, solid phase microextraction [12], hollow fiber microextraction [13], molecularly imprinted polymers [14, 15] or any other method that allow the isolation and the preconcentration of the target compounds thereby improving the selectivity and avoiding interferences of the matrix is needed. In this context, micro-solid phase microextraction (μSPE) is a new form of microextraction in a reduced packed sorbent [16]. Due to the porosity of the membrane sheet, analytes can diffuse through it [17] and be extracted by the sorbents. μSPE has been already used to extract drugs in oral fluids and analyzed by HPLC-MS [18]. The main advantage is that it can handle very complex matrices, but it generally suffers from relatively long extracting times [19]. To overcome this problem, vortex or magnetic stirring can be implemented to accelerate extraction step [20]. The development of new extraction procedures that

integrate extraction and stirring element in the same device [21] has demonstrated promising benefits as the one presented in this work. Nanomaterials such as carbon nanotubes and nanofibers have been widely used as sorbents for μSPE due to its high surface area that make them recommended for extraction purposes [22]. In this work, a combination of polymeric reversed-phase sorbent HLB, silica based sorbent C_{18} and multiwalled carbon nanotubes (MWCNTs) were used.

It is the first time that a mixture of these sorbents in a μSPE device has been used to extract these target analytes (benzene, toluene, butyraldehyde, benzaldehyde and tolualdehyde) in saliva samples from smokers and non-smokers as a model analytical problem. As well as, μSPE has not been used before in combination with IMS. These analytes were selected since they are included among 6000 substances which have been identified in cigarette smoke [23]. During tobacco smoking a large number of chemical compounds present in the mainstream are carcinogenic and also cause long-term toxics effects such as benzene and toluene [24]. Additives such as butyraldehyde, benzaldehyde and tolualdehyde are also added during the manufacturing process of cigarettes and can appear in the smoke. And finally is also important to taking into account that saliva is the fluid that is intimately in contact with the smoke swallowed during the smoking process before these compounds can be metabolized in other derivatives.

In summary, the aim of this work is to evaluate the potential of IMS within clinical analysis by using a home-made μSPE device to extract simultaneously toxic compounds of different nature that potentially can be present in saliva samples avoiding matrix and humidity interferences from the sample.

2. Experimental

2.1. Reagents and samples

Butyraldehyde, benzene, toluene, benzaldehyde and tolualdehyde were all purchased by Sigma-Aldrich (St. Louis, USA). Chemical information

is summarized in **Table 1**. Target analytes were prepared at 1 g L^{-1} in purified water by passage through a Milli-Q apparatus from Millipore (Bedford, MA, USA).

Table 1. Chemical information of target analytes used in this work.

Analyte	Molecular structure	Formula	MW (g mol^{-1})	Density (g cm^{-3})	Bp (ºC)	IE (eV)	PA (KJ mol^{-1})
Butyraldehyde	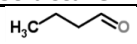	C_4H_8O	72.11	0.80	74.8	9.82	792.7
Benzene		C_6H_6	78.11	0.87	80.1	9.24	750.4
Toluene	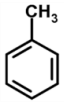	C_7H_8	92.14	0.86	110.8	8.83	784.0
Benzaldehyde		C_7H_6O	106.12	1.05	178.1	9.50	834.0
Tolualdehyde	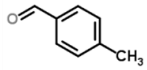	C_8H_8O	120.14	1.02	204	9.33	851.8

MW: molecular weight, Bp: boiling point, PA: proton affinity. PA of water is 691 KJ mol^{-1}.

These stock standard solutions were diluted with purified water or saliva to prepare mixed standards concentrations in the range of 0.1 µg mL^{-1} up to 5 µg mL^{-1}. Stock and working standard solutions were stored at 4 ºC in the refrigerator before analysis. Saliva samples were collected from 8 healthy individual and 8 smokers. Volunteers that participate in this research were not exposed to any chemical hazard(s) and were asked not ingest or drink anything apart from water 1 hour before giving the sample. Participants gave informed consent and were recruited from University of Cordoba staff, students and their social network. Samples were stored in the freezer at -18 ºC until it analysis.

2.2. Extraction procedure

The steps followed to build the packed sorbent or µSPE device consisting in an envelope with the sorbents for later perform the extraction of analytes in saliva are illustrated in **Figure 1**.

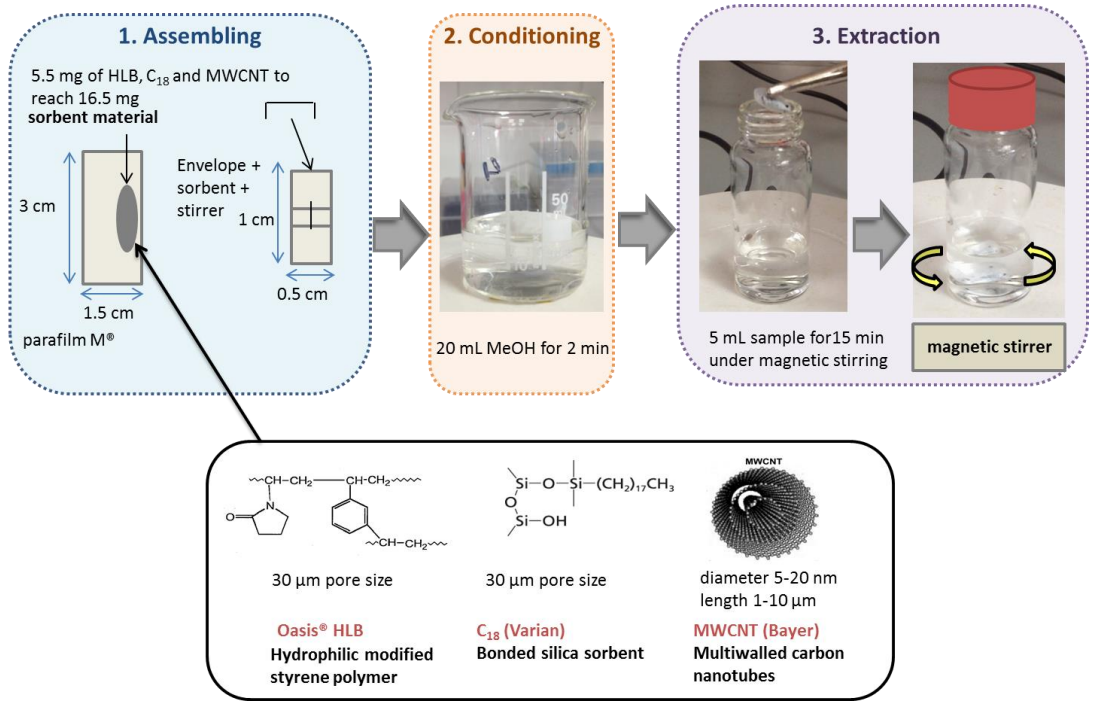

Fig. 1. Schema of the experimental set up followed for µSPE procedure.

Firstly 5.5 mg of polymeric reversed-phase sorbent HLB OASIS from Waters (Milford, MA, USA), silica based sorbent C_{18} from Varian (Harbor City, CA, USA) and multiwalled carbon nanotubes (MWCNTs) with a diameter of 5-20 µm and a length of 1-10 µm were used. A final mass of 16.5 mg was deposited in a piece (3 x 1.5 cm) of Parafilm M® supplied by Sigma-Aldrich (St. Louis, USA). It was folder to have the final dimensions of 1 x 0.5 cm. A staple was used working as integrated stirrer of the µSPE device. Each µSPE device was cleaned with methanol for 2 min. After that it was dried with lab tissue and inserted in a closed glass vial of 10 mL where the extraction of analytes takes part under magnetic stirring for 15 min. After that time, the µSPE device was taken out from the sample with tweezers. The excess of liquid from the packed sorbent was removed with paper tissue and then it was inserted in a 10 mL glass vial closed with magnetic cap and silicone septum prior to its analysis.

2.3. Equipment

An ion mobility spectrometer hyphenated with chromatographic column with the commercial name of FlavourSpec® from G.A.S. (Dortmund, Germany) was used. It was equipped with a heated splitless injector, which enabled direct sampling of the headspace via an automatic sampler unit (CTC-PAL, CTC Analytics AG, Zwingen, Switzerland). The device is equipped with a ^{3}H ionization source (St. Petersburg, Russia) with an activity of 300 MBq which is below the exemption limit of the EURATOM guideline (1 Gbq). This instrument can be operated in negative or positive ionization mode. For analysis, the μSPE device placed in a 10 mL glass vial was heated for 20 min at 80 ºC to ensure the transference of analytes from the sorbent to the headspace of the vial. Then, 200 μL of sample headspace was automatically injected by a heated syringe (80 ºC) into the GC–IMS equipment. Sample and drift gas used was pure nitrogen (99.999 %) supplied by Abelló Linde S.A. (Barcelona, Spain). After injection, the nitrogen carrier gas passing through the injector inserted the sample into the GC column which was 30 m long with an internal diameter (i.d.) of 0.25 mm and a 0.5 μm film thickness, consisting of methyl, phenyl and vinylsiloxane, from CS-Chromatographie Service GmbH (Dürem, Germany), in a 94:5:1 proportion. The GC column was heated and maintained at 40 ºC for timely separation. The analytes were eluted from the GC column and driven into the ionization chamber. Once ions are formed they are focused to a shutter grid (BN gate), prior to the separation in the 5 cm long drift tube. The BN gate opening time was set to 100 μs, allowing the ions to pass towards the separation chamber where ions differing in mobility were separated under a constant electrical field of 400 V cm^{-1}. The IMS drift tube was kept under atmospheric pressure (101 kPa) and heated at 75 °C. The data were acquired and displayed by the integrated computer within the equipment, and processed using the software LAV version 2.0.0 from G.A.S. All spectra were recorded in the positive ion mode.

3. Results and discussion

The combination of these sorbents of different nature in a home-made μSPE device was used for first time to retain toxics compounds with different polarities in saliva. The analyses were carried out with HS-GC-IMS. Parameters that affect the extraction procedure and its analysis by HS-GC-IMS were examined.

3.1. Evaluation of the extraction procedure

To evaluate the method proposed factors as type and amount of sorbent, extraction time, sample size, and pH that influence the extraction efficiency were studied. These parameters were tested with a stock standard containing the target analytes at 1 μg mL^{-1} prepared in ultrapure water. In **Table 2** are shown the conditions followed for the extraction procedure.

Table 2. Experimental conditions for μ-SPE used in this work.

Experimental parameter	Studied range	Optimum condition
Type of sorbent	C18, HLB and MWCNT	A mix of C18, HLB and MWCNT
Amount of sorbent (mg)	3, 16.5 and 30	16.5
Sample volume (mL)	1, 3 and 5	5
Extraction time	5, 15 and 25	15
Stirring method	Ultrasonic, magnetic, vortex	Magnetic

Type of sorbent

The kind of sorbent used in μSPE is essential to extract the analytes from the matrix because there occurs a dynamic portioning of analytes between the sorbent material and the matrix. High adsorption capacity, acceptable selectivity and desirable adsorption kinetics are some of the characteristics of an ideal sorbent [25] to be used in μSPE. A total of 60 mg of HLB, C_{18} and MWCNTs were tested individually and also a mixture of them in the μSPE device. Benzene was better retained with MWCNTs because of the π-π electrostatic interaction established and the large surface area of MWCNTs. Toluene was better extracted with C18 and also

MWCNTs because of the non-polar region of the analyte. And the most polar components tested (butyraldehyde, benzaldehyde and tolualdehyde) were better retained with HLB because of the hydrophilic part of this sorbent. Based on the different polarities of the target analytes a mixture of HLB, C_{18} and MWCNTs was chosen to be used simultaneously in the μSPE device. The combination of these three different sorbents resulted in the extraction of analytes of different polarities.

Extraction time, sample volume, pH and sorbent amount

Sample volume (1-5 mL), extraction time (5-25 min) and sorbent amount (3-30 mg) were studied simultaneously by using face centered central composite design (Statgraphics Centurion software) with 3 factors, 3 levels and 2 replicates resulting in 32 experiments. As can be seen in **Figure 2**, benzene and toluene responses are shown as example, the optimum conditions were obtained when using 5 mL of sample volume, 15 min for extraction time, and 16.5 mg of sorbent mixture.

The effect of sample pH in the range of pH 3-10 was also investigated. However, change in pH did not improve the extraction of the target analytes from saliva. Then saliva pH was maintained at its natural value between pH 7-7.4.

Effect of the type of stirring

μ-SPE involves dynamic partitioning of the target analytes between the sorbents and the sample solution. Since mass transfer is a time-dependent process, the sample was continuously agitated at room temperature (25°C) to accelerate the mass transfer process. Vortex, ultrasonic and magnetic stirring were tested. For all compounds magnetic stirring was the option at which highest signal intensities were obtained as can be seen in **Figure 3**. Benzaldehyde was the only analyte for which ultrasonic and magnetic stirring results in similar responses.

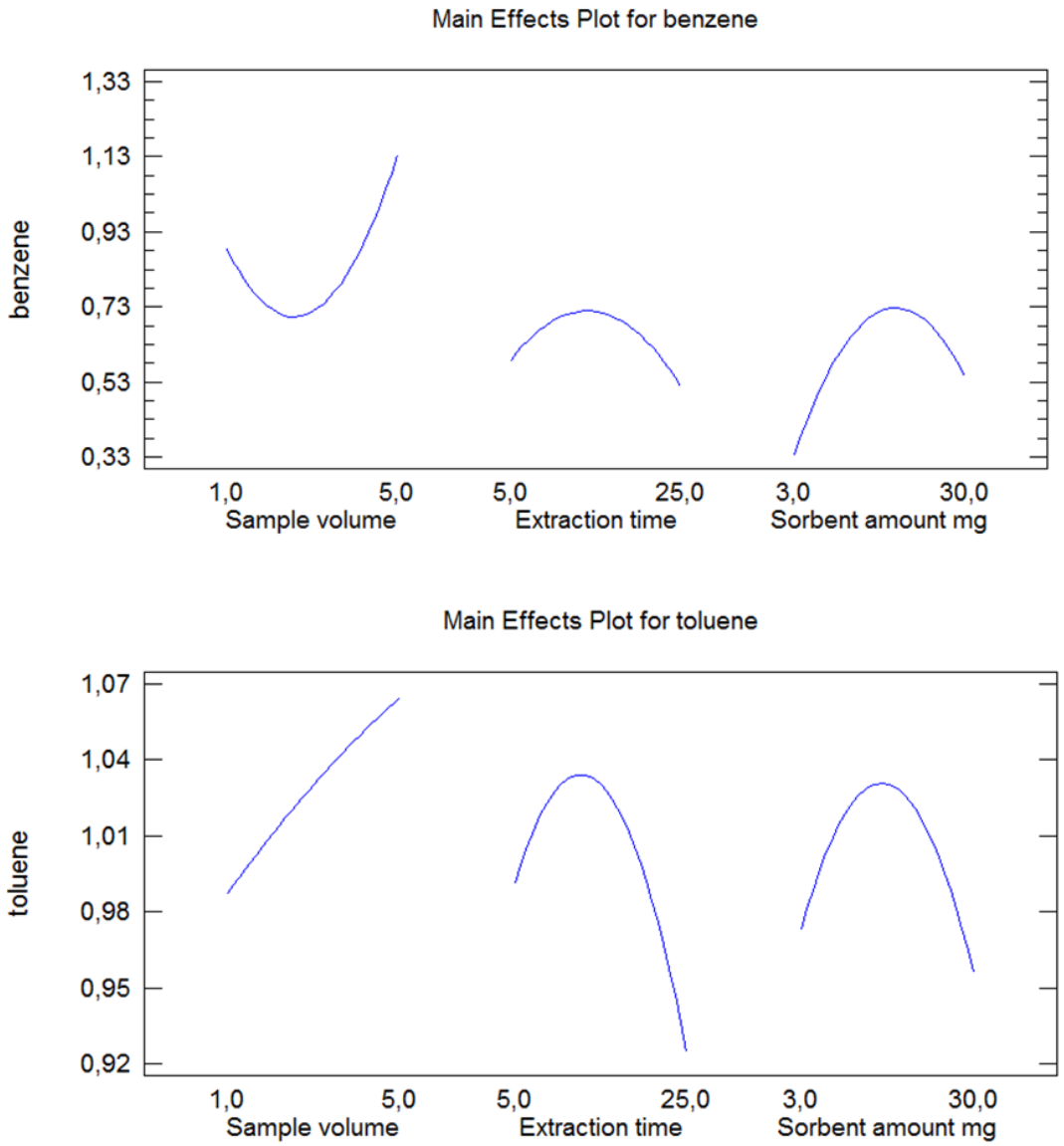

Fig. 2. Main effects plots obtained after multivariate optimization of sample volume, extraction time and sorbent amount for benzene and toluene.

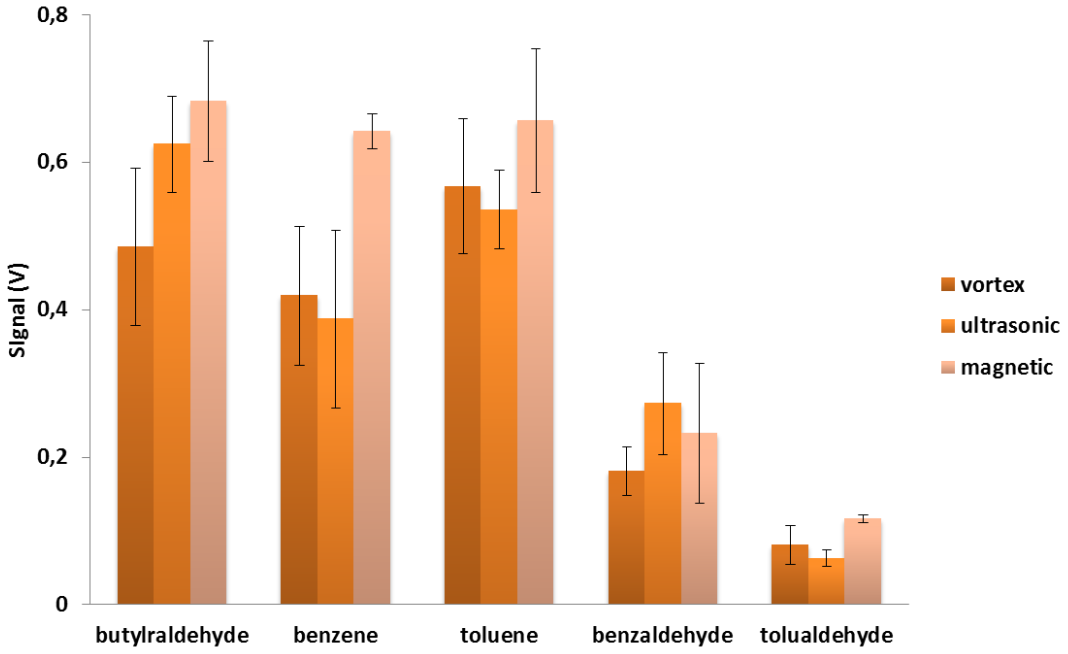

Fig. 3. Effect of the type of stirring on the extraction of target analytes.

3.2. Optimization of the instrumental parameters

The transference of the analytes from the μ-SPE device to the headspace is a critical step in the methodology for its later analysis by GC-IMS. In **Table 3** are summarized the instrumental parameters studied and the selected values. The heating time for desorption inside the autosampler was optimized in the range of 5-30 min, obtaining higher intensities of signal at 20 min as can be observed in **Figure 4 A**. At higher heating time (>20 min) signal decreased probably because of a negative effect on the porosity of the sorbents in the μ-SPE device due to prolonged heated. Heating temperature was set at the maximum value of the autosampler (80 ºC) to allow the vaporization of analytes previously retained in the μSPE device. 200 μL of the headspace was chosen since it provided an acceptable sensitivity level.

Table 3. Experimental conditions for HS-GC-IMS.

Experimental parameter	Studied range	Optimum condition
Carrier gas flow (mL min^{-1})	5-15	5
Drift gas flow (mL min^{-1})	-	250
Sample heating temperature (ºC)	30-80	80
Sample heating time (min)	5-30	20
Injection volume (µL)	200-1000	200
Analysis time (min)	-	30
HS Injector (ºC)	-	80
Gas column temperature (ºC)	40-70	40
Drift tube temperature (ºC)	45-75	75

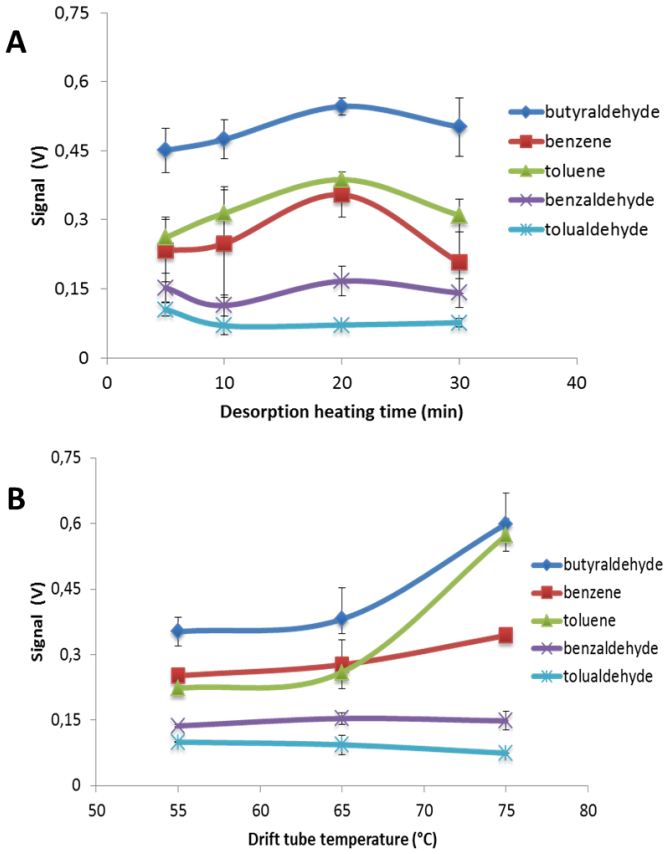

Fig. 4. (A) Effect of the heating time used for desorption of analytes retained in the µSPE device. (B) Influence of IMS drift tube temperature on signal intensity of the target analytes.

Temperature column was set at 40 ºC to allow the separation of analytes. Drift tube temperature was studied in the range of 45-75 obtaining higher signals intensities for all analytes at 65 ºC as can be seen in **Figure 4B**. But an increment of the signal was observed for butyraldehyde, benzene and toluene when 75 ºC was selected that can be ascribed to a reduction of clustering in the ionization source due to an increase of the temperature and consequently an improved ionization and higher signal obtained; finally 75 ºC was used for further experiments.

3.3. Improvement of signal with µSPE before GC-IMS analysis

The headspace from 1 mL of standard containing target analytes and from the µSPE device after extraction step were measured by HS-GC-IMS following the selected conditions. A standard solution of 1 µg mL^{-1} containing benzene, toluene, butyraldehyde, benzaldehyde and tolualdehyde prepared in ultrapure water was used for both. As observed in **Figure 5**, all compounds yielded monomer (MH^+), and also benzaldehyde and tolualdehyde gave a dimer (M_2H^+), visible in the IMS spectra at 1 µg mL^{-1}. Probably, dimer ions from benzaldehyde and tolualdehyde were more stable than the others dimer ions measured at the experimental conditions chosen and for this reason they can be detected by the faraday plate of the IMS.

The signal intensity for benzene, toluene and butyraldehyde was higher when using the µSPE device in comparison with direct HS measurement. Due to the lower proton affinity of benzene, toluene and butyraldehyde (<792.7 kJ mol^{-1}) their ionization can be problematic at that humid condition generated in the headspace from the saliva sample (99 % water) that is introduced into the ionization source of the IMS. Noted that at low water vapor concentration, the main proton carrier is $H^+(H_2O)$ which has a proton affinity of 697 kJ mol^{-1}. In the case where the water vapor concentration increases, the main proton carrier was found to be $H^+(H_2O)_2$ which has a higher proton affinity (808 kJ mol^{-1}) [10].

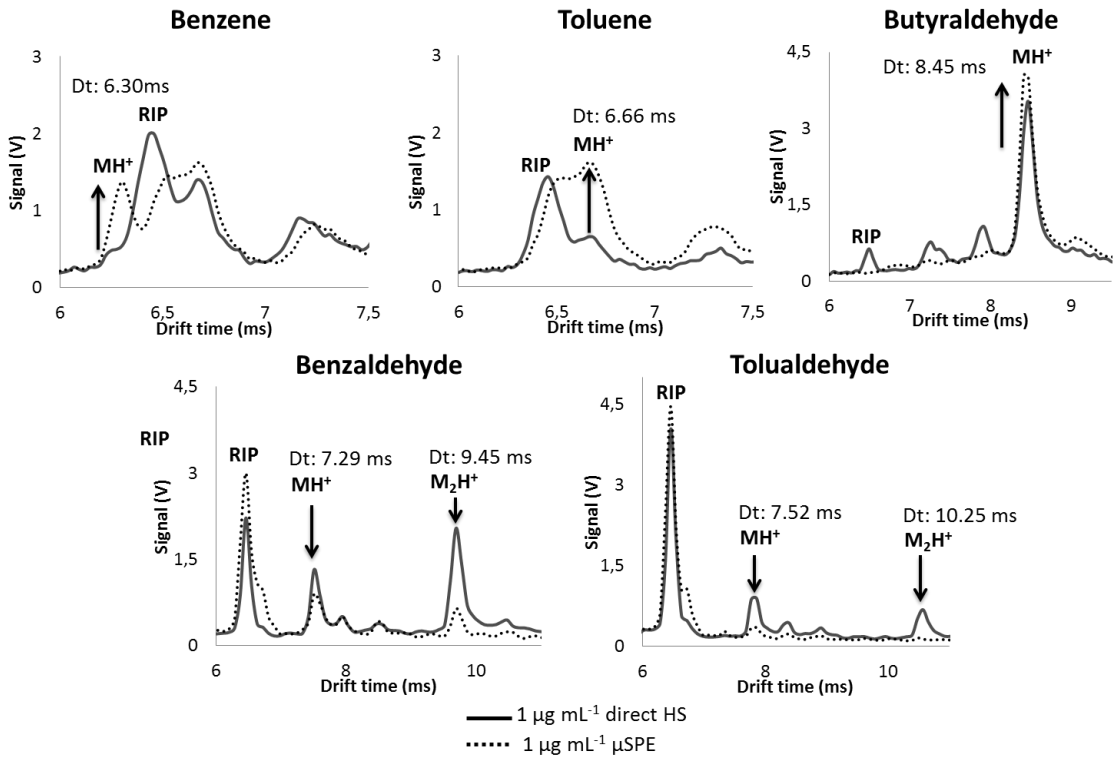

Fig. 5. IMS spectra of benzene, toluene, butyraldehyde, benzaldehyde and tolualdehyde obtained by direct headspace of the liquid standard or by desorption of µSPE device after the extraction procedure. An arrow was used to identify peak ion of each analyte.

This effect was considerably reduced when µSPE methodology was used, avoiding the moisture from the sample and improving the sensitivity of the method.

By contrast, benzaldehyde and tolualdehyde ions were produced without any affection from moisture due to its higher proton affinity values (834 and 851.8 kJ mol^{-1} respectively) which make possible its identification and quantification in all samples. This explains why direct HS analysis of benzaldehyde and tolualdehyde resulted in an intense IMS signal. However, when performing µSPE before HS-GC-IMS they gave a slightly reduced peak height intensity (tiny dimmer peak of tolualdehyde was not observed) in comparison with the signal obtained when they were determined by direct

HS analysis. A possible reason of this fact could be that the complete desorption of benzaldehyde and tolualdehyde from the packed sorbent to the headspace of the vial was not achieved at the desorption temperature chosen (80 ºC), taking into account the higher boiling point of these compounds (178.1 and 204 ºC respectively) compared with the rest compounds whose boiling point were lower than 110.8 ºC in all cases.

3.4. Analytical figures of merit

The validation of the method was carried out by establishing limits of detection (LOD) and quantification (LOQ), intra-day and inter-day precision and recovery values. Measurements were done by triplicate. Two calibration graphs for each target analyte (in ultrapure water and saliva) were built in order to study the matrix effect. Intensity height from monomer peak of each compound was used. LODs and LOQs were calculated as three and ten times respectively, the intercept deviation (Sb) divided by the slope. **Table 4** shows the analytical figures of merit of the proposed method obtained with ultrapure water and with the analytes dissolved in non-smoker saliva. By comparing the slopes of both calibrations curves slight decreased in the analytical signal was observed for the analytes dissolved in saliva as a result of the matrix effect.

The precision of the proposed method was assessed in terms of within-day and between-day precision, both expressed as RSD % and shown in **Table 5**.

Precision study was performed with spiked saliva samples at 2.5 µg mL^{-1} of each analyte. Within-day precision was assessed by applying the procedure six times on the same day and between-day precision by analysing three times the sample over three consecutive days. Precision values for drift time and retention time were in all cases lower than 3.5 %. But higher values for RSD were obtained for intensity peak height (RSD< 21.2 %). It can be attributed to irreproducibility in the µSPE device assembling (amount of sorbent weighted each time), or analyte losses while

performing the μSPE procedure that could cause variations in peak heights obtained in the measurements by HS-GC-IMS.

Table 4. Calibration curves and statistical figures of merit by μ-SPE-IMS method

Matrix	Compound	Calibration curve (*y= ax+b*)	R^2	S_a	S_b	LOD (mg L^{-1})	LOQ (mg L^{-1})
Water	Butyraldehyde	y= 0.789x + 0.409	0.989	0.081	0.102	0.31	1.03
	Benzene	y= 1.195x + 0.382	0.960	0.094	0.125	0.24	0.79
	Toluene	y= 0.530x + 0.621	0.958	0.031	0.055	0.18	0.59
	Benzaldehyde	y= 0.539x + 0.448	0.967	0.035	0.048	0.20	0.65
	Tolualdehyde	y= 0.315x + 0.143	0.968	0.025	0.025	0.24	0.81
Saliva	Butyraldehyde	y= 0.512x + 0.776	0.973	0.065	0.076	0.38	1.26
	Benzene	y= 0.623x + 0.689	0.972	0.103	0.056	0.49	1.66
	Toluene	y= 0.505x + 0.839	0.954	0.076	0.083	0.45	1.51
	Benzaldehyde	y= 0.406x + 0.315	0.986	0.067	0.073	0.41	1.37
	Tolualdehyde	y= 0.247x + 0.139	0.975	0.034	0.022	0.41	1.39

Table 5. Precision values for the determination of target compounds at 2.5 μg mL^{-1} in saliva samples by μSPE-IMS method.

Compound	Within-day precision (% RSD, n= 6)			Between-day precision (% RSD, *n= 9*)		
	Retention time	Drift time	Peak height	Retention time	Drift time	Peak height
Butyraldehyde	3.5	0.2	15.1	2.4	0.2	21.1
Benzene	3.2	0.2	13.9	3.1	0.2	21.2
Toluene	1.6	0.1	8.4	2.3	0.2	18.9
Benzaldehyde	1.2	0.2	13.7	1.0	0.6	18.0
Tolualdehyde	0.8	0.2	18.8	0.7	0.4	19.8

The efficiency of μSPE cartridge to retain analyte was assessed by conducting recovery test shown in **Table 6** involving triplicate in saliva samples from 7 saliva samples from smokers spiked with target analytes at 2.5 and 5 μg mL^{-1}. The method proposed gave recoveries values in the range of 78.8 and 99.8% and with RSD values between 6.5 to 15.8%. These results confirmed that the methodology proposed is effective for extracting low concentrations of butyraldehyde, benzene, toluene, benzaldehyde, and tolualdehyde from saliva samples with a simple and low cost μSPE device by using a non-invasive approach.

Table 6. Recovery study in smokers' saliva samples spiked with target analytes performing μSPE-IMS procedure and analyzed by HS-GC-IMS.

Compound	**2.5 μg mL^{-1}**		**5 μg mL^{-1}**	
	Recovery (%)	RSD (%) (*n*= 4)	Recovery (%)	RSD (%) (*n*= 3)
Butyraldehyde	99.8	13.0	86.9	15.8
Benzene	85.1	10.3	78.8	11.8
Toluene	82.6	6.5	81.4	11.4
Benzaldehyde	83.3	11.5	80.4	12.5
Tolualdehyde	73.6	12.3	73.2	13.2

When direct HS analysis was performed, with 1 mL of saliva sample, signals coming from other volatile substances present in saliva appeared in the IMS spectra as can be observed in **Figure 6**. Noted that for smoker saliva sample more complicated topographic plot was obtained, which differ significatively from non-smoker saliva sample. Signals appearing at the same retention time of expected analytes can difficult their correct identification or they can contribute to their wrong identification as false positives. The variability of matrix composition has proved to be a critical point in the method development, demonstrating the need to include a pre-treatment step prior to the introduction of analytes to the HS-GC-IMS.

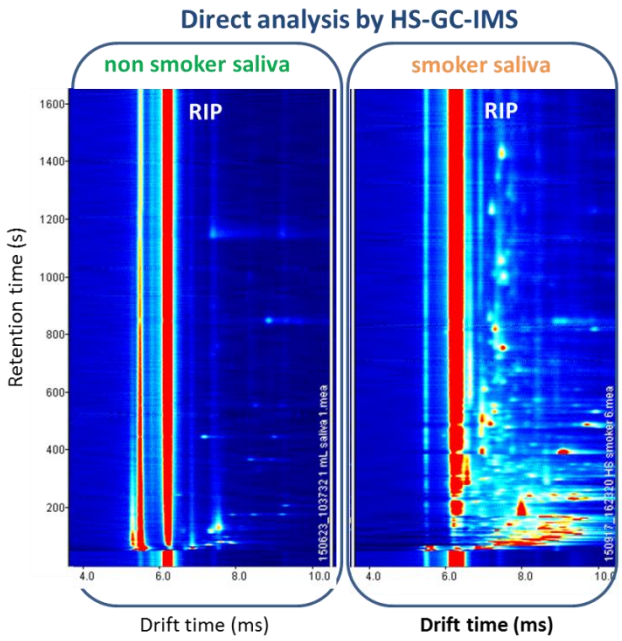

Fig. 6. IMS topographic plots from non-smoker and smoker saliva blanks samples obtained by performing direct HS-GC-IMS and μSPE combined with HS-GC-IMS.

In **Figure 7** is shown the topographic plot obtained from smoker saliva sample and the same sample with the analyte spiked. As can be seen, background signals and moisture from the matrix were reduced when using μSPE device and consequently increasing sensitivity and selectivity of the proposed methodology. Target analytes could be identified and quantified in saliva samples. Since the porous membrane used in this work afforded protection of the sorbent materials, direct desorption of the μSPE device can be done without further steps required. The hydrophilic part of HLB, hydrophobic chain of $C_{18;}$ and the large surface area and π-π electrostatic interaction with the analytes of MWCNTs, facilitated the adsorption of almost all analytes with good sensitivity and selectivity. The μSPE procedure is simple and affordable method to extract selectively toxic compounds in complicated matrix such as saliva and analyzed them by using HS-GC-IMS.

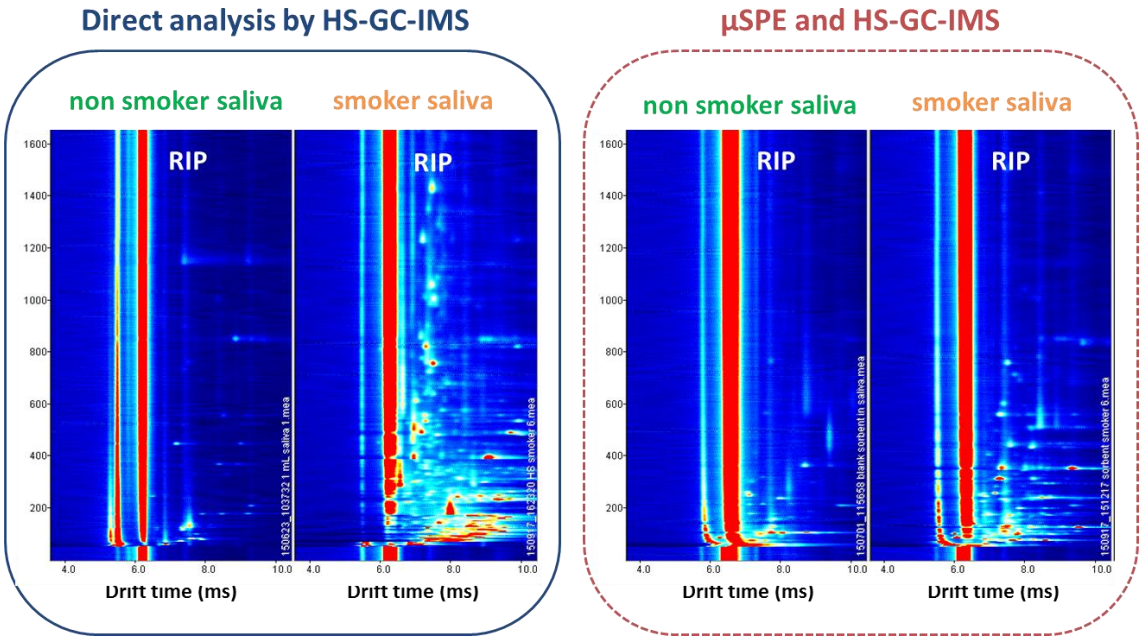

Fig. 7. Topographic plots obtained for a blank of smoker saliva and the same sample spiked at 5 µg mL^{-1} by µSPE combined with HS-GC-IMS.

4. Conclusions

This work opens up interesting prospect for IMS to monitor toxic compounds in the clinical field in combination of new sample preparation methodology based on µ-SPE. A home-made and low cost tool which consists of an envelope combining sorbents of different polarities was successfully applied to retain selectively target analytes present in saliva samples. Introduction of moisture and matrix components from saliva samples which can change ion chemistry inside the IMS complicating the spectra were avoided with this pretreatment step. The method has several other benefits such as simplicity and speed of analysis. As well, the packed sorbent used is easy to prepare in-house at reasonable time and cost. Potentially, this new developed microextraction strategy can be used to extract analytes from different complex matrixes such as other biological fluids.

Acknowledgements

The authors are grateful to Spain's DGICyT (Grant CTQ2014-52939R) for funding this work. L.Criado-García wishes to thank the Spanish Ministry of Education, Culture and Sport for award of a pre-doctoral grant (AP 2009-3528).

The authors have declared no conflict of interest.

References

[1] W. M. Bosker, M. A. Huestis, Oral fluid testing for drugs of abuse, Clin.Chem. 55 (2009) 1910-1931.

[2] M. Gröschl, H. Köhler, H. G. Topf, T. Rupprecht, M. Rauh, Evaluation of saliva collection devices for the analysis of steroids peptides and therapeutic drugs, J. Pharm. Biomed. Anal. 47 (2008) 478-486.

[3] G. A. Eiceman, Z. Karpas, Ion Mobility Spectrometry. Boca Raton, Fl 33487-2742, 2005.

[4] S. Armenta, M. Blanco, Pros and cons of benzodiazepines screening in human saliva by ion mobility spectrometry, Anal. Bional. Chem. 401 (2011) 1935-1948.

[5] S. Armenta, S. Garrigues, M. De la Guardia, J. Brassier, M. Alcalà, M. Blanco, Analysis of ectasy in oral fluid by ion mobility spectrometry and infrared spectroscopty after liquid-liquid extraction, J. Chrom. A 1384 (2015) 1-8.

[6] L. Criado-García, D.M. Ruszkiewicz, G.A. Eiceman, CLP. Thomas, Rapid and non-invasive method to determine toxic levels of alcohols and γ-hydroxybutiric acid in saliva samples by gas chromatography-differential mobility spectrometry, J. Breath Res. (2015) *in press*.

[7] M. T. Jafari, M. Javaheri, Selective method based on negative electrospray ionization ion mobility spectrometry (ESI-IMS) for direct analysis of salivary thiocyanate, Anal. Chem. 82 (2010) 6721-6725.

[8] W. M. Mullett, Determination of drugs in biological fluids by direct injection of samples for liquid chromatograhic analysis, J. Biochem. Biophys. Methods 70 (2007) 267-273.

[9] P. D. Harrington, E. S. Reese, P. J. Raunch, L. Hu, D. M. Davis, Interactive self-modeling mixture analysis of ion mobility spectra, Appl. Spectrosc. 51 (1997) 808-816.

[10] T. Mayer, H. Borsdorf, Accuracy of ion mobility measurements dependent on the influence of humidity, Anal. Chem. 86 (2014) 5069-5076.

[11] H. Borsdorf, P. Fiedler, T. Mayer, The effect of humidity on gas sensing with ion mobility spectrometry, Sensor Actuat B 218 (2015) 184-190.

[12] M. T. Jafari, H. Saraji, H. Sherafatmand, Polypyrrole/montmorillonite nanocomposite as a new solid phase microextraction fiber combined with gas chromatography-corona discharge ion mobility spectrometry for the simultaneous determination of diazinon and fenthion organophosphorus pesticides, Anal. Chim. Acta 814 (2014) 69-78.

[13] M. T. Jafari, H. Saraji, H. Sherafatmand, Electrospray ionization-ion mobility spectrometry as a detection system for three-phase hollow fiber microextraction technique and simultaneous determination of trimipramine and desipramine in urine and plasma samples, Anal. Bional. Chem. 399 (2011) 3555-3564.

[14] M. T. Jafari, B. Rezaei, B. Zaker, Ion Mobility spectrometry as a detector for molecular imprinted polymer separation and metronidazole determination in pharmaceutical and human serum samples, Anal. Chem. 81 (2009) 3585-3591.

[15] M. T. Jafari, Z. Badihi, E. Jazan, A new approach to determine salicylic acid in human urine and blood plasma based on negative electrospray ion mobility spectrometry after selective separation using a molecular imprinted polymer , Talanta 99 (2012) 520-526.

[16] C. Basherr, A. Alnedhary, B. S. Madhava, S. Valliyaveettil, H. K. Lee, Development and application of porous membrane-protected carbon nanotube micro-solid-phase extraction combined with gas chromatography/ mass spectrometry, Anal. Chem. 78 (2006) 2853-2858.

[17] C. D. Stalikas, Y. C. Fiamegos, Microextraction combined with derivatization, Trends. Anal. Chem. 27 (2008) 533-542.

[18] M. Sergi, D. Compagnone, R. Curini, G. D'Ascenzo, M. Del Carlo, S. Napoletano, R. Risoluti, Micro-solid phase extraction coupled with high-performance liquid chromatography-tandem mass spectrometry for the determination of stimulants, hallucinogens, ketamine and phencyclide in oral fluids., Anal. Chim. Acta 675 (2010) 132-137.

[19] C. Basheer, H. G. Chong, T. M. Hii, H. K. Lee, Application of porous membrane-protected micro-solid-phase extraction combined with HPLC for the analysis of acidic drugs in wastewater, Anal. Chem. 79 (2007) 6845-6850.

[20] C. Basheer, A. A. Alnedhary, B. S. Rao, S. Valliyaveettil, H. K. Lee, Development and application of porous membrane-protected carbon nanotube micro-solid-phase extraction combined with gas chromatography/mass spectrometry, Anal. Chem. 15 (2006) 2853-2858.

[21] R. Lucena, Extraction and stirring integrated techniques: examples and recent advances, Anal. Bional. Chem. 403 (2012) 2213-2223.

[22] W. Boonjob, M. Miró, M. A. Segundo, V. Cerdà, Flow-through dispersed carbon nanofiber-based microsolid-phase extraction coupled to liquid chromatography for automatic determination of trace levels of priority environmental pollutants, Anal. Chem. 83 (2011) 5237-5244.

[23] A. Rodgman, T. Perfetti, The chemical components of tobacco and tobacco smoke. CRS Press, Florida, 2013.

[24] D. Hoffmann, M. V. Djordjevic, I. Hoffmann, The changing cigarette, Prev. Med. 26 (1997) 427-434.

[25] M. Lashgari, C. Basheer, K. H. Lee, Application of surfactant-templated ordered mesoporous material as sorbent in micro-solid

phase extraction followed by liquid chromatography-triple quadrupole mass spectrometry for determination of perfluorinated carboxylic acids in aqueous media, Talanta 141 (2015) 200-206.

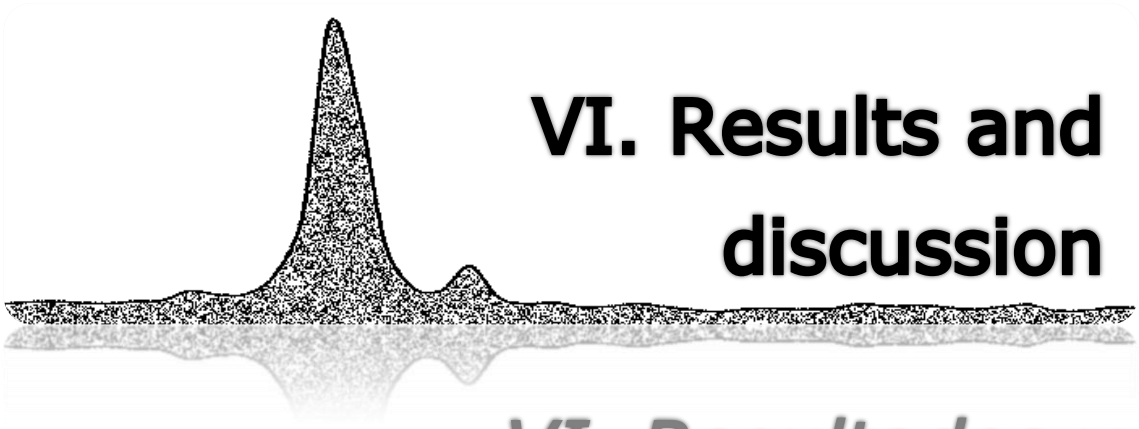

VI. Results and discussion

VI. Resultados y discusión

The main results of the research developed in this Doctoral Thesis are summarized in this section. Since the memory is a compilation of articles and the specific results of each paper have been previously discussed, the aim of this section is to give an integral approach to the experimental work carried out and presented in the memory, by comparing the strengths and drawbacks of each of them.

This block has been structured differently from the general scheme of the Thesis. It is divided into four sections, the first devoted to SISs coupled to ion mobility spectrometry to generate gaseous standards together with a focus on how to improve selectivity and sensitivity; the second section deals with the potential of ion mobility spectrometry as a rapid tool for monitoring target compounds in HTF and environmental samples; the third section discusses the potential of IMS in clinical analysis; and, finally the fourth presents an analysis of the ion mobility responses obtained in the experimental work carried out in this Doctoral Thesis.

VI.1. Sample introduction systems coupled to Ion mobility spectrometry

Inlets systems to deliver sample volatile analytes to the IMS must satisfy a requirement that gas-phase ions are produced from the sample at ambient pressure. The second requirement is that the IMS measurement provides an analytical reliable measure of the sample and the analyzer should not appreciably distort the chemical information sought from the sample [1]. In this Doctoral Thesis two home-made SISs were used to produce gaseous standards, one analyzing the headspace produced from a liquid pure standard and another by exponential dilution set-up. Both systems were compared with the response obtained by a gas generator. Another system which consists of a membrane holder with a PDMS membrane was used to remove humidity from the gaseous sample. Finally, TENAX® column was used to retain analytes prior to being injected into the

UV-IMS. **Figure 1** shows the plotting of the different SISs which have been used in the experimental works of this Doctoral Thesis.

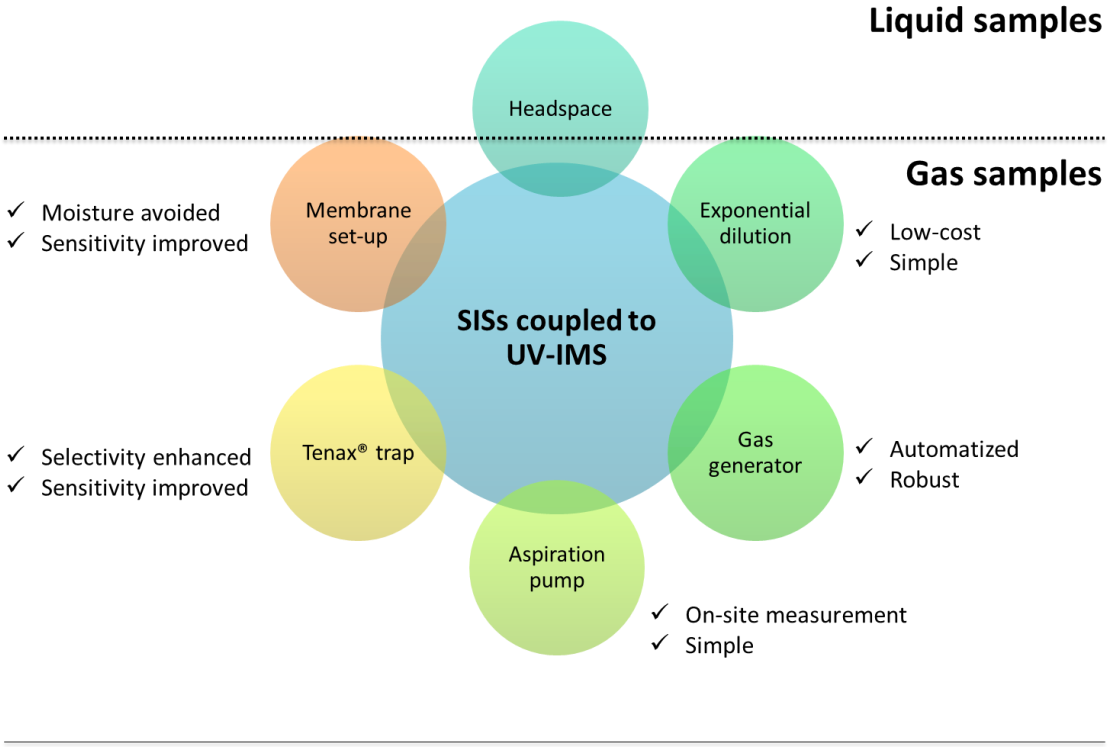

Fig. 1. Schematic of different SISs used for the introduction of volatiles from liquid and gaseous samples to UV-IMS.

Only the headspace system was dedicated to extract volatiles from liquid samples, the rest of the systems were used with gaseous samples to extract compounds that at ambient conditions are present in the gas phase. Note that the only automatized method used was the gas generator; the remaining SISs were operated manually. These systems are discussed in the following sections.

VI.1.1. SISs tested to calibrate the UV-IMS

Different strategies should be tested to generate gaseous standards depending on whether the target analyte is present (in a liquid or gaseous sample) taking into account the fact that calibration standards must be

prepared in a similar matrix or environment to that of the target analytes. The analytical features of each method proposed in this work are shown in this section. **Table 1** shows the LOD and LOQ values obtained for each analyte when using the SISs proposed. The excellent LOD of IMS may be attributed to the high efficiency of chemical ionization at ambient pressure through high collision rates and long residences times [2].

Table 1. Comparison of LOD and LOQ obtained with the three SISs studied.

Analyte	Headspace set-up		Exponential dilution		Gas generator	
	LOD mg L^{-1}	**LOQ** mg L^{-1}	**LOD** mg $L^{-1}_{(g)}$	**LOQ** mg $L^{-1}_{(g)}$	**LOD** mg $L^{-1}_{(g)}$	**LOQ** mg $L^{-1}_{(g)}$
Acetone	3.0	10.0	0.8	2.8	0.4	1.2
Ethylbenzene	3.4	11.5	1.1	4.1	0.1	0.4
Benzene	4.6	15.4	1.1	3.7	0.3	1.1
Toluene	3.6	11.8	1.6	5.4	0.1	0.3
m−Xylene	2.8	9.4	1.5	4.9	-	-
o−Xylene	2.3	7.7	1.5	4.9	-	-
p−Xylene	5.3	17.6	1.8	6.1	0.1	0.3

When the head-space method was used, the minimum concentration detected was much higher than the minimum concentration detected with exponential dilution set-up. The reason for this may be that when the head-space method was performed, the liquid sample was heated to generate volatiles compounds which represent only a fraction of the total compounds present in the liquid sample place inside the vial. Therefore, only the fraction of compounds passing to the gas phase was measured by UV-IMS [3]. Moreover, the effect of moisture should be taken into account when the gaseous fraction is measured from a liquid sample, since it might reduce the signal intensity [4]. Finally, LODs and LOQs were lower using the commercial gas generator in comparison with exponential dilution set-up due to the fact that major inaccuracies in the preparation of gaseous standards were avoided.

Precision expressed as RSD (%), was also assessed for target analytes when performing the head-space set-up, exponential dilution system and using the gas generator. Average values of RSD for head-space (3.57% for peak height and 0.40% for drift time) were slightly lower than the values obtained for exponential dilution set-up (10.46% for peak height and 0.54% for drift time). One reason for this may be the irreproducibility of preparing the gaseous samples in the dilution flask. Furthermore, the lower RSD values (0.30% for peak height and 0.22% for drift time) were obtained when using the gas generator due to the high precision of this commercial device to prepare individual standard solutions. Based on these values, the high precision values obtained with IMS can be demonstrated. In most cases the higher RSD values for some specific applications can be attributed to an error in the SISs selected. **Figure 2** shows a summary of analytical properties that each SIS tested offers.

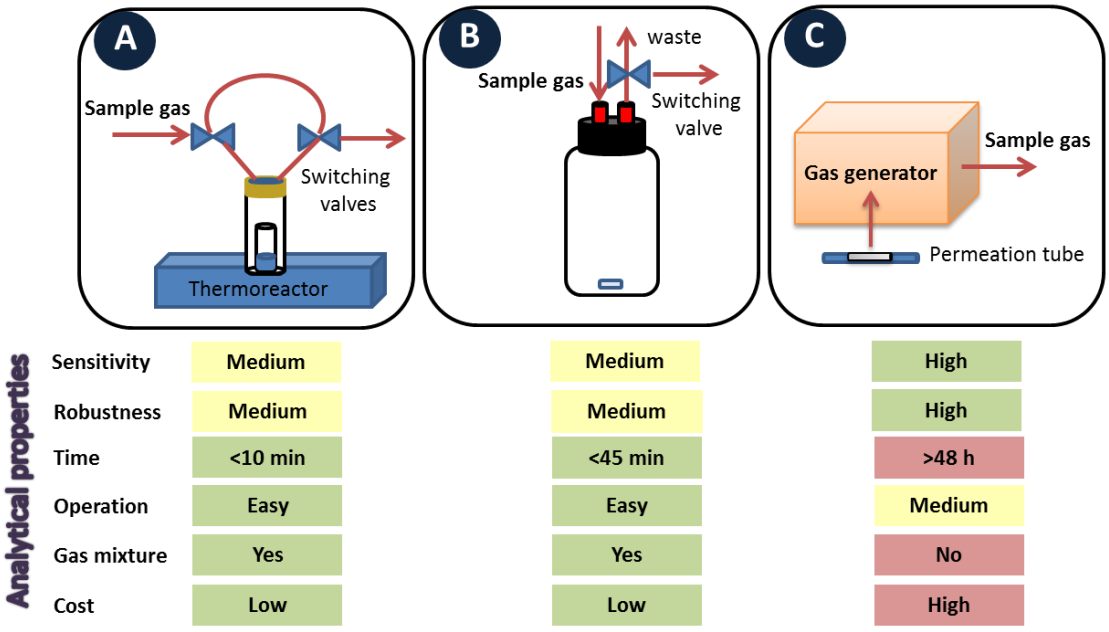

Fig. 2. Schematic of different SISs used for genarating gaseous standards and introducing them into the UV-IMS.
A: headspace, B: exponential dilution, C: gas generator.

The advantages of the home-made SISs proposed for liquid and gaseous samples are mainly the speediness, low cost, simplicity and acceptable sensitivity values obtained. The different optimized methods shown in this work can be used in the future to measure analytes present in different real samples by using UV-IMS technology. A real case is summarized in the following section.

VI.1.2. Measurements in the EUPHORE chamber

After studying how to generate gaseous standards and calibrate the UV-IMS, preliminary measurements of real air samples were performed in the atmospheric simulator, the European photoreactor (EUPHORE) at the CEAM institute (Valencia, Spain). The outlet port of the chamber was connected to the UV-IMS instrument and a pump to extract and measure the analytes that were in their gaseous state inside the chamber, which previously had been placed in the sample port of the EUPHORE chamber. For more details of the experimental set-up see Figure 7 in *Block II*. **Figure 3** shows, as an example, the IMS spectra which were obtained when toluene at 4.2 mg $L^{-1}_{(g)}$ were measured in a dry environment and when increasing humidity in the Euphore chamber.

Toluene peak decreased at these conditions due to the effect of moisture. Besides this, when a mixture of BTEX at 4.2 mg $L^{-1}_{(g)}$ was measured, only one peak was observed, appearing at a higher drift time (19.08 ms). The mixture was also affected by the increment of humidity inside the chamber, and its signal decreased at a high level of humidity. The same behaviour was observed for all BTEX compounds measured. Therefore, the main drawback found was related to the low selectivity of the UV-IMS, when a mixture of analytes which have similar chemical properties was measured. The same poor resolution was detected in real gaseous samples. Moisture can also modify the spectra affecting the ion chemistry of the ions generated when measured at high humid conditions.

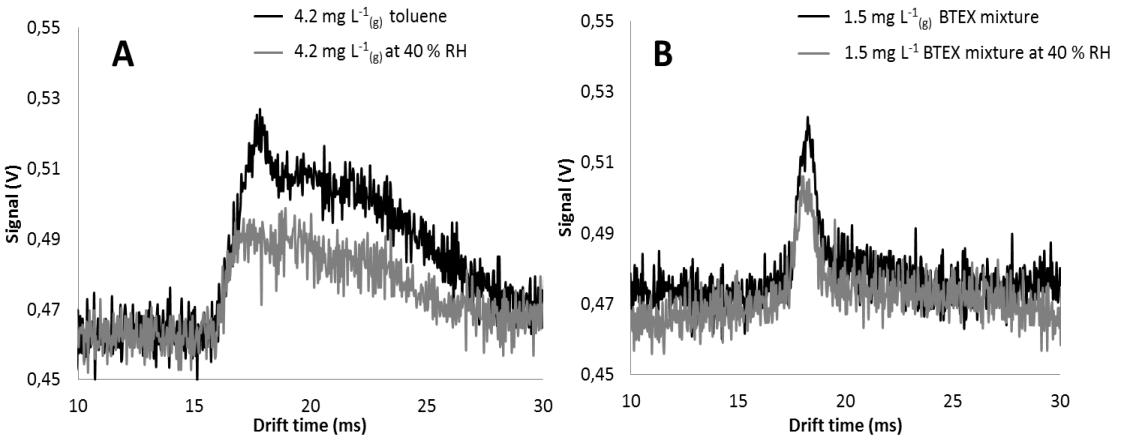

Fig. 3. IMS spectra obtained with a pump connected from the outlet port of the EUPHORE chamber to the UV-IMS instrument. (A) 4.2 mg $L^{-1}_{(g)}$ toluene in dry air and when humidity was increased to 40% RH. (B) 1.5 mg $L^{-1}_{(g)}$ mixture of BTEX in dry air and when humidity was increased to 40% RH.

VI.1.3. SISs used to improve the selectivity and the sensitivity of UV-IMS

The selectivity of the UV-IMS was studied by measuring at different concentration levels five BTX (benzene, toluene, *m*-xylene, *o*-xylene and *p*-xylene) using the headspace system or the exponential dilution set-up (SIS that were studied to generate gaseous standards), wherein a low resolution of the instrument was observed. The separation of ions that take part in the drift tube of the IMS was not enough to resolve all of them. Only one single peak appeared in the IMS spectra at longer drift time compared with the individual peak of each analyte measured independently. This confirmed that a pre-separation step needs to be included to improve resolution of this IMS instrument. Also, humidity can act as an interferent of the IMS measurement.

In order to reduce problems related to low selectivity and humidity interference, the following methods, which appear in **Figure 4**, were developed for their use coupled to the UV-IMS.

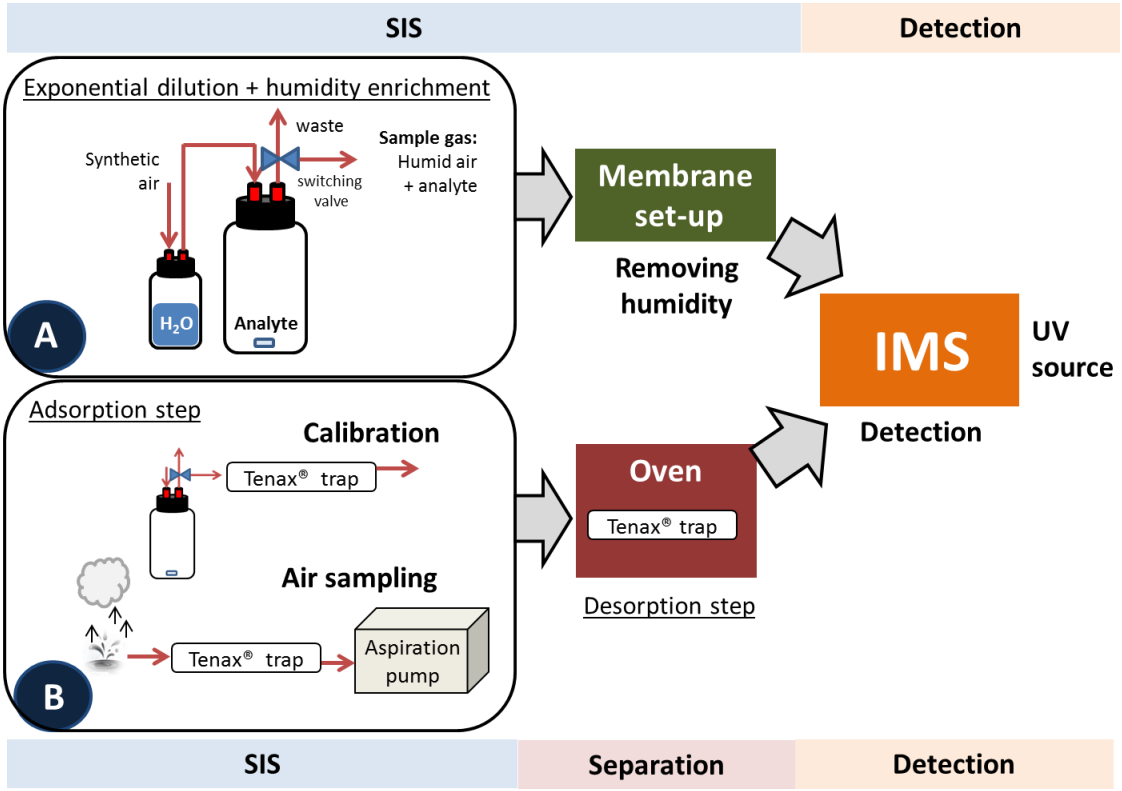

Fig. 4. Summary of different analytical methods used to improve the selectivity and sensitivity of the UV-IMS.
A: Exponential dilution set-up prior to humidity enrichment, B: Exponential dilution set-up used for parameters optimization and method validation and experimental set-up followed for air sampling using an aspiration pump.

A PDMS membrane in a home-made set-up, that can be easily connected when required, was implemented successfully to avoid the effect of humidity when using UV-IMS for on-field monitoring. This SIS offers a versatile, simple and inexpensive method suitable for on-site and direct analysis. Humidity that enriched the sample gas was generated with a home-made and low cost approach by using a flask filled with ultrapure water and connected to the sample flask in which analytes were injected. Humidity was measured inside the flask over time to check the relative humidity (%) achieved and the reproducibility of a home-made humidifier.

Note that the influence of moisture on the BTX signals using ion mobility spectrometry with an UV lamp as an ionization source was fully studied and reported for the first time. Experimentally, it was observed that increasing humidity (% RH) of the sample gas caused decreasing of signal intensity of the main peaks of all analytes, approx. 50.23% for benzene and toluene and 76.49% for xylene isomers. There was also the formation of new peaks at approx. 21 ms for benzene, toluene, m-xylene and o-xylene and around 15 ms for m-xylene and o-xylene when increasing the moisture content in the gaseous sample up to 75% RH. As well as this, there were slight differences in drift time values (<1.26%) of more intense peaks, which were observed for all compounds when humidity was increased in the sample gas (75% RH). Therefore, moisture did not provoke an intense drift shifting in the characteristic peaks for the target analytes.

Parameters which enable assessing the identity of ions, K_0 and Ω, were calculated for all analyte peaks that appeared in the IMS spectra. It must be highlighted that new peaks formed at high humidity conditions showed a lower reduced mobility (1.57-1.59 $cm^2\ V^{-1}\ s^{-1}$) and a larger size as indicated by the collision cross section values calculated (146.4-148.7 $Å^2$) compared with the characteristic analyte peaks observed in the IMS spectra. These clusters can be formed with analyte ions and water neutrals ($n \geq 1$) and may be the reason why these peaks appeared at longer drift times and K_0 values decreased when water content was increased inside the IMS. Furthermore, when the moisture inside the IMS cell increases, the potential cluster size increases but the strength of the attachment decreases [5]. Big and slow ions which were formed are instable and can be lost or even reach the Faraday-plate too late for detection [6]. This could explain why sometimes they were not observed, as was the case of *p*-xylene, resulting in a need to introduce previous step or treatment of the humid sample gas also containing the analyte prior to the introduction to the IMS device.

A study of the sensitivity and the selectivity obtained with the analytical method proposed can highlight the ability of this technology to

determine BTX in gaseous samples. LODs and LOQs values obtained measuring the target analytes at 75% RH when the membrane set up was used in combination with UV-IMS are in the same order of magnitude (LODs= 0.49-1.21 mg $L^{-1}_{(g)}$ and LOQs= 1.63-4.03 mg L^{-1}), as shown in a previous publication when BTX were measured without humidity interference [3]. Humidity interference was also reduced considerably when the membrane was used. Within-day RSD values were below 1.1% for drift time and 12.0% for peak height compared with the values obtained when no membrane was used: RSD; 3.7% for drift time and for peak height 24.5%. Consequently, precision was improved when using the membrane set up previous to UV-IMS measurement. Its use is recommended for analyzing real gaseous samples with high humid content by UV-IMS.

Related to the system used for improving the resolution of the IMS, the efficiency of determining benzene and toluene in air samples by thermal desorption-ultraviolet-ion mobility spectrometry (TD-UV-IMS) was tested. This combination along with thermal desorption improves the two basic analytical properties: sensitivity and selectivity, of the UV-IMS instrument.

The main contribution of this work was to separate benzene and toluene from a gaseous mixture of BTEX, illustrated in **Figure 5**. On a separate matter, it should be pointed out that although ethylbenzene and xylene isomers were included during the optimization study of the proposed method, the method developed did not allow separating them under the conditions followed. However, this method proved that they cannot interfere with benzene and toluene signals in the BTEX mixture.

The proposed system was fully validated in terms of selectivity, sensitivity and precision. The system was calibrated with benzene and toluene standard gas and a regression coefficient of greater than 0.98 was obtained with detection limit of 0.54 mg m^{-3} and 0.57 mg m^{-3} for benzene and toluene, respectively. Finally, the proposed method was tested using gasoline poured onto pavement. The system was able to quantify benzene and toluene after sampling air close to a gasoline spillage. Results showed

the decreasing tendency in the concentration of benzene and toluene over time.

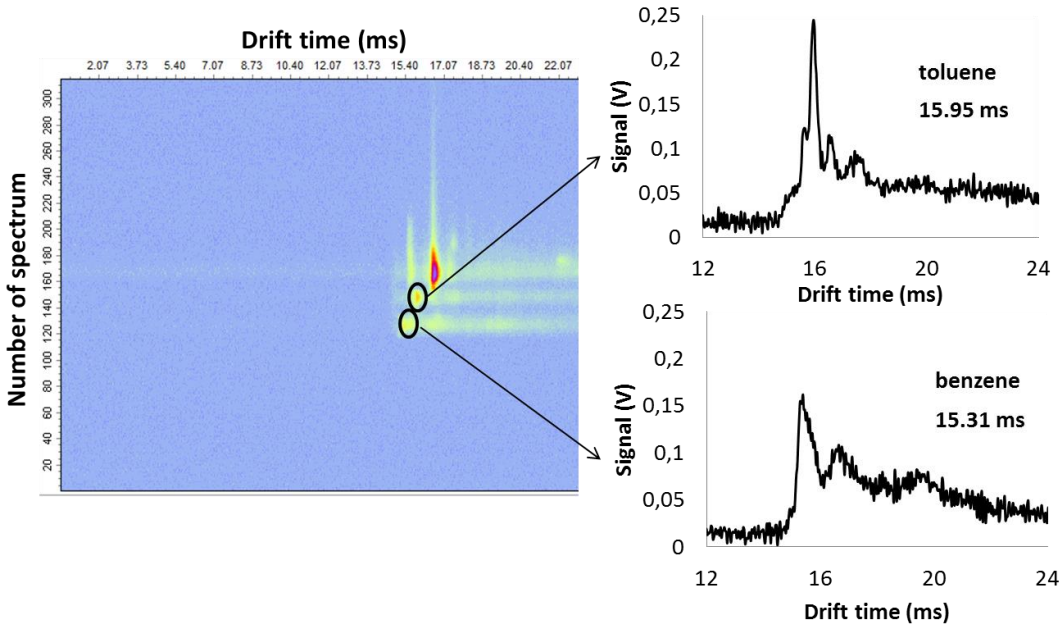

Fig. 5. IMS spectra obtained after adsorption step of 25 mg m^{-3} gaseous mixture of BTEX retained in Tenax TA trap and desorption step carried out in the oven and coupled to the UV-IMS for analysis.

VI.2. IMS for monitoring HTF and its degradation products

HTF is commonly used in heat transfer industrial processes such as those performed in thermosolar plants. Although HTF is thermally stable, the high temperatures used in such plants (around 400 ºC) and overheating in continuous cycles can alter its composition. The potential changes in its initial composition (biphenyl and diphenyl ether), and the likely production of new compounds, such as benzene and phenol, require using fast-response instruments to monitor its quality. Moreover, degradation products are potentially hazardous to workers and the environment and an alarm is needed to be set off in the event of leakage from a thermal circuit at a thermosolar plant.

For the first time HTF was characterized by using two IMS instruments. The simple one used a UV lamp as ionization source, UV-IMS, whereas the other included a chromatographic column coupled to a tritium source, GC-^{3}H-IMS. Other analytical techniques such as FT-MIR, GC-MS and GC-FID were also used for qualitative or quantitative analysis of the HTF. **Figure 6** summarizes the methods used for qualitative and quantitative analysis of HTF.

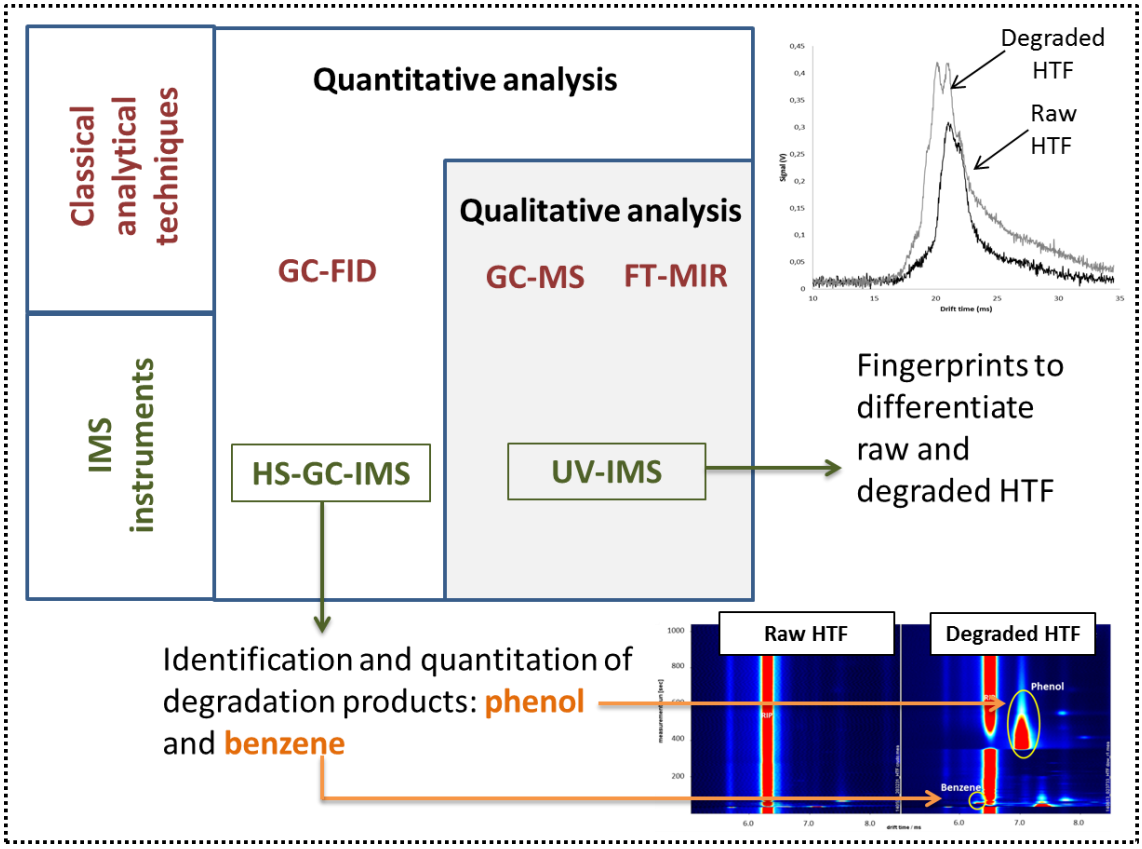

Fig. 6. Summary of different analytical methods used for the analysis of HTF.

The main aim of this work was to demonstrate the ability of IMS to distinguish raw and degraded HTF which required optimizing the operational parameters of this technique. After full optimization of instrumental parameters, raw and degraded HTF were distinguished by UV–IMS but no degradation compounds could be selectively identified by direct analysis of

the headspace because the UV-IMS instrument as commented before has a limited ability to separate ions. The required selectivity was obtained by using a GC column as a pre-separation step prior to IMS (GC–^{3}H–IMS) [7].

Benzene and phenol were identified in degraded HTF samples. As expected, benzene was the first compound to appear in the chromatogram (56 s) due to its low boiling point (80.1 ºC). Benzene is a non-polar compound with a low proton affinity (750.4 KJ mol^{-1}), but higher than the water value (691 KJ mol^{-1}); therefore, it can be ionized by a tritium source. Under the IMS conditions used in this work, benzene ions appeared a few milliseconds before the RIP in the spectrum, which was not observed for any compound that was measured before by using this instrument. Benzene ions detected probably resulted from a charge transfer reaction with NO^{+}. Nevertheless, phenol (817.3 KJ mol^{-1}) ions seem to react with the RIP as its signal appears after the RIP with a drift time of 7.01 ms.

Finally two classical instruments were used to analyze HTF samples. On one hand, FT-MIR measurements can be useful for obtaining general information about the compounds present in degraded HTF. However, the degradation products formed in raw HTF belong to the same family as the original compounds and are thus highly difficult to identify since they exhibit the same, typical bands of aromatics. In addition, FT-MIR measurements in this instrument require preparing KBr pellets with the samples prior to analysis; so they cannot be used for on-line analysis. On the other hand, GC–MS was also chosen for identifying the compounds present in the HTF samples. The initial components of HTF (biphenyl and diphenyl ether) were detected in all degraded HTF samples due to their high concentration. Also, degradation products (benzene and phenol) with other degradation compounds with a higher boiling point than benzene and phenol, dibenzofuran and triphenylmethane were also detected in degraded HTF samples. However, one major disadvantage of using GC–MS to check HTF degradation is that the less concentrated compounds (benzene and phenol) cannot be detected jointly with the more concentrated compounds (diphenyl ether and biphenyl) without saturating the MS detector. Also, the GC–MS

technique cannot be implemented in portable equipment for on-line use at a thermosolar plant.

In a second part of the HTF project, for the first time, a headspace module coupled to a gas chromatography column in combination with an IMS (with a tritium ionization source) was optimized and fully validated to simultaneously quantify benzene and phenol in HTF. Quantification of these compounds was essential in order to check the stability of HTF (it was checked in terms of production of benzene and phenol) in a thermosolar plant and to protect workers and the environment from the harmful effect of these toxic compounds. The LOD and LOQ achieved with the method proposed were 0.011 and 0.038 g L^{-1} and 0.004 and 0.014 g L^{-1} for benzene and phenol, respectively. The precision of the method was evaluated in terms of repeatability and reproducibility with all values lower than 9.2% and 13.3%, respectively. Results demonstrated that benzene and phenol were generated in the HTF heating process, and its concentration increased with heating time (approx. 483 h). Results obtained with the proposed methodology were compared with results obtained using a GC-FID method and they showed no significant difference to those obtained by GC-FID revealed by using *t student test* [8].

An important aspect of this work is related to the resolution of the benzene peak which appears jointly with the RIP. Results obtained with 5 cm drift tube IMS were compared with another IMS instrument with a drift tube of 10 cm. Two samples of raw HTF were spiked with 0.081 g L^{-1} and 0.162 g L^{-1} of benzene were analysed using both instruments. **Figure 7** shows the separation of the benzene peak from the RIP signal could be improved using this longer 10 cm drift tube.

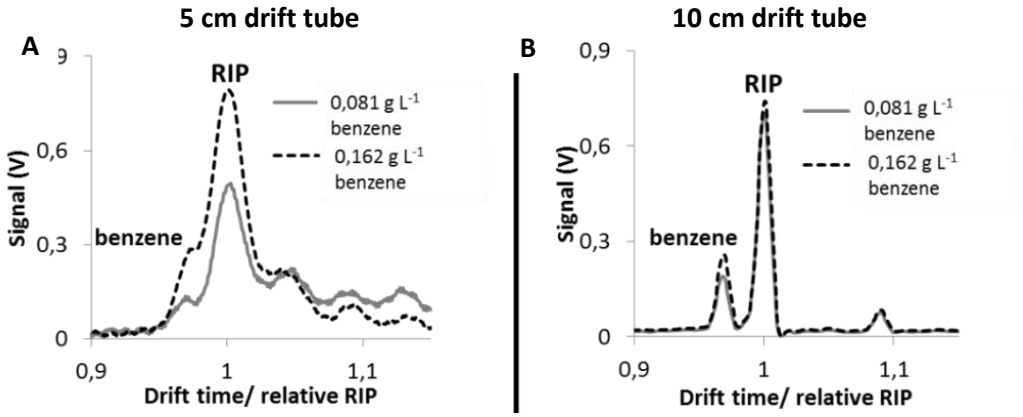

Fig. 7. Extracted IMS spectra of benzene using (A) 5 cm and (B) 10 cm drift tube length.

Also, narrower peaks were obtained when the 10 cm drift tube was used. Moreover, the resolution of the IMS was studied in this work calculating resolving power (Rp) for benzene peak which values were 63 for the 10 cm drift tube and 47 for the 5 cm drift tube. Therefore the resolution for the benzene using the longer drift tube (10 cm) was slightly improved.

Matrix effects posed by HTF samples on IMS signal were also investigated and only minor interference signals in the topographic plot were observed when HTF samples were analysed.

The third part of this block was developing a method to quantify low concentration of phenol in environmental samples in case of spillage. When direct analysis by HS-IMS was used a limit of detection of 0.94 μg mL^{-1} and 0.14 μg mL^{-1} was obtained for aqueous and soil samples, respectively. Special attention should be given to HS when it is selected as SIS, because of the low efficiency of HS detected in some cases. The potential of combining SPE before HS-IMS to improve the sensitivity of the method was studied in this work. A LOD value of 0.05 μg mL^{-1} was obtained by the proposed methodology when 15 mL of water sample was passed through HLB 60 mg SPE cartridge and eluted with 1 mL of dichloromethane without any observed interference from the solvent.

VI.3. Potential of Ion mobility techniques in the clinical field

Saliva is an attractive alternative to blood and urine for profiling and screening human subjects due to the non-invasive nature and the accessibility of the sample. Ion mobility techniques are sensitive instruments that have recently shown a higher applicability in the clinical and biomedical field. **Figure 8** illustrates the experimental diagram followed to determine analytes present in saliva samples by DMS and IMS.

Firstly, a DMS was used to determine toxics in a saliva sample in a non-invasive and a sensitive approach by using a polydimethylsilicone oral sampler to extract methanol, ethanol, ethylene glycol, 1,3-propandiol and γ-hydroxybutyric acid from samples of human saliva obtained using a passive-drool approach. The extracted compounds were recovered by thermal desorption, isolated by GC and detected with DMS, operating with a programmed dispersion field.

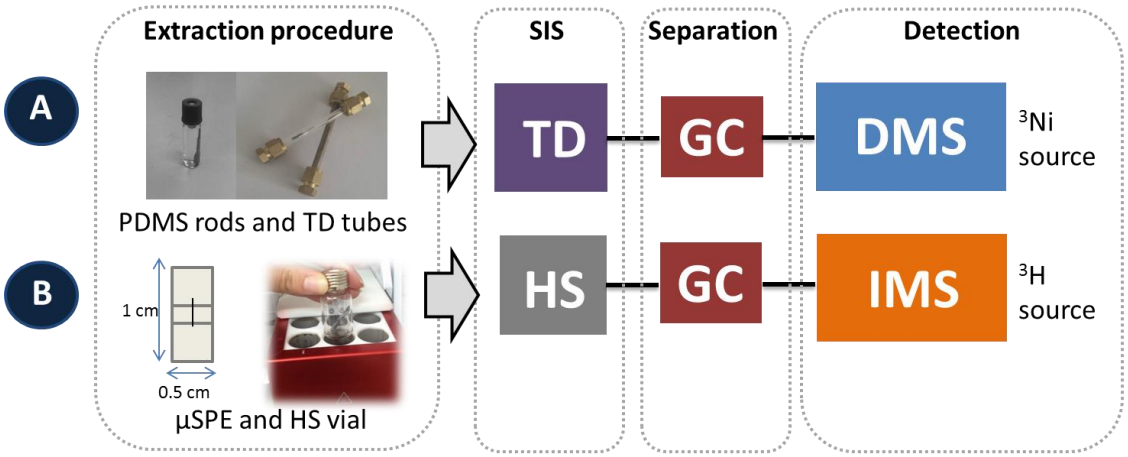

Fig. 8. Schema of the two methods used for the analysis (A) alcohols and sedatives by DMS and (B) toxics compounds by IMS.
PDMS: polydimethyl siloxane, µSPE: micro-solid phase extraction, HS: headspace, TD: thermal desorption, GC: gas chromatography, DMS: differential mobility spectrometry, IMS: ion mobility spectrometry.

Complex signal unobserved fragmentation behaviours were observed for the measurements carried out with the DMS. These yielded high-

mobility fragment peaks obscured within the reactant ion peak. Furthermore, compensation field maxima shifts were also observed, attributable to transport gas modification phenomena. Nevertheless, the robustness of the method developed is that the responses obtained indicated that in-vivo saliva sampling with TD-GC may be used to provide a semi-quantitative diagnostic screen over the toxicity threshold concentration ranges of 100 $mg.dm^{-3}$ to 3 $g.dm^{-3}$ [9].

Finally, a new method based on μSPE using a mixture of sorbents and their analysis by headspace-gas chromatography-ion mobility spectrometry (HS-GC-IMS) from oral fluid was developed to determine toxic compounds present in saliva. The preliminary step based on μSPE was included to avoid the interferences from moisture and matrix components of the sample and enhance sensitivity and selectivity.

The main limitation detected when measuring compounds with low proton affinity in humid environment is the effect on affecting their ionization process. Due to the lower proton affinity of benzene, toluene and butyraldehyde (<792.7 kJ mol^{-1}) their ionization can be problematic at the humid conditions generated in the headspace from the standard, which is later introduced into the ionization source of the IMS. This effect was considerably reduced when μSPE methodology was followed, avoiding the moisture from the sample and improving sensitivity of the method as shown in **Figure 9**. Once the extraction is performed, the desorption step was carried out in a headspace vial where the volatile compounds are desorbed and analysed by GC-IMS, providing enough separation between all the compounds. The method was fully validated in terms of sensitivity, precision and recovery. LODs and LOQs were in the range of 0.27-0.38 and 0.91-1.66 μg mL^{-1}, respectively. The relative standard deviations were <3.5% for retention time and drift time values. The recovery results (79-100%) indicate that the proposed method can be applied for toxic compound determination in saliva samples.

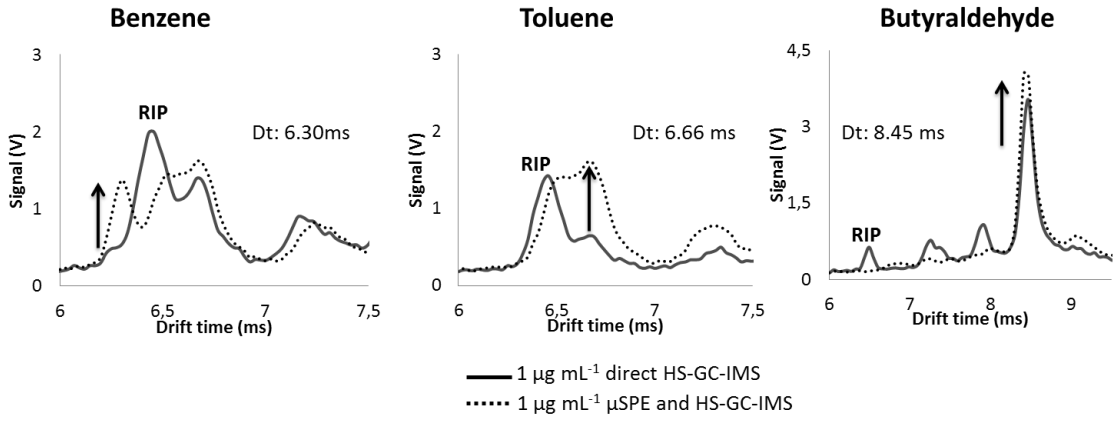

Fig. 9. IMS spectra of benzene, toluene and butyraldehyde obtained by direct HS-IMS analysis and also with extraction step with μSPE and desorption carried out in the HS autosampler and analysis by GC-IMS. An arrow indicates the characteristic peak ions of each analyte.

VI.4. Analysis of the ion mobility responses obtained in the experimental work

The following parts discuss aspects related to the IMS patterns that appeared in the IMS spectra and whose information can be extracted from it. **Table 2** summarizes the physical and chemical properties of all analytes measured by ion mobility techniques in the experimental work of this Doctoral Thesis.

VI.4.1. Monomer and dimmer product ions

As was exposed in *Block I Introduction*, gaseous molecules introduced into the IMS instruments are ionized by the ionization source (UV lamp, ^{3}H or ^{63}Ni). In the case of UV lamp (with energy of 10.6 eV), the molecules introduced must have an ionization energy below 10.6 eV to be ionized by the UV source of the IMS instrument used. For the radioactive sources (^{3}H or ^{63}Ni), the proton affinity of the target compounds must be higher than water proton affinity (690 kJ mol^{-1}). Thus, it is assumed that compounds

with ionization energy <10.6 eV (when using the UV-IMS) and high proton affinity (for ^{3}H or ^{63}Ni IMS instruments) dominate the ion mobility spectrum, even in low concentrations of the analyte.

When using IMS instruments with radioactive sources, reactant ions, $H^+(H_2O)_n$, which are formed from the supporting atmosphere by high energy primary electrons emitted by β source undergo collisions with volatile analytes molecules from the sample (M). The collisions yield an energetically excited intermediate adduct that may dissociate back to the reactants or may form product ions through other reaction pathways [2].

The protonated monomer, $MH^+(H_2O)_{n-x}$ is formed through association or transfer of a proton to the analyte molecule. As the concentration of the analyte molecules is increased further, the protonated monomer may be clustered with an additional analyte molecule forming a proton bound dimmer $M_2H^+(H_2O)_{n-x}$. In the equation (1) is shown the equilibrium between the reactions that take part in the positive mode inside the IMS instrument used in the experimental work.

$$M + H^+(H_2O)_n \leftrightarrow \mathbf{MH^+(H_2O)_{n-x}} + xH_2O + M \leftrightarrow \mathbf{M_2H^+(H_2O)_{n-x}} + xH_2 \quad (1)$$

In bold are signalled the monomer ion and dimer ion produced. Note that the likelihood of detecting an ion is controlled by the association of a molecule and a proton, which is governed by the enthalpy and entropy of the ion and by the level of moisture. When the clusters association is weak and the water levels are high the protonated dimer may undergo the reverse reactions to $MH^+(H_2O)_{n-x}$ and even dissociation to M and $(H_2O)_n$ [2]. Some ions (monomers and dimers) formed are unstable and in some cases they are not sufficiently long-lived. Consequently, their detection in IMS is limited.

Table 2. Physical and chemical properties of analytes measured by IMS instruments.

Family	IUPAC name	Molecular weight (g mol^{-1})	Boiling point (ºC)	Ionization energy (eV)	Proton affinity (kJ mol^{-1})	Vapor pressure* (mm de Hg)	IMS Instrument used
Alcohols	Methanol	32.04	64.7	10.84	754.3	127	^{63}Ni-DMS
	Ethanol	46.07	72.6	10.48	776	59.3	UV-IMS/ ^{63}Ni-DMS
	Ethylene glycol	62.07	197.3	10.55	815	0.06	^{63}Ni-DMS
	Propane-1,2-diol	76.09	188.2	10.80	876.2	0.13	^{63}Ni-DMS
Aldehydes	Butyraldehyde	72.11	74.8	9.82	792.7	111	^{3}H-GC-IMS
	Benzaldehyde	106.12	178.1	9.50	834.0	0.13	^{3}H-GC-IMS
	Tolualdehyde	120.14	204	9.33	851.8	0.25	^{3}H-GC-IMS
Aromatics	Benzene	78.11	80.05	9.24	750.4	94.8	UV-IMS/ ^{3}H-GC-IMS
	Ethylbenzene	106.17	136	8.77	788.0	9.6	UV-IMS
	Toluene	92.14	110.8	8.83	784.0	28.4	UV-IMS/ ^{3}H-GC-IMS
	m-Xylene	106.16	139	8.44	794.4	8.29	UV-IMS
	o-Xylene	106.16	144.5	8.56	796.0	6.61	UV-IMS
	p-Xylene	106.16	138.2	8.44	794.4	8.84	UV-IMS
Carboxylic acids	γ-Hydroxibutyric acid	104.10	295.6	nf	nf	0.13	^{63}Ni-DMS
Ketones	Acetone	58.08	56.3	9.70	812	231	UV-IMS
Phenols	Phenol	94.11	181.8	8.5	817.3	0.35	^{3}H-GC-IMS

The ionization energy of the UV lamp is 10.6 eV. Proton affinity of water is 691 kJ mol^{-1}. Vapor pressure values at 25 ºC, nf: not found data.

All substances measured in the IMS with ^{3}H source (benzene, toluene, butyraldehyde and phenol) showed only one monomer ion, MH^{+}. Benzene ions detected probably resulted from a charge transfer reaction with NO^{+}. Nevertheless, the rest of the compounds ions seemed to react with the RIP as their signals appeared after the RIP. Moreover, as was mentioned by other authors, higher temperatures do not favour the formation of large clusters (such as dimer ion) [10]. In the experimental work, drift tube temperatures in the range of 65-75 ºC were used. Only one single pattern was observed for the range of concentrations studied corresponding most probably to a monomer ion. A different behaviour was observed when benzaldehyde and tolualdehyde gave a monomer and also a dimer ion as can be observed in **Figure 10**.

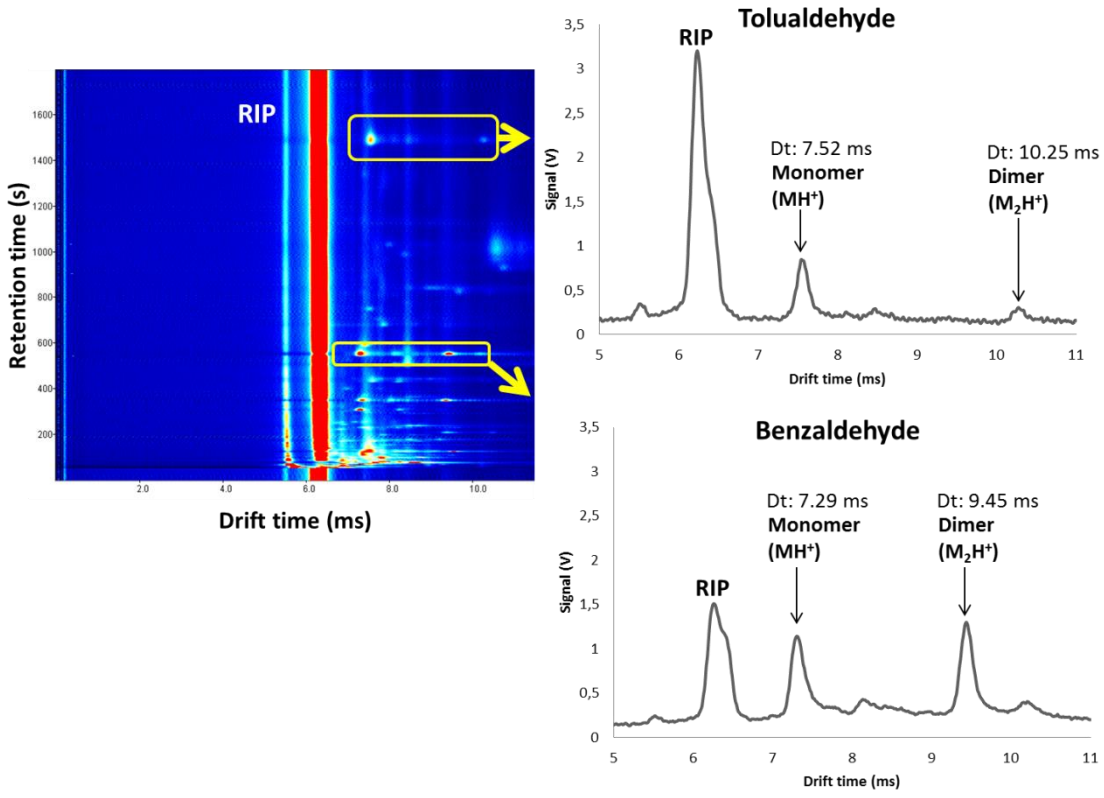

Fig. 10. A topographic plot of 5 μg mL^{-1} of benzaldehyde and tolualdehyde, obtained by μSPE and HS-IMS analysis. IMS spectra obtained for each of them at 562 s for benzaldehyde and 1514 s for tolualdehyde. The monomer and dimer peak ions obtained are signalled for each of them with an arrow.

A possible hypothesis to explain this fact is that, although unfavourable experimental conditions (75 ºC drift tube) to produce large ion products were followed, the dimer ions product formed with benzaldehyde and tolualdehyde were more stable in comparison with the rest of the compounds and could be detected by the Faraday plate of the IMS.

Related to the analytes that were measured by ^{63}Ni-DMS, methanol, ethanol, 1,2-propandiol and γ-hydroxybutyric acid yielded two peaks, hydrated protonated monomer cluster ion and a hydrated proton-bound dimer ion, while ethylene glycol produced a clearly resolved feature attributed to a proton bound dimer cluster ion and also an unresolved pattern obscured with the RIP that possibly could be a monomer ion. Aside from this, fragments ions were detected, because when the ionization potential of the analyte molecules is considerably lower than the reactant ions, charge transfer may be accompanied by fragmentation of the product ions, also favoured at 100 ºC DMS working temperature. These fragment ions were detected for ethanol which overlaid with the monomer ion and also were obscured with the RIP. GHB also showed a complex behaviour, two unresolved fragment ions were discernible with the RIP. Due to the complexity of patterns obtained, monomer and dimer of ethylene glycol, 1,2-propandiol and GHB were integrated for calibration and quantification purposes.

When the UV-IMS was used, no RIP appeared in the UV-IMS spectra due to the lower energy of the UV lamp, which was not enough to ionize N_2, H_2O and O_2. Our investigation was conducted at room temperature (25 °C), which explains the absence of fragmentation. When analyzing BTEX by UV-IMS, a single pattern was observed in the spectra which must correspond to a monomer ion. This intense peak observed is a M^+ ion already described for aromatic hydrocarbons [11]. Also, in some cases, shoulder peaks associated with the most intense peak appeared, most probably due to clusters-ion reactions and whose exact nature is unknown. It should be highlighted that the ion formation mechanism at ambient pressure is still unclear for many compounds, and the reactions that could take place are

not fully described [2]. The information about product ions that can be extracted from UV-IMS spectra is limited. In order to overcome limitations of UV-IMS, on one hand, using a pre-separation step such as GC can enhance resolution of the technique; or, by coupling a MS detector, more information about the ions produced in the IMS can be obtained.

References

[1] L. Arce, in R.A. Meyers (Editor), Encyclopedia of Analytical Chemistry. Applications, Theory and Instrumentation. John Wiley & Sons. Ltd, Chichester, 2011.

[2] G. A. Eiceman, Z. Karpas, H. H. Hill, Ion mobility spectrometry. 3rd ed. CRC press, Boca Ratón, 2013.

[3] L. Criado-Garcia, R. Garrido-Delgado, L. Arce, M. Valcárcel, A comparative study between different alternatives to prepare gaseous standards for calibrating UV-Ion Mobility Spectrometers, Talanta 111 (2013) 111-118.

[4] T. Mayer, H. Borsdorf, Accuracy of ion mobility measurements dependent on the influence of humidity, Anal. Chem. 86 (2014) 5069-5076.

[5] N. Krylova, E. Krylov, G. A. Eiceman, Effect of moisture on the field dependence of mobility for gas-phase ions of organophosphorus compounds at atmospheric pressure with field asymmetric ion mobility spectrometry, J. Phys. Chem. A 107 (2003) 3648-3654.

[6] W. Vautz, S. Sielemann, J. I. Baumbach, Determination of terpenes in humid air using ultraviolet air using ultraviolet ion mobility spectrometry, Anal. Chim. Acta 513 (2004) 393-399.

[7] L. Criado-Garcia, R. Garrido-Delgado, F. López, R. Peón, L. Arce, M. Valcárcel, Potential of ion mobility spectrometry versus FT-MIR and GC-MS to study the evolution of a heat transfer fluid after its heating process in a thermosolar plant, Microchem. J. 121 (2015) 163-171.

[8] L. Criado-Garcia, R. Garrido-Delgado, F. López, R. Peón, L. Arce, Simultaneous determination of benzene and phenol in heat transfer fluid by head-space gas chromatography hyphenated with ion mobility spectrometry, Talanta 144 (2015) 944-952.

[9] L. Criado-Garcia, D. M. Ruszkiewicz, G. A. Eiceman, C. Thomas, Rapid and non-invasive method to determine toxic levels of alcohols and ã-hydroxylbutyric acid in saliva samples by gas chromatography-differential mobility spectrometry , J. Breath Res. *in press* (2015).

[10] A. K. Viitanen, T. Mattila, J. M. Mäkelä, M. Marjamäki, O. Anttalainen, J. Keskinen, Experimental study of the effect of temperature on ion cluster formation using ion mobility spectrometry, Atmos. Res. 90 (2008) 115-124.

[11] D. Young, K. M. Douglas, G. A. Eiceman, D. A. Lake, M. V. Johnston, Laser desorption-ionization of polycyclic aromatic hydrocarbons from glass surfaces with ion mobility spectrometry analysis, Anal. Chim. Acta 453 (2002) 231-243.

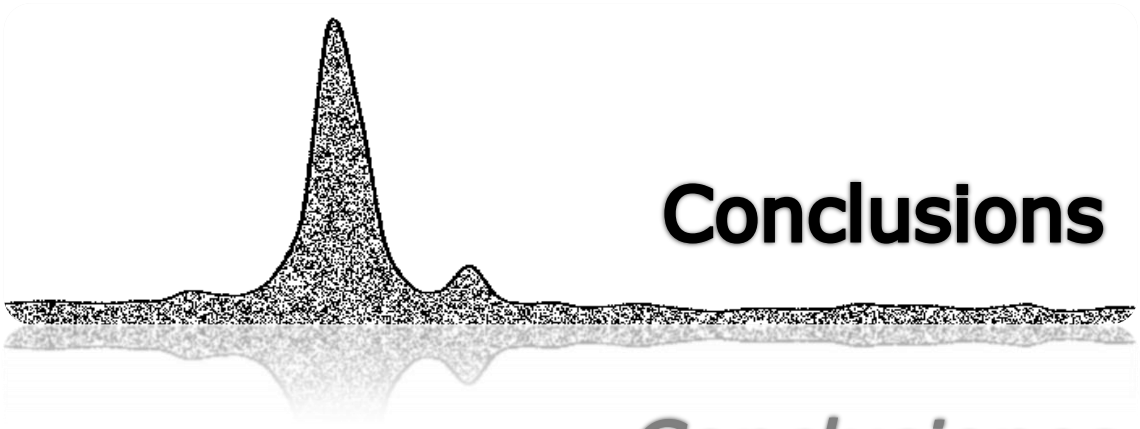

Conclusions

Conclusiones

The research carried out in this Doctoral Thesis is centered on the development of analytical methods focused on the determination of target compounds in environmental and clinical samples by ion mobility techniques. According to the general scheme of this Memory, the main conclusions of each of the issues addressed are presented as follows, divided into three sections. It starts by showing the potential of IMS for environmental analysis, followed by conclusions extracted from monitoring of HTF in thermosolar plant, and it ends with final remarks on applications of IMS in the clinical field.

Regarding the study of the suitability of **IMS for environmental analysis** (*Block III*), it should be pointed out that methods developed are simple, inexpensive and quick; data is obtained in a few minutes. The portability, especially needed for on-site analysis, is assured with this instrument. Experiments are carried out at atmospheric pressure and room temperature.

- ✧ The UV-IMS can be calibrated with **gaseous standards** (*Chapter 1*) generated by a head-space method when target analytes are present in liquid samples. For gaseous samples, exponential dilution set-up or generator gas calibrator devices are the most convenient systems to be used. The two home-made SISs gave us a cheap and a quick alternative to calibrate the IMS device, while the calibration gas generator allowed us to prepare lower concentrations of analyte in a more precise way. In many real applications the benefits of this automatic equipment do not outweigh the increased cost and time involved in the use of this device.
- ✧ Humidity is a variable to consider when IMS measurements are taken as it can affect the response of the detector. It has been demonstrated that the use of a PDMS membrane before the UV-IMS equipment significantly improves the precision values, LOD and LOQ in order to determine BTX in air (*Chapter 2*).

- ✧ The UV-IMS can be used as a sensor that provides a global response when measuring BTX in air samples. When a mixture of BTX was introduced inside the UV-IMS, only one peak was observed corresponding to a global signal sum of all analytes from the gaseous mixture appearing at a longer drift time compared to the individual signal of each analyte measured independently. This bigger product ion could not be resolved in the drift tube due to the structural similarities of the target analytes. Low **selectivity of the UV-IMS** was enhanced with a pre-separation step by using a Tenax TA column coupled to the ion mobility instrument (*Chapter 3*). This method offered a rapid and simple approach to enhance the basic properties that offer the IMS technology and contribute to reinforce its applicability for environmental analysis.

Controlling the lifetime of a heat transfer fluid over time in the thermosolar plant can be performed using the instruments UV-IMS working as a sensor, and HS-GC-^{3}H-IMS to quantify benzene and phenol in samples degraded HTF (*Block IV*).

- ✧ With the lab-scale reactor conditions at which HTF is exposed in the pipelines of a thermosolar plant could be reproduced. (*Chapter 4*). The UV–IMS instrument proved useful for the rapid monitoring of HTF degradation by obtaining a global IMS response. While the GC–^{3}H–IMS instrument additionally afforded the identification of degradation products such as phenol and benzene in degraded HTF. IMS results were also compared with two classical analytical techniques. FT-MIR spectra provide little information to distinguish between variably degraded HTF samples. By contrast, the GC–MS technique allows most HTF components to be detected. However, GC–MS cannot be used on-line at a thermosolar plant.
- ✧ Precision, sensitivity, selectivity and accuracy of the methodology proposed using HS-GC-^{3}H-IMS were acceptable to **quantify benzene and phenol in HTF samples** (*Chapter 5*). The results obtained by

HS-GC-^{3}H-IMS instrument showed no significant difference to those obtained by GC-FID revealed by using *t student test.*

- ✧ Direct analysis by HS-GC-IMS was used to determine phenol in contaminated water and soil samples. The sensitivity of the method was improved including **SPE before analysis by HS- IMS** (*Chapter 6*). The validation of the methodology in terms of sensitivity, precision and recovery proved effective in the environmental field for trace analysis.

Finally, regarding the **clinical field** (*Block V*), it has been shown that non-invasive sampling can be performed for health control of an individual. Ion mobility techniques (DMS and IMS) offer the advantage of a rapid response to determine low concentrations of analyte, compared to other techniques which are also used to determine toxic compounds in biological samples such as HPLC or GC- MS.

- ✧ A polydimethylsilicone rod was used to extract methanol, ethanol, ethylene glycol, propylene glycol and γ-hydroxybutyric acid from human saliva samples and analyzed by **TD-GC-DMS** operating with a programmed dispersion field (*Chapter 7*). This method provided a reliable approach for a rapid screen and evaluation protocol for a sedative and alcohols present at toxic levels. This pilot study demonstrates the effective recovery, detection and semi-quantitative estimation of all the analytes of interest selected in this work.
- ✧ A home-made **µ-SPE device** (*Chapter 8*) and HS-GC-IMS was used to determine analytes of different nature (benzene, toluene, butyraldehyde, benzaldehyde and tolualdehyde) present in saliva sample. It was really useful because a mixture of sorbents were combined in a single device to extract analytes polarity. With this pre-treatment, moisture and matrix components from saliva sample which can change ion chemistry inside the IMS were avoided. Consequently, the combination of **µ-SPE device** with the HS-GC-IMS improved considerably the selectivity and the sensitivity of the method.

La investigación desarrollada en esta Tesis Doctoral se ha enfocado en el desarrollo de métodos analíticos para la determinación de compuestos de interés en muestras ambientales y clínicas mediante el uso de técnicas de movilidad iónica. De acuerdo con el esquema general de esta Memoria, las conclusiones principales se han dividido en tres secciones, comenzando con el potencial de la IMS para el análisis ambiental, siguiendo con la monitorización de la vida útil de un fluido transmisor de calor usado en plantas termosolares y finalmente, se muestran las conclusiones obtenidas en los trabajos desarrollados en el ámbito clínico.

Con relación al estudio de la idoneidad de la **IMS para su aplicación en el análisis ambiental** (*Bloque III*), hay que destacar que los métodos desarrollados son simples, de bajo coste y rápidos ya que los datos se obtienen en pocos minutos. La portabilidad, especialmente necesaria para análisis in situ, está garantizada con este equipo ya que las medidas se llevan a cabo a presión atmosférica y a temperatura ambiente.

- ✧ El equipo de UV-IMS se puede calibrar con **patrones gaseosos** (*Capítulo 1*) generados con el método de espacio de cabeza si los analitos de interés están presentes en muestras líquidas. Para el caso de muestras gaseosas el sistema de dilución exponencial o el generador de gases automático son los métodos más indicados. Los métodos *home-made* ofrecen una alternativa barata y rápida para calibrar el equipo IMS, mientras que el generador de gases permite preparar concentraciones más bajas del analito de interés de una forma más precisa. En muchas aplicaciones reales no compensan los beneficios que aporta este equipo automático con respecto al incremento del coste y tiempo que supone el uso de este dispositivo.
- ✧ La **humedad** es una variable a estudiar cuando se realizan medidas de IMS ya que puede afectar a la respuesta del detector. Se ha demostrado que el uso de **una membrana de PDMS previa el equipo de UV-IMS** mejora significativamente los valores de precisión, LOD y LOQ para determinar BTX en aire (*Capítulo 2*).

- ✧ El equipo de UV-IMS se puede usar como un sensor que proporciona una respuesta global cuando se miden BTX en muestras de aire. La señal obtenida aparece a un tiempo de deriva mayor en comparación a la señal individual de cada analito ya que se forma un agrupamiento de los compuestos con mayor peso y carga total. La mezcla de los BTX no se pudo resolver en el tubo de deriva debido a las similitudes estructurales de los analitos presentes en la muestra. La baja **selectividad del equipo de UV-IMS** se mejoró acoplando una columna de Tenax TA al instrumento de movilidad iónica (*Capítulo 3*). Este método ofrece una aproximación rápida y sencilla para mejorar las propiedades básicas que ofrece la tecnología IMS y contribuyen a reforzar su aplicabilidad para el análisis medioambiental.

El control de la vida útil de un **fluido transmisor de calor** a lo largo del tiempo en las **planta termosolares** se puede realizar usando los instrumentos UV-IMS a modo de sensor y HS-GC-^{3}H-IMS para cuantificar benceno y fenol en muestras de HTF degradado (*Bloque IV*).

- ✧ Con el reactor diseñado se pudieron reproducir las condiciones a las que está expuesto el aceite HTF en las tuberías de una planta termosolar (*Capítulo 4*). El instrumento UV-IMS demostró ser útil para realizar un seguimiento rápido del proceso de degradación del aceite HTF monitoreando el incremento de la **señal global** que se obtiene al medir el HTF. Por otro lado, el instrumento GC-^{3}H-IMS permitió identificar el fenol y benceno en el aceite HTF degradado. Los resultados obtenidos se compararon con dos técnicas analíticas clásicas. Los espectros obtenidos con FT-MIR proporcionaron poca información para distinguir entre diferentes muestras de aceite HTF degradado. Por el contrario, la técnica GC-MS permitió la detección de la mayoría de los componentes del aceite HTF. Sin embargo, el equipo de GC-MS no se puede usar en línea en una planta termosolar.

- ✧ La precisión, sensibilidad, selectividad y exactitud usando HS-GC-^{3}H-IMS fueron aceptables para **cuantificar benceno y fenol en muestras de aceite HTF** (*Capítulo 5*). Los resultados obtenidos usando este instrumento no mostraron diferencias significativas a los obtenidos por GC-FID usando el test de la *t de student*.
- ✧ El análisis directo por HS-GC-IMS se usó para determinar fenol en muestras de aguas y suelos contaminados. La sensibilidad del método se mejoró incluyendo la **SPE antes del análisis mediante HS-IMS** (*Capítulo 6*). La validación de la metodología en términos de sensibilidad, precisión y recuperación demostró su eficacia en el campo del ambiental.

Por último, en relación con el **campo clínico** se ha demostrado como el control de la salud de un individuo se puede realizar a través de un muestreo no invasivo. Las técnicas de movilidad iónica (DMS e IMS) ofrecen la ventaja de ofrecer una respuesta rápida así como poder determinar bajas concentraciones de analito en comparación con otras técnicas que también se utilizan para determinar compuestos tóxicos en muestras biológicas tales como HPLC o GC-MS (*Bloque V*).

- ✧ El uso de un sorbente de polidimetilsilicona para extraer metanol, etanol, etilenglicol, propilenglicol y ácido γ-hidroxibutírico de muestras de saliva humana y su determinación mediante **TD-GC-DMS** (*Capítulo 7*) con un campo de dispersión programado, proporcionó un enfoque fiable para realizar una evaluación rápida de la presencia de un sedante y de alcoholes presentes a niveles tóxicos. Este estudio piloto demuestra la recuperación efectiva, detección y estimación semi-cuantitativa de todos los analitos de interés seleccionados en este trabajo.
- ✧ El uso de un **dispositivo de μ-SPE** (*Capítulo 8*) *home-made* y un equipo de HS-GC-IMS para determinar compuestos tóxicos de diferente naturaleza (benceno, tolueno, butiraldehído, benzaldehído y tolualdehído) en muestras de saliva, resultó muy útil ya que se combinaron mezclas de sorbentes para retener analitos de distinta

polaridad. Con esta etapa previa, se eliminó la interferencia de la humedad y los componentes de la matriz que pueden cambiar la química de iones dentro del IMS. La incorporación de la etapa previa de μ-SPE mejoró la selectividad y la sensibilidad del método HS-GC-IMS.

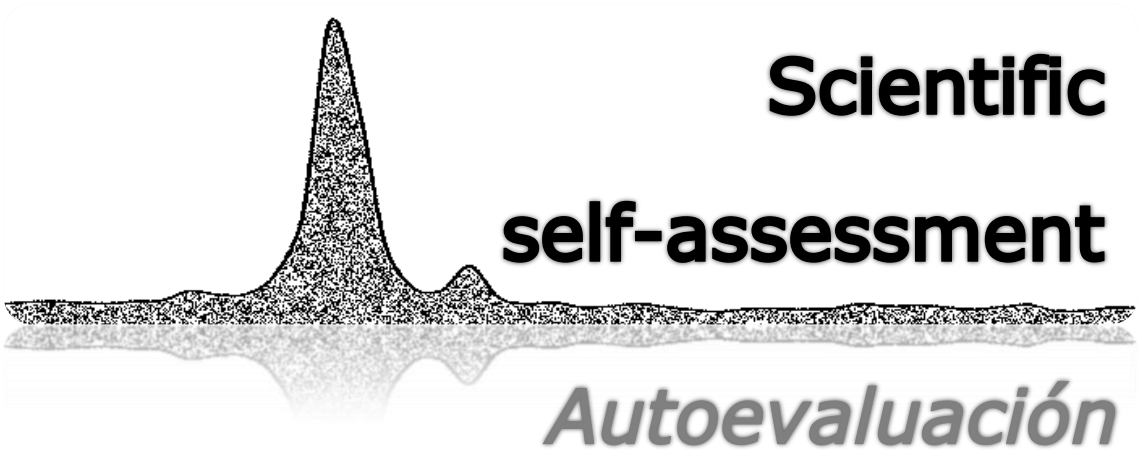

Scientific self-assessment

Autoevaluación científica

The experience gained during the development of this Doctoral Thesis and the preparation of this Memory, has provided an objective overview of the work presented here. In this part, a critical assessment of the results achieved has been conducted to evaluate the main contributions that the work can offer to the scientific community, as well as the drawbacks and shortcomings that might be addressed in future research.

The main contributions of this Doctoral Thesis are devoted to new methods development to be applied in the environmental and clinical fields.

In the work in which **methods to generate gaseous standards** (*Chapter 1*) are discussed, two home-made systems to introduce volatile compounds to the UV-IMS have been proposed; these two SISs were compared with a commercial gas generator.

- ✓ One main contribution of the headspace system proposed was a simple modification of the system, used before in our researching group. This modification prevented the gas flow from falling on the standard liquid, allowing liquid standards to be measured without overloading the IMS signal. Finally, the attractiveness of the home-made methods proposed for liquid and gaseous samples are mainly the speed, low cost, simplicity and acceptable sensitivity values throughout the operational range studied for all compounds studied.
- × The main limitation is that the LODs, LOQs, and RSD values were higher for both home-made methods compared with the values obtained using the calibration gas generator, due to possible inaccuracies in the preparation of gaseous standards. The separation of signals from similar compounds in a mixture was not achieved with this instrument. A pre-separation step can be included to improve selectivity as was shown in *Chapter 3*.

The high humidity values have a negative influence on the signal obtained by IMS. In this memory it was demonstrated that, by coupling a

membrane set-up to the UV-IMS, it was easy to avoid the effect of humidity on the IMS signal (*Chapter 2*).

- ✓ The main advantage of the method developed was that BTX signals from gaseous samples with high humidity content were identified in the spectra. LOD, LOQ and RSD values improved significatively when using the membrane set-up coupled to the UV-IMS when measuring gaseous samples with a higher % RH value.
- × A drawback of the method proposed is the analyte losses detected. Further work will be done with other membrane materials to overcome this problem and enhance analytical performance of this proposed set up. Besides this, other compounds from other families should be studied to demonstrate the potential of the membrane set-up.

The low selectivity of the methods developed by using UV-IMS was overcome by including a **pre-separation step coupled to the UV-IMS** (*Chapter 3*).

- ✓ With the Tenax TA column, analytes present in air samples were retained in the sorbent and separated by applying thermal desorption before their introduction to the UV-IMS. Sensitivity and selectivity was considerably improved.
- × The main shortcoming is that the separation achieved was not enough to differentiate compounds which have common chemical properties, as is the case with isomers of xylene and ethylbenzene. Other alternatives which can provide greater selectivity will be tested in future works.

Main contributions and limitations in relation to the **monitoring of degradation compounds produced in the thermosolar plant** (*Chapter 4 and 5*), are summarized below.

- ✓ A highlight of the method developed is that fingerprints of raw and degraded HTF obtained allow differentiating HTF samples by their analysis via UV-IMS. Degradation products generated in the HTF fluid

- ✓ could be identified and quantified by HS-GC-IMS without any sample preparation step. The main attractiveness of the IMS techniques used is its rapid analysis and responses, and also its portability to use these instruments for on-line measurements in the thermosolar plant.
- × A limitation of the method proposed is that compounds with a higher boiling point could not be identified with IMS (UV-IMS and HS-GC-IMS). Moreover, quantification was only achieved when using the IMS with a GC column. By contrast, these compounds could be detected by GC-MS and quantified by GC-FID.

Once demonstrated that prolonged use of HTF produces toxic compounds, methods to determine phenol in environmental samples are needed. A method which combines **SPE** with **HS-GC-IMS** analysis (*Chapter 6*) was proposed, sensitivity of the method was significatively improved.

- ✓ With the proposed methodology, LOD and LOQ values were reduced by one order of magnitude compared with the results obtained when only HS-GC-IMS was used to allow the quantification of low concentration of phenol in environmental water samples.
- × The main drawback of the proposed method is that the SPE step was performed off-line and is difficult to automate it.

In the last block of this memory, a sensitive method was developed using thermal desorption and gas chromatography coupled to **differential mobility spectrometry** (TD-GC-DMS) **to determine a sedative and alcohols in saliva samples**, a sensitive methodology was developed (*Chapter 7*).

- ✓ The use of TD-GC-DMS allowed a rapid detection of a sedative and alcohols present at toxic levels from saliva sample. These analytes could not be determined by HS-GC-IMS. This pilot study demonstrates the semi-quantitative estimation of all the toxic compounds of this work. Furthermore, alcohol and GHB product ions and their fragment ions were reported.

- × The study of fragmentation mechanisms, products and their ramifications for alcohol determination by DMS along with the development of detection and signal processing algorithms will be addressed in future works. As well as this, a clinical pilot study within an appropriate toxicology unit is needed in order to assess the efficacy of this approach in patients.

Potential toxic compounds in saliva were extracted by a **new preparation methodology based on µ-SPE** and analysed by HS-GC-IMS (*Chapter 8*).

- ✓ The main advantage of the extraction procedure proposed is that the home-made µ-SPE device could retain selectively analytes of a very different nature. Besides that, the autosampler of the GC-IMS instrument was used to desorb the analytes retained in the sorbent. Sensitivity and selectivity was improved when using µ-SPE compared with direct measurement of saliva headspace. The developed method could be used in future works to determine drugs and other toxic compounds.
- × The main disadvantage of the proposed method is the inefficient desorption achieved from the sorbent to the headspace of the vial for compounds with a higher boiling point (benzaldehyde and tolualdehyde), this limitation could be solved heating at temperatures higher than 80 ºC.

La experiencia adquirida durante el desarrollo de esta Tesis Doctoral y la preparación de esta memoria, ha permitido obtener una visión objetiva de los trabajos que aquí se presentan. En esta sección, se ha realizado una evaluación crítica de los resultados obtenidos, las principales contribuciones que los trabajos experimentales pueden ofrecer a la comunidad científica y, los inconvenientes y las deficiencias detectadas, que podrían abordarse en futuros proyectos de investigación.

Las principales aportaciones de esta Tesis Doctoral están centradas en el desarrollo de nuevos métodos para su aplicación en el campo ambiental y clínico.

En el trabajo en el que se incluyen **métodos** nuevos **para generar estándares gaseosos** (*Capítulo 1*), se han propuesto dos sistemas no comerciales para introducir los compuestos volátiles al equipo UV-IMS, estos dos SISs se compararon con un generador de gas comercial.

- ✓ La principal mejora del sistema de espacio de cabeza propuesto consistió en una simple modificación del sistema usado anteriormente en nuestro grupo de investigación. Esta modificación impidió que el flujo de gas incidiera sobre el estándar líquido, evitando la saturación de la señal de IMS. El atractivo de los métodos *home-made* propuestos para muestras líquidas y gaseosas fueron principalmente la rapidez, el bajo coste, la simplicidad y los valores de sensibilidad aceptables en el rango de concentraciones estudiado para todos los compuestos que fueron objeto de análisis.
- × La principal limitación encontrada reside en los valores de LOD, LOQ y RSD los cuales fueron más altos para los métodos *home-made* en comparación con los valores obtenidos utilizando el generador de gases comercial, debido a posibles irreproducibilidades en la preparación de los estándares gaseosos. Además usando el equipo de UV-IMS no se consiguió la separación de las señales de compuestos similares en una mezcla. En el caso de necesitar mejorar la

selectividad del método optimizado se debe incluir una etapa de pre-separación tal y como se ha demostrado en el *Capítulo 3*.

Los altos valores de humedad tienen una influencia negativa en la señal obtenida con los equipos de IMS. En esta memoria se ha demostrado que acoplando una **membrana al equipo de UV-IMS se evita fácilmente la influencia de la humedad** en la señal de IMS (Capítulo 2).

- ✓ La principal ventaja del método desarrollado fue que las señales características de BTX de muestras gaseosas con alto contenido de humedad se identificaron en los espectros de IMS. Los valores de LOD, LOQ y RSD se mejoraron significativamente cuando se utilizó el sistema de membrana acoplado a la UV-IMS en muestras gaseosas que presentaban valores altos de humedad relativa.
- × Un inconveniente del método propuesto es referente a la pérdida de señal de los analitos detectada con el uso del sistema de membrana. En un trabajo futuro, se probarán otros tipos de membrana para poder superar este problema y mejorar así el rendimiento analítico de este método propuesto. Además se estudiará el potencial del sistema de membrana acoplado al equipo UV-IMS con otros analitos.

La baja selectividad de los métodos usando equipos de UV-IMS se mejoró incluyendo una **etapa de pre-separación acoplado al equipo UV-IMS** (*Capítulo 3*).

- ✓ Con la columna de Tenax TA, los analitos presentes en las muestras de aire se retuvieron en el sorbente y se separaron mediante la aplicación de desorción térmica antes de su introducción en el UV-IMS. La sensibilidad y la selectividad se mejoró considerablemente.
- × La principal limitación detectada es que la separación lograda no fue suficiente para diferenciar los compuestos que tienen propiedades químicas comunes, como es el caso de los isómeros de xileno y etilbenceno. La sustitución de la columna Tenax TA por otras que aporten mayor selectividad se probaran en futuros trabajos.

Las principales aportaciones y las deficiencias de los métodos propuestos para la **monitorización de los compuestos de degradación que se producen en el fluido transmisor de calor** usado en las plantas termosolares (*Capítulo 4 y 5*) se resumen a continuación.

- ✓ Un punto destacado del método desarrollado es su utilidad como método de *screening* gracias a la obtención de las "huellas espectrales" para la diferenciación de muestras de HTF crudo y degradado mediante su análisis por UV-IMS. Los productos de degradación generados en el HTF se pudieron identificar y cuantificar por HS-GC-IMS sin ninguna etapa adicional de preparación de la muestra. El principal atractivo de las técnicas IMS utilizadas es la rapidez de análisis y respuesta, así como su portabilidad, pudiendo utilizar estos instrumentos para mediciones en línea en la planta termosolar.
- × Una limitación del método propuesto es que los compuestos con un punto de ebullición más alto no se pudieron identificar con los equipos de UV-IMS o HS-GC-IMS. Por otra parte, la cuantificación del benceno y fenol solo se logró cuando se utilizó el IMS con una columna de gases. Por el contrario, todos los compuestos de degradación se pudieron detectar por GC-MS aunque el benceno y el fenol solo se pudieron cuantificar en todas las muestras usando GC-FID.

Una vez demostrado que el uso prolongado de HTF produce compuestos tóxicos tales como benceno y fenol, se debe disponer de métodos que sean capaces de determinarlos en muestras ambientales. Para ello se propuso un método combinando **SPE** con el análisis **HS-GC-IMS** (*Capítulo 6*) mejorando considerablemente la sensibilidad.

- ✓ Con el método propuesto se obtuvieron LOD y LOQ de un orden de magnitud inferior a los obtenidos cuando solo se usa el equipo de HS-GC-IMS; pudiendo de esta forma cuantificar concentraciones más bajas de fenol en muestras de agua.

- × El principal inconveniente del método propuesto es que la etapa de SPE se realizó de forma *off-line* y resulta difícil automatización.

En el último bloque de esta memoria se desarrolló una metodología sensible usando desorción térmica y cromatografía de gases acoplado a la **espectrometría de movilidad diferencial** (TD-GC-DMS) **para determinar un sedante y alcoholes en muestras de saliva** (*Capítulo 7*).

- ✓ El uso de TD-GC-DMS permitió la detección rápida de un sedante y alcoholes presentes a niveles tóxicos en muestras de saliva. Sin embargo el mismo grupo de compuestos no se pudieron determinar por HS-GC-IMS. Este estudio piloto demuestra la estimación semi-cuantitativa de todos los compuestos seleccionados a niveles a los que son potencialmente tóxicos. Además, se estudiaron los iones producto de los alcoholes y sus fragmentos.
- × El estudio de los mecanismos de fragmentación, productos y sus ramificaciones para la determinación de alcohol por DMS, junto con el desarrollo de algoritmos de detección y procesamiento de señales se abordarán en un futuro trabajo. Además, se necesita un estudio clínico piloto dentro de una unidad de toxicología apropiada con el fin de evaluar la eficacia de esta metodología en pacientes.

Finalmente, una serie de compuestos tóxicos fueron extraídos de muestras de saliva mediante el uso de una nueva metodología basada en el **uso de µ-SPE y análisis mediante HS-GC-IMS** (*Capítulo 8*).

- ✓ La principal ventaja del procedimiento de extracción se atribuye a que el dispositivo µ-SPE *home-made* retiene selectivamente analitos de muy diferente naturaleza presentes en muestras de saliva, debido a la incorporación de sorbentes de distinta polaridad. Además en el automuestreador de HS del GC-IMS se desorbieron los analitos retenidos en el sorbente. La sensibilidad y la selectividad se mejoró al utilizar µ-SPE en comparación con la medición directa del espacio de cabeza producido al incorporar un volumen de saliva en un vial del

equipo. El método desarrollado se podría utilizar en futuros trabajos para determinar fármacos y otros compuestos tóxicos.

- La principal desventaja del método propuesto es la ineficiente desorción lograda desde sorbente al espacio de cabeza del vial de los compuestos con un punto de ebullición más alto (benzaldehído y tolualdehído), esta limitación se podría solucionar calentando a temperaturas superiores a 80 ºC.

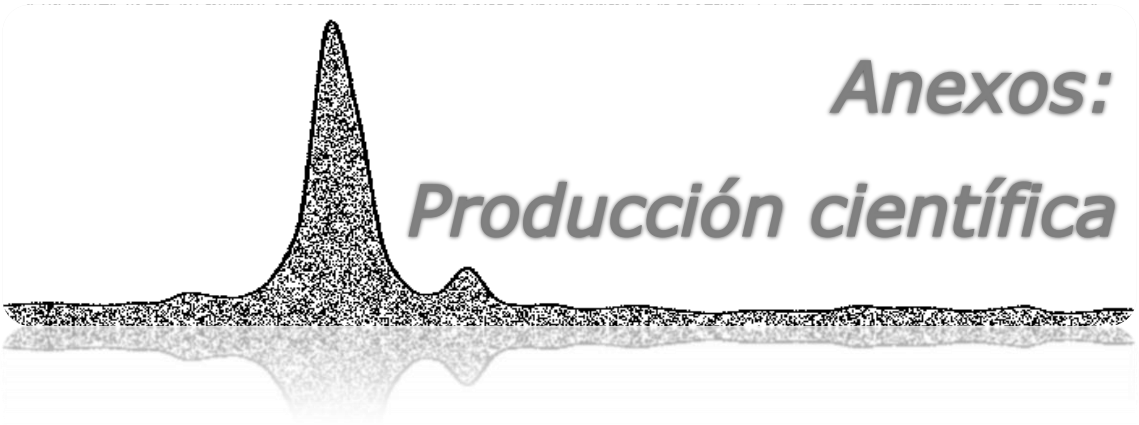

Anexos:
Producción científica

ANEXO A

Publicaciones científicas derivadas de la Tesis Doctoral

1. A comparative study between different alternatives to prepare gaseous standards for calibrating UV-Ion Mobility Spectrometers.

L. Criado-García, R. Garrido-Delgado, L. Arce, M. Valcárcel

Talanta 2013 (111) 111-118

2. Potential of ion mobility spectrometry versus FT-MIR and GC-MS to study the evolution of a heat transfer fluid after its heating process in a thermosolar plant.

L. Criado-García, R. Garrido-Delgado, F, López, R. Peón, L. Arce, M. Valcárcel

Microchemical Journal 2015 *(*121)163-171

3. Simultaneous determination of benzene and phenol in heat transfer fluid by head-space gas chromatography hyphenated with ion mobility spectrometry.

L. Criado-García, R. Garrido-Delgado, F, López, R. Peón, L. Arce, M. Valcárcel

Talanta 2015 (144) 944-952

4. Rapid and non-invasive method to determine toxic levels of alcohols and γ-hydroxylbutyric acid in saliva samples by gas chromatography-differential mobility spectrometry

L. Criado-García, D.M. Ruszkiewicz, G.A. Eiceman, C.L.P. Thomas.

Journal of Breath Research (in press)

5. Membrane set up combined with UV-IMS device to improve analytical performance and avoid humidity interference on the determination of BTX compounds in gaseous samples

L. Criado-García, L. Arce, M. Valcárcel

Submited to *Journal of Chromatography A*

6. Solid phase extraction to enhance sensitivity when headspace-gas chromatography-ion mobility spectrometer is used

L. Criado-García, L. Arce, M. Valcárcel

Submited to *Analytical Methods*

7. Extraction of toxic compounds from human oral fluid by magnetic stirring assisted micro-solid phase extraction (μ-SPE) step followed by headspace-gas chromatography-ion mobility spectrometry (HS-GC-IMS)

L. Criado-García, L. Arce, M. Valcárcel

In progress

8. Development and optimization of analytical method to determine benzene and toluene in air samples using Tenax TA coupled to UV-Ion Mobility Spectrometry

L. Criado-García, N. Almofti, L. Arce, M. Valcárcel

In progress

ANEXO B

Presentación de comunicaciones a congresos

IX Jornadas Doctorales Andaluzas (Mengíbar, España), del 18 al 23 de Septiembre de 2011

1. Presentación oral y póster: Determinación de compuestos orgánicos volátiles de trabajo mediante movilidad iónica (IMS) y análisis de movilidad diferencial (DMA), L. Criado-García.

13as Jornadas de Análisis Instrumental (JAI) (Barcelona, España), del 14 al 16 de Noviembre de 2011

2. Presentación poster: Comparative study of ion mobility techniques to determine VOCs in working air samples using atmospheric simulation chambers, L. Criado-García, L. Arce, E. Montoya, S. López-Vidal, M. Valcárcel.

3. Presentación poster: Rapid on-line measurement of hazardous BTEX by a home-made PDMS membrane coupled to UV Ion Mobility Spectrometry, L. Criado-García, R. Garrido-Delgado, L. Arce, E. Montoya, S. López-Vidal, M. Valcárcel.

II Congreso Científico de Investigadores en Formación (Córdoba, España), del 9 al 10 de Abril de 2012

4. Presentación oral: Determinación de compuestos orgánicos volátiles en ambientes de trabajo mediante técnicas analíticas de vanguardia: Espectrometría de Movilidad Iónica (IMS) y Análisis de Movilidad Diferencial (DMA), L. Criado-García, L. Arce, M. Valcárcel.

XXII Reunión Nacional de Espectroscopia. VI Congreso Ibérico de Espectroscopia (Córdoba, España), del 17 al 20 de Septiembre de 2012

5. Presentación oral: UV- Ion Mobility Spectrometry as screening technique to determine Volatile Organic Compounds in workplace air samples, L. Criado-García, L. Arce, M. Valcárcel.

22th International Conference on Ion Mobility Spectrometry (Boppard, Alemania), del 21 al 26 de Julio de 2013

6. Presentación oral: Validation of an Ion Mobility Spectrometric method for monitoring gaseous compounds in workplaces, L. Criado-García, R. Garrido-Delgado, L. Arce, M. Valcárcel.

XXIII Reunión Nacional de Espectroscopia. VII Congreso Ibérico de Espectroscopia (Logroño, España), del 9 al 11 de Julio de 2014

7. Presentación poster: Ion Mobility Spectrometry as a vanguard technology to assess the quality of Heat Transfer Fluid, L. Criado-García, R. Garrido-Delgado, L. Arce, M. Valcárcel.

23th International Conference on Ion Mobility Spectrometry (Asheville, EEUU), del 27 Julio al 1 de Agosto de 2014

8. Presentación oral: Comparative study of IMS, GC-FID/MS and IR techniques to identify a mixture of organic compounds in a Heat Transfer Fluid, L. Criado-García, R. Garrido-Delgado, L. Arce, M. Valcárcel.

9. Presentación oral: Rapid and non-invasive method to determine toxic substances present in saliva samples by gas chromatography- differential mobility spectrometry, L. Criado-García, D.M. Ruszkiewicz, C.L.P. Thomas.

24th International Conference on Ion Mobility Spectrometry (Córdoba, España), del 26 al 30 de Julio de 2015

10. Presentación poster: Solid phase extraction as an alternative to enhance sensitivity of ion mobility spectrometry: determination of phenol in environmental samples as a case of study, L. Criado-García, L. Arce.

11. Presentación poster: Determination of benzene, toluene, ethylbenzene in gaseous samples using sorbent trap coupled to UV-IMS, L. Criado-García, N. Almofti, L. Arce.

18th edition the European Conference on Analytical Chemistry, EUROANALYSIS (Burdeos, Francia), del 6 al 10 de Septiembre de 2015

12. Presentación poster: A new approach to determine toxic substances present in saliva samples by ion mobility spectrometry, L. Criado-García, L. Arce, M. Valcárcel.

ANEXO C

Pósters

DETERMINACIÓN DE COMPUESTOS ORGÁNICOS VOLÁTILES (VOCs) MEDIANTE TÉCNICAS ANALÍTICAS DE VANGUARDIA

*Laura Criado García**
Lourdes Arce Jiménez y Miguel Valcárcel Cases
Departamento de Química Analítica, Grupo FQM-215, Campus de Rabanales, Universidad de Córdoba

OBJETIVO

Diseñar métodos de muestreo acoplados a técnicas de movilidad iónica para la determinación de **compuestos orgánicos volátiles (VOCs)** en muestras de aire tomadas en el interior de los lugares de trabajo mediante dos **tecnologías analíticas de vanguardia:**

Análisis de Movilidad Diferencial (DMA)

Se basa en la **clasificación** de las partículas cargadas o iones en en función de su movilidad eléctrica.

Espectrometría de Movilidad Iónica (IMS)

Los iones formados a presión atmosférica migran en un campo eléctrico en dirección contraria de un gas de deriva. Los iones de distinta **masa**, **carga** y **forma** alcanzan **velocidades diferentes** y por tanto **se separan**.

OBJETIVOS ESPECIFICOS

- Estudio del potencial del equipo de IMS y DMA
- Diseñar sistemas de captación de contaminantes
- **Calibrar los equipos con patrones de analitos puros**
- Comparar de los resultados obtenidos para ambas tecnologías: IMS y DMA
- Obtener información cualitativa e índices globales de los VOCs estudiados

EXPERIMENTAL : Espectrómetro de movilidad iónica UV

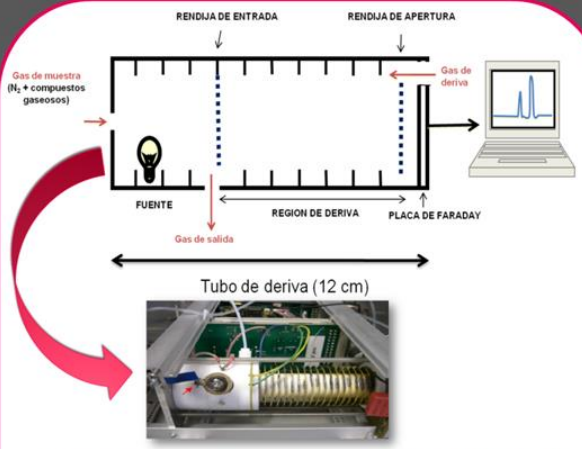

1. Los iones se cargan positivamente por una **fuente de ionización** (lámpara UV)
2. Los iones cargados se mueven a través de la **región de deriva** en un campo eléctrico débil a presión atmosférica
3. Llegan al detector y son detectados por la **placa de Faraday**

RESULTADOS

Un ejemplo de aplicación ya desarrollada como trabajo experimental de la tesis doctoral es la **generación de un patrón gaseoso de etanol medido por UV- IMS**

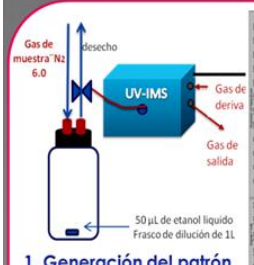

1. Generación del patrón gaseoso de etanol mediante en método de DILUCIÓN EXPONENCIAL

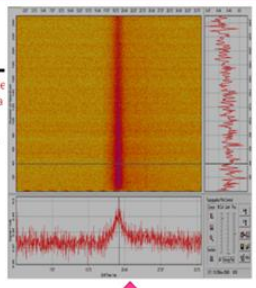

2. Espectro de etanol obtenido mediante UV-IMS

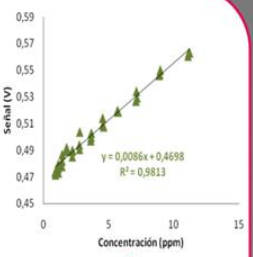

3. Curva de calibración

CONCLUSIONES

Inconvenientes	Ventajas
Interpretación de resultados	Rápida
Interacción ión molécula	Versátil
	Económica

* a42crgal@uco.es

Comparative study of Ion Mobility Techniques (Differential Mobility Analyzer and Ion Mobility Spectrometry) to determine VOCs in working air samples using EUPHORE atmospheric simulation chambers

L.R. Criado-García [1], R. Garrido-Delgado [1], E. Montoya [2], S. López-Vidal [2], L. Arce [1], M. Valcárcel [1]
[1]Department of Analytical Chemistry. Annex C-3 Building. Campus Rabanales. University of Córdoba. 14071-Córdoba. Spain. E-mail: qa1mejob@uco.es
[2]RAMEM S.A. 28027-Madrid.Spain. /www.ioner.eu/

DIA-P04

Objective

This work focuses on extending the range and versatility of two new vanguard techniques UV-DMA and UV-IMS for the determination of atmospheric pollutants in order to be an alternative to classical analysis method (such as GC-MS and FTIR). All the experiments were performed in the EUPHORE photoreactor chambers which simulate atmospheric conditions such as humidity, temperature, photoionization, pressure and other parameters. In this simulation chamber, it is possible to determine real concentrations of pollutants and their generated products.

Fundamentals

UV-IMS

The ions generated by an UV ionization source move in a weak electric field at atmospheric pressure towards the drift region. During their drift they collide with a drift gas flowing in the opposite direction. A Faraday plate used as detector is positioned at the end, where ions are separated depending on their shape, charge and mass. The number of ions reaching the detector is a measure of the concentration of the analyte.

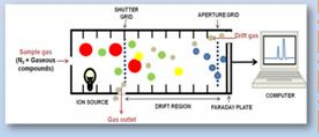

UV-DMA

A DMA can be seen as a wind tunnel where ions with different electrical mobilities (i.e., sizes) are separated through the superposition of two perpendicular forces, one given by a high sheath flow rate and the other by an electric field. The combination of both forces is responsible of the Resolving Power (RP) achievable by the instrument. Ramen DMAs specially developed for molecules achieve a RP close to 60, but higher RP will be reached with future developments .

Experimental

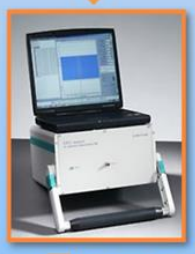

➢ Each simulation chamber consits of **half spherical Teflon bag** with a volume of about **200 m³**. Ports for input of the reactants and sampling lines for the analytical instruments are located on the floor of the chamber.
➢ The chamber is equipped with atmospheric sensors and conventional analytical instrumentation: GC-MS, GC-MS/MS, GC-FID, GC-ECD, GC-PID and HPLC. There are also state-of-the-art in-situ measurement techniques such as long-path Differential Absorption Spectroscopy (DOAS), long-path FT-IR and Tunable Diode Laser.

Working conditions:
- Sample gas 100 mL min^{-1} of air
- Drift gas 100 mL min^{-1} of N_2 6.0

Working conditions:
- Sample gas 450 mL min^{-1} of air
- Sheath flow rate 160 L min^{-1} of air

Results

Acetone, formaldehyde, benzene, toluene and isomers of xylene were measured under experimental conditions with rutine instrumentation and vanguard techniques proposed in this work: IMS and DMA.

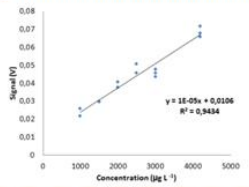

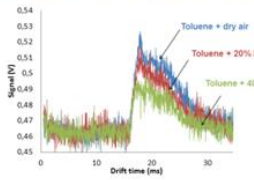

Toluene as an example

Calibration curves performed in both equipments

Limits of detection obtained were under Permisive Exposure Limit values (PEL). So these technologies can be used to determine this analyte in air.

	LOD (µg L^{-1})	LOQ (µg L^{-1})
UV-IMS	568	1894
UV-DMA	129	428
FTIR	5.4	-
GC	1.54	3.01

PEL = 200 mg L^{-1}

A preconcentration system and a more energetic ionization source (e.g. tritium) could be used to improve sensibility.

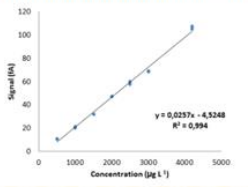

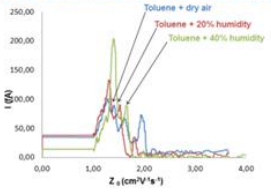

Study of the influence of the humidity over measurement of toluene for both techniques

Toluene (4.25 mg L$^{-1}_{(g)}$) was measured in humid air (20 or 40 % of humidity). For both techniques humidity strongly affects the results obtained. A reduction of the signal in the spectrum of toluene was observed when UV-IMS was used; otherwise, the signal from DMA was increased in the presence of humidity so it is an interferent. Membrane system before introducing the sample into the equipment should be used in both cases.

Conclusion

The proposed new vanguard techniques UV-DMA and UV-IMS are two useful tools for the determination of atmospheric pollutants compared with routine techniques and atmospheric control sensors due to the fact that they provided rapid detection, they are cheaper and portable for in-situ analysis. Therefore, they could be considered as an alternative to classical analysis method. Instruments based on ion mobilities give a quantification of compounds with statistically acceptable results for the determination of toluene and other analytes in EUPHORE chambers. This work opens up interesting prospect for the IMS and DMA to screening analytes in air samples.

Rapid on-line measurement of hazardous BTEX by a home-made PDMS portamembrane coupled to UV-Ion Mobility Spectrometry

L.R. Criado-García [1], E. Montoya [2], S. López-Vidal [2], L. Arce [1], M. Valcárcel [1]
[1]Department of Analytical Chemistry. Annex C-3 Building. Campus Rabanales. University of Córdoba. 14071-Córdoba. Spain. E-mail: qa1mejob@uco.es
[2]RAMEM S.A. 28027- Madrid. Spain. /www.ioner.eu/

UV-Ion Mobility Spectrometry

UV-Ion Mobility Spectrometry (UV-IMS) is a reliable, solventless and inexpensive technique which permits efficient monitoring of Volatile Organic Compounds (VOCs) such as BTEX (benzene, toluene, m-xylene, o-xylene and p-xylene). The technique has still limitations such as relatively poor resolution of the species formed and **interferences** in the measurement which can **disturb the ionization process** such as **humidity**.

Objective

The aim of this work is to develop a miniaturized home-made **portamembrane** coupled to UV-IMS for direct measurement of BTEX at low concentration in humidity gas-phase samples without pretreatment steps.

Principle of working

The ions generated by an UV **ionization source** move in a weak electric field at atmospheric pressure towards the **drift region**. During their drift they collide with a **drift gas** flowing in the opposite direction. A **Faraday plate** used as detector is placed at the end, where ions are separated depending on their shape, charge and mass.

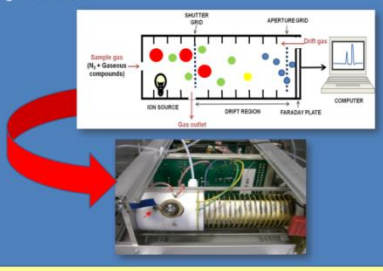

Experimental

In this work, we used a 100 mL flask filled with water to generate humidity coupled to other flask (1000 mL) in which gaseous analytes were generated. This sample gas went into the portamembrane in which analytes diffused along the membrane and they were conducted by carrier gas to the UV-IM Spectrometer.

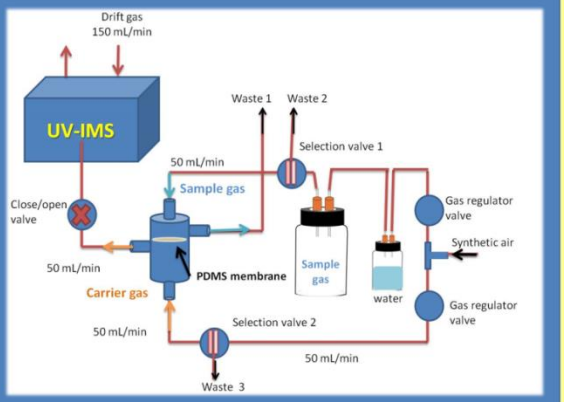

PDMS

The home-made portamembrane utilized a microporous **polydimetil siloxane** membrane (PDMS) for avoiding humidity in the measurement. PDMS, which is a well-known material, is among the more popular gas permeable materials available.

Properties

- From the **siloxane**: strength, stability and flexibility.
- From their attached **methyl group**: inertness and water repellency.

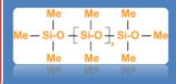

Preliminary results

Xylene isomers measured in a **dry** and **humid air**

Without membrane | **With membrane**

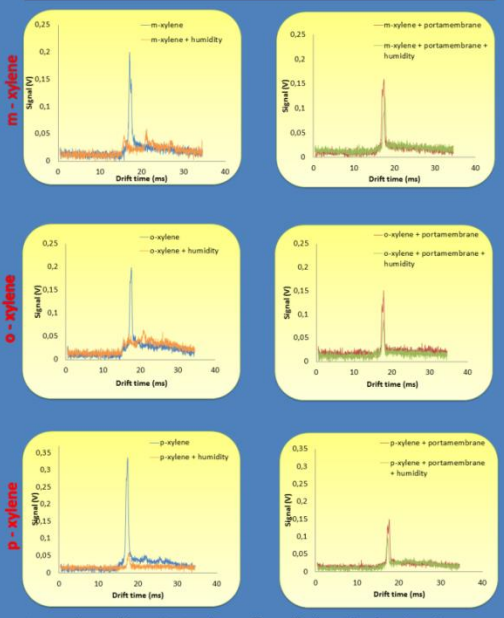

It was observed how IM signal was affected by humidity for all analytes tested without membrane. This signal reduction was almost avoided using a PDMS membrane inside a home-made portamembrane.

Conclusion

The home-made portamembrane coupled to UV-IMS has been successfully proposed to avoid humidity in gaseous samples. This work propose a PDMS portamembrane as a new interface which extend the range and versatility of UV-IMS to determinate BTEX potentially present in workplace areas such as factories, gas station and garages which are difficult to detect with UV-IMS at atmospheric air conditions due to interferents such as humidity.

ION MOBILITY SPECTROMETRY AS A VANGUARD TECHNOLOGY TO ASSESS THE QUALITY OF A HEAT TRANSFER FLUID (HTF)

UNIVERSIDAD DE CÓRDOBA

L. Criado-García, R. Garrido-Delgado, L. Arce , M. Valcárcel*
Department of Analytical Chemistry. Annex C-3 Building. Campus Rabanales. University of Córdoba. 14071-Córdoba. Spain. *E-mail: qa1mejob@uco.es

XXIV RNE – VIII CIE ESPECTROSCOPIA

Analytical problem

HTF is a mixture of two compounds: biphenyl and diphenyl ether which is used in thermosolar plants.

- **Efficiency and productivity**
  - It is necessary to control the lifetime of HTF due to the presence of degradation products: benzene and phenol.
- **Safety and occupational health**
  - Sampling could be dangerous due to high temperatures and release of toxics compounds.

Objective

- Differentiate between raw and degraded HTF by H^3-GC-IMS and UV-IMS
- Identify compounds formed in HTF when it is heated at high temperatures (aprox. over 400 ºC) by H^3 -GC- IMS and UV-IMS.

ION MOBILITY SPECTROMETRY

RUTINARY TECHNIQUES

Experimental

UV-IMS

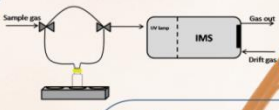

Parameter	UV-IMS	GC-H^3-IMS
Sample gas N_2 (mLmin^{-1})	100	10
Drift gas N_2(mLmin^{-1})	100	250
Volume (µL)	100	100
Head space sampling volume (µL)	-	200
Incubation temperature (º C)	30	30
Incubation time (min)	-	5
Syringe temperature (º C) T3	-	80
Column temperature (º C)T2	-	40
Drift tube temperature (º C) T1	-	65
Agitation speed (rpm)	-	250
Fill speed (µLs^{-1})	-	100
Pull up (s)	-	1.0
Flushing (min)	-	10
Acquisition time(min)	-	32

GC-H^3-IMS

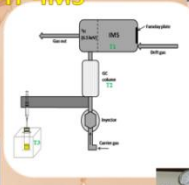

Reactor and degraded HTF samples

FT-MIR

Spectra were obtained by **transmission mode** in a **FT-MIR Bruker Tensor 27** (Bruker Optik GmbJ) spectrophotometer with CsI beamsplitters and a DTGS detector. OPUS v. 6.5 software (Bruker Optik GmbH; Rudolf-Plank-Str. 27; 76275 Ettlingen; GERMANY) was used to collect the transmission spectra

GC-FID/GC-MS

GC-MS

HTF samples were diluted in DCM (1 g/50 mL). 1 µL of sample was injected at 265 ºC working with split 1/50. Chromatographic column used was composed of 5% phenilsilicone (30 m, 0.25 mm d.i. y 0.25 micas). Helium as carrier gas at 1 mL min^{-1}. Temperature program:35 ºC (2 min), 10 ºC/min up to 285 ºC (5 min).
Ion detection was carried out at fullscan mode, m/z:45-400 (0.5 s/scan).

GC-FID

HTF samples were diluted in DCM (1 g/50 mL). 1 µL of sample was injected at 265 ºC working with split 1/20. Chromatographic column used was composed of 5% phenilsilicone (30 m, 0.25 mm d.i. y 0.25 micas) SLB5-MS. Helium as carrier gas at 1mL min^{-1}.
Temperature program: 37 ºC 3 min, 4 ºC/min hasta 150C, 8 ºC/min up to 300 ºC (5 min).
Detector FID: 300 ºC, rango:11; H_2: 30 mL min^{-1}, air: 300 mL min^{-1}, auxiliary gas: 30 mL min^{-1}.

Results

QUALITATIVE ANALYSIS

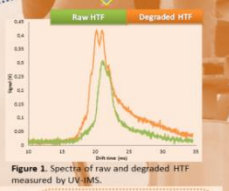

Figure 1. Spectra of raw and degraded HTF measured by UV-IMS.

Figure 2. Global IMS signal from degraded HTF heated at 400 ºC for a long period of time measured by UV-IMS.

Raw and degraded HTF samples can be differentiated by UV-IMS. HTF signal increased when HTF sample was heated at 400 ºC for 200 h (see signals from 1 to 4 in Figure 2). More heating time resulted in no significant increase in the IMS global signal intensity.

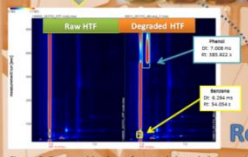

Figure 3. Topographic plots of raw and degraded HTF measured by H^3-GC-IMS.

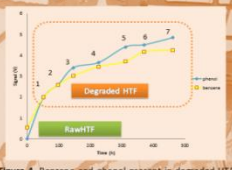

Figure 4. Benzene and phenol present in degraded HTF heated at 400 ºC for a long period of time measured by ^{3}H-GC-IMS.

Raw and degraded HTF samples can also be differentiated by H^1-GC-IMS. Moreover, benzene and phenol, that appear as degradation products of HTF exposed at high temperatures, can be successfully identified.

QUALITATIVE ANALYSIS

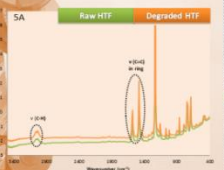

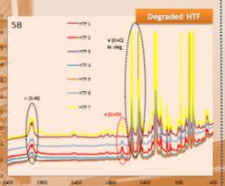

Figure 5. (**5A**) FT-IR spectra from raw and degraded HTF. (**5B**) FT-IR spectra from degraded HTF heated at 400 ºC for a long period of time.

Vibrations associated with aromatic compounds can be successfully identified in the IR spectra. Increases in the transmittance values from aromatic bands were observed when more degraded HTF samples were measured by FT-IR.
One band (related to the C-O bond) could be coming from the phenol among other degradation products present in degraded HTF samples.

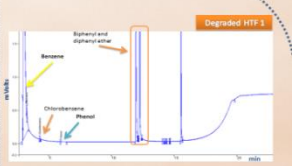

Figure 6. Chromatogram of degraded HTF 1 measured by GC-FID.

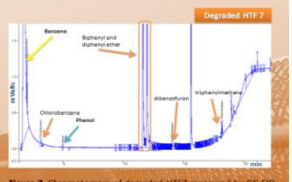

Figure 7. Chromatogram of degraded HTF7 measured by GC-FID.

Initial ingredients of raw HTF: biphenyl and diphenyl ether and degradation products: benzene, phenol and chlorobenzene were successfully identified in the GC-FID chromatogram of degraded HTF (see Figure 6 and 7).
An increase in the signal of degradation products were observed when more degraded HTF samples were measured as well as the appearance of new degradation products: dibenzofuran and triphenylmethane in the chromatogram (see Figure 7).

Quantitative study ^{3}H-GC-IMS

Benzene and phenol signals obtained for the concentration range studied were successfully adjusted to a second order polynomial equation.

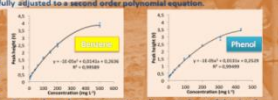

Notice that at low concentration, a linear tendency of the signal was observed.

	Linear interval (mg L^{-1})	Equation	R^2	LOD (mg L^{-1})	LOQ (mg L^{-1})
Benzene	32.3-150	Y=0.0085x+0.5202	0.993	9.7	32.3
Phenol	14.9-150	Y=0.0121x+0.2537	0.990	4.4	14.9

Quantification of benzene and phenol in degraded HTF samples:

HTF	Degradation time (h)	Concentration (ppm) Benzene	Phenol
1	51	714	629
2	99	1525	487
3	147	1930	932
4	227	2863	925
5	311	4175	1562
6	462	6610	1645
7	534	6727	2685

Precision study for UV-IMS

Degraded HTF	Global IMS signal	
	Drift time	Peak height
Repeatability (% RSD)	0.5 %	2.6%
Reproducibility (%RSD)	1.8 %	4.7%

Precision study for ^{3}H-GC-IMS

Degraded HTF	Benzene			Phenol		
	Drift time	Peak height	Retention time	Drift time	Peak height	Retention Time
Repeatability (% RSD)	0.1 %	3.3 %	0.6 %	0.1 %	2.9 %	1.2 %
Reproducibility (%RSD)	0.1 %	4.5 %	1.1 %	0.1 %	3.5 %	1.6 %

Analytical properties	GC-H^3-IMS	UV-IMS	FT-IR	GC-MS GC-FID
Sensitivity	ppm level	ppm level	ppm level	ppt level
Robustness	High	Medium	High	High
Time per analysis	<60 min	<5 min	15 min	45 min
Cost	Low	Low	High	High
Sample pretreatment	No	No	Yes	Yes
Portability	No	Yes	No	No

Conclusion

In this work, two different IMS instruments were used to study the suitability for monitoring the HTF lifecycle. One was an IMS with UV lamp, which was proved to be useful to monitor the degradation of HTF in a quick and easy way giving a global IMS response. Another was an IMS with Tritium (^{3}H) source and GC column, which was really powerful to identify degradation products such as phenol and benzene in degraded HTF samples. Results obtained by IMS techniques were comparable with the ones obtained by routine techniques: Gas chromatography with Flame Ionization Detector, Mass Detector and Near Infrared Spectroscopy. IMS was demonstrated in this work to be a reliable, quick, portable and inexpensive technique that can be useful for HTF quality control in thermosolar plants.

Solid phase extraction as an alternative to enhance sensitivity of Ion Mobility Spectrometry: Determination of phenol in environmental samples as a case of study

Laura Criado-García, Lourdes Arce
Department of Analytical Chemistry, Annex C-3 Building, Campus Rabanales, University of Córdoba. 14071-Córdoba, Spain. e-mail: qa1arjil@uco.es

Objectives

The aims of this work were to propose a method to determine directly phenol in environmental samples (soil and water samples) by headspace Ion Mobility Spectrometry (HS-IMS) and also demonstrate the potential of combining solid phase extraction (SPE) with HS-IMS to enhance sensitivity to determine low concentrations of phenol in environmental water samples.

Experimental

Oasis® HLB 60 mg

Hydrophilic modified styrene polymer

The interactions that took part in the hydrophilic part of the sorbent dominated the retention of phenol.

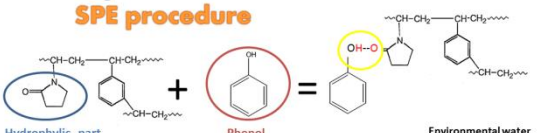

SPE procedure

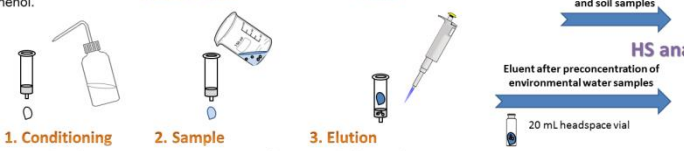

1. Conditioning
5 mL methanol
5 mL distilled water

2. Sample
15 mL aqueous sample acidified (pH= 3) adding 2 M HCl

3. Elution
1 mL dichloromethane
~~methanol~~
~~acetonitrile~~

No interfences observed. Only yields ion in negative mode
Discarded due to interference in the IMS signal in positive mode

HS-IMS

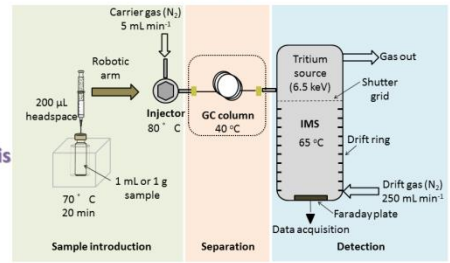

Results

1. Optimization procedure

Sample volume and mass

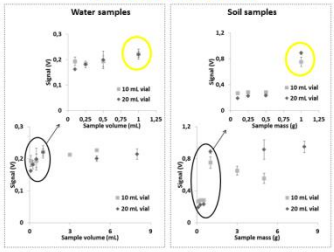

The higher intensity values for phenol were achieved when using 1 mL or 1 g of sample in 20 mL headspace vial.

Heating time and temperature to create the HS

IMS signal obtained for water samples

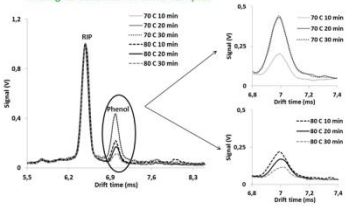

Phenol **peak intensity was higher when heating at 70 °C for 20 min.** Heating for more time resulted in no increment in phenol peak intensity. When heating at 80 °C the signal was lower since phenol signal could be affected by humidity (increased at that condition). Same behaviour was observed for soil samples.

SPE cartridge

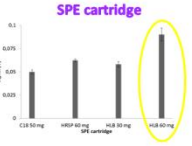

Sample volume for SPE

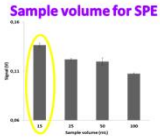

2. Method validation

Sensitivity

Method	Matrix	Calibration curve (y= ax+b)	R^2	$S_{y/x}$	Sa	Sb	LOD (mg L^{-1})	LOQ (mg L^{-1})
HS-IMS	Water	y= 0.033x + 0.056	0.974	0.020	0.010	0.002	0.94	3.13
	Soil	y= 0.283x + 0.033	0.984	0.018	0.013	0.014	0.14	0.45
SPE-HS-IMS	Water	y= 0.056x + 0.037	0.995	0.002	0.001	0.002	0.05	0.18

Precision values for drift time and retention time were in all cases lower than 1.9 %. Higher RSD % values were obtained for phenol peak height.

LOD and LOQ were one order of magnitude lower when SPE was used prior to HS-IMS

Precision

Precision values	Matrix	Concentration added (mg L^{-1})	HS-IMS Peak height	HS-IMS Drift time	HS-IMS Retention time	Concentration added (mg L^{-1})	SPE-HS-IMS Peak height	SPE-HS-IMS Drift time	SPE-HS-IMS Retention time
Within-day (% RSD, n= 6)	Water	4	5.5	0.2	0.2	0.5	7.7	0.3	0.5
	Soil	1	2.2	0.3	0.9				
Between-day (% RSD, n= 9)	Water	4	6.7	0.3	1.6	0.5	15.5	0.7	1.9
	Soil	1	10.1	0.4	1.2				

Recovery

Added concentration (mg L^{-1})	River water Found concentration (mg L^{-1})	River water Recovery (%)	Stream water Found concentration (mg L^{-1})	Stream water Recovery (%)	Well water Found concentration (mg L^{-1})	Well water Recovery (%)
0.5	0.45±0.03	90	0.35±0.12	69	0.47±0.06	95
0.8	0.70±0.08	88	0.49±0.11	61	0.53±0.11	66

The results shown than **HLB 60 mg** was an **effective sorbent material** for extracting **phenol** from **environmental samples.**

The **IMS headspace analysis of the eluent** in which phenol was present was carried out **without any interference from the solvent** (dichloromethane).

3. Analysis of real samples

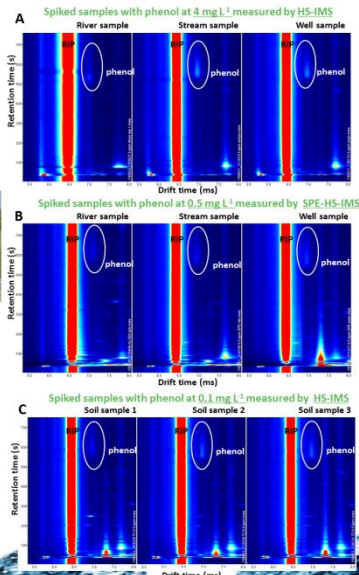

Soil sample 1 (parking area of Rabanales campus), soil sample 2 (train station area) and soil sample 3 (park in Córdoba city center)

Conclusion

Strengths of the methodology developed

SPE: • Sensitive • Selective

HS-IMS: • Rapid • Simple • Precise

SPE-HS-IMS: • Sensitive • Selective • Rapid • Simple • Precise

All these advantages allow using SPE-HS-IMS as a suitable approach for environmental trace analysis

Determination of benzene, toluene, ethylbenzene in gaseous samples using sorbent trap coupled to UV-IMS

Laura Criado-García, Nouman Almofti, Lourdes Arce
Department of Analytical Chemistry. Annex C-3 Building. Campus Rabanales. University of Córdoba. 14071-Córdoba. Spain. *E-mail: qa1arjil@uco.es

Objective

The main objective of this work is based on the development of a method to trap BTEX present in gaseous samples and desorbed them using thermal desorption unit and carried them to UV-IMS for their identification and determination.

Experimental

1. Preparation of the gaseous standards

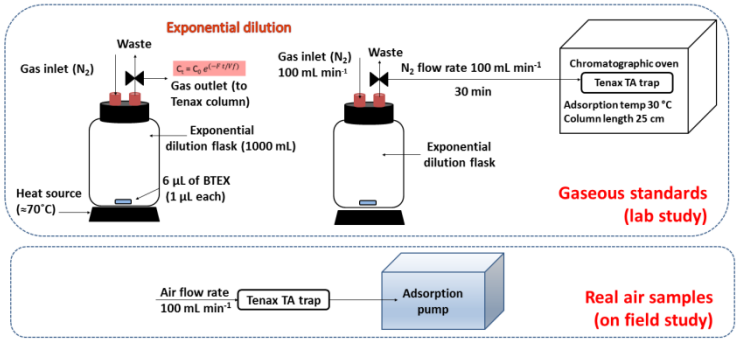

2. Adsorption step

3. Desorption step and UV-IMS analysis

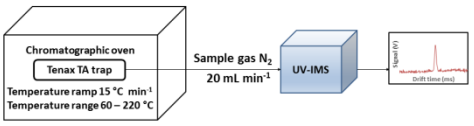

Adsorption and desorption conditions

Parameters	Studied values	Optimum value
Adsorption step		
Adsorption time	5, 15 and 30 min	30 min
Adsorption flow rate	100, 200 and 300 mL min^{-1}	100 mL min^{-1}
Desorption step		
Temperature ramp	5, 15 and 20 °C min^{-1}	15 °C min^{-1}
Sample gas flow rate	20, 30 and 40 mL min^{-1}	20 mL min^{-1}
Drift gas flow rate	100, 200 and 300 mL min^{-1}	100 mL min^{-1}

UV-IMS conditions

Parameters	Value
Drift and sample gas	N_2 (5.0 = 99.999%)
Drift gas flow rate	100 mL min^{-1}
Sample gas flow rate	20 mL min^{-1}
Drift voltage polarity	Positive
Ionization source	UV lamp (10.6 eV)
Trigger delay	0.4 ms
Grid Pulse width	100 µs
Repetition rate	50 ms
Sampling frequency	30000 Hz
Electric field strength	333 V/cm
Length of the drift tube	12 cm

Results

Two full factorial design DOE (design of experiment) using Minitab 17 software were established.
Each design consisted of 2 factors at 3 levels, making up a total of 18 runs

1. Optimization of sample and drift gas flow rate for desorption step

Surface plots obtained for benzene and toluene for sample gas and drift gas flow rate.
20 and 100 mL min^{-1} resulted the optimum values for **sample and drift gas flow rate.**

2. Optimization of adsorption flow rate and time for adsorption step

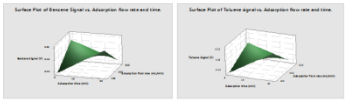

Surface plots obtained for benzene and toluene for adsorption flow rate and time.
100 mL min^{-1} and **30 min** resulted the optimum values for **adsorption flow rate and time.**

3. Preconcetration achieved with Tenax TA trap coupled to UV-IMS

Benzene as an example

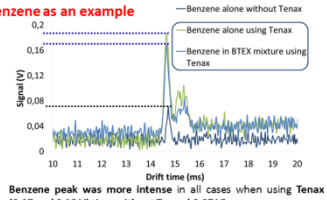

Benzene peak was more intense in all cases when using **Tenax (0.17 and 0.18 V)** than **without Tenax (0.07 V)**

4. Identification of BTEX compounds in the IMS spectra

Compound	Signal (V)	Drift time (ms) Tenax TA	Drift time (ms) Flask	Retention time (min)	K_0 Calculated (Tenax TA)	K_0 reported [1]
Benzene	0.402	14.61	14.70	7.15	2.28	2.11
Toluene	0.252	15.57	15.48	8.35	2.13	2.00
	0.253	16.80	16.19	8.50	1.98	
Ethylbenzene	0.315	16.23	16.23	9.25	2.05	1.89
m-xylene	0.575	16.19	16.19	9.45	2.05	1.91
o-xylene	0.419	16.36	16.23	9.60	2.03	1.92
p-xylene	0.712	16.20	16.14	9.30	2.05	1.97

[1] L.Criado-Garcia et al. Talanta 111 (2013) 11-118.

IMS spectra obtained for each BTEX compound measured individually by Tenax- UV-IMS

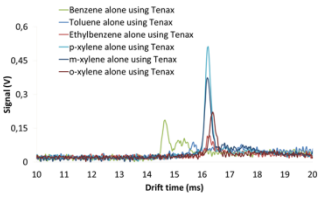

5. Validation of the Tenax trap-UV-IMS method

Sensitivity

Analyte	Concentration range (mg m^{-3})	Regression coefficient (R^2)	LOD (mg m^{-3})	LOQ (mg m^{-3})
Benzene	0.10 – 9.50	0.987	0.73	2.43
Toluene	0.10 – 9.39	0.990	0.78	2.60
Ethylbenzene	0.10 – 9.39	0.982	1.04	3.49

Precision

	Compounds	Intensity (%RSD)	Drift time (% RSD)	Retention time (% RSD)
Repeatability n=6	Benzene	13.11	1.24	0.81
	Toluene	19.95	0.98	0.74
	Ethylbenzene	22.05	0.89	1.14
Reproducibility n=9	Benzene	12.71	1.43	0.78
	Toluene	16.38	1.18	0.66
	Ethylbenzene	22.06	1.10	0.97

Selectivity

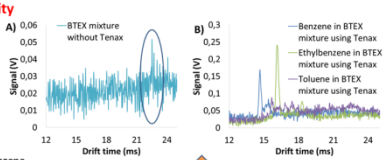

A) Only one peak was observed in the IMS spectra corresponding to a cluster ion from the mixture of BTEX when using only UV-IMS

B) Individual peaks from each compound of the BTEX mixture were obtained when Tenax TA sorbent trap was used combined with UV-IMS

6. Real samples: monitoring air from a gasoline spillage in a parking area

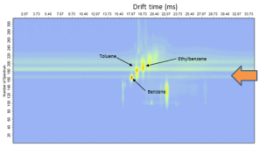

Topographic map of the air from gasoline spillage on the pavement after 5 min (sampling 1)

Benzene, toluene and ethylbenzene were identified and pointed by arrows.

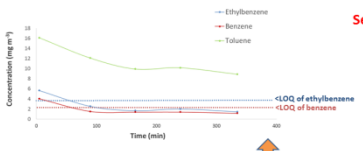

5 mL gasoline spillage on pavement	Time (min)	Concentration (mg m^{-3}) Benzene	Toluene	Ethylbenzene
Sampling 1	5	4.02	16.12	5.64
Sampling 2	90	<LOQ	12.09	<LOQ
Sampling 3	165	<LOQ	9.91	<LOQ
Sampling 4	240	<LOQ	10.17	<LOQ
Sampling 5	335	<LOQ	8.89	<LOQ

Sampling number	Sampling time	Temperature (°C)	Humidity (RH %)	Wind speed (Km h^{-1})	Time interval (min)
1	12:20	28	42	7	5
2	13:50	31	34	6	90
3	15:10	32	33	3	165
4	16:20	35	20	3	240
5	17:35	37	15	6	335

Tendence of concentration of benzene, toluene and ethylbenzene present in air after a gasoline spillage (5 mL) on pavement of a parking area along time detected by the proposed method (Tenax-UV-IMS)

The decreasing concentration was clearly observed for the three compounds along time

Conclusion

In this work has been demonstrated for the first time, the potential of coupling Tenax TA column to UV-IMS to determine BTEX compounds in air samples. This new methodology was implemented successfully to identify benzene, toluene and ethylbenzene in real air samples close to a gasoline spillage. Collection of more real air samples (from factories, traffic areas and petrol station) and improvement of separation of xylene isomers by coupling a multicapillary column or using other sorbent material coupled to UV-IMS will be considered in future work

A new approach to determine toxic substances present in saliva samples by ion mobility spectrometry

EUROANALYSIS 2015 — 18th edition of EuroAnalysis, the European Conference on Analytical Chemistry

L. Criado-García, L. Arce, M. Valcárcel
Department of Analytical Chemistry. Annex C-3 Building. Campus Rabanales. University of Córdoba. 14071-Córdoba. Spain. *E-mail: qa1meobj@uco.es

Introduction

- **Within the clinical field,** rapid and reliable tests are necessary to determine the **presence of compounds in saliva.** The non-invasive nature and ready accessibility of the sample suggest that saliva may be an attractive alternative to blood and urine for profiling and screening human subjects.
- **Ion Mobility Spectrometry (IMS)** is a sensitive technique that has been shown a higher selectivity in explosive and chemical agent applications. Sensitive and rapid methods are needed to be implemented in the clinical field as the one proposed in this work.
- **µSPE** is the extraction method suggested before GC-IMS analysis. It will avoid the problems related to the effect of the matrix, specially moisture from saliva samples which can interfere with the IMS signal.

Over **6000 substances had been identified in cigarette smoke,** from BTEX such as **benzene** and **toluene**, to other additives that can be present in flavored tobacco such as **butyraldehyde, benzaldehyde** and **tolualdehyde.**

Experimental

Analytes

butyraldehyde, benzene, toluene, benzaldehyde, tolualdehyde

Extraction of analytes from saliva

Magnetic stirred assisted-µSPE

1. Assembling
Sorbent material: 5.5 mg of each **(HLB, C_{18} and MWCNT)** to reach 16.5 mg of sorbent mix
Envelope: parafilm M®
Integrated stirred: staple

2. Conditioning
20 mL MeOH 2 min
+ dried with lab tissue to remove the excess of liquid

3. Extraction
5 mL sample (water or saliva) 15 min with magnetic stirring + dried with lab tissue to remove the excess of liquid

Sorbents

Different sorbents were mixed in a µSPE system to retain target analytes of different polarity.

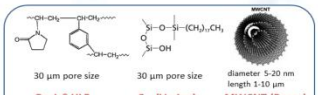

Oasis® HLB — Hydrophilic modified styrene polymer
C_{18} (Varian) — Bonded silica sorbent
MWCNT (Bayer) — Multiwalled carbon nanotubes

Desorption and signal acquisition

Headspace-gas chromatography-Ion mobility spectrometry (HS-GC-IMS)

The analytes were thermally desorbed from the µSPE system using the headspace autosampler of the IMS.

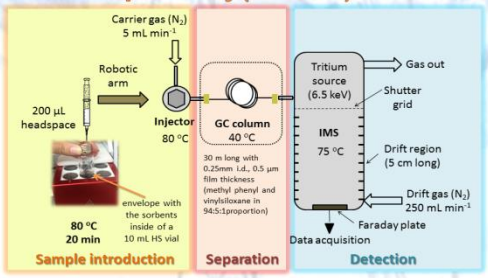

IMS theory

The ions generated by **tritium ionization source** move in a weak electric field at atmospheric pressure towards the **drift region.** During their drift, they collide with a **drift gas** flowing in the opposite direction. A **Faraday plate** used as detector is positioned at the end, where ions are separated depending on their **shape, charge and mass.** The number of ions reaching the detector is a measure of the concentration of the analytes.

Results

µSPE-HS-GC-IMS was used for first time to determine benzene, butyraldehyde, toluene, benzaldehyde and tolualdehyde in saliva samples from smoker and non smoker.

Identification of analytes in saliva samples

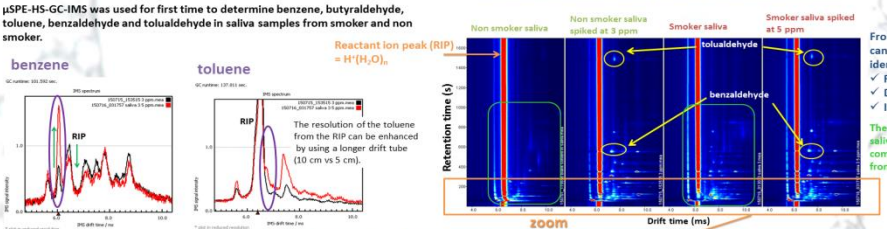

From the topographic plot can be extracted and identified each analyte:
- ✓ Retention time (s)
- ✓ Drift time (ms)
- ✓ IMS signal intensity (V)

The fingerprint of the smoker's saliva sample is different compared to a saliva sample from a non-smoker individual.

benzene

toluene

The resolution of the toluene from the RIP can be enhanced by using a longer drift tube (10 cm vs 5 cm).

butyraldehyde

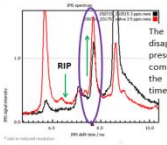

The RIP signal almost disappeared due to the presence of other components eluting at the same retention time.

zoom

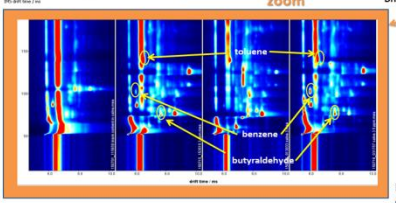

Analyte	Molecular weight (g mol^{-1})	Boiling point (°C)	Proton affinity (KJ mol^{-1})	Reduced mobility (K_0) cm^2 V^{-1} s^{-1}
Butyraldehyde	72.11	74.8	792.7	1.40
Benzene	78.11	80.1	750.4	1.92
Toluene	92.14	110.8	784.0	1.74
Benzaldehyde	106.12	178.1	834.0	1.57
Tolualdehyde	120.14	204	851.8	1.53

K_0 value is specific of each ion on IMS.

Boiling points determine the elution order and retention time (s) from the GC column.

The compound with higher proton affinity value will preferentially acquire the charge from the RIP.

tolualdehyde

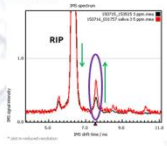

benzaldehyde

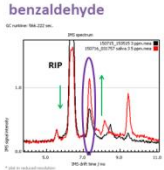

Calibration curves obtained by µSPE-IMS method

Matrix	Compound	Calibration curve (y= ax+b)	R^2	Sa	Sb	LOD (mg L^{-1})	LOQ (mg L^{-1})
Saliva	Butyraldehyde	y= 0.512x + 0.776	0.973	0.065	0.076	0.38	1.26
	Benzene	y= 0.623x + 0.689	0.972	0.103	0.056	0.49	1.66
	Toluene	y= 0.505x + 0.839	0.954	0.076	0.083	0.45	1.51
	Benzaldehyde	y= 0.406x + 0.315	0.986	0.067	0.073	0.41	1.37
	Tolualdehyde	y= 0.277x + 0.126	0.975	0.040	0.042	0.27	0.91

*Calibrations were also performed in ultrapure water.; LOQs obtained were around or slightly below 1 ppm for all analytes.
**Benzaldehyde and tolualdehyde resulted in the better R^2 values since their corresponding peaks were well resolved compared to the other analytes. In both cases, the LOQs were lower than the one obtained for the other analytes since their proton affinity values were higher than for the other compounds.

Precision for the µSPE-IMS method

The RSD values show that the method optimized is more accurate for identification (RSD values for drift and retention time were in all cases lower than 3.5 % RSD) than for quantification purpose (RSD < 21 % for peak height).

Analyte	Within-day precision (% RSD, n= 6)			Between-day precision (% RSD, n= 9)		
	Retention time	Drift time	Peak height	Retention time	Drift time	Peak height
Butyraldehyde	3.5	0.2	15.1	2.4	0.2	21.1
Benzene	3.2	0.2	13.9	3.1	0.2	21.2
Toluene	1.6	0.1	8.4	2.3	0.2	18.9
Benzaldehyde	1.2	0.2	13.7	1.0	0.6	18.0
Tolualdehyde	0.8	0.2	18.8	0.7	0.4	19.8

(2.5 ppm of each component spiked in saliva sample was used for precision study)

- ✓ non-invasive
- ✓ accessibility of the sample

Conclusion

- ✓ sensitive
- ✓ working at ambient pressure
- ✓ quick responses

This work opens up interesting prospect for **ion mobility spectrometry to screening toxic compounds in clinical field** in combination with a new sample preparation methodology: **µSPE.**